DIFFERENTIAL CONTRIBUTIONS OF SUBREGIONS OF THE DORSAL ANTERIOR CINGULATE CORTEX TO NEGATIVE EMOTION IN THE COMMON MARMOSET

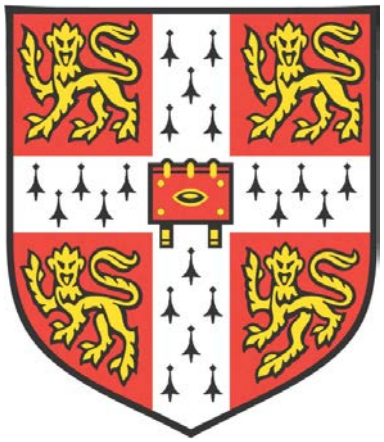

SUFIA SABURAN RAHMAN

DEPARTMENT OF PHYSIOLOGY, DEVELOPMENT & NEUROSCIENCE

UNIVERSITY OF CAMBRIDGE

JANUARY 2018

This dissertation is submitted for the degree of Doctor of Philosophy

Dedicated to my parents,

who inspired me to start this thesis.

And to my niece,

Noura Amelia Rahman,

who inspired me to finish it.

if

the ocean

can calm itself,

so can you.

we

are both

salt water

mixed with

air.

- Nayyirah Waheed

PREFACE

The following work was carried out at the Department of Physiology, Development and Neuroscience, University of Cambridge, during the years 2013 - 2018, under the supervision of Professor Angela C. Roberts.

This dissertation is the result of my own work and includes nothing which is the outcome of work done in collaboration except where specified in the text below. It has not been previously submitted, in part or whole, to any university or similar institution for any degree, diploma, or other qualification.

The experiments in this thesis could not have been carried out without the support of a number of people in the laboratory. Thus, I acknowledge and thank my supervisor, Angela Roberts, for performing telemetry implantation surgeries; research associates, Andrea Santangelo and Nicole Horst for performing cannulation surgeries, and Christian Wood for support in analysis of tracing data; and finally, research associates Gemma Cockcroft and Lauren Anderson for support in counter scoring and histological processing.

This dissertation does not exceed the prescribed word limit of 60,000 for the Degree Committee of Biology.

This work was funded by a BBSRC studentship and an MRC Programme grant.

Sufia Saburan Rahman

31st January 2018

ACKNOWLEDGEMENTS

First and foremost, I would like to express my sincere gratitude to my primary supervisor, Professor Angela Roberts, for her support throughout the duration of this project and for helping me to “find the plot.” I would also like to thank my secondary supervisor Dr Andrea Santangelo for her guidance and encouragement.

I am grateful to my colleagues at the Innes, past and present, many of whom have become good friends. All have contributed to the completion of this thesis in some way, whether through practical help assisting with marmoset infusions, intellectual and humorous conversations in the office (which often turned into lively debates), provision of a constant supply of treats by the kettle, or simple words of kindness.

The excellent marmoset care provided by Colin Windle (NACWO), Jo Keeley (NVS), and the brilliant laboratory technicians; Danielle Oberle, Ollie Tyrtania, Lucy Mulderrig (and Natalie and Dom) is greatly appreciated.

I am also grateful to the friends that kept me grounded and provided some of my best memories of the past few years:

Nessie – Lydia and Stacey, who supported me through 2nd year (the “rmd”) and who I can always count on for advice on anything from recipes (courgette pie!) to life choices; and Laith(y), my gym/desk/SfN/NYC buddy, whose infectious enthusiasm lifted my spirits many a time.

Zuzanna B - for being cool.

The members of S.T – friends who I have grown up with and who have inspired me with their successes.

Finally, I thank my parents, my brother, and of course my twin sister, Zarina, for believing in me when I didn’t believe in myself.

ABSTRACT

The dorsal anterior cingulate cortex (dACC) has been implicated in a broad range of cognitive and emotional functions, including the processing of negative emotion. Furthermore, abnormalities in dACC activity have been associated with anxiety and depression, disorders in which negative emotion is dysregulated. Thus, a better understanding of the precise contributions of the dACC to negative emotion could give us important insights into the neurobiological mechanisms underlying these debilitating neuropsychiatric disorders. However, despite extensive study of the dACC, its precise role in negative emotion is unclear. Instead there is mounting evidence that rather than being one functionally homogeneous region, subregions of the dACC may have distinct functional roles. This evidence is largely correlational, and interventional studies in experimental animals are required to address this.

Accordingly, the work in this thesis causally assessed the contributions of two spatially distinct subregions of the dACC (rostral and caudal) to the regulation of the behavioural and cardiovascular correlates of negative emotion in the common marmoset (Callithrix jacchus). These dACC subregions were targeted with indwelling cannulae to enable pharmacological manipulations to be carried out in a range of tasks, used to assess distinct components of negative emotion, such as conditioned fear and anxiety.

The findings suggest that the rostral dACC and the caudal dACC do indeed have distinct contributions to the expression of negative emotion and the regulation of anxiety, respectively. Furthermore, an assessment of the anterograde projections of these subregions provides anatomical support for the observed functional differences.

TABLE OF CONTENTS

LIST OF FIGURES

LIST OF TABLES

1 |GENERAL INTRODUCTION

Neuropsychiatric disorders are highly prevalent and can cause considerable personal suffering, as well as large societal and economic costs (Kessler et al., 2009). They are the leading cause of years lived with disability worldwide, and of these, depression and anxiety are associated with the greatest disease burden (Whiteford et al., 2013). However, our understanding of these disorders is inadequate. Even if it were possible to provide the best existing treatments to the maximum number of patients, the majority of disease burden is simply unavoidable given our current knowledge (Andrews et al., 2004). This highlights the necessity for further study into the causes and mechanisms underlying these disorders to accelerate the development of improved treatments.

Abnormalities in the structure and function of the dorsal anterior cingulate cortex (dACC) have been observed in anxiety and depression, indicating its contribution to these disorders of negative emotion (Pizzagalli, 2011; Shin and Liberzon, 2010). By virtue of its connectivity with higher cortical regions of the brain and with limbic regions, it has been suggested that the dACC is a key node in the brain for the integration of cognition and emotion (Ray and Zald, 2012; Stevens et al., 2011). Impairments in both functional domains are apparent in disorders of negative emotion. Indeed, neuroimaging studies in healthy individuals have implicated the dACC in cognitive functions, such as decision-making and conflict, and affective functions, such as in fear and anxiety (Maier et al., 2012; Shackman et al., 2011; Ullsperger et al., 2014). However, despite extensive study of the dACC, its precise role in negative emotion is uncertain. Instead, there is mounting evidence that rather than being one functionally homogeneous region, the dACC may have functionally dissociable roles which can be mapped onto distinct anatomical subregions.

1.1 Structure of the dACC

The cingulate cortex refers to the band of cortex that wraps around the corpus callosum, below the superior frontal gyrus on the medial walls of the frontal lobe. This was referred to as *"le grande lobe limbique* by Broca in 1878, in reference to its oval shape (limbique translates to hoop), and he theorised that it was a uniquely mammalian structure. The cingulate cortex can be divided into the anterior cingulate cortex (ACC) and the more posterior cingulate cortex (PCC) based on location as well as clear differences in cytoarchitecture (layer IV is agranular in ACC but granular in PCC) (Brodmann, 1909) and connectivity (Vogt and Pandya, 1987; Vogt et al., 1979). However, due to the recognition that the ACC is not a unitary functional area, with no functional study activating its entirety, it is often divided into subregions based on positions relative to the genu of the corpus callosum (Figure 1.1) to allow for more precise localisation of functional areas. The dorsal ACC (dACC) describes the region located above the corpus callosum and posterior to the genu, the perigenual ACC (pgACC) is the region surrounding the genu, and the subgenual ACC (sgACC), below the genu.

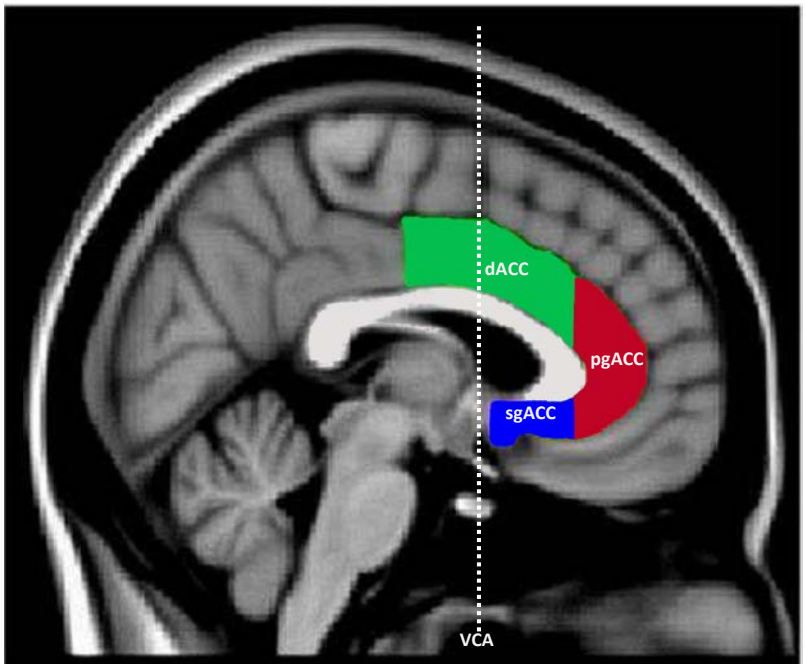

Figure 1.1 Parcellation of ACC based on position relative to corpus callosum and genu. dACC, dorsal anterior cingulate cortex; pgACC, perigenual anterior cingulate cortex; sgACC, subgenual anterior cingulate cortex. White dashed line indicates the vertical line of the anterior commissure (VCA) Figure adapted from (Gunning-Dixon et al., 2009)

Although these terms are commonly used, they are spatial designations, anchored to the corpus callosum and are not based on stable anatomical characteristics. Thus, they do not have clear boundaries. This has resulted in researchers using various nomenclatures to describe the dACC based on different methodology and criteria. Some refer to this region as

Brodmann area 24, which, although does include the dACC, also extends to the pgACC and sgACC. The region specifically surrounding the cingulate sulcus has been referred to as the "rostral cingulate zone" (Picard and Strick, 1996) based on functional similarity to motor regions in the macaque. Others prefer to use the all-encompassing term "dorsomedial prefrontal cortex (dmPFC)/dACC" to refer to the dACC and the adjacent neocortex above (Maier et al., 2012; Robinson et al., 2014). Finally, mounting evidence supports the proposal that the dACC is not a subregion of the ACC, but rather a separate functional entity designated the midcingulate cortex (MCC), which has anterior and posterior subdivisions (aMCC; pMCC) (Vogt, 2016; Vogt et al., 2003) and this has led to yet another nomenclature for this region. These names have been used interchangeably (and sometimes incorrectly) in the literature, and this lack of consensus regarding what the dACC comprises, and further, what to call it, has undoubtedly led to some of the confusion in ascribing functions to the dACC. A thorough understanding of the structure and homology of the dACC is thus crucial before then considering its function in emotion.

1.1.1 Anatomical parcellation of the dACC

A long-standing goal in neuroscience is the parcellation of the brain into distinct areas based on differences in structure and function. This is based on the theory of localisation of function, that specific areas of the brain are responsible for specific functions. Parcellation of the brain thus provides the necessary means of breaking down the overwhelming complexity of the brain in order to begin to understand how it works. Furthermore, a brain map allows for comparison and synthesis of findings across studies and research groups. However, for this to be effective, the technical challenge of accurate and reliable definitions of regional boundaries must be met.

Brain structure is intimately related to function and as a result, various anatomical techniques have been used to parcellate the brain, using sectioned, post-mortem tissue. These include analyses at the cellular microscale of the arrangement of neurons in layers (cytoarchitecture), of myelinated nerve fibres (myeloarchitecture) and of neurotransmitter receptors (chemoarchitecture) following staining for various markers, and macroscale analysis of the anatomical connectivity between different brain regions. The latter requires invasive infusions of tracers, and thus much of our knowledge of brain connectivity in humans is inferred from studies carried out in closely related nonhuman primates, highlighting the crucial need for creation of homologous maps between species. Use of these different techniques has in some

cases resulted in complementary findings, strengthening proposed regional boundaries, but in other cases resulted in inconsistent findings.

1.1.1.1 Human

The first detailed regional map of the human brain to gain widespread consensus, and which remains in common use today, was hand drawn by Korbinian Brodmann over a century ago, alongside regional brain maps of non-human primates and other lower mammals (Brodmann, 1909). In this seminal monograph, Brodmann divided the cerebral cortex into distinct areas based on differences in cytoarchitecture, comparing homologies between species. Typically, cell bodies are arranged in six cortical layers, each with a different characteristic organisation of neuronal cell types (Figure 1.2). However, there are regional variations in the distribution, density, shape, and size of neuron cell bodies from this, which are apparent upon examination of Nissl stained brain tissue sections. Cytoarchitectonic boundaries were described by Brodmann as follows:

> *"The transition between two neighbouring types, that is, the laminar differentiation between these types occurs more or less in a circumscribed manner, at some points so suddenly, that a sharp linear border is present between the neighbouring fields" (Brodmann, 1909).*

Brodmann used a numerical system to label distinct cytoarchitectural regions, now referred to as Brodmann areas (BA). Although he only identified 43 areas in the human brain, his numbered labels go up to 52, as he left out labels for areas that he could observe in other species but not in human. The cingulate gyrus was divided into a precingulate and a postcingulate area based on differences in granularity (precingulate is agranular i.e. no layer IV). The precingulate area was divided dorsoventrally into BA32, BA24 and BA33, a thin strip of rudimentary cortex buried in the callosal sulcus. The dACC in humans is located in this precingulate area and includes parts of BA32, BA24, and BA33 and thus crosses cytoarchitectural boundaries (Figure 1.3A). Notably, no further rostro-caudal divisions of the precingulate area were made by Brodmann. Although, Brodmann's map is the most well-known and has had most impact in the field, particularly in neuroimaging, throughout the 20th century various other researchers also developed maps of the human brain. These have broadly similar parcellations to Brodmann's, but with differences in areal sizes, shapes, number and nomenclature (Zilles and Amunts, 2010). However, other maps of the cortex have defined more regions within the cingulate cortex than Brodmann.

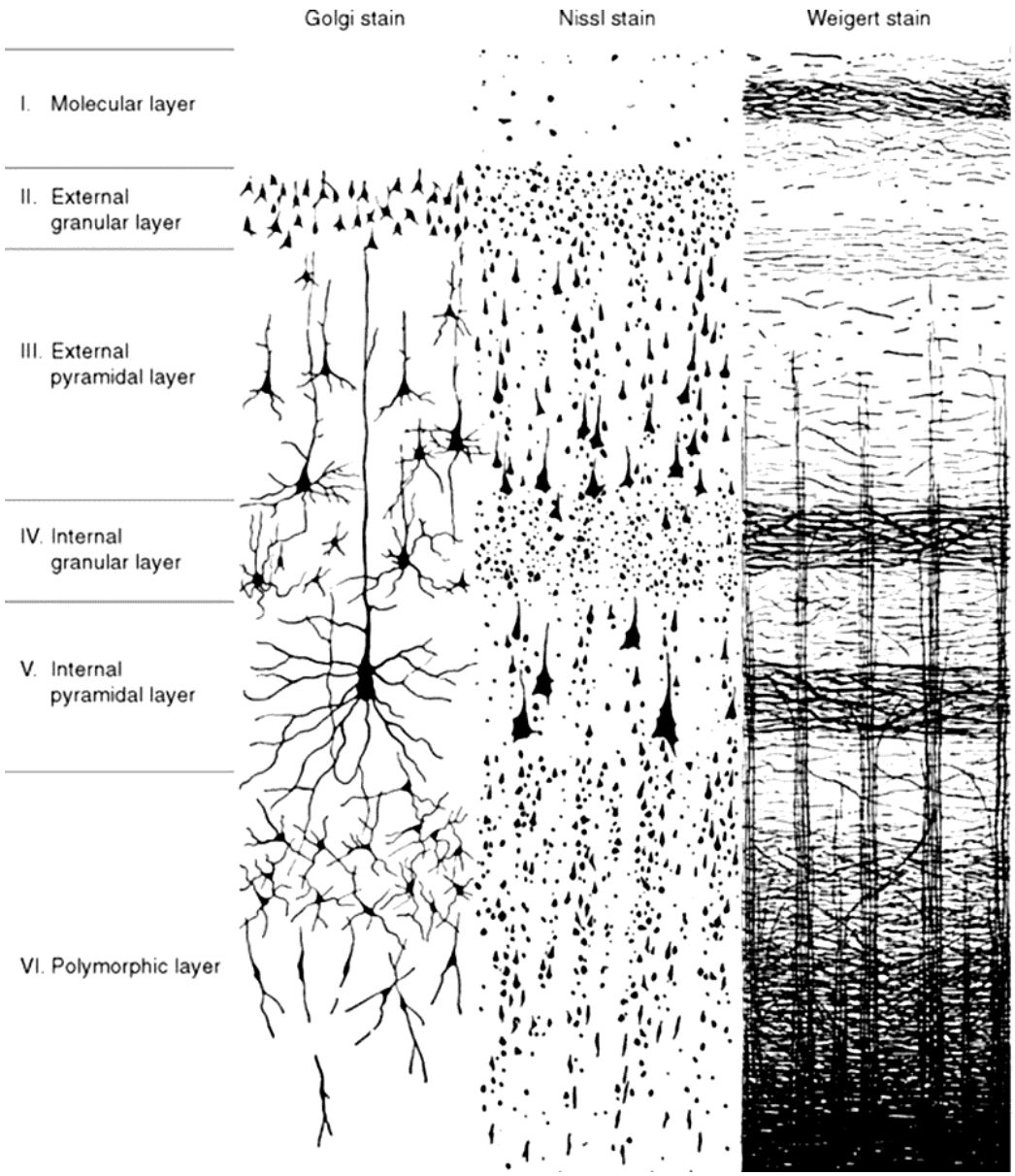

Figure 1.2 Cross-section of human neocortex stained by three different methods showing the typical six cortical layers. The Golgi stain completely staining a small number of cells, revealing the shapes of the arborization; the Nissl method stains the cell bodies of all neurons, revealing their shapes and packing densities (cytoarchitecture); the Weigert method stains myelin, revealing horizontally oriented bands and the vertically oriented bands of cortical afferents and efferents (myeloarchitecture) (Brodmann, 1909).

Smith examined sections of fresh brain with the naked eye and mapped out differences in thickness, texture and colouration (Smith, 1907), and thus identified four divisions of the cingulate cortex, which he called callosal areas (Figure 1.3B). Cecile and Oskar Vogt, created a cortical map based on regional differences in myeloarchitecture, in which over 200 areas were defined, including rostro-caudal and dorso-ventral divisions of the dACC (Figure 1.3C) (Vogt and Vogt, 1919). These maps suggest greater structural complexity within the cingulate cortex than appreciated by Brodmann.

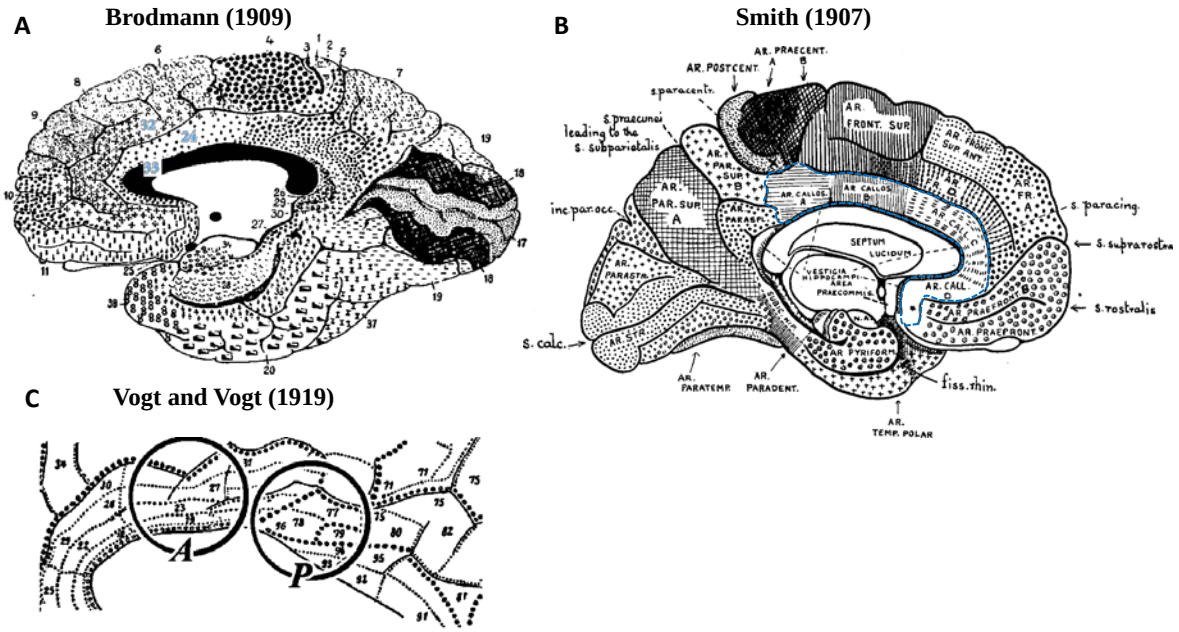

Figure 1.3 Regional maps of the cingulate cortex. A. Brodmann (1909) with areas included in the dACC highlighted in blue; B. Smith (1907) with the cingulate cortex bounded in blue; C. Vogt and Vogt (1919), taken from Vogt et al. 2003, showing anterior (A) and posterior (P) divisions of the dACC.

Despite the utility of architectural maps of the human brain, in order to meaningfully relate functional and structural insights from animal studies, in which invasive experiments can be carried out, to humans, cross-species homologies need to be determined. In this regard, Brodmann's maps offered the advantage over those of his contemporaries of including maps for multiple species carried out with the same methodology. However, Brodmann recognised that the same numbered areas in his cytoarchitectural maps of different species were not always homologous, particularly in the frontal lobe, as these were difficult to determine. This is specifically stated in reference to BA32 in human and monkey (guenon) which share the same number 32 due to the similarity in their anatomical locations (Brodmann, 1909). To resolve this issue and enable a better comparison of regions between species, various researchers have worked towards modifying and extending Brodmann's maps in non-human primate.

1.1.1.2 Cross-species homology with macaque

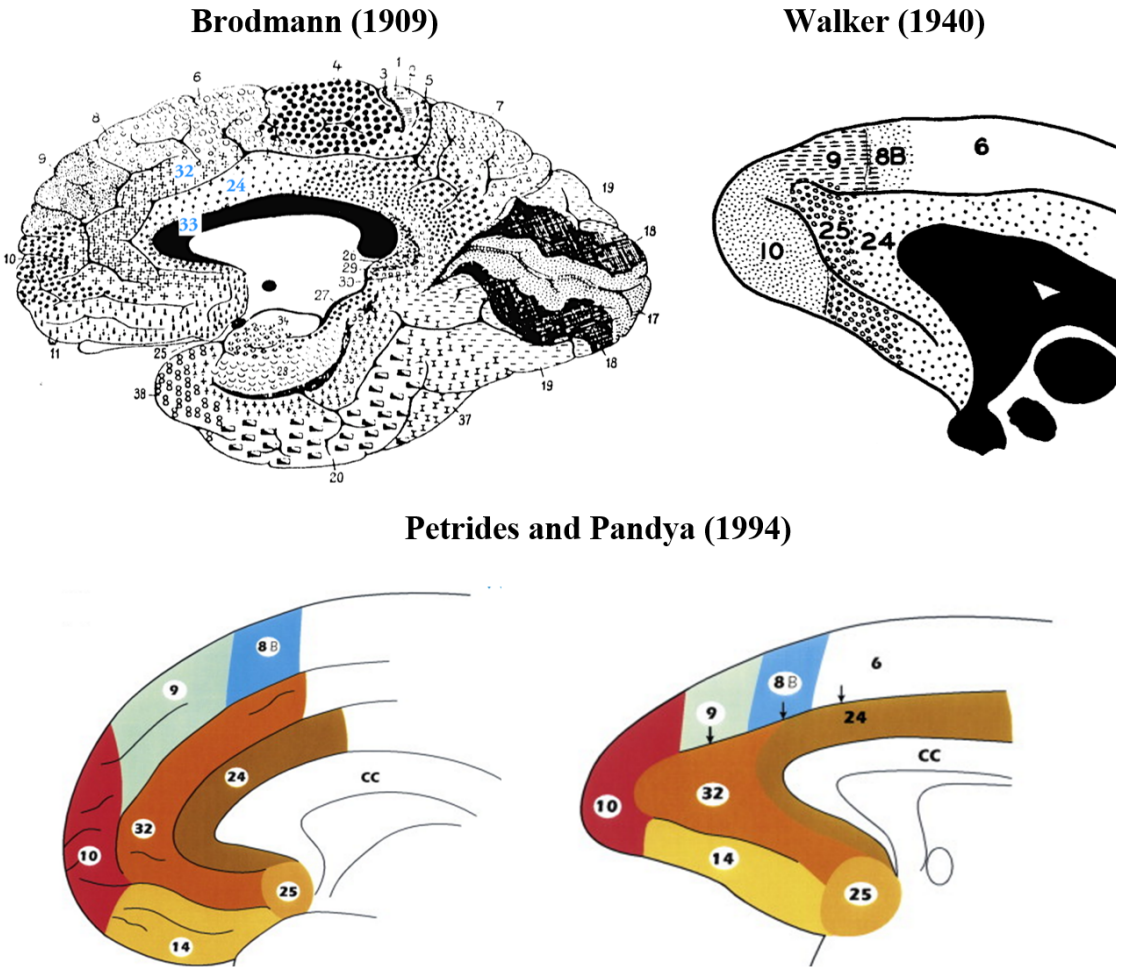

Figure 1.4 Cytoarchitectonic parcellation of medial wall of human brain. Adapted from Brodmann (1909), map of medial surface of macaque brain adapted from Walker (1940), comparative cytoarchitecture of human and macaque (Petrides and Pandya, 1994).

Walker produced a cytoarchitectural map of the rhesus macaque *(Macaca mulatta)* frontal cortex that was intended to align better with Brodmann's human map than Brodmann's existing macaque map (Walker, 1940). However, he compared the cytoarchitecture of the macaque frontal cortex to Brodmann's human map. Thus, there are some notable discrepancies; Walker's area 24 extends to the basal surface of the brain and is homologous with BA25, and he did not define an area 32 (Figure 1.4). Despite these inconsistencies, Walker's was the standard macaque map used for several decades. In 1994, Petrides and Pandya then produced maps based on a direct comparison between human and macaque cytoarchitecture, using the same experimental methods and criteria, to allow for experimental research from macaques to be meaningfully related to structural and functional findings in human arising from neuroimaging (Petrides and Pandya, 1994, 2002; Petrides et al., 2012). Accordingly, their human and macaque maps show a large degree of homology (Figure 1.4).

However, these cross-species maps just focus on cytoarchitecture. In order to create more detailed and reliable maps of the frontal lobe, several researchers have attempted to integrate findings from cytoarchitectural studies with those using other techniques to assess structure. Vogt et al. specifically studied the connectivity of the cingulate cortex alongside its cytoarchitecture in the macaque (Vogt, 1987; Vogt and Pandya, 1987). They divided area 24 into three regions along the ventrodorsal axis; 24a, located directly above the corpus callosum and which had the least laminar differentiation; 24b, which had better defined layers II and III; and 24c, ending at the ventral bank of the cingulate sulcus, which had a very dense layer III (Vogt, 1987) (Figure 1.5). These divisions were supported by differences in connectivity between area 24a and b compared to 24c such as projections to area 23 (Vogt and Pandya, 1987). In addition, although they found no strong cytoarchitectural basis to differentiate rostral and caudal dACC, analysis of connectivity provided evidence of differing afferent terminations. Tracer injections into the amygdala (lateral and accessory basal nuclei) and the rostral superior temporal gyrus strongly labelled the perigenual ACC and only the very rostral portion of the dACC (rostral area 24 and area 25), whilst injection into the inferior parietal cortex labelled only the caudal dACC and the PCC (caudal area 24 and area 23). Thus, these studies in macaque provide anatomical evidence for both dorso-ventral and rostro-caudal divisions of the cingulate cortex, similar to those described in the early maps in human (Figure 1.3).

Around the same time, Carmichael and Price noted that Walker's cytoarchitectonic regions were relatively large and did not fully reflect the structural diversity of the medial PFC (Carmichael and Price, 1994). To resolve this, they used multiple histological and immunohistochemical stains, including for Nissl and myelin, to further parcellate the orbital and medial PFC, including aspects of the ACC, in three species of macaque. They produced a map similar to Vogt's, with three subdivisions of area 24, with agreement in the 24a designation, however their areas 24b and c are larger and have slightly different boundaries.

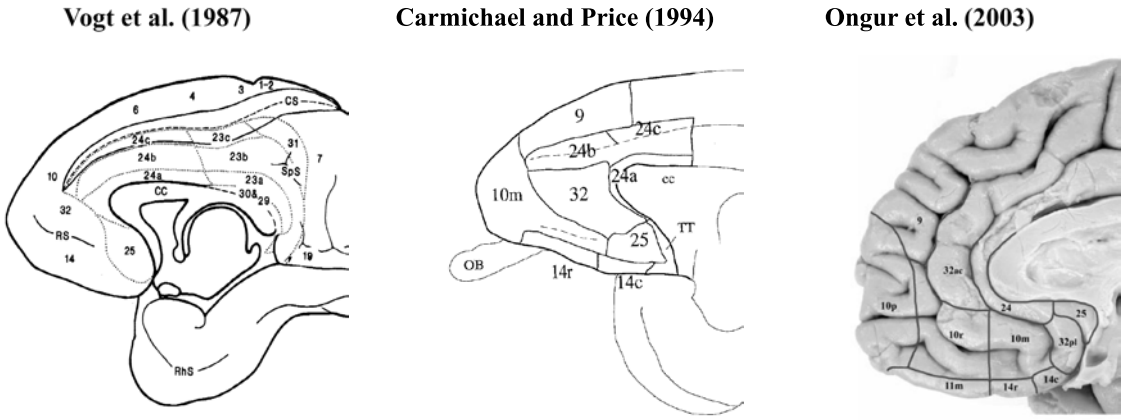

Figure 1.5 Architectonic maps of the medial wall in macaque. (Vogt et al 1987; Carmichael and Price 1994) and human (Ongur et al. 2003).

With the creation of more detailed maps of the macaque cerebral cortex but no corresponding development of the human map, the problem of not being able to carry out a direct comparison between human and macaque experimental findings arose yet again. Thus, Öngür et al. analysed the architecture of the human brain using similar staining techniques and criteria to those used by Carmichael and Price (Öngür et al., 2003), focussing on the ventromedial portion of the PFC (vmPFC). Of note, they labelled Brodmann's human area 32 as 32ac, in reference to its location in the anterior cingulate region, and labelled the region corresponding to Brodmann's monkey area 32 as 32pl, in reference to its prelimbic location. This map is commonly used alongside Carmichael and Price's macaque map to compare between human and monkey orbital and vmPFC (Wallis, 2012), but it omits parcellation of the dorsomedial surface in which the dACC is located.

1.1.1.3 Cross-species homology with common marmoset

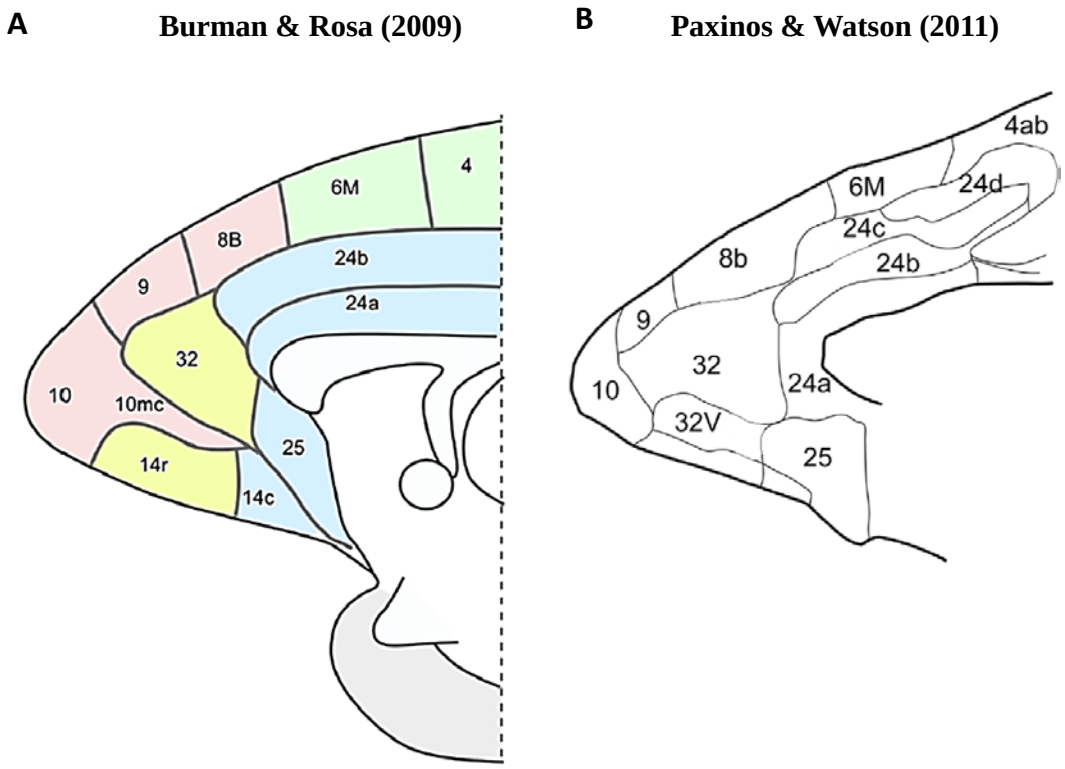

Figure 1.6 Cytoarchitectonic division of the medial frontal surface of the common marmoset. A. from Burman and Rosa (2009)(yellow, dysgranular cortex; blue, agranular cortex; pink, granular cortex; green, motor and premotor areas). B. Figure adapted from Reser et al. (2016) based on 3D reconstruction of medial cortical surface of marmoset brain presented in Paxinos and Watson (2011) atlas.

Being the closest evolutionary relative of humans commonly used in invasive research, researchers have focussed on creating comparative maps for the macaques, however the common marmoset (*Callithrix Jacchus*), a small-bodied, new world primate, is an experimental species that has become increasingly popular in behavioural neuroscience (Prins et al., 2017), consequently an architectonic map has been produced for the marmoset frontal lobe (Burman and Rosa, 2009). Divisions are, based on regional differences in cytoarchitecture and myeloarchitecture (Figure 1.6A). The marmoset area 24 maps onto Brodmann's human area 24 well, and as in humans, it is agranular. Area 24 was originally subdivided in two along the ventrodorsal axis, due to the presence of larger cells in layer V in 24a, and denser myelin staining in deeper layers compared to the more dorsal 24b (Burman and Rosa, 2009). However, in creating a stereotaxic atlas of the marmoset brain, using more extensive criteria four ventrodorsal divisions of area 24 were identified (24a-d) (Paxinos et al., 2011). Area 24d appears more caudally and shows transitional cingulate and premotor cortical characteristics (Figure 1.6B). A clearly distinguishing feature of the marmoset brain compared to macaque and human is its smooth surface. The lissencephalic marmoset cortex offers a

practical advantage over macaques, as regions which in the latter may be buried in sulci, the cingulate sulcus in the case of the dACC, are more accessible. Also, no rostro-caudal divisions have yet been identified on the basis of anatomical structure in the marmoset.

1.1.1.4 Cross-species homology with rat

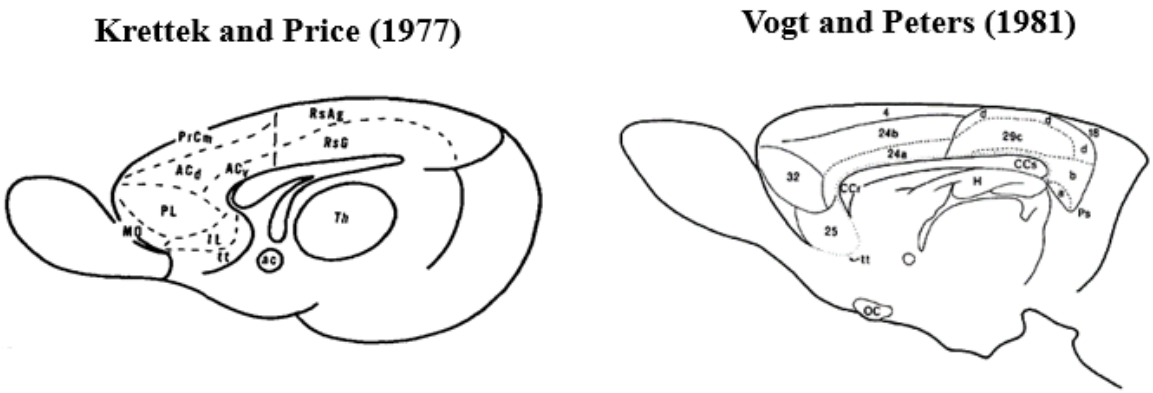

Figure 1.7 Architectonic map of rat brain. Figures from Krettek and Price (1977) and Vogt and Peters (1981).

Although cortical homologies between human and non-human primate bear much greater resemblance than to rodents, the latter are the most commonly used species in basic neuroscience and provide a foundation for much translational research. Thus it is important to determine cortical homology between rodents and higher species (Vogt et al., 2013). Although some have suggested a criterion for identifying PFC regions, based on their projections from the mediodorsal nucleus of the thalamus (Rose and Woolsey, 1948), others note that the rat prefrontal cortex is completely agranular, distinguishing it from primates, and thus question whether it has a comparable PFC (Uylings et al., 2003). Krettek and Price used this criterion, along with cytoarchitecture, to create a map of the frontal pole of the rat (Figure 1.7) (Krettek and Price, 1977). They identified four major subregions in the anterior medial surface; the infralimbic area (IL), prelimbic area (PL) , anterior cingulate area (AC) and medial precentral area (PrC). The naming of these regions was based on how similar they were to regions described by either Brodmann or Rose and Woolsey in other species (Brodmann, 1909; Rose and Woolsey, 1948). The rat anterior cingulate area, which can be divided further into a dorsal and ventral region (ACd, ACv; also referred to as Cg1 and Cg2), was stated to correspond to BA24.Vogt's and Peter's initial cytoarchitectural analysis, described broadly similar regions but using Brodmann's nomenclature, designating the ACd and ACv as 24b and 24a respectively (Vogt and Peters, 1981). Despite their support for the use of Brodmann's nomenclature in line with that most commonly used for primates, the use

of PL, IL and AC/Cg are more widespread in the rodent literature. Controversy exists as to whether the rat AC is functionally homologous to the primate ACC, or despite its lack of granularity in rats, the dorsolateral PFC (dlPFC), or some combination of the two (Öngür and Price, 2000; Seamans et al., 2008; Uylings et al., 2003).

1.1.2 Functional parcellation of the cingulate cortex

Functional neuroimaging studies enable for changes in brain activity to be localised and correlated with behaviour. However, there is uncertainty in this localisation due to individual differences in brain anatomy (Brett et al., 2002). Particularly relevant to the study of the cingulate cortex are individual differences in rostral cingulate anatomy, specifically the presence or absence of a paracingulate sulcus, which impacts the layout and relative volume of proposed architectonic areas (Shackman et al., 2011). In addition, although the spatial resolution for neuroimaging techniques such as functional magnetic resonance imaging (fMRI) is high (millimetre range), for meaningful interpretation of neuroimaging data across subjects and comparison to other research, images must be mapped onto normalised anatomical templates such those provided by the Montreal Neurological Institute (MNI) or Talairach and Tournoux (Talairach and Tournoux, 1988). In the latter, brains are aligned to the anterior commissure and posterior commissure, and then scaled on to a grid. As a result, imaging foci do not have clearly demarcated boundaries that occur within precise anatomical or cytoarchitectural regions but are more probabilistic.

Another important point is that, although Brodmann areas are widely used in reference to imaging foci, these labels are derived from Talairach and Tournoux's map in which the authors note, *"the brain presented here was not subjected to histological studies and the transfer of the cartography of Brodmann usually pictured in two dimensional projections sometimes possesses uncertainties."* Thus, these should only be taken as approximations.

The complexity involved in localising function based on neuroimaging data was recently discussed (Shackman, 2015) specifically in relation to the dACC, in response to the controversy surrounding the claim that based on reverse inference of fMRI studies, that the dACC is primarily involved in pain (#cingulategate) (Lieberman and Eisenberger, 2015). It is argued that due to the authors failure to use probabilistic templates that inherently account for the issues described above (individual variation in anatomy and normalisation error) their conclusion is invalid (Shackman, 2015).

Thus, the most appropriate method of parcellating the cingulate cortex must take into account anatomical, cytoarchitectural and functional findings in an integrated manner.

1.1.3 A neurobiological model of the cingulate cortex

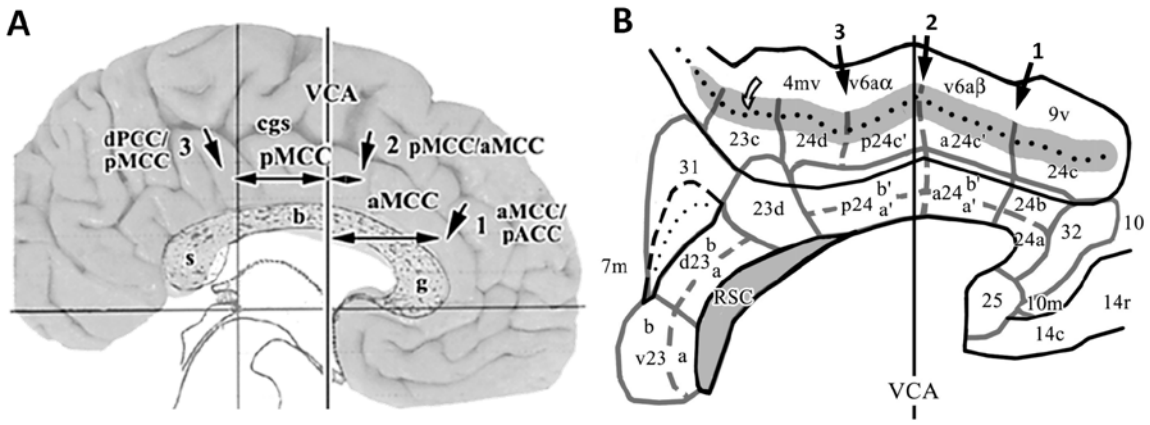

Figure 1.8 Parcellation of the human and macaque ACC by Vogt and colleagues according to cytological differences. ***A****. medial surface of human brain showing cytological borders (numbered and labelled arrows) and regional designations (pACC, perigenual ACC; aMCC, anterior midcingulate cortex; pMCC, posterior midcingulate cortex; dPCC, dorsal PCC; cgs, cingulate sulcus; g,b,s, genu body and splenium of cingulate cortex; VCA, vertical line through the anterior commissure. Figure from Vogt et al., 2003.* ***B*** *Flattened reconstruction of the medial surface of the macaque brain. Cytoarchitectural regions and subdivisions are labelled and bounded with solid and dashed grey lines respectively. The cingulate sulcus is shaded in grey. Numbered red arrows show cytological borders. Figure adapted from Vogt et al. 2005.*

Towards the end of the 20th century, a number of functional findings in humans and macaques relating to the cingulate cortex had emerged. Based on these, as well as the previously described differences in connectivity with the parietal cortex and amygdala in macaque (Vogt and Pandya, 1987), area 24 was divided into rostral area 24 which was included in the "affect" division of the ACC, a region involved in autonomic regulation (Kaada, 1951), and caudal 24' which was included in the "cognition" division of the ACC, a region not involved in emotion but in skeletomotor activity (Devinsky et al., 1995). This broadly corresponds to the pgACC/dACC division. Further assessment of the cingulate cortex has emphasised this distinction and led to Vogt's four-region neurobiological model of the cingulate cortex, consisting of the anterior cingulate, midcingulate, posterior cingulate, and retrosplenial cortices (ACC, MCC, PCC, and RSC, respectively). In this, the midcingulate cortex (MCC) is introduced as a structurally and functionally distinct entity located between the ACC and PCC (Vogt, 2009, 2016; Vogt et al., 2003). Rather than just being a transition zone, it is argued that there is no quantitative progression of structure and function between these areas making the MCC a unique area. However, the affect/cognition functional divide was refuted, and instead a functional distinction between noxious cutaneous thermal stimulation activating the MCC, but not the pgACC, was established (Vogt et al., 2003). The MCC has been further divided into anterior and posterior subregions (aMCC and pMCC) (Figure 1.8A), with this division supported by differences in neuron density in layers Va and Vb, and functional imaging differences revealing relatively greater fear-related activity in the aMCC compared to the

pMCC (Vogt et al., 2003). However, it must be borne in mind that the functional imaging findings are correlational and do not necessarily indicate causal roles. More recently, a study of multi-receptor architecture found that regional borders between the distribution patterns of multiple neurotransmitter receptors matched Vogt's model (Palomero-Gallagher et al., 2009). This latter study also supported further division of area 24c across the dorsal and ventral sulcus.

Similar, putatively homologous regional distinctions have been identified in non-human primates (Figure 1.8B). Structural differences in parvalbumin immunoreactivity in macaques and cynomolgus monkeys, differentiate area 24 (pgACC) from area 24' (MCC), which has a higher layer Va activity and further reveal a more diffuse layer Va in posterior 24' (pMCC) than anterior 24' (aMCC) (Vogt et al., 2005). Analysis of striatal projections from the cingulate cortex in macaque also found rostro-caudal divisions in the cingulate cortex, although the boundaries differ slight to Vogt's designations (Figure 1.10B) (Heilbronner et al., 2016). In addition, this distinction is supported by anatomical and electrophysiological studies, dividing the cingulate motor areas in the vicinity of the cingulate sulcus in macaques into three separate motor areas (CMAs); the rostral cingulate motor area (CMAr) and the caudal cingulate motor areas, in the ventral bank of the sulcus (CMAv), and in the dorsal bank of the sulcus (CMAd) (Picard and Strick, 1996). The CMAr is distinguished from the CMAv and CMAd based on its relatively weak influence on motor activity as determined by electrical stimulation (Luppino et al., 1991). Functional imaging data in humans resulted similarly in the identification of three motor areas which have provisionally been associated with CMAs; the anterior rostral cingulate zone (RCZa) with the CMAr; the posterior rostral cingulate zone (RCZp) with the CMAv; and the caudal cingulate zone (CCZ) with the CMAd (Figure 1.9) (Picard and Strick, 2001). These are proposed to have different functions with the RCZa thought to be involved in conflict monitoring, the RCZp in response selection and the CCZ in movement execution (Picard and Strick, 2001). However, it should be noted that in macaques, motor areas in the cingulate sulcus are distinct from the cingulate gyrus (Dum and Strick, 1993), whilst in humans due to limitations in spatial resolution in imaging studies, such distinction is ambiguous. The RCZ lies in Vogt's aMCC and the CCZ largely in the pMCC.

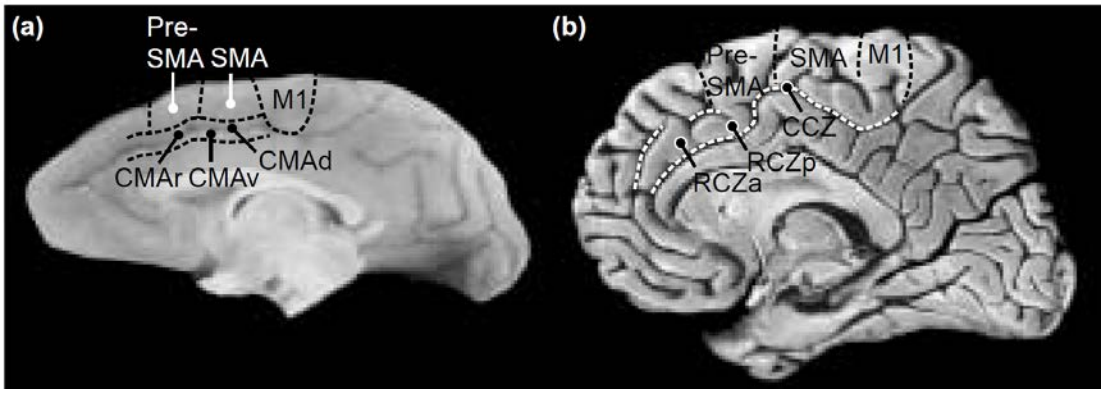

Figure 1.9 Motor areas of the frontal lobe in macaque (a), with putative homologous areas in human (b). Figure from Picard and Strick (2001).

The ACC and MCC have also been structurally differentiated, by neuronal size in all layers, in rats and these are suggested homologues of these regions in non-human primate and human (Figure 1.10A) (Vogt and Paxinos, 2014). However, a comparison between rat and primate cingulate connections with the striatum, found no rostro-caudal differences in Cg terminations, although these were present in primate (Figure 1.10B (Heilbronner et al., 2016), indicating important differences across species and the need for caution when relating findings from cingulate regions in rat to humans. Of the primate cingulate subregions, Cg terminations showed greatest similarity to caudal area 24 (pMCC) (Figure 1.10Bii). On the basis of function in behavioural studies, the PL has been proposed to be homologous to the aMCC in humans as these regions are both thought to be involved in fear expression (Milad and Quirk, 2012). However, similar behavioural outputs could reflect different neural bases, thus suggestion of functional homology on its own should be taken with caution.

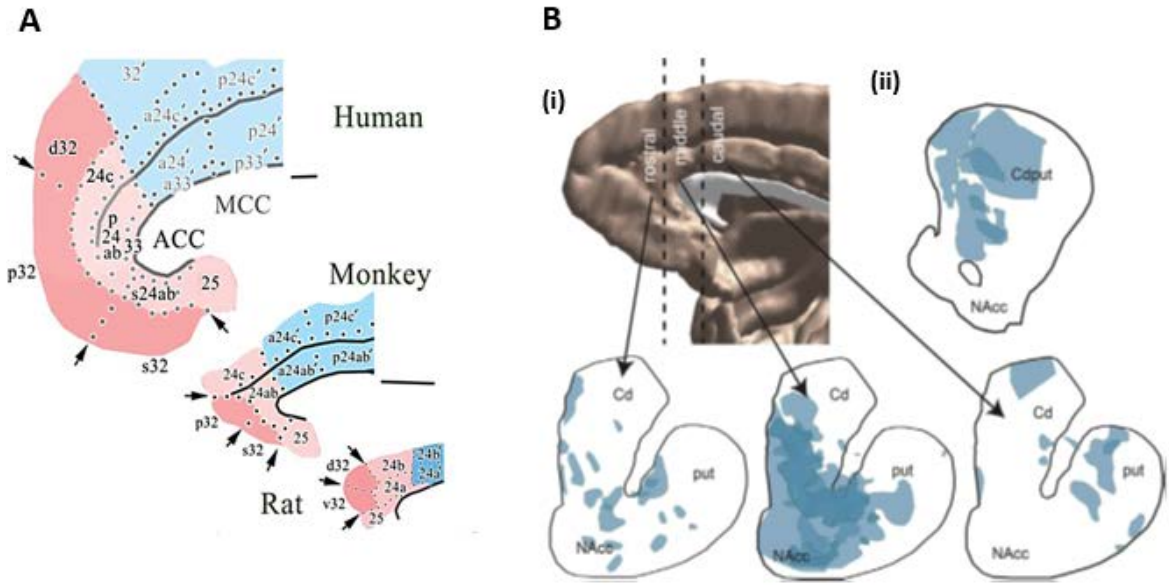

Figure 1.10 Medial surface of frontal lobe in human, macaque, rat showing ACC and MCC homology (colour coding and arrows)(A). Figure modified from Vogt et al. 2013. B. Medial surface of frontal lobe in showing divisions of the cingulate cortex and striatal projection patterns in macaque (i) and striatal projection pattern in rat (ii). Figure modified from Heilbronner et al. 2016.

1.1.4 Nomenclature of ACC subregions

Based largely on Brodmann's designation of area 24 (Brodmann, 1909), the ACC has long been referred to as if it were a homogeneous region in terms of structure and function, although in some cases regions of interest widely differ within it (Vogt, 2016). The region of interest in this thesis is commonly referred to as the dACC based on spatial location (Figure 1.1), with the anterior half referred to as the rostral dACC (rdACC) and the posterior half the caudal dACC (cdACC). However, recent integrated neurobiological analyses of cytoarchitecture, connectivity and function in humans and macaques, indicate the existence of structurally distinct subregions along the rostro-caudal axis in the ACC extending from the genu of the corpus callosum to the granular PCC. In this neurobiologically based model of the ACC (Vogt and Paxinos, 2014; Vogt and Vogt, 2003; Vogt et al., 2003), the region referred to as the dACC on the basis of spatial location is identified as a distinct entity from the ACC, and thus is named the MCC, to emphasise this distinction. The MCC is further divided into anterior and posterior subregions designated as the aMCC and pMCC. This nomenclature more effectively describes parcellation of the cingulate cortex, as it is based on structural and functional characteristics and thus where possible will be adopted in this thesis when describing functional findings in human and macaque. However, in some instances ROIs do not directly map on to the pgACC, aMCC or pMCC, crossing these subregional boundaries.

Thus, in these cases spatial designations will be used including mid-dACC (mdACC) in reference to the middle third of the dACC, and rostral ACC (rACC) in reference to the rdACC and pgACC together.

1.2 The role of the dACC in negative emotion

The dACC has long been implicated in emotion and its dysregulation in disorders of negative emotion, however its precise role remains elusive. Before reviewing the specific contribution of the dACC to emotion, it is useful to first address key concepts relevant to the study of emotion.

1.2.1 What is emotion?

Despite being so integral to the human experience, it is difficult to accurately and scientifically define emotion due to its heterogeneous and multifaceted nature. It is generally accepted that emotions consist of conscious subjective experiences, physiological responses, and behavioural responses. However, opinion is divided as to which of these components cause emotion and which result from it.

In the pioneering work of Charles Darwin in "*The Expression of the Emotions in Man and Animals*" published in 1872, emotions are described as "states of mind". Based on similarities in the facial expressions of emotions in humans around the world, and across species, he proposed that certain emotions are innate and evolutionarily conserved due to their adaptive value. That is, they protect the organism or prepare it for action, with additional important communicative roles, and this improves survival. A century later, Paul Ekman built on Darwin's proposal of universal facial expressions, describing six basic emotions; happiness, sadness, fear, surprise, anger, and disgust, that were recognised and held the same meaning across cultures, including preliterate cultures (Ekman et al., 1969). This evolutionary theory of emotion forms a conceptual basis from which to study emotion in animals to gain insight into emotion in humans. Furthermore – the theory that certain emotions evolved to solve adaptive problems is one that has been refined and persists today. For example, the contemporary neuroscientist, Edmund Rolls, has defined emotions as *"states elicited by rewards and punishers"* (Rolls, 2005), emphasising the role of positive emotions in promoting approach behaviours, and negative emotions in promoting avoidance behaviours.

Shortly after Darwin's publication, describing the facial expression of emotions, William James and Carl Lange independently developed similar theories on how we experience emotion (1884). The James-Lange theory proposed that the conscious experience of emotion follows the peripheral bodily response to an emotive stimulus and further, that each emotion has its own physiological profile. For example, the sight of a snake causes an increase in heart rate, sweaty palms and other physiological reactions which are then interpreted by the brain to generate the conscious experience of fear. The view that "feelings are mental experiences of

bodily state (Damasio and Carvalho, 2013) and similar (Craig, 2009) are prominent among some scholars today.

The classification of emotion into discrete basic units, argues that distinct emotions are subserved by distinct neural processes. There is evidence that shows some emotions can indeed be distinguished based on autonomic activity, can be induced artificially (Ekman et al., 1983) and even have distinct neural signatures (Kassam et al., 2013) but the latter is strongly contested (Lindquist et al., 2012). This modular approach is countered by a dimensional approach that posits that all emotions arise from two common neurophysiological systems to varying degrees; one for valence (positive/negative) and one for arousal (Posner et al., 2005). The latter allows for overlap between emotions and can describe a wider range of emotions. Both discrete and dimensional approaches are useful for the study of emotion, as each can be relevant to different aspects of emotion (Ekman, 2016)

Finally, a recent theory places conscious subjective experience at the forefront of emotion (LeDoux and Brown, 2017). According to this view, although behavioural and physiological responses contribute to emotion, and the circuits underlying these are conserved, they are at most indirect markers of the subjective experience. Thus, the only way to directly assess emotion is through verbal self-report. It is proposed, that emotion terms such as “fear” and “anxiety” should only be used to describe the subjective experience whilst behavioural and physiological responses to emotion, should be referred to as “defensive behaviours” and “defensive physiological adjustments” respectively (LeDoux and Pine, 2016). This is because use of the same emotion term apparently implies that these distinct components involve a common circuit. However, in the field of behavioural neuroscience, use of emotion terms to refer to these different components is generally understood and thus will be used with appropriate context in this thesis.

1.2.2 Neural correlates of emotion

Cannon's and Bard's lesions in cats were the earliest experiments aimed at determining the neural correlates of emotion and were the first to study emotion using experimental animals (Cannon, 1927). They contested the James-Lange theory and instead proposed that physiological arousal and generation of emotion occurred at the same time. To substantiate their theory, they studied the behaviour of cats following surgical removal of the neocortex. This resulted in an excessive anger response to innocuous stimuli, an emotional display that was dubbed "sham rage" on the basis that animals were not believed to have a conscious awareness of rage. It was asserted that this disproved the James-Lange theory, as emotion could clearly be expressed in subjects that had no sensory or motor cortices with which to detect physiological arousal. Building on this, they found that if the hypothalamus remained intact "sham rage" was diminished and thus argued that release of the hypothalamus from inhibition by the neocortex was necessary for the "uncontrolled" expression of emotion (Bard, 1934).

In 1937, an alternate influential neurobiological theory of emotion was proposed by James Papez, this time centred on the cingulate cortex (Papez, 1937). Papez wrote:

> *"The cortex of the cingular gyrus may be looked on as the receptive organ for the experiencing of emotion as the result of impulses coming from the hypothalamic region."*

Papez proposed a circuit for emotion, now known as the Papez circuit, by synthesising what was known of the anatomy of the brain with experimental and clinical findings at the time (Figure 1.11). Cases of rabies virus infecting the hippocampus, were associated with emotional changes and thus the hippocampus was given prominence in the Papez circuit, which was further characterised by monitoring the brain progression of rabies virus injected into a cat's hippocampus. Although the cingulate cortex was not yet well-studied, there were clinical reports in which tumours of the corpus callosum resulted in emotional changes such as states of depression and "loss of spontaneity in emotion." The Papez circuit originated with sensory information entering the thalamus that then separated into two streams. The "stream of thought" continued "upstream" to the lateral cortex to generate thought, perception, and memories while the "stream of feeling" continued "downstream" to the mammillary bodies of the hypothalamus to generate the bodily response to emotion. Crucially, within this circuit, the cingulate cortex was placed to integrate information from the sensory cortices with information from the hypothalamus, to generate the experience of emotion. Furthermore top-

down regulation of emotion could occur via downstream projections from the cingulate to the hypothalamus via the hippocampus. Many, though not all, of the regions that form the Papez circuit, including part of the cingulate cortex, are still recognised as key nodes in the circuitry of emotion. However, a key region was missing – the amygdala.

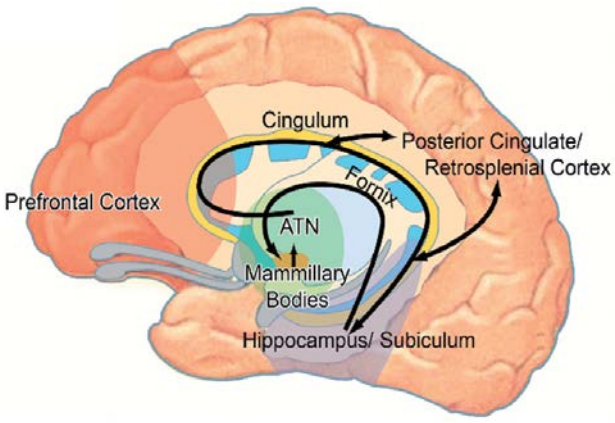

Figure 1.11 Schematic of Papez circuit (shown in black). ATN, anterior thalamic nuclei. Figure from Aggleton et al. 2016.

The amygdala was implicated in emotion two years later when Klüver and Bucy published their observations of behavioural changes in rhesus monkeys following bilateral lesions of the temporal lobe. These included emotional blunting, such as lack of fear to a snake, among other changes such as hypersexuality and tameness. It was later shown that specific bilateral lesions of the amygdala, the almond-shaped region located within the temporal lobe, were sufficient to diminish fear (Weiskrantz, 1956). These findings were incorporated alongside Papez theory of emotion and Darwin's evolutionary theory of emotion by Paul Maclean.

In what Maclean called the triune brain, he proposed that the brain consisted of three distinct but interconnected brain systems that were sequentially added as layers across evolution (MacLean, 1990). These were the "reptilian brain", consisting of the striatum and basal ganglia, involved in basic autonomic function and primitive emotions such as aggression; the "visceral brain", consisting of a group of structures in Broca's limbic lobe, including a number of those in Papez circuit i.e. cingulate cortex, thalamus, hypothalamus, hippocampus in addition to the amygdala and septum, with a collective role in emotion; and finally the "paleomammalian brain" consisting of the neocortex, responsible for higher cognitive functions. Maclean's triune brain concept has come under much criticism and its theory of layered brain evolution has largely been disproved (Smith, 2010). The notion of a brain system exclusively for emotion, the visceral brain, later renamed the limbic system or sometimes the Papez-Maclean circuit, has questionable empirical validity as limbic structures

do not necessarily work concertedly as an emotion system and furthermore many limbic structures have been implicated in functions besides emotion (Kötter and Meyer, 1992; LeDoux and Brown, 2017). However, the term “limbic” is useful as a general term to refer to structures that are involved in emotion, and limbic system to refer to the neural circuitry involved in emotion. As our knowledge of this has increased, various structures have been added and removed from Maclean’s original model, however the dACC is one region that has remained limbic.

1.2.3 Emotion dysregulation

Emotions serve an adaptive role, for example fear alerts us to danger and motivates appropriate behavioural responses. However, emotions can be dysregulated when they occur out of context or unpredictably, or are exaggerated or prolonged, and this impairs our ability to control behaviour effectively. Emotion regulation describes the monitoring, evaluation and modifying of behavioural responses that is necessary for adaptive goal-directed behaviour (Gross, 1998; Thompson, 1994). This can include conscious processes e.g. distraction, reappraisal, and non-conscious automatic processes. Impairments in emotion and emotion regulation i.e. emotion dysregulation are common to many psychiatric disorders (Gross and Jazaieri, 2014). Much of what we know about the dACC in relation to emotion, is in fact garnered from studying the dACC in dysregulated emotion.

Historically, the first indication that the dACC might causally be involved in psychiatric disorders came from the outcomes of anterior cingulotomy, carried out on mentally ill patients in the 1960s. In humans, although it is rare for lesions to arise naturally in specific circumscribed regions, for the study of the dACC, lesions in the form of anterior cingulotomy give us a unique insight into the causal function of this region, with the key caveat that fibres of passage, including those in the cingulum that project to other cingulate regions and subcortical structures are also damaged.

Anterior cingulotomy was developed as a refinement of lobotomy, the destruction of portions of the frontal lobe, which was carried out extensively in the 1950s in the US, to “cure” a range of psychiatric disorders including schizophrenia, depression, chronic pain, and anxiety disorders for which there were no treatments at the time. The rationale behind lobotomy was to sever the connections between the prefrontal cortex and the rest of the brain, and thus prevent the spread of abnormal activity thought to be responsible for psychiatric symptoms. This was reportedly extrapolated from a single study of performance in a cognitive task in two chimpanzees, Becky and Lucy, before and after bilateral frontal lobe ablation. Following the

lesion neither animal was able to perform the task, and in addition Becky in particular, showed a marked emotional change. Before she would respond with violence and anger after an incorrect choice and non-reward but now she was calm (Fulton and Jacobsen, 1935). Based on this study Antonio Egas Moniz carried out the first lobotomies in humans which he declared successful (Moniz, 1937). However, it was the American doctor, Walter Freeman, who really championed the technique and was responsible for its widespread use to treat thousands of patients with mental illness. However, his surgical procedure was crude, performed without visualising the brain region being damaged; an instrument was inserted into the brain, either through burr holes in the side of the head or through the orbits, and moved around to destroy the tissue. He was criticised as reckless due to his disregard of usual medical practices of sterility and his showmanship. Some patients died of haemorrhage or had fatal seizures following surgery. Those that survived showed mixed results, with some patients displaying marked and lasting improvement of symptoms, and some no change (Barahal, 1958). A disturbing effect of lobotomy, although welcomed by some as it made patients "more manageable," was the apathetic, inert, and emotionless state patients were left in.

The more focussed surgical procedure of anterior cingulotomy was first carried out in 1948 with the hope that it would be a more anatomically precise and effective method of treating mental illness than lobotomy (Whitty et al., 1952). This was based on animal experiments, limited clinical data, and Papez theory implicating the ACC in emotion. A bone flap was created to visualise the underlying brain, and the region corresponding to Vogt's aMCC, was removed bilaterally by suction. The authors of this first study concluded that the surgery *"produced definite though sometimes transient changes in the mental symptoms of almost all our patients."* Despite a marked decline in the popularity of psychosurgery due to rising criticism and more importantly the discovery in 1950 of the first psychiatric drug, chlorpromazine, anterior cingulotomy continued to be refined and remains in use. Nowadays anterior cingulotomy is guided by MRI and is stereotactically guided, making it much more precise. It is however reserved as a last resort for severe, intractable cases of certain conditions; chronic pain, depression and OCD – all disorders involving negative emotion (Steele et al., 2008; Wendy et al., 1996; Wilkinson et al., 1999).

A wealth of data from anterior cingulotomy studies suggest that the dACC (specifically the aMCC) is dysregulated in disorders of negative emotion. Indeed, it has been demonstrated that sufferers of depression and anxiety disorders had the best outcomes compared to other disorders after this procedure (Ballantine et al., 1987). However, the mechanism by which

anterior cingulotomy causes clinical benefit remains elusive. Thus, these findings need to be integrated with those from structural and functional studies of the dACC in depression, anxiety, and negative affect in humans and (the latter) in experimental animals. Before doing so it is necessary to review our current knowledge of the neurobiology underlying disorders of negative emotion.

1.2.4 Disorders of negative emotion

Major depressive disorder (MDD) or depression, is a mood disorder characterised by low mood or loss of interest or pleasure (anhedonia). It is extremely common, affecting over 300 million people globally (World Health Organization, 2017) and is an episodic illness in which recurrence of depressive episodes is common (Burcusa and Iacono, 2007). Furthermore, depression carries a significant disease burden – it was the leading cause of disability worldwide (measured as years lost due to disability; 2015 figures), and carries a strong risk for suicide (Hawton et al., 2013). At present, the most common treatments for depression are selective serotonin reuptake inhibitors (SSRIs) and cognitive behavioural therapy (CBT). However, up to a third of patients fail to respond to multiple therapeutic interventions and thus display treatment-resistant depression or experience residual symptoms (Rush et al., 2006), highlighting the urgent need for better treatment options.

Anxiety disorders are also extremely common- they are the most prevalent class of mental disorder worldwide (Kessler et al., 2009). They often have an early onset and a chronic, recurring course and thus can cause a significant burden and impairment of function (Baxter et al., 2014; Kessler et al., 2005a). Anxiety and depression are highly comorbid, with up to 90% of patients with anxiety disorder experiencing clinical depression in their lifetime (Gorman, 1996) suggesting overlapping aetiology (Kessler et al., 2005b). Treatment of anxiety disorders is largely similar to that of depression, with SSRIs and CBT at the forefront, although drugs targeting the GABAergic system are also used. Different treatments are recommended for certain disorders such as pregabalin, which acts to increase extracellular GABA, for generalised anxiety disorder (GAD), rapid-acting benzodiazepines for panic attacks and exposure therapy for specific phobia (Bandelow et al., 2012).

1.2.4.1 Diagnosis and classification

5 of 9 symptoms, present during the same two-week period (including at least one of depressed mood or loss of interest or pleasure) and representative of a change from previous functioning:

- Depressed mood
- Diminished interest/pleasure in all or almost all activities
- Worthlessness or guilt
- Poor concentration, indecisiveness
- Thoughts of death, suicidal ideation
- Appetite/weight changes
- Sleep disturbances; insomnia or hypersomnia
- Changes in psychomotor activity; agitation or retardation
- Fatigue or loss of energy

Box 1-1 Diagnostic criteria for major depressive disorder (adapted from DSM-V).

There are no reliable diagnostic biomarkers for depression or anxiety. Clinical diagnosis of these and other neuropsychiatric disorders, occurs on the basis of symptom presentation according to standard criteria designated by the Diagnostic and Statistical Manual of Mental Disorders (DSM) or alternatively the International Classification of Diseases (ICD). Thus, clinicians largely rely on self-report of symptoms with the use of screening and diagnostic tools such as the Beck Depression Inventory and the Hamilton Depression Rating Scale.

Depression is characterised by a major depressive episode, which, according to DSM-V, requires at least one core symptom of low mood/anhedonia along with other cognitive and somatic symptoms (Box 1-1). Although major depressive episodes are also a common feature of bipolar disorder i.e. bipolar depression (American Psychiatric Association, 2013), occurrence of a manic episode is essential for diagnosis of this disorder.

Anxiety disorders are characterised by excessive fear or chronic anxiety and associated physiological responses. They encompass a number of disorders that are diagnostically differentiated according to the type of situation that causes a maladaptive response (American Psychiatric Association, 2013) (Box 1-2). For example, phobic disorders involve persistent excessive fear responses or avoidance of a specific external object or situation e.g. heights (specific phobia), social situations which may involve negative judgement (social anxiety disorder; SAD) and situations in which escape may be difficult (agoraphobia). In contrast, GAD involves excessive anxiety and worry about numerous concerns. Anxiety disorders can also be distinguished according to the type of response they elicit, such as panic disorder,

which is characterised by recurrent unexpected panic attacks, abrupt surges of intense fear with no obvious trigger.

However, there is significant overlap in symptom criteria between depression and anxiety (Ressler and Mayberg, 2007). In addition, these disorders are heterogeneous and may manifest in different ways. This is typified by the 636,120 possible symptom combinations that can lead to a diagnosis of post-traumatic stress disorder (PTSD) (Galatzer-Levy and Bryant, 2013). Thus, one diagnostic category can include a number of distinct symptoms, each caused by distinct biological mechanisms, which in turn can cross diagnostic boundaries. In addition, recent changes in DSM classifications made in DSM-V released in 2013 have been controversial. Notably, obsessive-compulsive disorder (OCD) was reclassified under the distinct category of obsessive-compulsive related disorders rather than under anxiety disorders. In a similar vein, PTSD was reclassified under the category of trauma and stressor-related disorders due it being triggered by exposure to an identifiable traumatic event. However, the neurobiological evidence supporting removal of OCD and PTSD from the anxiety disorder category is strongly contested (Radua et al., 2010; Zoellner et al., 2011).

The focus on a symptom-based approach to diagnosis of neuropsychiatric disorders favoured by DSM-V, has been accused of hampering research and the development of treatments targeting underlying pathophysiological mechanisms (Insel et al., 2010). The Research Domain Criteria (RDoC), a framework for research into neuropsychiatric disorders, was developed as an alternative to allow better translation of research findings to clinical diagnosis (Insel et al., 2010). It integrates behavioural and neurobiological measures into dimensional constructs under five different functional domains relevant to psychiatric disorders. Thus, the focus is shifted away from indistinct overlapping diagnoses towards defined neurobiological functions. This is hoped to lead to exploration of different potential pathophysiological mechanisms of psychiatric disorders at various levels of analysis from genetic to circuit-based to neuropsychological.

According to the RDoC criteria depression falls under two functional domains, the negative valence system under the construct of loss, and the positive valence system under the reward-related constructs. Anxiety disorders also fall under RDoC's negative valence system but under the constructs of acute threat (fear), potential threat (anxiety) and sustained threat, although reward-related deficits (positive valence domain) can also occur.

Specific phobia: Patients are fearful or anxious about, or avoidant of, circumscribed objects or situations. The fear, anxiety, or avoidance is almost always immediately induced by the phobic situation, to a degree that is persistent and out of proportion to the actual risk posed. There are various types of specific phobias such as to animals, natural environments, blood/injection/injury, or certain situations.

Social anxiety disorder (SAD) is characterised by a marked or intense fear or anxiety of social situations in which the individual may be scrutinized by others.

Panic disorder (PD): Patients experience recurrent unexpected panic attacks and are persistently concerned or worried about having more panic attacks or change their behaviour in maladaptive ways because of the panic attacks. Panic attacks are abrupt surges of intense fear or intense discomfort, that reach a peak within minutes, and are accompanied by physical and/or cognitive symptoms.

Agoraphobia: Patients are fearful and anxious about two or more of the following situations: using public transportation, being in open spaces, being in enclosed places, standing in line or being in a crowd, being outside of the home alone. These situations are feared because of thoughts that escape might be difficult, or that help might not be available in the event of developing panic-like or other incapacitating or embarrassing symptoms. These situations almost always induce fear or anxiety and are often avoided.

Generalized anxiety disorder (GAD) is characterised by persistent and excessive anxiety and worry about various domains of life, that the individual finds difficult to control. Patients experience physical symptoms such as restlessness, irritability, being easily fatigued, difficulty concentrating, muscle tension and sleep disturbance.

Obsessive-compulsive disorder (OCD) is characterised by the presence of obsessions and/or compulsions. Obsessions are recurrent and persistent thoughts, urges, or images, that are experienced as intrusive and unwanted. In most individuals these cause marked anxiety or distress. Compulsions are repetitive behaviours or mental acts that an individual feels driven to perform in response to an obsession. They are often carried out according to rules that must be applied rigidly. These are aimed at preventing or reducing anxiety or distress or preventing some dreaded event or situation.

Post-traumatic stress disorder (PTSD) develops after exposure to actual or threatened death, serious injury, or sexual violence. The disorder is characterised by recurrent involuntary and intrusive distressing memories of the event, nightmares, a sense of reliving the experience (illusions, hallucinations, or dissociative reactions such as flashbacks), intense psychological distress, physiological reactions and avoidance in response to cues that resemble the traumatic event. Symptoms must be present for more than 1 month.

Box 1-2 Short descriptions of anxiety and related disorders (adapted from DSM-V).

1.2.4.2 Pathophysiology of negative emotion

Both depression and anxiety are thought to have complex genetic, developmental, and experiential causes and reflect pathophysiological abnormalities across multiple brain circuits and neurotransmitter systems. Although there are undoubtedly differences in the underlying neurobiological constructs, due to the large overlap between anxiety and depression in terms of comorbidity, diagnostic symptoms, and functional domains, it is sometimes useful from a research perspective to consider them together as disorders of negative emotion (Ressler and Mayberg, 2007) and at other times to consider specific constructs.

1.2.4.2.1 Genetic and environmental risk factors

A modest genetic component in depression has been shown in a meta-analysis of familial studies, which revealed an estimated heritability of 37% (Sullivan et al., 2000). In addition, approximately 66% of the genetic variance in depression symptoms is shared with that of anxiety symptoms, highlighting a genetic overlap between the two. However, identification of susceptibility loci is difficult – a mega-analysis including 9240 MDD cases found no evidence for a genetic variant associated with depression (Ripke et al., 2013). This is because depression and other psychiatric disorders, are thought to be polygenic and result from the combined effects of multiple genes with small individual contributions. Large sample sizes are thus required to identify these, and indeed recent larger meta-analyses have just started to identify genetic variants involved in MDD (reviewed in Mullins and Lewis, 2017), however the molecular mechanisms by which these have their effect remain to be explored. Genetic risk factors for anxiety disorders have yet to be confirmed (Otowa et al., 2016)

Environmental influences account for the remaining variance (63%) (Sullivan et al., 2000) in susceptibility to depression, with exposure to stressful life events such as divorce, injury and childhood abuse increasing risk (Kendler et al., 1999; Shapero et al., 2014). Gene-environment interactions (GxE), in which genetic effects are moderated by environmental influences, are considered important in the aetiology of disorders of negative emotion. One of the best studied candidate genes for GxE in depression and anxiety is a polymorphism in the promoter region of the serotonin transporter gene (5HTTLPR), the gene which encodes the drug target of SSRIs. An influential study in 2003 found that this interacted with stressful life events to moderate risk of depression (Caspi et al., 2003). In addition, this polymorphism has been associated with amygdala reactivity to environmental threat (Hariri et al., 2002, 2005) and cingulate-amygdala functional connectivity (Pezawas et al., 2005), regions involved in emotion regulation, indicating possible mechanisms by which the polymorphism confers

disease risk. However, results relating to this GxE have not been reliably replicated, and a recent large meta-analysis found no evidence for any association between 5HTTLPR alone or its interaction with stress in the development of depression (Culverhouse et al., 2018).

1.2.4.2.2 Neurobiology of depression

Much research over the past 60 years has focussed on the monoamine theory of depression – that depression is caused by reduced transmission of serotonin, noradrenaline, or dopamine in the brain. This is based on the serendipitous discoveries of two drugs that were found to relieve depressive symptoms; iproniazid which was developed to treat tuberculosis, and imipramine, a chlorpromazine analogue developed as an antipsychotic. Research into the mechanism of action of these drugs revealed that iproniazid irreversibly inhibits the enzyme responsible for metabolising monoamine neurotransmitters, monoamine oxidase (MAO), while imipramine inhibits the reuptake of noradrenaline and serotonin from the synapse (Wong and Licinio, 2004). Thus, through different mechanisms, both antidepressant drugs result in an increase in monoamine neurotransmission. Imipramine became the first tricyclic antidepressant drug and subsequent research focussed on developing drugs with a similar mechanism of action but reduced side-effects. This resulted in the development of the second generation of antidepressants, selective serotonin reuptake inhibitors (SSRIs) and serotonin-noradrenaline reuptake inhibitors (SNRIs), which are widely used today . The fact that all current antidepressant drugs act on the monoamine systems, as well as the discovery of the 5HTTLPR, although its role is inconclusive, support the monoamine theory of depression. However, several flaws exist in this theory. Most critically, although the pharmacological action of SSRIs increases synaptic serotonin almost immediately, it often takes weeks of chronic treatment for antidepressant effects to be apparent clinically (Trivedi et al., 2006). Furthermore, less than 50% of patients given SSRIs show a clinical response, and only about a third achieve remission (Trivedi et al., 2006). The monoamine systems project widely across the brain and modulate activity of neurons, suggesting broad regulation of various functions. So, despite having a role in depression, it is likely that monoamine deficiency is a downstream adaptive response to primary dysfunctions that directly cause depression. Identification of these could lead to antidepressant drug targets with a more rapid onset.

The role of the glutamate system in depression has recently come to the fore following clinical trials in which a single dose of ketamine, an NMDA receptor antagonist, resulted in rapid and robust antidepressant effects in patients with treatment-resistant depression (Zarate et al., 2006). However, it has been argued that a metabolite of ketamine is in fact responsible for its antidepressant effect, and controversy currently exists as to whether the mechanism of

action is independent of NMDA receptor inhibition being caused instead by AMPA receptor activation (Suzuki et al., 2017; Zanos et al., 2017; Zanos P et al., 2016). As glutamate is the major excitatory neurotransmitter in the brain and involved in most brain functions, further research is needed to determine specific abnormalities in glutamate signalling in depression.

The neuroplasticity theory of depression posits that neurogenesis and other structural changes, largely mediated by glutamate and triggered by exposure to chronic stress, cause depression (Jacobs et al., 2000; Pittenger and Duman, 2008). As previously mentioned, stress is a known risk factor for depression (Kendler et al., 1999). The basis of this theory is that chronic stress results in upregulation of the hypothalamic-pituitary-adrenal axis, elevating levels of the glucocorticoid cortisol. This in turn results in a number of downstream structural changes including reduced hippocampal neurogenesis and reduced dendritic branching and synaptic plasticity thought to be caused by reduced levels of brain derived neurotropic factor (BDNF). Furthermore, antidepressants block or reverse these morphological changes i.e. increase hippocampal neurogenesis and synaptogenesis, at a timescale similar to that of their therapeutic lag (Malberg et al., 2000). These mechanisms are difficult to study in humans, and despite the neuroplasticity theory convincingly integrating various cellular and molecular findings albeit largely from preclinical research, much controversy exists. For example, in relation to the role of adult hippocampal neurogenesis, hippocampal volume is reduced in patients with depression and this reduction correlates with number of depressive episodes (Videbech and Ravnkilde, 2004), but neural cell proliferation is not reduced in depression (Reif et al., 2006), although it is increased by antidepressant treatment (Boldrini et al., 2012). Thus, structural alterations, particularly in the hippocampus, appear to contribute to depression risk but further research is required to determine causality.

Cognitive theories of depression, emphasise the contributing role of cognitive biases such as biased attention, biased memory, biased thoughts and rumination to the onset and maintenance of depression (Disner et al., 2011). For example, it has been observed that compared to controls, depressed patients display exaggerated responses to negative feedback on cognitive tasks which disrupts subsequent performance (Elliott et al., 1996; Murphy et al., 2003; Pizzagalli, 2011) . In addition, negative biases, particularly relating to oneself are commonly reported (Gotlib and Joormann, 2010; Mogg and Bradley, 2005), and it has been proposed that antidepressants may work by remediating these biases (Harmer et al., 2009).

Neuroimaging and post-mortem studies in humans have identified abnormalities in various brain regions in depression. These include the dACC, sgACC, dlPFC, ventral striatum, hippocampus, and amygdala. Furthermore, normalisation of aberrant activity between these

regions is associated with therapeutic benefits (Pizzagalli, 2011) leading to various neurocircuitry based models of depression.

It is important to note that the majority of studies investigating the neural correlates of depression are correlational. Many of the symptoms involved in depression, such as sadness, guilt and suicide ideation cannot convincingly be studied causally in animals, as they rely on human self-report of symptoms (Nestler and Hyman, 2010). Widely used behavioural assays in rodents, the forced swim and tail suspension tests, proposed to model behavioural despair, only show predictive validity i.e. behavioural effects that are sensitive to antidepressant treatments. In non-human primates, studies largely focus on early life stress (Gilmer and McKinney, 2003) and while these can provide insights into the pathophysiology of negative emotional disorders, early adverse events are likely to contribute to the development of both anxiety and depression. Anhedonia, is a core symptom of depression, although also apparent in schizophrenia, and thus may be a construct that is more amenable for investigation of causality in animals (Nestler and Hyman, 2010; Treadway and Zald, 2011).

1.2.4.3 The role of the dACC in depression

1.2.4.3.1 Structural findings

A recent meta-analysis of structural MRI studies of regions of interest (ROI), investigating volumetric changes in depression, found the greatest effect (Cohen's d = -0.769), a volumetric reduction, occurred in the ACC (Koolschijn et al., 2009), and this was most pronounced in the left ACC. In this study the entire ACC, was defined a priori, and it thus included studies that defined specific subregions (sgACC, pgACC and dACC/MCC), and so volumetric differences in different subregions of the ACC, proposed to be functionally distinct (Devinsky et al., 1995; Vogt, 2016), were not assessed. A specific study of the dorsal cingulate cortex (dorsal pgACC and dACC/MCC) and PCC, has shown bilateral grey matter reductions in both regions in unipolar depression and intriguingly, reduced volume of the left dACC only remained present in remitted patients (Caetano et al., 2006). This implies that bilateral dorsal cingulate cortex volume reduction is a state-dependent change in depression, whereas changes specifically in left dACC volume may be more trait related. Supporting this, symptom severity in depression has been negatively correlated with bilateral dACC volume, and the latter predicts antidepressant treatment response (Chen et al., 2007).

A meta-analysis of voxel-based morphometry (VBM) studies, a technique which allows for regionally unbiased assessment of volumetric differences across the whole brain, also consistently found a reduction in grey matter in depression but found this specifically

localised to the pgACC (Bora et al., 2012). Investigations of specific morphological abnormalities in depression have revealed reductions in glial cell density and neuronal size in layer 6 of area 24b (Cotter D et al., 2001) and reduced cortical thickness in the dACC (Li et al., 2014; Schmaal et al., 2017). Furthermore, while in controls cortical thickness in the dACC correlated with Glx (glutamate/glutamine, balanced cycling between these two neurochemicals indicates normal glutamatergic neurotransmission), it did not in depressed patients, suggesting glutamatergic dysregulation could underlie the observed reduction in cortical thickness in depression (Li et al., 2014) (Figure 1.12C). Interestingly, although no overall difference was found between Glx in the pgACC in depression vs controls, a reduction was observed in a subgroup of severely depressed patients. Similarly, Wagner et al. found no difference in grey matter volume of the dACC or pgACC in MDD patients vs controls but comparison of a subsample of MDD patients with a high risk of suicidality to matched controls, did yield reduced grey matter in both the pgACC and dACC (Wagner et al., 2011). These last two studies highlight the importance of accounting for clinical heterogeneity when studying patient populations, as different types of depression (severity, symptoms) likely have different pathologies which may well account for the differing findings in the extent of ACC changes in depression.

1.2.4.3.2 Functional findings

Abnormalities in different ACC subregions have been shown in functional neuroimaging studies of depression. They support the implication from anterior cingulotomy that the aMCC is involved in depression and further implicate the pgACC and sgACC (Drevets et al., 1997; Mayberg et al., 1997, 2005). However the pMCC does not appear to have a significant role, as it has been shown that patients with posterior anterior cingulotomy sites in the pMCC had poorer responses, and this was located outside the region shown in meta-analysis of prefrontal regions to have functional abnormality in depression (Figure 1.12A) (Steele et al., 2007, 2008).

A meta-analysis has shown that MDD patients consistently show greater activity in the dACC (aMCC) as well as the amygdala and insula, in response to negative stimuli (compared to positive stimuli) (Hamilton et al., 2012). These regions (dACC, amygdala and insula) are all nodes in the salience network, a large scale brain network thought to be involved in detecting and processing behaviourally relevant stimuli (Seeley et al., 2007). In addition, heightened baseline pulvinar nucleus (thalamic) activity in depression was demonstrated. The authors

proposed a model of depression in which pulvinar nuclear activity potentiates responding of salience network activity to negative stimuli (Figure 1.12B) – a model consistent with cognitive theories of depression implicating negative cognitive biases in the pathophysiology of depression (Gotlib and Joormann, 2010; Harmer et al., 2009).

Functional imaging studies comparing activity of ACC regions before and after antidepressant treatment have been highly informative. Using positron emission tomography (PET), Mayberg et al. first discovered resting hypermetabolism of the rACC (pgACC and rostral dACC; Brodmann area 24a/b) in MDD patients that showed symptom improvement after 6 weeks of antidepressant drug treatment, whilst non-responders showed hypometabolism of the same region (Mayberg et al., 1997). This finding has been replicated in a larger sample (Mayberg et al., 2000) and in a study that measured baseline theta activity using EEG (Pizzagalli et al., 2001), indicating that reduced pre-treatment rACC activity is predictive of poor treatment response. This link has also been demonstrated in task-related studies which show greater pre-treatment activity in the rACC in response to negative vs neutral stimuli is predictive of treatment response to venlafaxine (Figure 1.12D) (Davidson et al., 2003), and greater pre-treatment functional activity in a sad facial affect processing task predictive of faster symptom improvement during 8 weeks of fluoxetine treatment (Chen et al., 2007). Thus, both heightened resting activity and emotional task-related activity in the rACC are predictive of antidepressant treatment response whilst reduced activity is not.

The dACC has also been implicated in anhedonia, a core symptom of depression (Box 1-1). Impaired reward processing may underlie anhedonia and a comparison of functional studies in reward processing in humans with primate anatomical studies has highlighted the importance of corticostriatal circuitry including the dACC, sgACC, and dlPFC (Haber and Knutson, 2010). Few studies have specifically assessed causality, however, lesion of the sgACC in macaque appears to impair anticipation of reward (Rudebeck et al., 2014). Notably, this study used aspiration lesions, which could have damaged fibres of passage to or from the dACC. Recent work has specifically associated rdACC activity with the anti-anhedonic response of ketamine. In a randomised placebo-controlled study, a single ketamine infusion had rapid-acting anti-anhedonic effects that lasted up to 2 weeks, independent of antidepressant effects, in patients with treatment-resistant bipolar depression (Lally et al., 2014). A subset of patients had resting state FDG-PET scans at 2h post infusion which revealed significantly increased glucose metabolism in the rdACC after ketamine compared to placebo, and this was associated with the specific anti-anhedonic effect of ketamine. This finding has been replicated in patients with treatment-resistant depression, however anhedonia after ketamine

infusion was compared to baseline rather than placebo (Figure 1.12E) (Lally et al., 2015). Although it is unclear whether this increased activity in the rdACC reflects normalisation of hypoactivation as described by Mayberg and colleagues (Mayberg et al., 1997) these findings support a role for the rdACC in mediating antidepressant response.

The interaction between the dACC (aMCC) and the sgACC (Brodmann area 25 is thought to be particularly important in depression. In treatment-resistant depression, baseline hypermetabolism of the sgACC, along with hypometabolism in the dACC (area 24) has been demonstrated (Figure 1.12C) (Mayberg et al., 2005). After chronic deep brain stimulation of the white matter adjacent to the sgACC, resting activity in these regions normalised in treatment responders i.e. activity increased in the dACC and decreased in sgACC. This landmark study supports the view that depression is caused by dysfunction in distributed corticolimbic circuits rather than isolated abnormalities in particular regions (Mayberg, 1997). The sgACC has strong connections to the pgACC and dACC via white matter tracts in the cingulum bundle, and this is one of three tracts found to be essential for DBS antidepressant response (Riva-Posse et al., 2014). Further evidence highlighting sgACC and dACC interactions as key to the circuitry of depression comes from functional connectivity analyses, that have reported negative functional connectivity between the sgACC and the dACC in depressed individuals. Furthermore, the strength of this was positively associated with clinical response to antidepressant medication (Kozel et al., 2011). To summarise, both structural (volumetric reductions) and functional (reduced baseline activity) abnormalities have been described in ACC regions in depression. Although there is some variation in terms of which subregions of the dACC contribute (Figure 1.12), activity of the rACC appears to be particularly important for symptom improvement following antidepressant treatment, whilst the interaction of the aMCC with other corticolimbic brain regions appears to be dysregulated in depression.

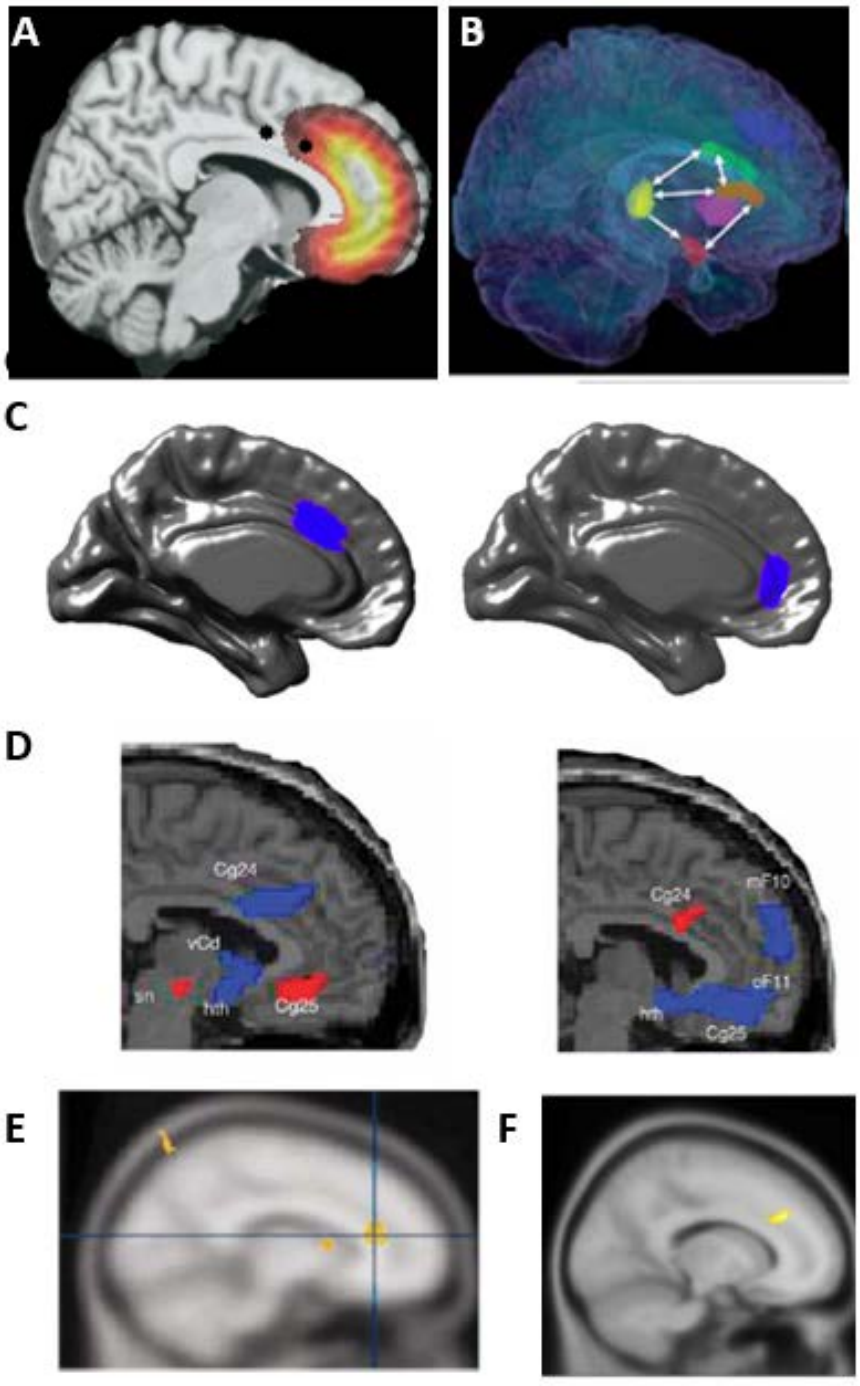

Figure 1.12 Selected findings implicating the ACC in depression. A. Coloured region shows result of meta-analysis of functional abnormalities in prefrontal cortex in depression. Black dots show anterior cingulotomy lesion sites – the more anterior site is associated with better clinical response (Steele et al. 2007,2008); B. Proposed model of negative bias in depression – high baseline pulvinar (yellow) activity, potentiates responding in the amygdala (red), insula (orange) and dACC (green), nodes shown to be hyperactive in depression (Hamilton et al. 2012). C. Visualisation of dACC and pgACC in two dimension surface, regions that show differences in Glx according to depression severity (Li et al. 2014); D. PET image showing hyperactivity of sgACC (Cg25) and hypoactivity of dACC (Cg24) in treatment-resistant depression (left), that normalises after 3 months continuous DBS treatment (shown as change from baseline) (Mayberg et al. 2005; E. Baseline activity in rACC that predicts antidepressant treatment response (Davidson et al. 2003); F. rdACC region that shows increased glucose metabolism after ketamine compared with baseline in treatment resistant depression, associated with anti-anhedonic effect (Lally et al. 2015).

1.2.4.4 Neurobiology of anxiety disorders

1.2.4.4.1 Fear conditioning

Anxiety disorders are characterised by excessive fear, and as a result much research focusses on the neural circuits involved in fear responses. Fear and anxiety differ in that fear is the response to a specific immediate threat, and is normally associated with short-lived arousal and defensive behaviours such as fleeing and freezing, whilst anxiety is the response to a perceived distant or uncertain threat and is associated with more prolonged arousal, and vigilance (Gross and Canteras, 2012; Sylvers et al., 2011). However, they are both negative emotions that occur in response to threats, and serve evolutionarily adaptive survival roles in allowing organisms to rapidly detect threats in the environment and respond appropriately, and evidence suggests that fear and anxiety may be served by overlapping neuronal circuits (Tovote et al., 2015).

In contrast to depression, our understanding of the aberrant circuitry in anxiety disorders owes much to translational research into the neurobiology of fear conditioning and extinction (Milad and Quirk, 2012). Laboratory-based paradigms for classical (Pavlovian) fear conditioning involve repeated pairing of a neutral cue (CS) to an aversive stimulus (US) resulting over time in the cue being able to elicit a fear response on its own in the absence of the US. Extinction of this fear response is achieved by repeated presentations of the CS without the aversive stimulus. As the fear response can be restored by pairing an extinguished CS with the US (reinstatement) or by presenting the CS in a new context (renewal), the original fear conditioning memory is thought to remain after extinction but to be inhibited by the new fear extinction memory (Bouton and Moody, 2004). Conscious threat appraisal or anticipatory anxiety, which describes the negative affective state experienced when expecting threatening stimuli, can be studied using instructed fear paradigms. In these, participants are informed that a CS will be followed by an aversive outcome, usually “threat of shock.” An advantage of using the fear conditioning model to study anxiety, is that it produces many of the behavioural symptoms commonly displayed in anxiety disorders such as avoidance, vigilance, and physiological symptoms. Furthermore, exposure therapy, a form of CBT, comparable to fear extinction, is an effective treatment for some anxiety disorders (Hofmann, 2008).

Various abnormalities in fear processing are apparent in anxiety disorders and these may contribute to mediating anxiety states. Impairments in fear extinction are observed in anxious populations, for example patients with panic disorder displayed greater physiological arousal during fear extinction than healthy controls (Michael et al., 2007). A meta-analysis of simple

fear conditioning across anxiety disorders reported modest increases in conditioned fear responses during both acquisition and extinction in anxiety patients (Lissek et al., 2005). This suggests that anxiety patients experience greater fear in response to threat-related stimuli than controls.

In discrimination learning paradigms, which involve a fear cue (CS+) linked to an aversive outcome and a perceptually similar safety cue (CS-) linked with a neutral outcome, anxiety patients were worse at distinguishing between the cues as indexed by their conditioned fear response (Lissek et al., 2005, 2014). This occurs even when patients report being aware of the CS- US contingency (Lissek et al., 2005) indicating an impaired ability to suppress fear responses in the presence of safety cues, a phenomenon referred to as fear generalisation. These findings could explain symptoms such as hypervigilance and a heightened startled response.

Fear conditioning is particularly applicable to the study of PTSD, as this disorder is characterised by excessive, uncontrollable fear. Accordingly, heightened fear responses, impaired fear extinction and impaired extinction recall have all been described in PTSD patients (Milad et al., 2008; Norrholm et al., 2011; Orr et al., 2000).

The amygdala is a key node in fear circuitry and a wealth of evidence in both animals (1.2.2) and humans indicates that it mediates expression of fear (LeDoux, 2000; Maren, 2001). Fear conditioning studies in animals have elaborately detailed fear circuits within the amygdala. Briefly, the lateral nucleus (LA) largely receives sensory input from the cortical regions and the thalamus while the basolateral and basomedial nuclei receive contextual input from the hippocampus. These nuclei directly project to the central nucleus (CeA) which projects to regions that mediate fear expression such as the hypothalamus, periaqueductal gray, and bed nucleus of the stria terminalis (LeDoux, 2003). Although neuroimaging studies in humans lack the detailed resolution to discriminate between nuclei of the amygdala, they show that this structure, as well as the insula, is hyperactive in response to negative emotional stimuli across anxiety disorders, and in healthy participants during fear conditioning (Etkin and Wager, 2007). The dACC/aMCC and the vmPFC have been implicated in mediating conditioned fear expression and extinction respectively, with abnormalities apparent in anxiety disorders (Graham and Milad, 2011a). Furthermore these regions are thought to exert top-down control over amygdala activity (Linnman et al., 2012b, 2012a; Milad and Quirk, 2012), consistent with the theory that anxiety disorders are associated with hyperactivity of fear circuits.

1.2.4.4.2 Attentional bias

Another common feature of anxious individuals is an attentional bias toward threat-related stimuli and an increased likelihood of interpreting ambiguous stimuli as threatening (Bishop, 2007). Threat-related biases have been suggested to play a causal role in the development of anxiety (Mathews and MacLeod, 2002). They can be captured using various tasks involving threat related distractors and some form of measured response latency. For example, in the emotional Stroop test participants are asked to name the colour of threat-related and neutral printed words. A threat-related bias is demonstrated if response times are longer to threat-related than to neutral words. Although the effect size is modest (Cohen's d = 0.45), a threat-related bias is robust across anxiety diagnoses and occurs in various paradigms, both involving conscious perception and subliminal exposure to threats (Bar-Haim et al., 2007). Intriguingly, this is not apparent in MDD in which biases to self-referential negative information are common and therefore it may be a distinguishing feature of anxiety disorders (Mogg and Bradley, 2005). However, although various models have been proposed, beyond involvement of a non-conscious threat detection system there is disagreement over the mechanism that mediates the attentional bias to threat (Cisler and Koster, 2010). As for the processing of fear, the amygdala has emerged as a key structure involved in the automatic detection of threat (Öhman, 2005).

1.2.4.5 The role of the dACC in anxiety

Human neuroimaging studies have revealed activation across the ACC and dmPFC during processing of fear and anxiety (Etkin et al., 2011). The variation in the activation foci correlated with fear and its regulation is noteworthy (Figure 1.13). Although activity related to fear expression predominantly occurs in the aMCC, the pMCC is also implicated. However, a number of cognitive processes are thought to occur between presentation of a fearful stimuli and a fear response. This includes an initial appraisal/evaluation of the stimulus and context. Due to the low temporal resolution of fMRI it is difficult to differentiate between neural activations related to appraisal and those directly mediating the fear response. Thus, these different regions may have subtle differences in their function in fear that may be teased apart by studying different sub-processes related to fear in more detail. Towards this, a meta-analysis of uninstructed (Pavlovian) and instructed fear paradigms was carried out. In the latter participants have prior information on CS-US contingency and thus the process of fear learning is reduced, and conscious appraisal of threat occurs. This revealed that the aMCC was consistently activated (fMRI) in both uninstructed (Pavlovian) and instructed fear paradigms suggesting a specific role of the aMCC in the expression of fear (Figure 1.14A)

(Mechias et al., 2010), whilst the rostral dmPFC was only activated in the latter suggesting a specific role in conscious fear appraisal. This finding is further corroborated by Milad and colleagues who show that aMCC activity positively correlates with fear expression, as measured by skin conductance response, during a fear conditioning task (Figure 1.14B) (Milad et al., 2007a). In addition, Kalisch and colleagues introduced high and low cognitive load during an instructed fear task. Both conditions elicited a similar conditioned response. However, during the low load condition, when cognitive resources enable greater conscious appraisal, activation in a different more anterior region, in the pgACC was increased compared to the high load condition. This suggests that more dorsal and rostral regions adjacent to the aMCC including the rostral dmPFC and pgACC may have a greater role in conscious threat appraisal rather than expression of fear per se (Figure 1.14C) (Kalisch and Gerlicher, 2014; Kalisch et al., 2006; Maier et al., 2012). However, this does not account for the fear-related functional activity also observed in the pMCC.

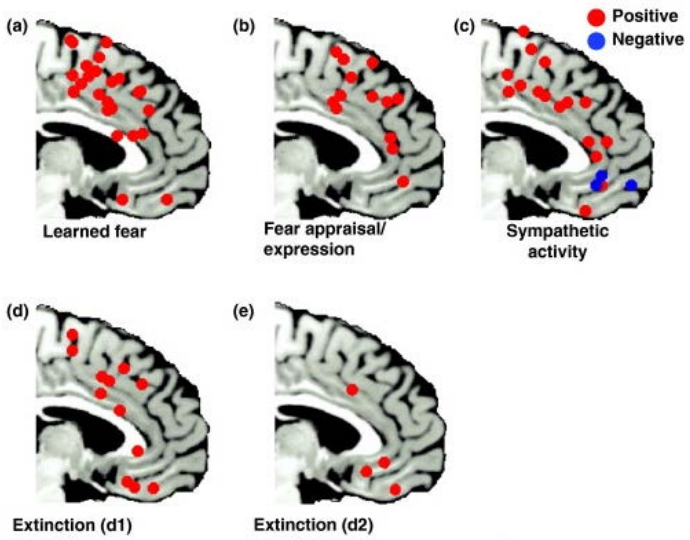

Figure 1.13 Variation in activation foci associated with fear and its regulation. Figure from Etkin et al. 2011.

Straube and colleagues show that the pMCC is also involved in anticipatory anxiety (Figure 1.14D) (Straube et al., 2009), and further that variation in activity of subregions of the ACC relate to threat intensity. In this study healthy individuals anticipated electrical shocks of differing intensities and whilst activity of the pMCC positively correlated with anxiety during anticipation of strong threat, activity of the pgACC was negatively correlated, and further showed a positive correlation with anticipation of moderate threat. The authors suggest that this is due to a shift in threat processing from low level avoidance to hypervigilance and readiness for action i.e. a threat bias. Recent studies support this suggestion and specifically implicate a dACC-amygdala circuit in mediating an adaptive threat bias (Vytal et al., 2014),

however the ROIs involved appear to vary along the dACC and dmPFC depending on the manipulation and subject group involved. The rostral dmPFC showed significantly greater positive functional connectivity with the amygdala during the processing of fearful faces when anticipatory anxiety was present (threat of shock) and this was paralleled by faster behavioural responses to the stimuli ((Figure 1.14E) (Robinson et al., 2012). Acute tryptophan (a precursor for serotonin) depletion also significantly increased positive aMCC–amygdala coupling during the processing of aversive stimuli suggesting this circuit is regulated by serotonin (Robinson et al., 2013). Furthermore, patients with unmedicated GAD and SAD also showed significantly increased caudal dmPFC-amygdala connectivity when processing fearful vs happy faces compared to controls, and this correlated with their self-report anxiety symptoms (Robinson et al., 2014). Thus, this dACC-amygdala circuit is hypothesised to cause aversive amplification whereby in healthy people the dACC amplifies amygdala responses in the presence of threats resulting in an adaptive threat bias, but in patients with anxiety disorder, chronic overactivity of this circuit leads to a negative affective bias.

Although implicated in various anxiety disorders, the dACC is most consistently implicated in PTSD. A meta-analysis of neuroimaging studies during a negative emotional condition found that the dACC was hypoactive compared to controls in PTSD but not in SAD or specific phobia (Etkin and Wager, 2007). As the amygdala is hyperactive in PTSD, one circuit-based theory is that the dACC and other cortical structures exert top-down regulation of amygdala activity and this is impaired in PTSD resulting in excessive fear (Pitman et al., 2012; Rauch et al., 2006). In support of this circuitry, in healthy individuals, rdACC (aMCC) volume covaries with amygdala volume and dACC has negative functional connectivity with amygdala (Figure 1.14F) (Pezawas et al., 2005). Furthermore, dACC activity may be a familial risk factor for PTSD, as it was found that veterans with PTSD and their twins had significantly higher resting glucose metabolism in the cdACC (pMCC) compared with veterans without PTSD and their twins (Figure 1.14G) (Shin et al., 2009).

As in MDD, activity of the rostral dACC in anxiety may also be predictive of treatment outcome. This was shown in patients with GAD, in which increased activity of the rostral dACC during anticipation of an aversive stimulus predicted better treatment outcomes to an SSRI (Nitschke et al., 2009). Intriguingly this was a similar region to that predicting treatment response in depression indicating overlap between the neurobiological basis of treatment of these disorders.

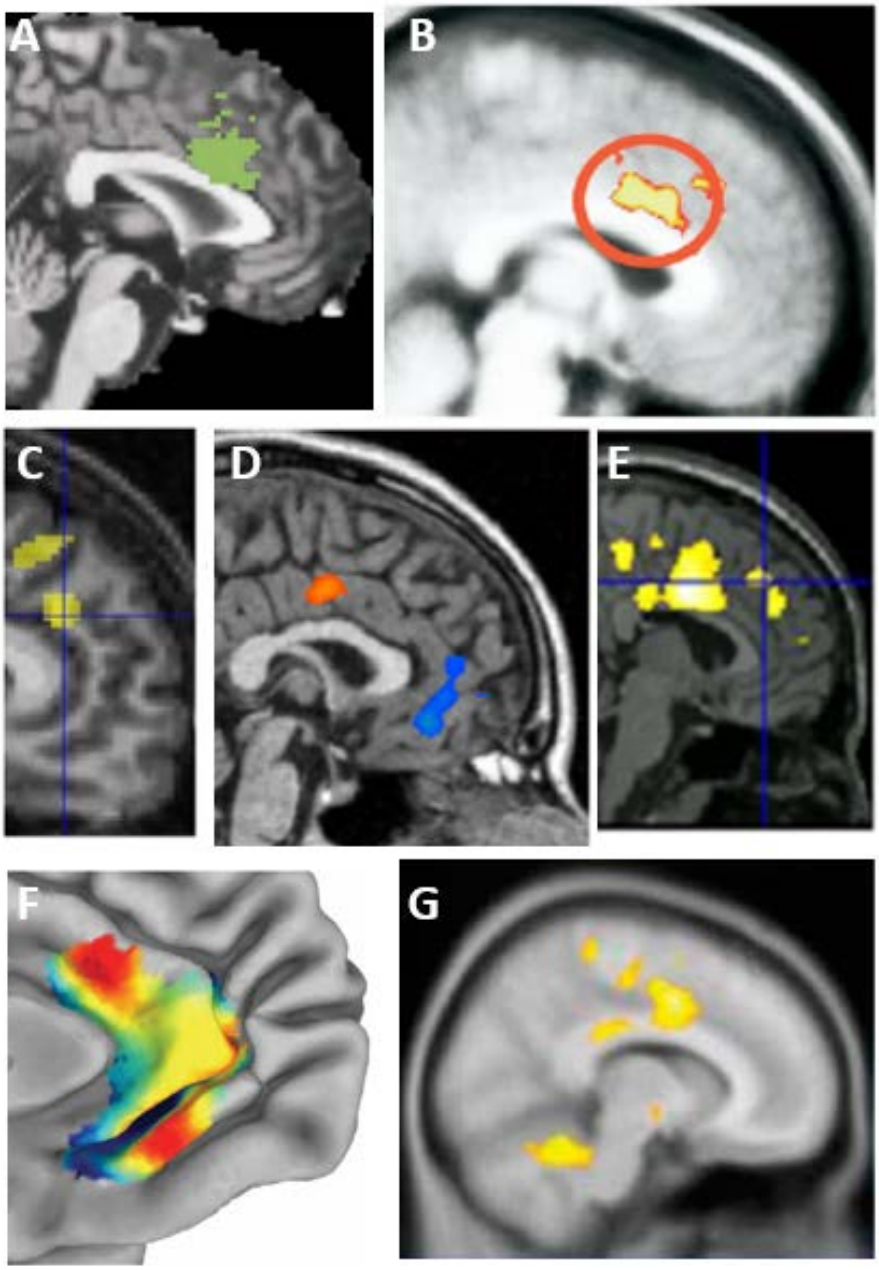

Figure 1.14 Selected findings implicating the ACC in anxiety. A. Overlap of fMRI activation of dACC during uninstructed and instructed fear (Mechias et al. 2010);B. dACC region that positively correlates with fear expression (Milad et al. 2007);C. more rostral dACC region shows greater activity during low cognitive load instructed fear (Kalisch et al. 2006);D. cdACC activity correlates with anticipation of anxiety during strong threat (Straube et al. 2009); E. rostral dMPFC activation to fearful faces shows enhanced coupling to amygdala during instructed fear; F. Volume of the rdACC in healthy individuals covaries with the amygdala (peaks shown in red) (Pezawas et al. 2005) G. resting glucose metabolism is higher in the pMCC is greater in veterans with PTSD and their identical twins compared to veterans without PTSD and their identical twins(Shin et al. 2009).

1.3 Non-emotion related functions of the dACC

Historically, the dACC was implicated in emotion by virtue of it prominent position in Papez limbic system (Papez, 1937). Human lesion studies supported this role (Brown and Lighthill, 1968) and as discussed, the dACC is implicated in processing negative emotion. However,

with the advent of neuroimaging techniques in the 1990s came the identification of a vast array of functions besides emotion with which the dACC has come to be associated with today. Indeed, the dACC is one of the most consistently activated regions across neuroimaging studies (Yarkoni et al., 2011), although other experimental approaches such as lesion, stimulation, and single-unit recordings in humans and non-human primates have undoubtedly contributed to our understanding of the dACC. These functions include but are not limited to, conflict monitoring (Botvinick et al., 2004), reward-based decision-making (Bush et al., 2002; Kennerley et al., 2006), salience detection (Menon and Uddin, 2010), and autonomic arousal (Critchley et al., 2003).

There are two possible explanations for functional heterogeneity within the dACC, both of which are likely to contribute to some degree; 1) the dACC has a broad computational role that contributes to multiple overlapping functions; 2) the dACC has functional subdivisions that are responsible for distinct roles. As a result, some researchers have attempted to integrate the diverse unitary roles of the dACC into overarching models of its function while others have attempted to identify functional divisions upon which to parcellate the dACC. Although the focus of this thesis is the role of the dACC in emotion and its regulation, a comprehensive knowledge of the broader functions of the dACC can inform our understanding of this specific role. Thus, I will now briefly summarise some of the key reported functions of the dACC and their possible bearing to emotion.

1.3.1 Cognition

Early reviews of the ACC that incorporated neuroimaging findings, functionally segregated the ACC into a dorsal cognitive division and a rostral/ventral emotional division (Bush et al., 2000; Devinsky et al., 1995). This was primarily based on data comparing activity during the classic cognitive coloured-word Stroop task and the emotional Stroop task. There is ample evidence to suggest that these regions are differentially engaged during cognition vs emotion (Mohanty et al., 2007). However, it is also apparent that the dACC is activated by both cognition and emotion and neither exclusively (Etkin et al., 2011; Shackman et al., 2011). It has been argued that dissociation between cognition and emotion is problematic as these functions are integrated in the brain (Pessoa, 2008). Indeed, on the basis of its anatomical connectivity with both the limbic system and the prefrontal cortex, the dACC can be described as a cognitive-emotional hub region (Pessoa, 2008)

Many of the cognitive functions in which the dACC has been implicated broadly relate to cognitive control, a set of processes that adaptively guide behaviour according to current

internal goals. Successful goal-directed behaviour requires monitoring of the environment and action outcomes (performance monitoring), decision-making, and flexible behavioural adaptation (Ullsperger et al., 2014). However, controversy exists as to what activity in the dACC represents. Initially, the dACC was thought to be involved in error detection. The error-related negativity (ERN), a negative component found in EEG recordings is consistently seen 50-100ms after an error response (Gehring et al., 1993) and is thought to arise from the region (Carter et al., 1998; Dehaene et al., 1994). Error monitoring was found to be too narrow a function to describe the dACC, as when error responses occur, ongoing processing of the correct response often leads to belated activation of the correct response and thus, in the post-response period, both correct and incorrect responses may be activated. Thus this activity likely reflects post-response conflict and has now been incorporated into the "conflict monitoring" theory, in which the dACC detects conflicts and responds by triggering adjustments in cognitive control that serve to reduce conflict in subsequent performance (Botvinick et al., 2001, 2004). Conflict signals the need for cognitive control. This accounts for the observed activation of the dACC during various tasks involving activation of competing responses, overriding prepotent responses and commission of errors. The latter is conceptualised to represent conflict between the incorrect and correct response. Evidence from human neuroimaging studies supports this view, with activity largely centred on the sulcul part of the dACC. Only recently were conflict-related signals detected in non-human primates (Ebitz and Platt, 2015), overcoming a major hurdle in this line of enquiry. Prior to this single-unit recordings in macaques had failed to find conflict-related activity (Cole et al., 2009) suggesting the imaging studies in human did not reflect conflict but a broader function (Cole et al., 2009; Ebitz and Platt, 2015; Shenhav and Botvinick, 2015)

1.3.2 Action selection

More comprehensive views of dACC function emphasize its role in reinforcement-guided action selection (Rushworth et al., 2004). Supporting evidence largely comes from lesion studies and recordings in non-human primates, and again the sulcul region of the dACC is implicated. Lesions of the entire anterior cingulate sulcus (including dACC) in macaques did not impair behavioural performance directly after errors, but did impair ability to sustain a rewarded response in a reinforcement guided task (Kennerley et al., 2006). However, these lesions were ablations that damage fibres of passage, so it is not absolutely clear that the deficits observed were related to damage specifically within the ACC itself. Single-unit recordings have identified neurons in the pgACC sulcus that encode unsigned reward-prediction errors or surprise signals (Hayden et al., 2011), as well as the value of various decision-making variables (predicted reward, probability of success and cost) and multiplexed representation of these variables (Kennerley and Walton, 2011). Importantly, reward-related signals in the rdACC have been linked to subsequent adaptations in behaviour in both macaques (CMAr) (Shima and Tanji, 1998) and humans (aMCC) (Williams et al., 2004). Two dominant models of dACC have arisen from these data.

The “expected value of control theory” posits that the dACC integrates information about potential rewards and costs to estimate a net value associated with allocating cognitive control to a given task (Shenhav et al., 2013, 2016). This signal is used to select between multiple task options and is graded to specify how much control to allocate. Alternatively, the behavioural adaptation model proposes that the dACC integrates multiple valuation signals such as recent reward history and value of the environment to specifically signal the value of switching from the current behavioural strategy (Kolling et al., 2016; Rushworth et al., 2012). Both models agree that the dACC is important for decision-making and evaluating costs and benefits but differ in their interpretation of the function of cognitive control between competing tasks vs behavioural change from the default. While they go some way in accounting for the various cognitive functions of the dACC they largely ignore the role of the dACC in emotion. The dACC’s involvement in cognitive and emotional processes may reflect its more general role in modulation of autonomic responses related to adaptive behavioural control (Critchley et al., 2003).

1.3.3 Pain

Pain is defined as an “unpleasant sensory and emotional experience” (International Association for the Study of Pain) and is thus clearly recognised to have both nociceptive and affective components. Functional imaging studies in humans consistently show activity of the dACC in response to physical pain (Peyron et al., 2000), and it has been suggested that this function overlaps with social pain, the negative affect experienced following social separation or rejection (Eisenberger, 2012; Eisenberger et al., 2003), thus emphasising the role of the dACC in the affective component of pain. Indeed, anterior cingulotomy is reported to be effective for the treatment of chronic intractable pain (Wilkinson et al., 1999), and was initially developed to treat this condition (Foltz and White Jr, 1962) before later being used to treat depression and anxiety disorders (Ballantine et al., 1987). Intriguingly, it is this affective component of chronic pain that may be altered by targeting the dACC. This was specifically examined in a study in which the efficacy of deep brain stimulation (DBS) of the mdACC to treat patients with chronic pain was assessed (Boccard et al., 2014). Although patients still sensed their pain they were less bothered by it and this was reflected by significant improvements in quality of life measures.

In the “neural alarm theory” of dACC function, developed to account for the roles of the dACC in distress and conflict, the dACC is proposed to first detect goal-related conflicts and then “sound the alarm” to signal a problem (Eisenberger and Lieberman, 2004). This integrates the pain and conflict accounts of dACC function and was later expanded to emphasize detection of “survival-relevant” conflicts and include other “distress-related” emotions (distress, fear, negative affect) (Lieberman and Eisenberger, 2015).

1.3.4 Salience

Salient stimuli are those that have behavioural significance, and these can be driven by emotional, motivational, and cognitive factors. The aMCC and anterior insula (AI) are core nodes in the salience network. This is an intrinsically connected, large-scale network proposed to detect salient stimuli and coordinate other regions to respond appropriately to guide behaviour (Menon and Uddin, 2010; Seeley et al., 2007; Sridharan et al., 2008). The salience network is consistently activated during cognitively demanding tasks as well as pain, uncertainty, and fear – all of which can be considered behaviourally salient. Subcortical limbic regions such as the amygdala are also variably included in the salience network. Other networks have been identified in a similar manner, through the use of functional connectivity

analyses of fMRI data taken from subjects at rest. These are the default-mode network which is most active during rest and deactivates during tasks (Raichle et al., 2001) and the central executive network which is most active during cognitive tasks (Seeley et al., 2007) and the salience network may be involved in switching between these other networks (Sridharan et al., 2008). The role of the dACC in salience aligns well with its role in emotion may be considered the most behaviourally salient stimuli.

1.4 Summary and aims

A recent controversy surrounding the dACC (#cingulategate) occurred in response to the claim that the *best* psychological description of dACC function was related to pain processing (Lieberman and Eisenberger, 2015). This disagreement largely related to how the authors analysed data (reverse inference analyses) from a database of fMRI studies to arrive at this conclusion, with many showing it to be invalid (Shackman, 2015; Wager et al., 2016; Yarkoni, 2015). However, it also raised the broader issue of attributing function to the dACC, which as a whole is highly unlikely to have one selective role but rather is involved in numerous functions that can impact on each other. As discussed above broad models of dACC function often integrate the role of the dACC in emotion.

In the present review, the role of the dACC is assessed specifically in relation to negative emotion (1.2), a function it is consistently implicated in. Variation in activity across the rostro-caudal axis of the dACC is observed suggesting the existence of functional subdivisions of the dACC that may have distinct roles relating to negative emotion. Although anatomical studies in macaques and humans support this suggestion, it is largely based on correlational studies in humans with few causal studies in experimental animals contributing. Furthermore, given that dysregulation of negative emotion is critical in the pathophysiology of neuropsychiatric disorders, such as anxiety and depression, a precise understanding of the roles of subregions of the dACC in negative emotion could give us a greater insight into the neurobiological mechanisms underlying these disorders.

The marmoset has a highly developed prefrontal cortex, with a well-defined granular area 24 comparable to that of humans. It displays complex cognitive and emotional behaviour making it ideal for the assessment of the dACC in these processes, relevant to negative emotion. In this thesis I investigate the roles of two topographically distinct regions of the dACC, the rdACC and cdACC, in the regulation of negative emotion in the common marmoset (Figure 1.15).

Specifically, I assess the contributions of these subregions to:

1. regulation of anxiety in response to an uncertain threat (Human Intruder Task)
2. baseline cardiovascular activity
3. regulation of conditioned fear (Fear extinction task)
4. approach-avoidance decision-making (VI decision-making task)
5. anatomical projections throughout the brain (anterograde tracing)

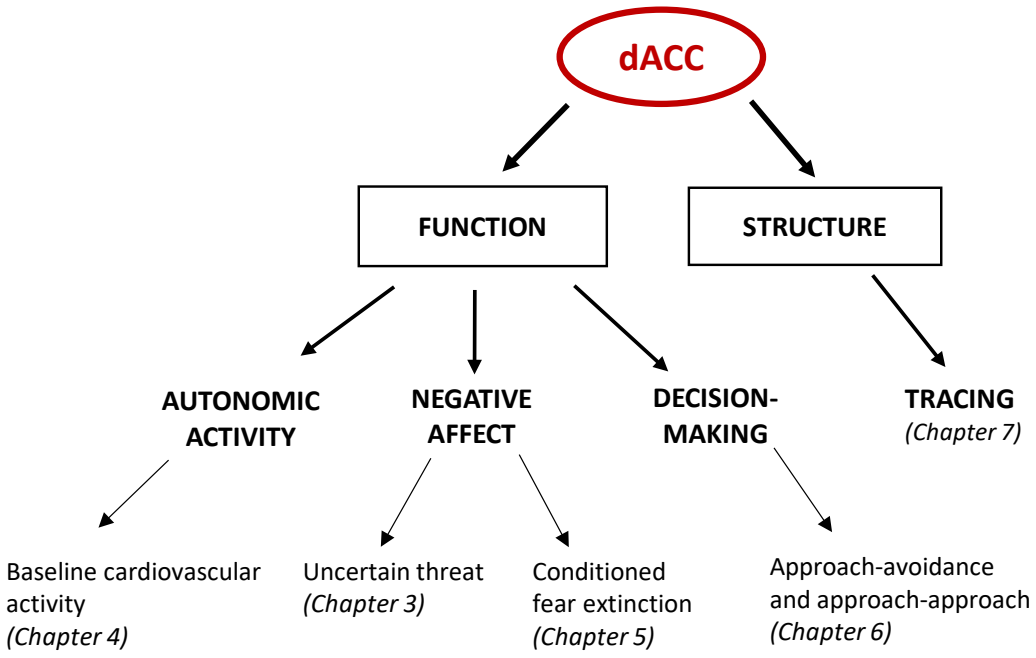

Figure 1.15 Overview of experimental chapters in this thesis.

1.5 Targeting the dACC

Although the aim of this thesis was to investigate the role of two subregions of the dACC – the rdACC located at the level of the lateral septum (AP 11.9), and the cdACC, located posteriorly closer to the anterior commissure (AP 10.5) (Paxinos et al., 2011) - the dACC has never been targeted with cannulae before in the marmoset and significant difficulty was encountered in doing so due to the wide interindividual variation in brain size. This resulted in some cannulae being placed (i) in the "mid" dACC (mdACC), that later in this thesis may be seen as a transition zone between the rdACC and cdACC, and (ii) more anteriorly in the pgACC. Thus, as part of this work it was necessary to determine which surgical adjustments would minimise variation in cannula placement within the dACC. Future studies will be able to use these adjustments to more precisely target dACC regions. This unexpected obstacle resulted in a more extensive analysis of dACC subregions. Where feasible data from these additional regions will be presented as well as data from the intentional regions of interest (rdACC and cdACC).

2 |MATERIALS & METHODS

2.1 Subjects

A total of twenty marmosets (*Callithrix jacchus,* 10 females and 10 males) were used in the experiments described in this thesis (Table 2.1). The mean age at the outset of behavioural testing was 41 months (SD = 4.2) and marmosets were experimentally naïve prior to this, with the exception of some (Trixie, Wall-e, Cucumber and Snowball) that received structural MRI scans as infants as part of separate developmental study. As conducted in all experimental marmosets in the colony, subjects underwent a behavioural screening protocol conducted by the Senior Research Technician, Gemma Cockcroft, consisting of two non-invasive tests of anxiety and of fear: the human intruder test (Agustín-Pavón et al., 2011) and the rubber snake test (Shiba et al., 2014), to provide an indication of trait anxiety. Based on their scores on these, subjects that were "high anxious" were excluded from the decision-making task as lower anxious marmosets are trained on the touchscreen more easily.

Marmosets were bred on site at the Innes Marmoset Colony (Behavioural and Clinical Neuroscience Institute) and housed in male/female pairs (males were vasectomised), under temperature (22 ± 1 °C) and humidity (50 ± 1%) controlled conditions, in purpose-built cages. A variety of environmental enrichment aids were provided including beams, branches, and ropes. A 12h dawn/dusk-like light-dark cycle was maintained and marmosets were provided with a varied and balanced diet with water available ad libitum. During the week, this included rusk or peanuts in the morning and sandwich and a piece of fresh fruit in the afternoon, with treats given over the weekend. Only marmosets that were included in the touchscreen approach-avoidance task (Chapter 6) were fed a restricted diet from Sunday evening to Friday afternoon after their daily behavioural testing session, during which they were fed 20g of pellets MP.E1 primate diet (Special Diet Services, Essex, UK) and 2 pieces of carrots in the afternoon and were restricted to 2h per day of free access to water to ensure a high response rate in the task. At the weekend, they received the same variety of treats as all other marmosets and had 48 hours of free access to water. This research has been regulated under the Animals (Scientific Procedures) Act 1986 Amendment Regulations 2012 following ethical review by the University of Cambridge Animal Welfare and Ethical Review Body

(AWERB) All procedures were performed in accordance with the UK Animals (Scientific Procedures) Act 1986, the personal and project licences and the AWERB policies.

*Table 2.1 Overview of infusion sites and study inclusion for each subject. Sites shown in brackets are predicted locations based on surgical coordinates, which remain to be verified by histological assessment post-mortem. * Lilin's posterior site was discovered to be too posterior, hitting the midcingulate cortex rather than cdACC, thus data from this site is not included.*

Subject	Infusion site				Study				
	pgACC	rdACC	mdACC	cdACC	Human intruder	Baseline autonomic	Fear extinction	Decision-making	Tracing
Jalapeno		✓	✓		✓	✓	✓		
Toba		✓	✓		✓	✓	✓		
Garbanzos			✓	✓	✓	✓	✓		
Banshee		(✓)		(✓)	✓	✓	✓		
Trixie		(✓)	(✓)		✓	✓	✓		
Watercress			✓	✓	✓		✓		✓
Snowball		✓	✓		✓	✓	✓		✓
Azuki		✓		✓	✓	✓	✓		✓
Wall-e	✓	✓			✓	✓			
Yeti	✓		✓		✓	✓			
Privet			✓	✓				✓	
Ptolemy			✓	✓				✓	
Golem		✓		✓				✓	
Lilin*			(✓)					✓	
Twinkle			✓	✓				✓	
Cucumber		✓		✓				✓	
Jumbee	(✓)	(✓)			✓			✓	
Buttercup		(✓)	(✓)		✓			✓	
Nemesis		✓							✓
Lemongrass			✓						✓
TOTAL:	3	12	13	10	12	9	8	8	5

2.2 Overview of Experiments

Figure 2.1 shows the various ways subjects included in this study progressed through experiments, including training stages, surgeries, and movement across experiments.

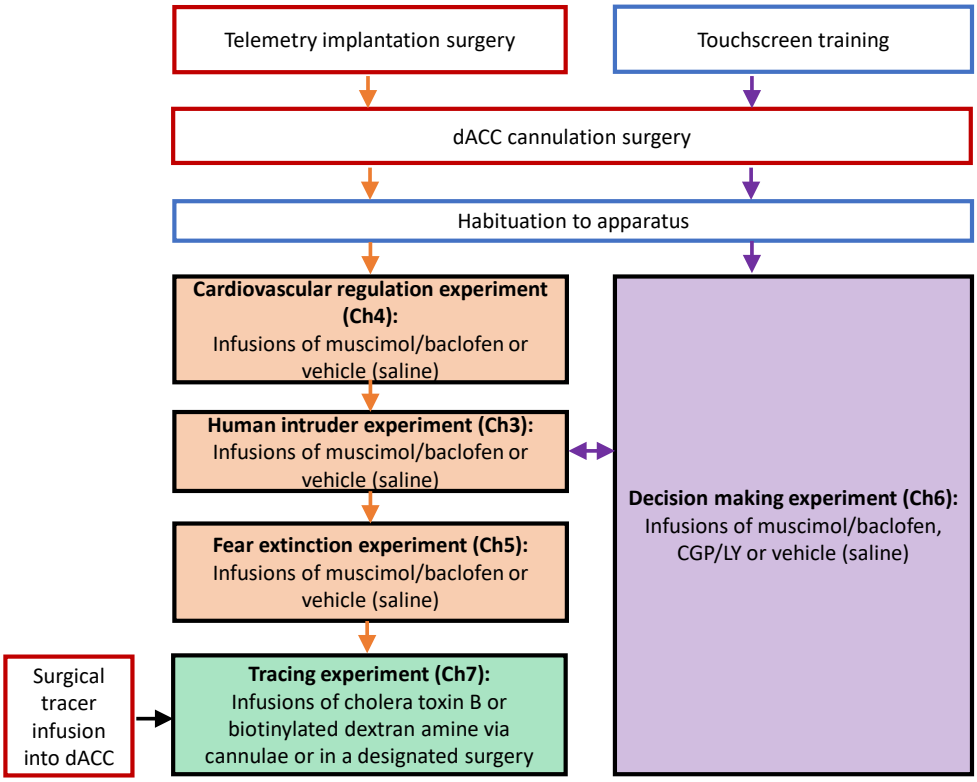

Figure 2.1 Summary of subject progression through experiments

2.3 Behavioural Testing Apparatus

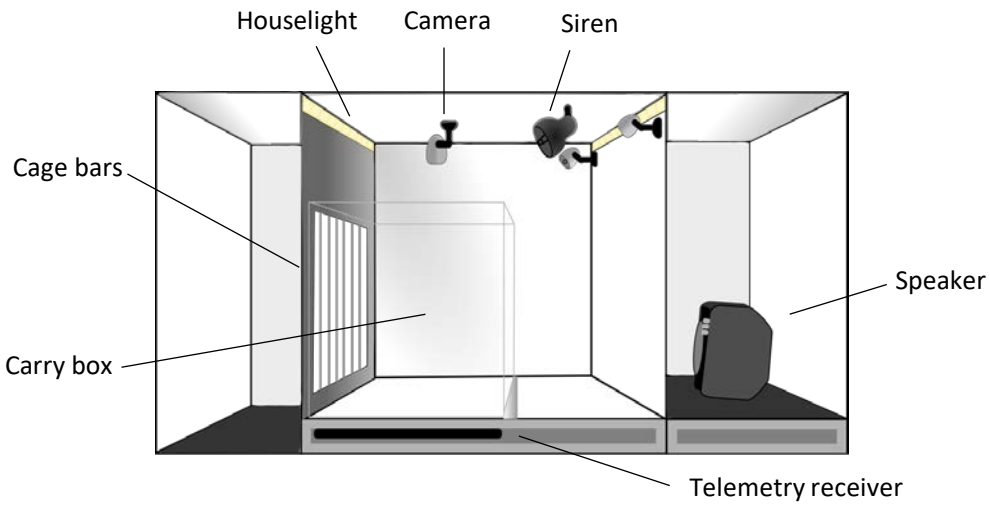

Figure 2.2 Labelled diagram of the front view of the behavioural testing apparatus

Testing for the baseline autonomic, fear extinction, and decision-making studies occurred in a custom-built, automated test apparatus, enclosed within a sound-attenuated box, and located in a designated testing room. Marmosets were first trained by positive reinforcement (marshmallow reward), to freely enter a transparent Perspex carry box (H 260x W 200x D 230mm) containing airholes and apertures for presenting marshmallows (Figure 2.3A). This was used to transport the test subject from the homecage to the behavioural apparatus into which it slotted (Figure 2.2). Prior to study onset, subjects were taken to the test apparatus with the houselight 'on' for 10-20min daily sessions, repeated at least 5 times to habituate them. Familiarisation with the apparatus was determined by evaluating behaviour across sessions such as relaxation of posture, reduced locomotion within the box and reduced vocalisations, and where possible (in subjects with implanted telemetry probes) reductions in heart rate and blood pressure. The human intruder test took place in the animal's homecage. Further details of the paradigms used in these studies will be described in the relevant chapters.

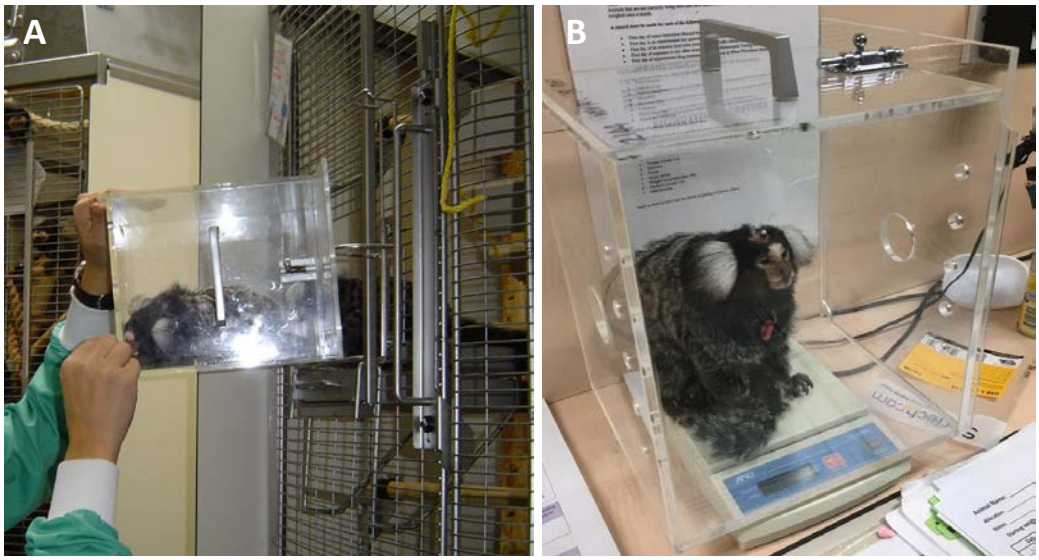

Figure 2.3 A. A marmoset being trained to enter the carry box using marshmallow as a positive reinforcer. B. A dACC cannulated marmoset (Banshee) being weighed in the carry box.

2.4 Surgery

2.4.1 Pre-surgical procedures

Marmosets were weighed at least once a week before a planned surgery and again the day before (Figure 2.3B). If the weight dropped by more than 5% of the first weight, surgery was postponed. Marmosets were not given any food for at least 12hrs prior to surgery to avoid likelihood of vomiting during surgery. In addition, one day prior to a telemetry implantation surgery, they were given prophylactic antibiotic treatment (Synulox; 0.1ml of a 50mg/ml solution, oral; Pfizer, Kent, UK).

All surgical tools and drapes were purchased in sterile pouches or were sterilised by autoclaving (Elara D table top autoclave; Tuttnauer Europe B.V., Breda, Netherlands) or using ethylene oxide. Sterile pouches were laid out in preparation for surgery but remained sealed until required for use. All surfaces in the pre-surgery and surgery areas were disinfected.

On the morning of surgery, the marmoset to be operated on was divided from its cage-mate and brought to the pre-surgery area. Here it was sedated with ketamine hydrochloride (Vetelar; 0.05 ml of a 100 mg solution, i.m.; Amersham Biosciences and Upjohn, Crawley, UK) and placed in a heated incubator while this took effect. Once the marmoset was sedated, it was placed on a heat mat and the area surrounding the incision site (for telemetry surgery, the abdomen from the base of the ribs to top of the inner thigh; for cannulation surgery, the scalp, avoiding ear tufts) was shaved. Hands and feet were also shaved to allow pulse-oximeter recordings to be taken. A long-lasting prophylactic analgesic was administered (Carprieve; 0.03ml of 50mg/ml carprofen, s.c.; Pfizer, Kent, UK) and the marmoset was taken with the heat mat to the surgery table.

2.4.2 Anaesthesia induction

Anaesthesia was achieved by administration of a mixture of vaporised isofluorane (Novartis Animal Health, Herts, UK) and O_2, using an anaesthetic machine (Compact Anaesthesia Systems, VetTech Solutions Ltd., Cheshire, UK). This was initially supplied at a flow rate of 4% isoflurane in $0.5 l min^{-1}$ O_2 using a facemask, held over the animal's mouth and nose. Anaesthesia was confirmed using O_2 saturation (95-100%), pulse rate readings (200-250) and assessing physical parameters including loss of the pedal reflex. Subsequently, the face mask was removed, and a topical anaesthetic was applied to the back of the throat (Intubeaze 20 mg/ml lidocaine hydrochloride spray; Dechra Veterinary Products Ltd., Shropshire, UK) and

the animal was intubated with an intra-tracheal tube. This was attached to the anaesthetic machine with anaesthesia maintained at ~2.5% isoflurane in 0.3 l/min O_2. Throughout anaesthesia, pulse-rate, O_2 saturation, respiratory rate, and CO_2 saturation, were monitored by pulse-oximetry and capnography (Microcap Handheld Capnograph, Oridion Capnography Inc., MA, USA) and core body temperature was monitored by a rectal thermometer (TES-1319 K-type digital thermometer, TES Electrical Electronic Corp., Taipei, Taiwan). Isofluorane percentage and the heat mat temperature were adjusted to maintain stable readings. 1.0ml of warmed saline (s.c.) was given every 60 minutes to prevent dehydration and the body was turned every 30 minutes to stimulate blood flow.

2.4.3 Telemetry implantation surgery

The marmoset was positioned on its back on a sterile drape placed on top of the heat blanket and in the centre of the surgery table. Sterile drapes were used to cover its legs and for placement of sterile surgical instruments. The abdomen was first cleaned with bactericidal povidone-iodine surgical scrub (Vetasept; Animalcare Ltd., York, UK) and then covered with an incision drape (Ioban 2 antimicrobial incision drape). A midline incision was made along the animal's abdomen using a surgical scalpel blade to cut through the skin and surgical scissors to cut through the muscle wall. Metal retractors were used to position the intestines to the sides of the abdominal cavity. The aorta was localised and pulled away from the vena cava and surrounding connective tissue using pressure swabs. A length of the aorta was cleared of fatty sheath and a piece of thread was clamped in place around the aorta close to the bifurcation. Pressure was applied to the aorta, as high up as possible, to occlude blood flow (for a maximum of 3 minutes to avoid paralysis of the lower limbs). The thread was tensed to cut off back flow of blood and an incision was made into the aorta. The vessel wall at the incision site was lifted using a vein pick, and then the catheter of the telemetry probe (PhysioTel implant, model PA-C40 or HD-S10; Data Sciences International (DSI), St. Paul, MN, USA) was inserted into the lumen of the aorta. The catheter was glued in place using 5µl tissue adhesive glue (Vetbond; 3M, UK). This was allowed to dry (a few seconds) before slowly releasing tension on the thread and pressure from the aorta to allow normal blood flow. A cellulose patch was positioned over the insertion site and more glue was applied.

The telemetry probe was tested to ensure it was detecting blood pressure by switching it on with a magnet and using a radio tuned to the appropriate frequency to pick up the transmitted signal. The thread was removed from around the aorta, the retractors removed, and the intestines repositioned. The body of the probe was placed on top of the intestines and the catheter looped around the side of the abdominal cavity. The muscle wall was sewn up in a continuous running stitch using a non-absorbable suture (3.0 Ethilon, polyamide 6, non-absorbable; Ethicon, Puerto Rico, USA). Half way through closure, the probe body was incorporated into the stitch to attach it to the muscle wall. The ioban drape was removed and the area beneath cleaned. Then the abdomen was covered with a sterile incision drape and the skin was sewn together using continuous sub-cutaneous suturing (3.0 Vicryl, polygactin 910, re-absorbable; Ethicon, Puerto Rico, USA). Tissue adhesive was applied along the line of incision, to completely seal it.

2.4.4 Stereotaxic surgery

The marmoset was positioned on its front on a heat mat and both were placed on a stereotaxic frame, specially modified for the marmoset (David Kopf, Surgical Instruments)(Figure 2.4). The marmoset's head was secured in place by inserting ear bars, positioning eye bars in the supraorbital foramen of the eye sockets, and a mouth bar against the roof of the mouth. Ophthalmic ointment (Lacri-lube; Allergan Inc., California, USA) was applied to the eyes to prevent desiccation. A sterile polythene operating cover (Buster Sterile Op Cover; VetTech Solutions Ltd.) was placed over the body of the marmoset. The head was wiped with bactericidal povidone-iodine surgical scrub (Vetasept; Animalcare Ltd., York, UK) and an antimicrobial incision drape (Ioban 2 Antimicrobial Incise Drape; 3M, Minnesota, USA) was then placed over it, also securing the operating cover. An incision was made down the midline of the scalp. A metal tissue spreader (eye speculum) was inserted to keep the skin and muscle apart, to keep the skull exposed.

A fine probe (Smooth Dental Broach; Micro-Mega, Besancon, France) was attached to the stereotaxic arm and this was used to take reference measurements. The anteroposterior (AP) zero coordinate, was taken at the interaural line as measured from the apex of the ear bars. The probe was then moved to AP +17.5 (all coordinates given in mm), and a dental drill (Dental Unit Polisher/Drill Unit II; Eickemeyer, Tuttlingen, Germany) with attached burr (Ash Steel Burs; Dentsply Ash Instruments, Surrey, UK) was used to drill a small trench across the midline (approximated by visible skull features) , to reveal the superior sagittal sinus. The lateromedial (LM) zero coordinate was taken at the centre of the superior sagittal sinus.

Figure 2.4 Back view of stereotaxic equipment with ear bars and a stereotaxic arm secured.

2.4.4.1 Standardisation of stereotaxic coordinates

To account for inherent individual variability in the size of the frontal lobes, a "depth check" was carried out for each marmoset and target coordinates were adjusted accordingly. This involved measuring the thickness of the brain at a standard reference co-ordinate (AP +17.5, LM -1.5), from the dorsal surface of the cortex to the base of the skull. A fine probe (Smooth Dental Broach; Micro-Mega, Besancon, France) was slowly lowered and a microscope (S5 Opmi-MD microscope; Carl Zeiss Ltd., Cambridge, UK) was used to determine the point at which a small lateralised movement of the probe occurred at the surface of the brain indicating that the tip of the probe had touched the base of the skull. If the depth was within the range 6.2-6.8mm, no adjustments were made to the target coordinates. If the depth was outside this range, further measurements were taken at 0.5mm intervals along the AP axis (anteriorly if the depth was >6.8mm, posteriorly if the depth was <6.2mm) until it was within range (Figure 2.5A). The total deviation from the reference coordinate was recorded and all target AP co-ordinates were adjusted by this amount.

In light of post-mortem histological assessment in the initial animals, which revealed variation in brain size within the cingulate region, a second depth check reading was introduced for the remaining subjects (Figure 2.5B). This second, "area 25 depth check" was taken at the level of area 25 near to the genu of the corpus callosum which is a closer

reference point to the target coordinates within the dACC and was recorded in the same way as above but at AP +14.0 / LM -1 with any prior adjustments from the original depth check applied to this. If the depth was within the range 8.9-9.1 mm, no adjustment was made. If the depth was outside this range, further measurements were taken in 0.5mm intervals along the AP axis (anteriorly if the depth was >9.1mm, posteriorly if the depth was <8.9mm) until it was within range. The total deviation from the reference coordinate was recorded and all subsequent AP coordinates were adjusted by the combined adjustments determined by the two depth checks.

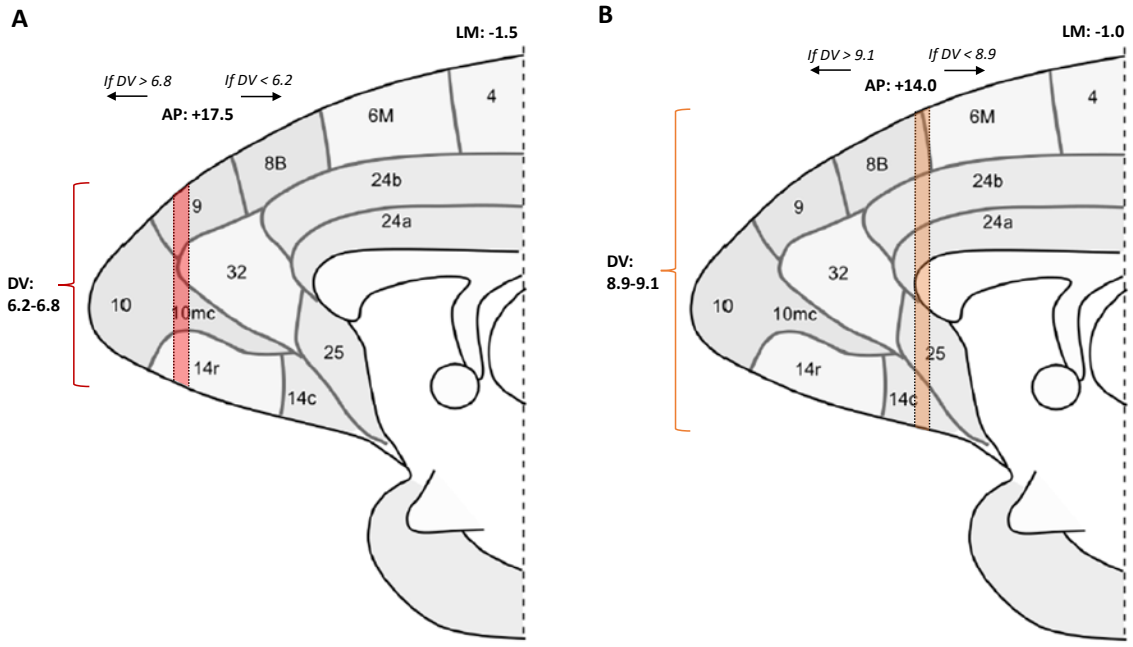

Figure 2.5 Schematic showing standardisation of stereotaxic coordinates. A. Original "depth check" B. "area 25 depth check". AP - anteroposterior from ear bars, LM -lateromedial from sagittal sinus, DV – dorsoventral from cortical surface. All coordinates given in mm (not to scale). Adapted from Burman and Rosa 2009.

2.4.4.2 dACC cannulation surgery

Bilateral guide cannulae with a 2mm centre to centre distance, extending 3.5mm beyond the pedestal (Plastics One, Roanake, VA, USA) (Figure 2.7A), were implanted at the depth-adjusted target coordinates (Figure 2.6;Table 2.2).

First, small holes were drilled into the skull at the target coordinates, using the dental drill and a needle was used to pierce the dura. Additional holes were manually made in the skull using a small hand drill and steel skull screws (0.80 x 1/16, Plastics One, Roanake, VA, USA) were attached into these using a screwdriver (Drill bit, drill holder and screwdriver; Plastics One). An adhesive (Super-Bond C&B; Sun Medical Co. Ltd., Shiga, Japan) was applied to the exposed surface of the skull and around the screws, with care taken not to let it enter the

craniotomies. This adhesive improved the bonding quality of the implant to the skull and protected the skull surface from the potentially damaging effects of dental acrylic. The rostral dACC site was implanted first, and for this the guide cannula (Figure 2.7A) was attached to the stereotaxic arm and this was rotated at an angle of 40^{o} anteriorly. The point at which the guide cannulae first touched the surface of the brain was taken as the dorsoventral zero coordinate, and from here the stereotaxic arm was slowly lowered to the initial surgical target depth (Table 2.2). If the pedestal sat proud of the skull with the guides exposed, the implant was lowered in 0.5mm increments until it sat just above the skull. This measurement was recorded and subsequently injector (Figure 2.7D) lengths were tailored according to this. Vetbond was applied to protect any exposed cortical surfaces near the cannula. Dental acrylic was applied over the skull screws and around the guide cannula to secure it in place. When this was dry, the guide cannula(e) was released from the stereotaxic arm, and the arm was carefully raised. The stereotaxic arm was returned to vertical for implantation of the second guide cannulae targeting the caudal dACC site, carried out as above. When both cannulae guides were secured, dental acrylic was applied to join the two sites with a smooth surface. After fully dry, the skin around the cannulation site was sewn together using single sutures (3.0 Vicryl, polygactin 910, re-absorbable, Ethicon, Puerto Rico, USA), to promote closure of the incision sites anterior and posterior to the implant in order to protect the skull surface. Sterile dummy injectors (Figure 2.7B;Plastics One, Roanoke, VA, USA) were then inserted into the guide cannulae to maintain patency and metal caps (Figure 2.7C; Plastics One, Roanoke, VA, USA) screwed on top for protection. A liquid plaster (Germolene New Skin; Perrigo, Devon, UK) was applied to the line of sutures and the animal was taken out of the stereotaxic frame. Marmosets were given dexamethasone (i.m., 0.2ml), prophylactically to prevent any brain swelling.

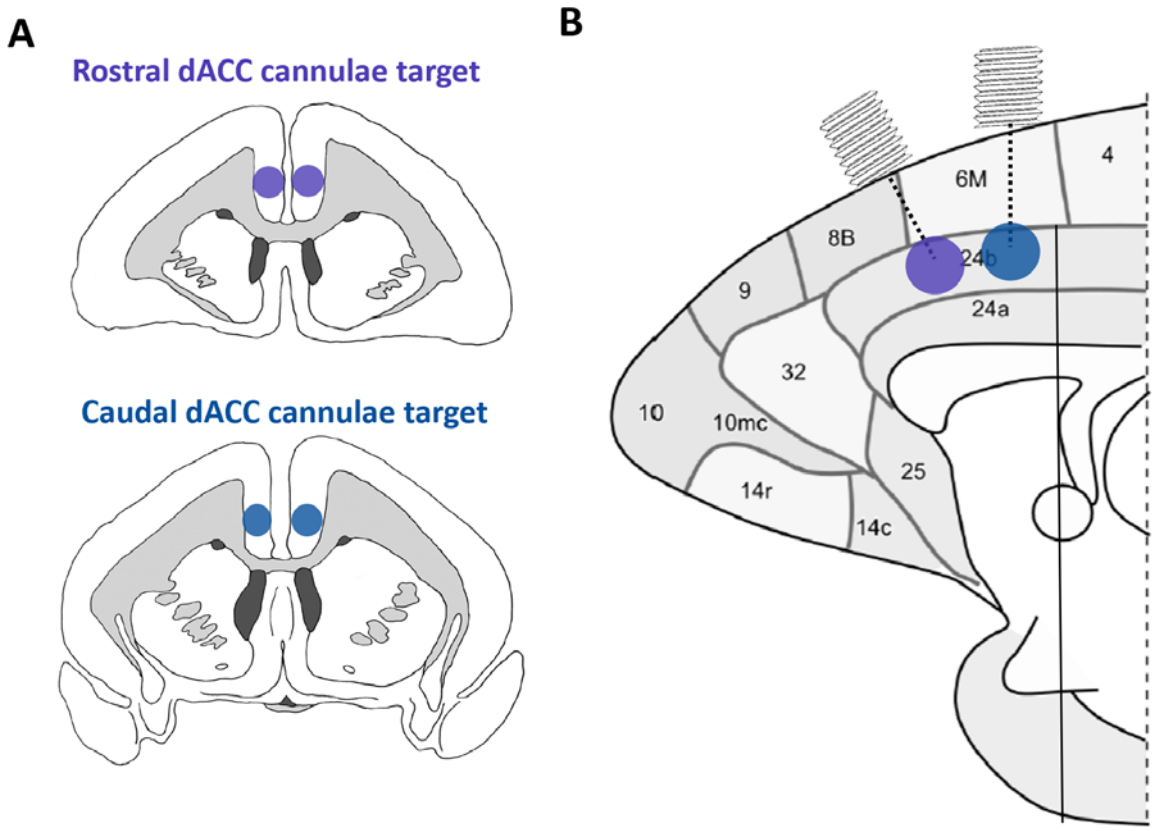

Figure 2.6 Schematic of cannulae target sites in the rostral and caudal dACC. A. Coronal view (hand drawn sections matched to the marmoset stereotaxic atlas (Paxinos and Watson, 2012); B. Sagittal midline section (adapted from Burman and Rosa 2009).

Table 2.2 Cannulae plus injector target coordinates. AP from ear bar, LM from sagittal sinus, DV from cortical surface (including injector projection).

Cannulae targets	**Target coordinates (mm)**		
	AP	**LM**	**DV**
Rostral dACC	+13.5	±1	-3.3
Caudal dACC	+11.0	±1	-3.8

2.4.5 Post-surgical care

The vaporiser was switched off and the marmoset allowed to regain consciousness. The intra tracheal tube and rectal thermometer were gently removed. O_2 was given via the anaesthetic tube until the marmoset was able to maintain O_2 saturation >98% unaided. The animal was placed in a heated incubator to recover from anaesthesia. The marmoset was closely monitored, with checks made at least every 15mins for the first hour after being placed in the incubator and at least every 30mins thereafter. Water and food were introduced after 1-2hrs.

The researcher determined when the marmoset had fully recovered from anaesthesia taking things like muscle tone, alertness, and interest in food into account. This usually occurred within 2 hours of surgery finishing, and at this point the marmoset was returned to its homecage. Observation continued until the researcher was satisfied that the marmoset was able to be left without further monitoring.

All animals were given an analgesic (Metacam, 0.1 ml of a 1.5 mg/ml oral suspension; Boehringer Ingelheim, Germany) for 3 days post-surgery. After telemetry surgery animals were additionally given antibiotic (Synulox; 50mg/ml solution, Pfizer, Kent, UK) on the day and for 7 days post-surgery.
Cannulation sites were cleaned, and dummy injectors and caps were changed for clean sterile ones at least once weekly to avoid occurrence of infection.

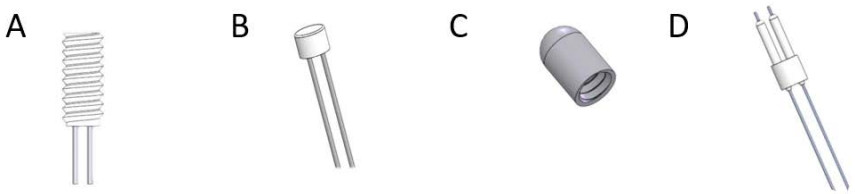

Figure 2.7 Cannulae components. A. bilateral guide cannula, B. dummy injector C. metal dust cap D. Injector. Diagrams from PlasticsOne online catalogue.

2.5 Intracerebral infusions

Intracerebral infusions were carried via the guide cannulae to temporarily inactivate (Chapters 3,4,5,6) or activate (Chapter 6) the target subregion of the dACC to assess the effect on behaviour. Drug or vehicle (control condition) was infused at a specified time before task onset (Table 2.3). No more than one drug infusion was carried out per week.

2.5.1 Drug preparation

Drug powders (Sigma-Aldrich, Missouri, US) were prepared as solutions in advance. They were dissolved in vehicle to the correct concentration, filtered for sterility and stored as aliquots in sterile eppendorfs at -20°C.

Pharmacological inactivation: 0.1mM muscimol/1.0mM baclofen (mb)

Muscimol - a selective $GABA_A$ receptor agonist which acts to reduce neuronal activity. The $GABA_A$ receptor is an ionotropic Cl^- channel, and activation of it causes Cl^- influx and neuronal hyperpolarization.

Baclofen - a selective $GABA_B$ receptor agonist, which acts to reduce neuronal activity. The $GABA_B$ receptor is a metabotropic $G_{i/o}$-protein coupled receptor, and activation of it causes neuronal hyperpolarization through a signalling cascade involving inhibition of adenylyl cyclase, downregulation of protein kinase A and subsequent activation of inward rectifying K^+ channels.

This drug mixture has previously been used in the Roberts laboratory to transiently inactivate regions of the prefrontal cortex in the marmoset in order to assess behavioural effects (Clarke et al., 2015; Wallis et al., 2017). Histological analyses of drug (muscimol) infusion spread into rat cerebral cortex has shown that this is localised to 0.5–1 mm from the injection site and unlikely to extend beyond the targeted region (Allen et al., 2008; Eddy et al., 2016).

Pharmacological activation: 100pg/µL CGP52432/ 10ng/µL LY341495 (CGP/LY)

CGP52432 is a selective $GABA_B$ receptor antagonist (Lanza et al., 1993)

LY341495 is a preferential $mGluR_{2/3}$ antagonist (Schoepp et al., 1999). Group 2 and 3 metabotropic glutamate receptors are involved in signalling cascades that cause presynaptic inhibition.

This drug mixture has been shown to enhance presynaptic glutamate release thereby causing pharmacological activation (in hippocampal slices), and causes an anxiolytic effect in rats when infused into the hippocampus (Marrocco et al., 2012). This drug mixture has previously

been used in marmosets in the Roberts laboratory and with the infusion parameters shown (Table 2.3) has produced behavioural effects (unpublished).

Table 2.3 Cerebral drug infusion parameters

Drug	Infusion rate	Volume infused	Wait time	Effect
mb	0.25 µl/min	0.50 µl (in 2mins)	20-25mins	Inactivation
CGP/LY	0.50 µl/min	1.00 µl (in 2mins)	15-20mins	Activation

2.5.2 Intracerebral infusion procedure

2.5.2.1 Infusion set up

All infusions were carried out in a designated minor procedures room, using sterile (autoclaved/ethylene oxide-exposed) equipment where possible. The table surface and infusion pump (Kd Scientific, Massachusetts, USA) were wiped with disinfectant. A sterile drape was laid out and the sterile infusion equipment was set up on this (Figure 2.8). Two gastight Hamilton syringes (10µl, Sigma-Aldrich, Missouri, USA) were filled with saline (sodium chloride 0.9% w/v; Hameln Pharmaceuticals Ltd., Gloucester, UK) and attached to a double injector of the appropriate length (determined from surgery coordinates based on the depth of the guide cannulae). This was done using PTFE tubing (inner diameter 0.3mm, VWR International Ltd, UK) connected to the syringe on one end and the injector on the other end with solva tubing (inner diameter 0.38mm, Pulse Instrumentation, Wisconsin, USA) adapters. The tubing and injector were flushed and filled with saline before being connected to the Hamilton syringes to ensure an air-tight set up. The Hamilton syringes were placed in the infusion pump and the plunger of each syringe was manually depressed to push out saline at the tip of the injector. The plungers were immediately pulled back to load a small amount of air into the tubing. The injector was then submerged in drug or vehicle solution and this was back-loaded into the tubing. The air bubble was marked, and its movement was used to indicate a working infusion set up.

2.5.2.2 Infusion procedure

The test marmoset was divided off from its cage partner, and into the top right quadrant of the homecage. One researcher acted as an assistant and in this role caught the marmoset whilst wearing protective handling gloves with disposable nitrile gloves underneath. The handling gloves were removed, and the marmoset was transferred into a secure one-handed grip in

which the index finger wound over the marmoset's shoulder and the thumb and other fingers beneath the arms and around the body. The marmoset was then taken to the minor procedures room where the experimenter was waiting with infusion set-up prepared. First the experimenter removed the caps and dummy injectors from the guide cannulae and cleaned the cannulation site using 70% alcohol wipes. Next, using sterile gloves the injectors were carefully inserted into the guide cannula and the microinfusion pump was switched on for two minutes (Table 2.3). The injectors were left *in situ* for a further minute after the infusion to allow for diffusion. The injectors were removed, and fresh sterile dummy injectors and caps were inserted in the guide cannulae.

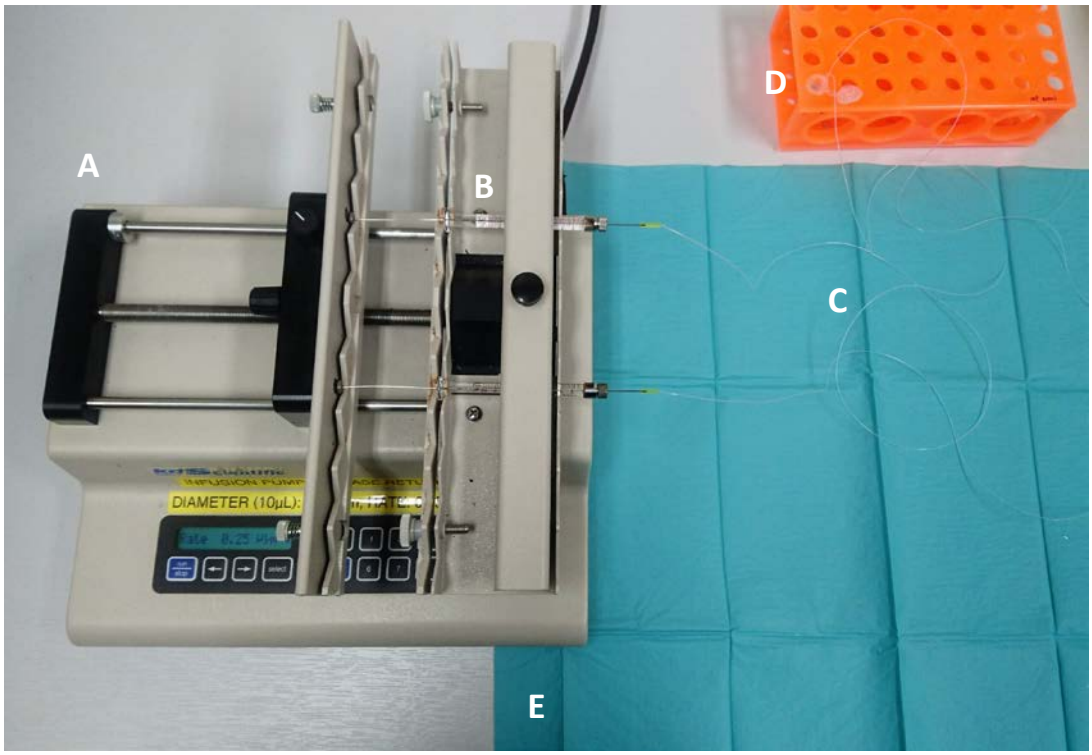

Figure 2.8 Infusion apparatus set up. Infusion pump (A) with saline filled Hamilton syringes (B) inserted, connected via PTFE tubing (C) to an injector submerged in vehicle solution (D). Infusion apparatus was set up on a sterile drape (E).

The assistant returned the animal to the home cage and dividers were removed. Prior to real infusions, numerous "mock infusions" were carried out to habituate animals to being caught and to the whole infusion procedure. This was carried out in exactly the same way as a real infusion except rather than inserting infusion injectors, dummy injectors were changed.

2.6 Telemetry data collection

Blood pressure data were recorded in the baseline autonomic and fear extinction studies. The implanted telemetry probe was switched on using a magnet prior to placing the carry box in the test apparatus. This continuously detected blood pressure from the marmoset and transmitted it using radio-frequency signals to a receiver (RPC-1; DSI) located beneath the behavioural testing chamber (Figure 2.2). An ambient pressure reference monitor (APR-1; DSI) and calibrated pressure output adapter (R11CPA;DSI), converted the absolute pressure received into a gauge pressure measured in millimetres of mercury (mmHg). These signals were sampled at a rate of 100Hz through an analogue-to-digital convertor (Micro 1401; Cambridge Electronic Design (CED), Cambridge, UK) and recorded onto a PC using data acquisition software (Spike2 Version 8;CED). Data were stored offline for further analysis.

Systolic and diastolic blood pressure events were extracted from the blood pressure trace as local maxima or minima respectively. Interbeat intervals (IBIs) were measured as the time interval between successive systolic blood pressure events and heart rate was derived from this (HR = IBI/60). Data were processed to remove outliers (values outside the pressure range 20-200mmHg, and the IBI range of 0.1-0.4).

2.7 Euthanasia

To euthanise, the marmoset was first premedicated with ketamine hydrochloride (Vetalar, 0.05mL of a 100mg/mL solution, i.m; Pharmacia and Upjohn), then administered with sodium pentobarbital (Dolethal, 1 ml of 200mg/ml solution, i.v in femoral vein; Vetoquinol UK Ltd, Buckingham, UK). A stethoscope was used to confirm the heart had stopped beating. The marmoset was taken to the post-mortem room for perfusion.

2.8 Perfusion and histology

Marmosets were transcardially perfused, with 400mL of 0.1M PBS, followed by 400mL of 10% neutral buffered formalin ((Sigma-Aldrich, Missouri, US) as a fixative over ~20min. The entire brain was then dissected and placed in fixative solution for 12-24hrs. The brain was transferred to a 30% sucrose/0.1M PBS solution for at least 48h for cryoprotection. The brain was frozen using crushed dry ice and mounted on a freezing microtome. Coronal brain sections (60μm) were taken and stored in well plates filled with 0.01M PBS. Every third section was mounted on to microscope slides and stained with Cresyl Fast Violet (Sigma-Aldrich, Missouri, US). Stained sections were viewed under a Leitz DMRD microscope (Leica Microsystems, Wetzlar, Germany) to verify cannulae placements.

2.9 Statistical analysis

Data were organised using Microsoft Excel 2013. Statistical analyses were carried out using, GraphPad Prism version 7.03 (GraphPad Software Inc., California, US) and the statistical language and environment R (version 3.4.2) (R Core Team, 2017) with the R Studio interface (version 1.1).

3 | THE ROLE OF THE dACC IN THE REGULATION OF RESPONSES TO AN UNCERTAIN THREAT

3.1 Introduction

An excessive response to uncertain threats is considered a common feature across anxiety disorders (Grupe and Nitschke, 2013). Uncertainty creates potential conflict between competing motivational drives and this distinguishes anxiety from fear, in which there is more certainty regarding the nature and timing of threat.

Studies in rodents have used a range of tasks to assess anxiety, with classical tasks (those developed before 1985) still predominating research (Haller et al., 2013). The most commonly used are exploratory-based tasks, including the open field test and elevated plus maze (EPM). These generate conflict between the drive to approach and explore novel areas and to avoid potential threats, exploiting rodents' natural aversion to open spaces. The former measures time spent in the centre of the field, and the latter, time spent in the exposed arms of the maze. Less time spent in these locations is associated with increased anxiety. However. findings in rodent are conflicting and difficult to extrapolate to human due to controversy surrounding regional homologies. Electrolytic lesion of the PL, the putative functional homologue of the dACC (Milad and Quirk, 2012), increased anxiety in both the open field and the EPM tasks (Jinks and McGregor, 1997). However, this lesion technique does not spare fibres of passage. Excitotoxic lesions, and temporary inactivation of the mPFC, using muscimol, instead have shown an anxiolytic effect across a range of tasks (Shah and Treit, 2003; Shah et al., 2004), but these targeted a large area including IL, PL and AC. Later studies, involving temporary inactivation specifically of the PL found an anxiolytic effect on the EPM (Stern et al., 2010). Excitotoxic lesions targeted to the rostral AC, the putative cytoarchitectural homologue of dACC, had no effect on the EPM, but did have a pro-depressant effect on a task involving helplessness (modified forced swim test) (Bissiere et al., 2006). These findings suggest that

the PL is involved in anxiety while the AC is involved in other aspects of emotion regulation. However, the predictive validity of these classical tasks of anxiety is poor and despite extensive preclinical research into anxiety in rodents, including the development of novel tasks, this has seldom translated into discovery of clinically effective anxiolytics (Griebel and Holmes, 2013; Haller et al., 2013).

Non-human primates (NHPs) show much greater similarity to humans than rodents do, in relation to brain structure, behaviour and physiology (Coleman and Pierre, 2014; Miller et al., 2016), supporting their use to study the neurobiology of anxiety. Human threat has been widely used to provoke anxiety in various primate species including the macaque and the common marmoset (Barros and Tomaz, 2002; Kalin, 2004). In the human intruder test (HI Test) an unfamiliar human "intruder" enters the room and stands in front of the animal while its behavioural responses are recorded. Although experimentally reared animals are accustomed to human interactions, these could be positive such as when food treats are offered, or they could potentially be aversive, such as when drugs need to be administered. Thus, the intent of an unfamiliar human is uncertain and can induce approach-avoidance conflict.

Kalin and colleagues have used the HI Test in a series of experiments investigating anxious temperament in rhesus macaques (Kalin, 2004; Kalin and Shelton, 1989; Kalin et al., 2001, 2005). In their version of the paradigm, the subject is taken out of the home-cage to a socially isolated, novel test room, where it is alone for a short period of time, before an intruder enters and presents their profile without making eye contact, in what is described as the human intruder no eye contact condition (NEC) (Kalin and Shelton, 1989; Kalin et al., 2005). In macaques, direct eye contact is an unambiguous threat, and thus the 'no eye contact' condition is used to increase uncertainty and provoke anxiety (Kalin et al., 2005; Machado and Bachevalier, 2008). They have shown that in infant macaques anxiolytic compounds reduced freezing and defensive behaviours (Kalin and Shelton, 1989) and that an anxiogenic compound did the opposite (Kalin et al., 1992). Furthermore, in adult macaques, increased freezing during the NEC compared to the alone condition correlated with increased activity of caudal area 24c of the dACC, as well as regions of the lateral thalamus and brainstem, measured by FDG uptake, suggesting that these regions are involved in the contextual regulation of freezing behaviour (Kalin et al., 2005). The relatively caudal dACC region involved, has direct projections to regions involved in motor activity which may explain this role.

The HI Test (or "human threat test") was first carried out in marmosets by Costall and colleagues and subsequently validated by Carey and colleagues for its ability to induce defensive anxiety-related behaviours based on previous ethological descriptions of marmoset behaviour (Carey et al., 1992a; Costall et al., 1988; Stevenson and Poole, 1976). In addition, a significant increase in plasma cortisol immediately following threat was reported, indicating activation of the stress response (Ash et al., 2018; Carey et al., 1992a). Marmosets differ to macaques in that they do not exhibit freezing responses to human threat but a range of defensive responses. Behavioural responses on this task, most consistently time spent at the front of the cage, are sensitive to clinically effective anxiolytic agents such as diazepam as well as serotonergic agents and thus the HI Test shows predictive validity (Barros and Tomaz, 2002; Cagni et al., 2009; Carey et al., 1992a; Costall et al., 1988, 1992). Although, typical anxiogenic (FG7142, caffeine) agents did not appear to modify behaviour (Carey et al., 1992a), in the Roberts laboratory anxiogenic like responses have been observed in response to manipulations (see below) indicating that the task is sensitive to both reductions and increases in anxiety(Agustín-Pavón et al., 2012; Santangelo et al., 2016).

The Roberts laboratory has developed their own version of the HI Test based on the marmoset human threat test (Agustín-Pavón et al., 2012; Carey et al., 1992a; Shiba, 2013). Following an initial 8-minute separated condition, in which the subject is divided away from its cage-mate into a quadrant of its home-cage, a 2-minute intruder phase occurs in which an unfamiliar human enters the room, stands 40cm in front of the subject's cage and makes direct eye contact. Unlike macaques, marmosets do not exhibit gaze avoidance behaviour and thus direct eye contact is thought to be less of an overt threat, but still likely anxiety provoking (Mitchell and Leopold, 2015). Using this paradigm, excitotoxic lesions of the vlPFC and anterior OFC(Agustín-Pavón et al., 2012), caused behavioural responses opposite to those of anxiolytics, indicating an anxiety-like response. In addition, a positive correlation between marmoset pgACC/rdACC volume and proportion of time spent at the front zone of the cage (TSAF) has been reported (Mikheenko et al., 2015). Anxiolytic drug treatment has previously been shown to increase TSAF in the HI Test (Carey et al., 1992a), suggesting that decreased volume of this region is associated with increased anxiety.

In humans, reduced pgACC/rdACC volume has been reported in anxiety disorders including panic disorder and PTSD (Asami et al., 2008; Radua et al., 2010). Thus, structural changes in the rdACC in both marmosets and humans appear to contribute to anxiety, with lower volumes being unfavourable.

To summarise, correlational studies in non-human primates have implicated two different subregions of the dACC in the regulation of anxiolytic (rdACC) and anxiogenic (cdACC) responses to human threat, however the specific functional contributions of these regions have not been causally examined, rather structural changes of the rdACC, and activity of the cdACC have been associated with anxiety. Given that abnormalities of similar regions have also been described in anxiety disorders in humans, casual studies of the roles of these regions in anxiety could give us insights into these disorders. Thus, the aim of this study is to determine the functional contributions of the rdACC and cdACC to anxiety using the HI Test, a well-validated test involving uncertain threat.

3.2 Methods

3.2.1 Subjects

A total of twelve marmosets took part in this study. (Table 2.1). Of these, ten had completed the baseline autonomic study and two were undergoing touchscreen training (Jumbee and Buttercup). All had previously received dACC cannulation surgery.

3.2.2 Human intruder test (HI Test) paradigm

This test was carried out in the marmoset's home-cage. The test subject was separated from its partner by dividing it into the top right quadrant of the cage, and the partner in the bottom left quadrant. A video camera and microphone were set up in the holding room and directed at the test subject to record behaviour. After 8 minutes of this "separated" condition, an experimenter, the "human intruder", entered the room and stood in front of the cage (40cm), and where possible made direct eye contact with the subject for 2mins (intruder phase) (Figure 3.1A). The intruder then quietly left the room, and the subjects behaviour was recorded for a further 5mins (post-intruder phase). At the end of recording (15 minutes total), the recording apparatus was packed away and the dividers removed from the home-cage.

The HI Test was carried out five times per subject with a minimum of 7 days between consecutive tests. This repeated measured design allowed for separate infusions of saline (control) and mb into each cannulated area and a final control infusion to test for habituation, carried out 20 minutes prior to test onset. The intruder wore a white laboratory coat, laboratory gloves, blue scrub trousers, and wore one of a set of life-like human masks (Figure 3.1C) to disguise themselves and thus appear to be a novel human intruder. The order of infusions and masks was counterbalanced between subjects.

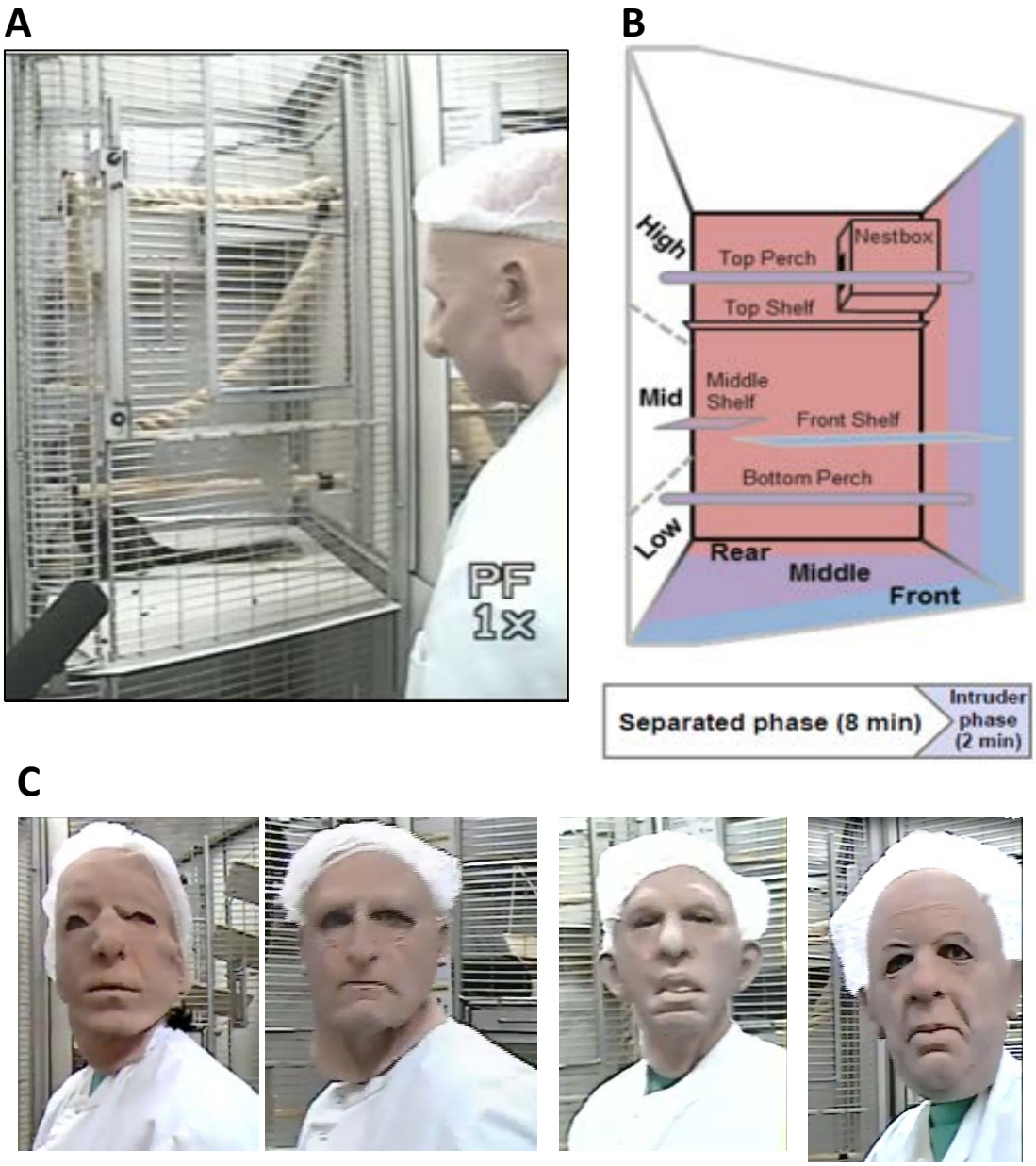

Figure 3.1 The HI Test. ***A*** *Video still during intruder phase of the HI Test.* ***B.*** *Schematic of top right quadrant of homecage (i.e. test quadrant) showing division into zones for height and depth (adapted from Santangelo et al. 2016)* ***C*** *Video stills showing the different masks used by the human intruder as a disguise.*

3.2.3 Behavioural scoring

A quantitative behavioural analysis program (Jwatcher V1.0) was used to score a range of different behaviours during the 2 min intruder phase from playback of video recordings of the HI Test sessions:

1. Distance measures

   The proportion of time spent in each depth zone and height zone (Figure 3.1B) was scored. The average height was calculated by multiplying the proportion of time spent in each height zone by the middle point in cm of that zone from the floor of the quadrant (Figure 3.2) .

2. Locomotion

   The proportion of time spent in locomotion, defined as translational movement in which all four limbs changed location, was scored.

3. Head and body bobs

   The number of head and body bobs, a marmoset behaviour indicative of anxiety, were counted (Agustín-Pavón et al., 2011; Carey et al., 1992b; Santangelo et al., 2016).

4. Jumps forward

   The number of jumps forward (towards the intruder), an approach behaviour, were counted.

   In addition, the number and type of vocalisations made during the intruder phase were scored. Audio editing software (Audacity, ver. 1.3.13, http://audacity.sourceforge.net/) was used to extract audio from the video recordings and this was converted into a waveform (Syrinx, V2.6h). Calls were classified as tsik, tsik-egg, egg, tse or tse-egg based on differences in sound, length and frequency range (Figure 3.3) (Bezerra and Souto, 2008).

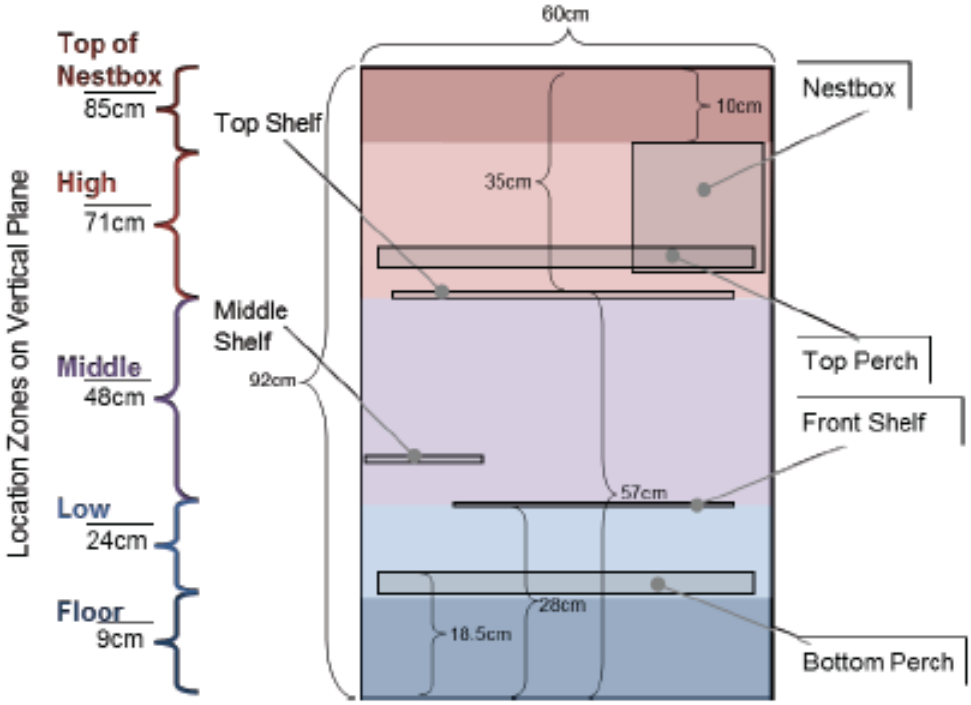

Figure 3.2 Front view of the HI Test quadrant with the dimensions of furniture within and the middle points of the height zones (figure from Santangelo et al. 2016 Supplementary methods). Note "top of nestbox" is only scored when the marmoset is physically on top of the nestbox, other positions in this zone are scored as "high".

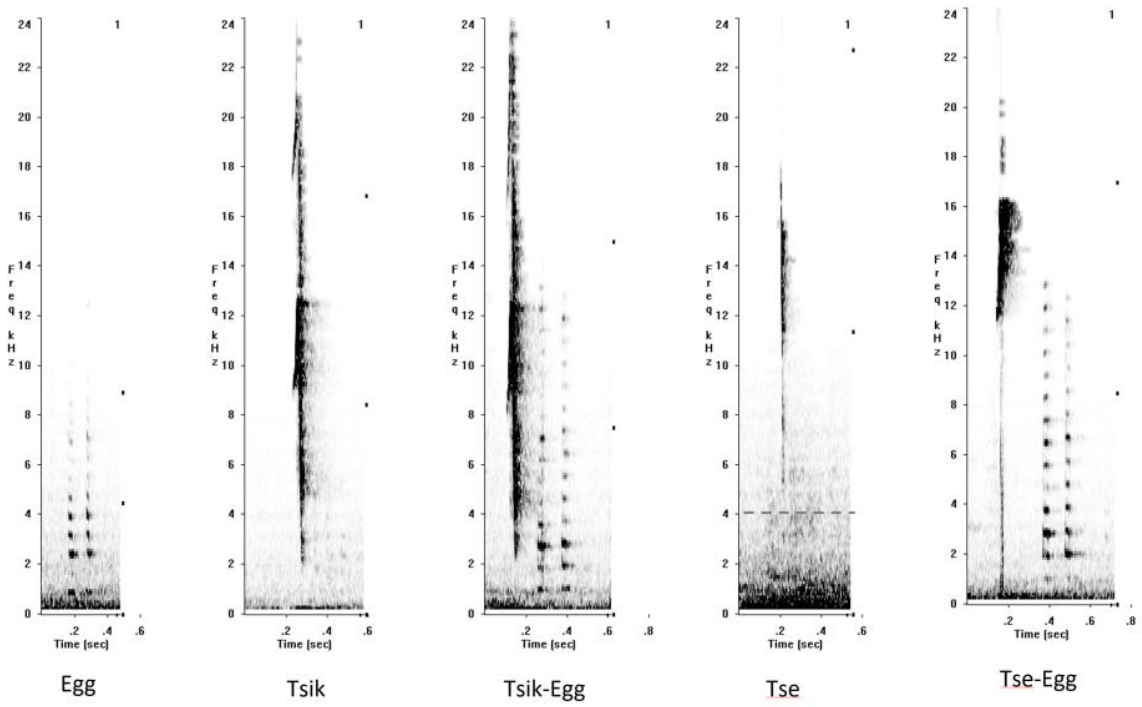

Figure 3.3 Sonogram excerpts showing characteristics of each vocalisation. The tse call differs from tsik in that the frequency does not go below 4kHz (shown by dotted line). Figure from Santangelo et al. 2016, supplementary methods.

3.2.4 Data analysis

An exploratory factor analysis (EFA) with a principal axis factoring extraction method has been performed on HI Test scores from sessions carried out as part of a screening procedure on 161 naïve marmosets from the colony (Shaun Quah, unpublished data). This model predicts the extent to which the different behaviours in the human intruder test are driven by an underlying latent variable, e.g. anxiety. Initial runs of the exploratory factor analysis included: proportion of TSAF and time spent at the back of the cage, average height, proportion of time spent on locomotion, number of bobs, number of jumps towards the human intruder, egg calls, tsik call, tsik-egg calls, tse calls, and tse-egg calls. Instead of average depth, the proportion of time spent at the front and the back of the cage were used, as these measures reflect approach and avoidance movements respectively. Tse calls were removed from the exploratory factor analysis as its measure of sampling adequacy was below the standard of .5 defined in Field, 2009 (MSA = .435). The Kaiser-Meyer-Olkin measure of sampling adequacy for the final model verified the sampling adequacy for the analysis, KMO = .84 ('great' according to (Hutcheson and Sofroniou, 1999)). Bartlett's test of sphericity was significant (χ^2 (45) = 486.70, $p < .001$), indicating that correlations between items were sufficiently large for a factor analysis. Due to the low level of communalities after extraction, the scree plot was consulted to decide the number of factors to extract instead of using

Kaiser's criterion (Field, 2013). Only 1 factor was extracted based on the point of inflexion on the scree plot (Figure 3.4). This factor accounted for 38.9% of the variance. There were 18 (40.0%) nonredundant residuals with absolute values greater than 0.05, below the recommended value of 50%, reflecting that our one factor model is a good fitting model. The pattern in which the items cluster on this factor suggest that this factor represents the animal's anxiety towards the human intruder (Table 3.1) .

Table 3.1 Factor loading of each measure extracted from the EFA

Measures	**Factor loading (Anxiety)**
Time spent at front (proportion)	**-0.77**
Time spent at back (proportion)	**0.67**
Average Height	**0.83**
Locomotion (proportion)	**-0.58**
Bobs	**0.79**
Jumps	**-0.52**
Egg calls	**0.33**
Tsik-egg calls	**0.35**
Tse-egg calls	**0.42**
Tsik calls	**-0.10**

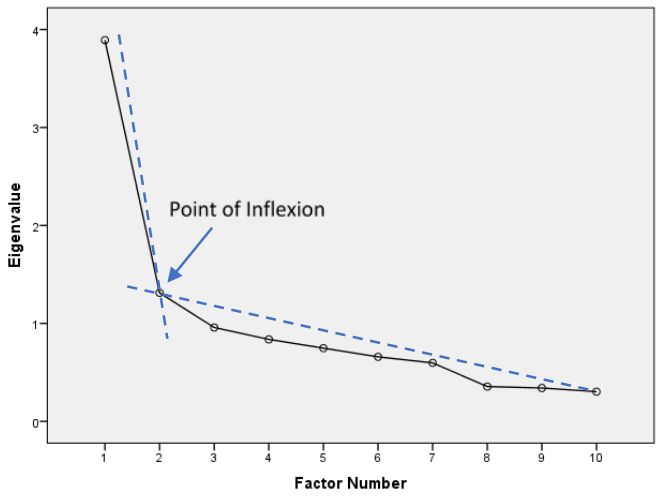

Figure 3.4 Scree plot

Table 3.2 shows the factor coefficient matrix from the final output of the EFA, revealing the measures that load on to the factor. Scores for each HI Test session for the subjects included in this study were standardised (z-score) using the mean and standard deviation for the HI Test scores from the laboratory cohort to provide an overall measure of anxiety.

Table 3.2 Output of exploratory factor analysis showing measures that are affected by anxiety. Also shown are the mean and SD of each of these measures taken from the laboratory cohort, used to standardise measures from individual sessions.

Measures	**Coefficient**	**Mean**	**SD**
Time spent at front (proportion)	**-0.24**	0.31	0.25
Time spent at back (proportion)	**0.16**	0.30	0.29
Average Height	**0.33**	57.93	15.30
Locomotion (proportion)	**-0.11**	7.98	6.66
Bobs	**0.26**	21.84	22.64
Jumps	**-0.09**	2.93	2.93
Egg calls	**0.05**	9.21	10.19
Tsik-egg calls	**0.05**	9.83	16.67
Tse-egg calls	**0.06**	11.49	14.85
Tsik calls	**-0.01**	2.76	7.66

3.3 Results

3.3.1 Determining cannulae placements within the dACC

Cannulae placements have been determined for eight of the twelve marmosets that took part in this study by post-mortem histological assessment of cresyl Fast blue stained coronal sections (2.8). This revealed huge variation in brain size and within the cingulate region which made it difficult to determine cannulae location by schematising on to drawings of standard marmoset brain coronal sections and creating composite diagrams as has been done previously (Clarke et al., 2015), highlighting a need to establish additional anatomical landmarks to determine the location of the cannulae. This was especially important considering there are no reported differences in cytoarchitecture in the anterior-posterior direction of area 24 (Burman and Rosa, 2009; Paxinos et al., 2011). Thus, in order to establish cannulae placements objectively, a number of anatomical landmarks were identified on each subject's cresyl-stained series of sections through area 24 and the absolute distances between each of these and the anterior cannulation site (site 1) and posterior cannulation site (site 2) were calculated (Figure 3.5). Of these anatomical landmarks, the appearance of the lateral septum (LS) and the disappearance of the islands of Calleja (IC) were taken as an anterior cingulate marker and posterior cingulate marker respectively. Since the absolute distance between the LS and IC disappearance ranged from 900-1620μm (±100), reflecting the inter-individual variability in brain anatomy in this region, the distances between each cannulation site and the LS and IC were standardised to the total distance between the LS and IC disappearance (IC-) for each marmoset (Figure 3.6). Based on this analysis four topographically distinguishable dorsal cingulate regions were identified in which cannulae sites occurred. Using the following criteria; perigenual ACC (pgACC) - site very anterior to LS; rdACC – site at a similar level to the LS; mdACC – site located behind the LS but very anterior to IC- ; cdACC – site located close to or posterior to IC-. The remaining four marmosets are still undergoing experimentation and thus their data is grouped according to predicted placements based on their surgical coordinates. Unlike the earlier animals, the "area 25 depth check" (2.4.4.1) was used in the surgeries of these final four marmosets, as an additional procedure to more accurately correct for individual variation in brain size within the cingulate region. The location of the anterior and posterior cannulation site for each subject based on this analysis is shown in Table 3.3. Although the pgACC and mdACC were not a priori planned regions of interest, a sufficient number of animals were had cannulae sites located in these regions and thus results from these regions were included in some of the analysis.

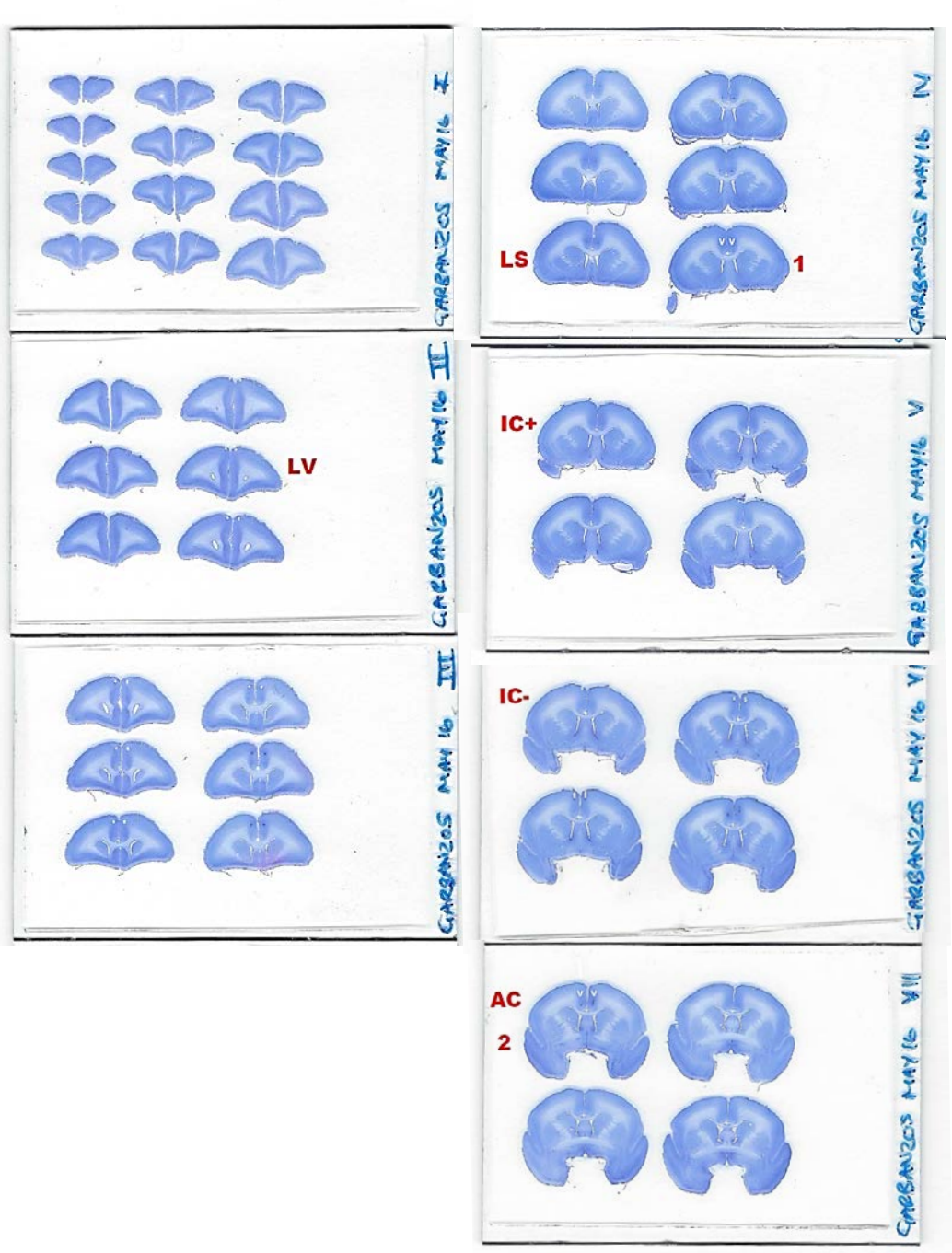

Figure 3.5 Example of a series of stained coronal sections, from a dACC cannulated marmoset (Garbanzos), with labelled anatomical landmarks. (LV = lateral ventricles, LS=lateral septum, 1 = anterior cannulation site, IC+ = appearance of islands of Calleja, IC- = disappearance of islands of Calleja, AC = anterior commissure, 2 = posterior cannulation site. White arrow heads show injection sites.

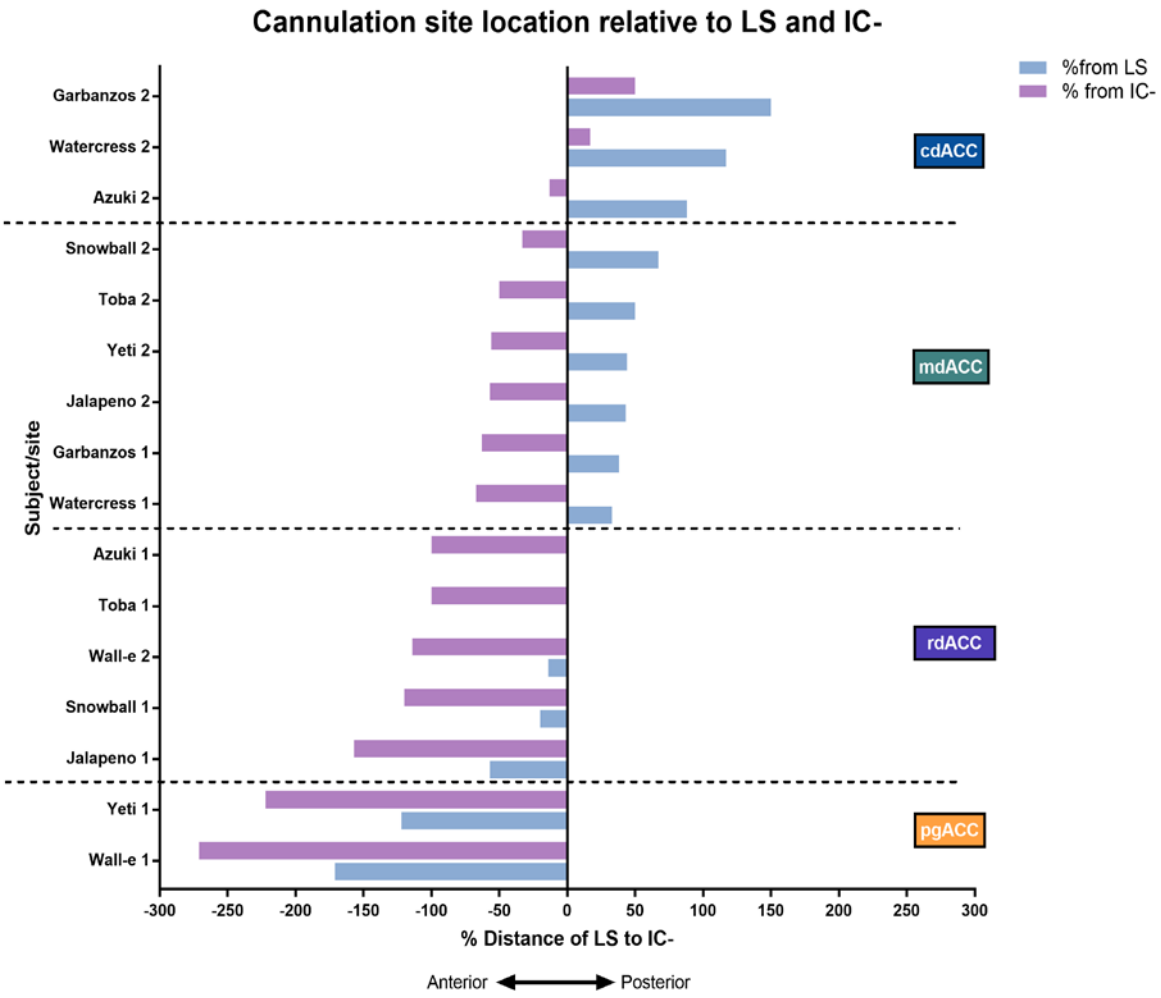

Figure 3.6 Cannulation sites showing distance between from the anterior (1) and posterior (2) cannulation sites to the lateral septum (LS) and the disappearance of the islands of Calleja standardised to the entire LS to IC- distance for each subject.

Table 3.3 Cannulation site placements for each subject included in the HI study with totals per region. Predicted placements shown in italics/brackets

SUBJECTS	Cannulation sites			
	pgACC	rdACC	mdACC	cdACC
Jalapeno		✓	✓	
Toba		✓	✓	
Garbanzos			✓	✓
Watercress			✓	✓
Snowball		✓	✓	
Azuki		✓		✓
Wall-e	✓	✓		
Yeti	✓		✓	
Banshee		*(✓)*		*(✓)*
Trixie		*(✓)*		*(✓)*
Jumbee	*(✓)*	*(✓)*		
Buttercup		*(✓)*	*(✓)*	
TOTAL	**3**	**9**	**7**	**5**

3.3.2 Anxiety response to the human intruder

3.3.2.1 Habituation

To test for potential habituation to a novel intruder on repeated HI Test sessions, the EFA score for the first, middle and last control infusions (saline), regardless of area infused, were compared (Figure 3.7). A one-way repeated measures ANOVA found no significant effect of infusion order on EFA score ($F_{2,22} = 2.306$, $p = 0.130$). Thus, subsequently each mb infusion was compared to its matched control infusion.

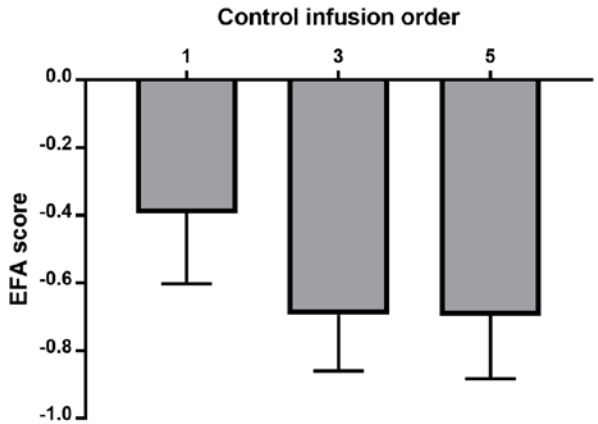

Figure 3.7 Effect of control infusion order on EFA score in response to a human intruder (bars show mean+SEM). There was no significant effect of saline order.

3.3.2.2 Inactivation of ACC subregions differentially affected anxiety response to the human intruder

A mixed model ANOVA was performed to analyse the effect of inactivation on EFA scores. Fixed effect factors included: region (pgACC, rdACC, mdACC or cdACC), treatment (saline or mb), and a random effect factors of subject to account for inter-individual differences between marmosets, and for the different combinations of cannulation sites. There was no significant main effect of drug ($F_{1, 29} < 1$) or region ($F_{3, 33} < 1$) on EFA score. However, there was a significant drug by region interaction ($F_{3,29} = 2.978$, $p = 0.049$)(Figure 3.8). A separate analysis including just the planned regions of interest (i.e. region: rdACC or cdACC) also revealed a significant drug by region interaction ($F_{1,14} = 2.978$, $p = 0.001$) with no main effect of drug or region (drug: $F_{1,14} < 1$; region: $F_{1,21} < 1$).

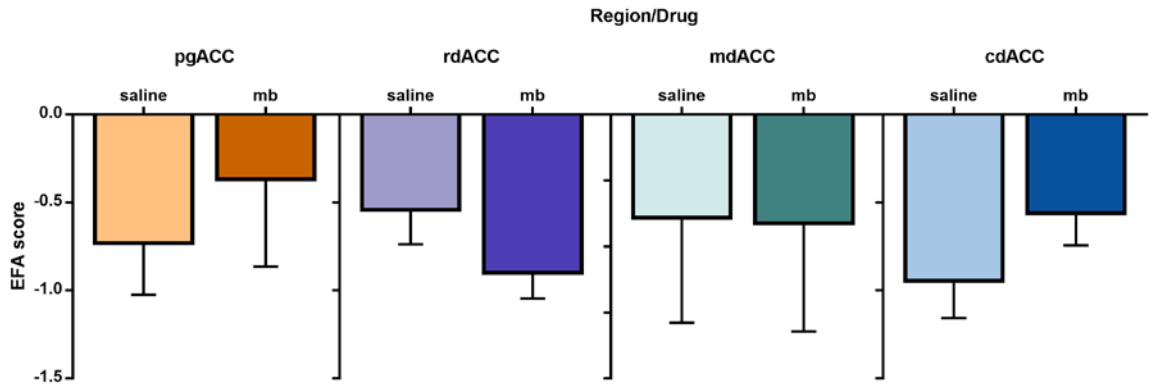

Figure 3.8 Effect of infusion of saline or mb in each region on EFA scores in response to a human intruder (bars show mean+SEM). There was a significant drug by region interaction.

The difference in EFA score during mb inactivation relative to saline control was calculated (Figure 3.9). A mixed model ANOVA with region as a fixed factor and subject as a random factor showed that a main effect of region on EFA difference score just failed to reach significance ($F_{3,20} = 2.947$, $p = 0.058$). However, a separate analysis, including just the planned regions of interest (i.e. region: rdACC or cdACC) did find a significant main effect of region on EFA difference score ($F_{1,8} = 9.079$, $p = 0.017$). One sample t-tests were performed on the EFA difference score for each region.

Inactivation of the rdACC had a trend anxiolytic response, reducing the EFA score ($t_8 = -2.086$, $p = 0.070$). In contrast. inactivation of the cdACC had an anxiogenic response significantly increasing the EFA score ($t_4 = 4.182$, $p = 0.014$)

Inactivation of the mdACC or pgACC had no overall effect on the EFA score (mdACC: ($t_4 = -0.070$, $p = 0.946$; pgACC: $t_2 = 1.780$, $p = 0.217$).

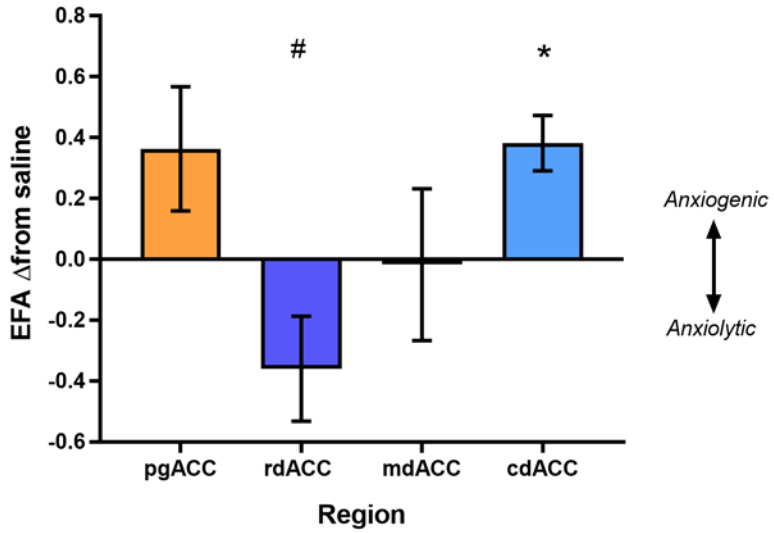

*Figure 3.9 Effect of inactivation on change in EFA score (mb minus saline). Values >0 indicate an anxiogenic effect of mb while values <0 indicate an anxiolytic effect of mb. Inactivation of the rdACC caused a trend reduction in EFA score #p<0.1 and inactivation of the cdACC caused a significant increase in EFA score *p<0.05. Bars show mean±SEM.*

3.3.3 Individual behavioural measures of the HI Test

Table 3.4 shows the raw measured values for each behavioural measure on each HI Test session as well as the calculated scores from the EFA and for average height, following infusions into different subregions of the dACC.

Table 3.4 All measures for all HI Test sessions grouped by region (continued on next page)

Area	Subject	Drug	EFA score	% in depth zones			% in height zones					Average Height	Locomotion (%)	Bobs	Jumps	CALLS					
				Front	Middle	Back	Top of NB	High	Middle	Low	Floor					Tsik	Tsik-Egg	Tse	Tse-Egg	Egg	TOTAL
pgACC	Jumbee	saline	-1.23	75.37	15.84	9.43	0.00	17.43	38.40	8.97	35.82	36.19	1.87	0	2	0	2	1	0	0	3
	Jumbee	mb	-1.23	56.17	18.85	25.54	0.00	17.28	36.68	3.26	43.34	34.56	6.36	0	7	0	0	0	0	0	0
	Wall-e	saline	-0.73	32.27	39.74	27.87	19.77	3.33	24.12	6.56	46.11	36.47	2.47	5	5	18	6	9	10	0	43
	Wall-e	mb	-0.36	32.67	50.29	16.95	0.00	42.89	27.34	10.28	19.40	47.79	1.17	15	4	14	23	12	0	3	52
	Yeti	saline	-0.26	37.52	45.03	18.19	0.00	67.17	33.57	0.00	0.00	63.81	1.74	6	5	0	0	0	0	0	0
	Yeti	mb	0.45	7.93	54.11	38.66	35.27	65.43	0.00	0.00	0.00	76.44	0.24	0	2	0	0	0	0	0	0
	Mean	**saline**	**-0.74**	**48.39**	**33.54**	**18.50**	**6.59**	**29.31**	**32.03**	**5.18**	**27.31**	**45.49**	**2.03**	**4**	**4**	**6**	**3**	**3**	**3**	**0**	**15**
		mb	**-0.38**	**32.26**	**41.09**	**27.05**	**11.76**	**41.87**	**21.34**	**4.51**	**20.91**	**52.93**	**2.59**	**5**	**4**	**5**	**8**	**4**	**0**	**1**	**17**
rdACC	Jalapeno	saline	-0.27	33.71	66.15	0.63	5.97	27.26	36.93	5.84	24.49	45.76	1.84	28	4	19	49	0	6	0	74
	Jalapeno	mb	-1.28	54.43	41.72	2.74	0.00	20.48	17.40	11.33	49.69	30.08	2.40	1	5	5	0	0	5	1	11
	Snowball	saline	-0.58	50.27	42.75	7.42	0.00	41.40	34.04	11.20	13.81	49.66	1.77	6	0	0	0	0	0	3	3
	Snowball	mb	-1.04	65.82	11.67	23.21	5.97	32.61	19.07	6.60	36.45	42.25	2.36	1	5	3	0	0	0	0	3
	Wall-e	saline	-1.11	49.72	28.98	22.03	13.64	0.00	28.45	2.55	56.09	30.91	3.53	6	8	4	8	9	12	0	33
	Wall-e	mb	-1.12	47.30	41.54	11.63	7.51	8.24	22.69	2.27	59.77	29.05	2.77	2	4	1	2	4	8	0	15
	Toba	saline	0.58	0.00	74.44	26.02	10.25	57.02	12.62	15.66	4.91	59.45	1.10	28	2	0	23	0	16	8	47
	Toba	mb	-0.12	40.40	38.97	21.27	0.00	42.39	30.64	6.70	20.92	48.29	1.38	25	0	0	5	0	12	7	24
	Azuki	saline	-0.98	74.18	26.43	0.00	0.00	0.00	95.93	4.68	0.00	47.17	0.25	0	1	6	0	0	3	0	9
	Azuki	mb	-0.38	31.25	30.61	38.80	20.08	14.55	37.14	3.87	25.03	48.40	0.79	0	2	1	0	0	0	1	2
	Banshee	saline	-0.30	32.01	40.11	28.46	8.81	53.13	18.34	0.66	19.64	55.94	1.37	5	5	0	0	10	5	0	15
	Banshee	mb	-0.89	54.47	37.95	8.32	0.00	49.58	15.06	0.85	35.25	45.80	1.75	0	5	0	0	4	0	8	12
	Buttercup	saline	-0.32	84.06	15.85	0.00	11.53	73.30	15.07	0.00	0.00	69.08	1.06	10	0	0	1	6	22	13	42
	Buttercup	mb	-1.24	76.22	24.50	0.00	0.00	30.18	29.23	2.41	38.89	39.54	5.44	1	1	0	0	0	0	0	0
	Jumbee	saline	-1.22	70.59	23.16	6.86	0.00	14.94	37.53	11.38	36.77	34.66	1.64	1	2	2	1	1	0	2	6
	Jumbee	mb	-1.21	67.44	11.34	21.85	3.33	13.90	38.20	1.95	43.26	35.39	2.21	0	5	0	0	0	0	0	0
	Trixie	saline	-0.76	66.80	10.72	23.15	0.00	41.38	43.95	0.30	15.04	51.90	0.88	0	3	1	0	2	0	1	4
	Trixie	mb	-0.91	59.05	21.95	19.76	0.00	20.00	57.68	2.97	20.12	44.41	1.73	0	4	0	0	0	0	0	0
	Mean	**saline**	**-0.55**	**51.26**	**36.51**	**12.73**	**5.58**	**34.27**	**35.87**	**5.81**	**18.97**	**49.39**	**1.49**	**9**	**3**	**4**	**9**	**3**	**7**	**3**	**26**
		mb	**-0.91**	**55.15**	**28.92**	**16.40**	**4.10**	**25.77**	**29.68**	**4.33**	**36.60**	**40.36**	**2.31**	**3.33**	**3.44**	**1.11**	**0.78**	**0.89**	**2.78**	**1.89**	**7.44**

Area	Subject	Drug	EFA score	% in depth zones			% in height zones					Average Height	Locomotion (%)	Bobs	Jumps	CALLS					
				Front	Middle	Back	Top of NB	High	Middle	Low	Floor					Tsik	Tsik-Egg	Tse	Tse-Egg	Egg	TOTAL
mdACC	Watercress	saline	-1.24	57.88	23.03	19.68	0.00	8.24	24.25	0.00	68.10	23.62	1.04	0	1	0	0	0	0	0	0
	Watercress	mb	-1.65	81.76	9.77	9.17	0.00	0.00	22.93	0.00	77.77	18.00	1.08	0	1	0	0	0	0	0	0
	Garbanzos	saline	-0.49	42.19	48.03	9.59	0.00	40.36	33.19	12.73	13.53	48.86	0.79	7	3	0	0	0	0	19	19
	Garbanzos	mb	-0.03	40.93	28.58	31.05	0.00	50.86	49.70	0.00	0.00	59.97	0.46	16	3	0	3	0	0	15	18
	Jalapeno	saline	-0.71	42.56	53.16	4.68	0.00	8.58	57.44	11.79	22.59	38.53	0.82	13	3	8	21	4	0	0	33
	Jalapeno	mb	0.52	8.49	85.79	6.81	0.00	66.93	22.58	11.58	0.00	61.14	1.15	44	5	13	56	9	4	0	82
	Yeti	saline	0.91	5.48	17.53	76.72	0.00	98.71	1.02	0.00	0.00	70.57	0.45	17	1	0	0	0	0	30	30
	Yeti	mb	0.28	19.42	26.14	55.01	0.00	77.95	22.63	0.00	0.00	66.20	0.65	4	3	0	0	0	1	12	13
	Toba	saline	0.77	0.00	69.31	31.24	0.00	60.80	39.75	0.00	0.00	62.25	0.93	35	1	0	18	0	4	18	40
	Toba	mb	0.45	0.00	66.83	33.83	0.00	33.66	16.05	50.95	0.00	43.83	0.66	38	1	0	30	0	6	14	50
	Snowball	saline	-0.62	39.15	54.19	7.36	0.00	44.46	25.60	13.17	17.46	48.59	3.17	19	10	3	0	0	0	15	18
	Snowball	mb	-1.07	42.98	57.74	0.00	0.00	0.00	54.69	22.45	23.58	33.76	1.48	7	7	2	0	0	0	5	7
	Buttercup	saline	-0.85	70.30	30.27	0.00	0.00	45.34	33.93	8.77	12.51	51.71	1.28	3	2	0	0	0	0	4	4
	Buttercup	mb	-0.85	71.99	6.47	22.27	10.25	18.83	61.51	0.00	10.14	52.51	2.07	0	4	0	0	0	0	1	1
	Mean	**saline**	**-0.32**	**36.79**	**42.22**	**21.32**	**0.00**	**43.78**	**30.74**	**6.64**	**19.17**	**49.16**	**1.21**	**13**	**3**	**2**	**6**	**1**	**1**	**12**	**21**
		mb	**-0.34**	**37.94**	**40.19**	**22.59**	**1.46**	**35.46**	**35.73**	**12.14**	**15.93**	**47.92**	**1.08**	**16**	**3**	**2**	**13**	**1**	**2**	**7**	**24**
cdACC	Azuki	saline	-1.29	77.96	1.05	21.66	0.00	0.00	55.44	0.00	45.23	30.68	0.94	0	2	0	0	0	0	3	3
	Azuki	mb	-0.73	40.67	56.47	3.57	0.00	19.52	64.55	1.51	15.14	46.57	0.98	0	3	0	0	1	0	1	2
	Watercress	saline	-1.50	83.07	11.01	6.08	0.00	4.10	41.79	0.69	53.57	27.96	1.16	0	2	0	0	0	0	0	0
	Watercress	mb	-1.06	44.30	56.37	0.00	0.00	0.00	28.81	56.32	15.53	28.75	0.26	0	0	0	0	1	0	0	1
	Garbanzos	saline	-0.44	47.77	33.03	19.57	0.00	43.14	31.21	9.79	16.22	49.42	2.72	14	2	0	0	0	2	10	12
	Garbanzos	mb	-0.02	10.89	56.35	33.42	0.00	18.24	71.28	0.00	11.14	48.16	1.48	8	0	0	0	0	3	10	13
	Banshee	saline	-0.96	42.84	37.04	20.79	17.79	14.99	10.57	9.52	47.80	37.42	5.86	0	6	0	12	1	0	6	19
	Banshee	mb	-0.51	41.18	41.65	17.87	10.01	48.10	20.17	0.00	22.41	54.36	2.11	3	5	0	0	0	5	2	7
	Trixie	saline	-0.58	64.20	6.85	29.65	0.00	29.66	71.04	0.00	0.00	55.15	1.44	0	1	0	0	0	0	0	0
	Trixie	mb	-0.55	27.06	71.59	1.79	0.00	45.33	26.59	12.12	16.39	49.33	1.13	0	3	0	0	0	0	0	0
	Mean	**saline**	**-0.96**	**63.17**	**17.79**	**19.55**	**3.56**	**18.38**	**42.01**	**4.00**	**32.56**	**40.13**	**2.42**	**3**	**3**	**0**	**2**	**0**	**0**	**4**	**7**
		mb	**-0.57**	**32.82**	**56.49**	**11.33**	**2.00**	**26.24**	**42.28**	**13.99**	**16.12**	**45.43**	**1.19**	**2**	**2**	**0**	**0**	**0**	**2**	**3**	**5**

The effect of inactivation of the rdACC and cdACC on individual behavioural measures was assessed using mixed model ANOVAs with fixed factors of region (rdACC or cdACC) and drug (saline or mb) and subject as a random factor. Where significant drug effects were observed each region was analysed separately.

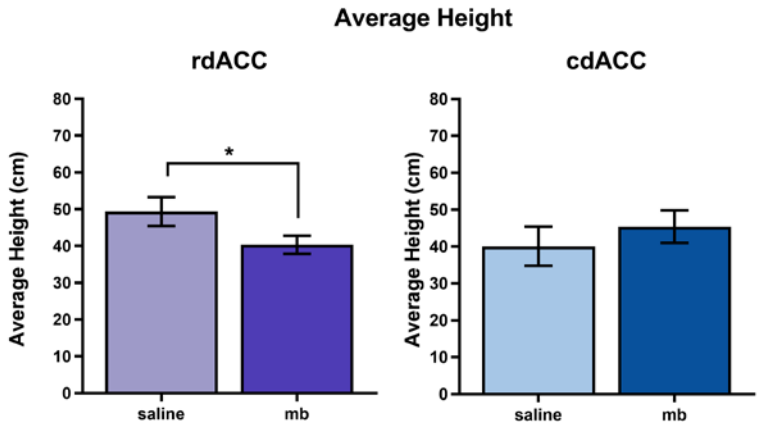

*Figure 3.10 Effect of infusion of saline or mb in the rdACC and cdACC on average height in response to a human intruder. Inactivation of the rdACC caused a significant reduction in average height *p<0.05. Bars show mean±SEM.*

There was a significant overall drug by region interaction on average height ($F_{1,14}$ = 6.868, p = 0.020). Further analysis revealed that inactivation of the rdACC caused a significant reduction in average height ($F_{1,8}$ = 8.079, p = 0.022), whereas inactivation of the cdACC had no effect ($F_{1,4}$ = 1.296, p =0.318) (Figure 3.10).

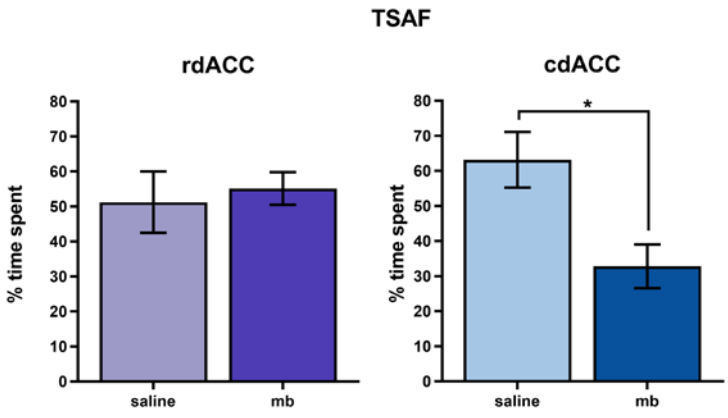

*Figure 3.11 Effect of infusion of saline or mb in the rdACC and cdACC on % time spent at the front of the cage in response to a human intruder. Inactivation of the cdACC caused a significant reduction in TSAF *p<0.05. Bars show mean±SEM.*

There was a significant overall drug by region interaction on proportion of TSAF ($F_{1,14}$ = 8.257, p = 0.013). Further analysis revealed that inactivation of the cdACC caused a

significant reduction in proportion of TSAF ($F_{1,4} = 17.867$, $p = 0.013$), whereas inactivation of the rdACC had no effect ($F_{1,8} < 1$)(Figure 3.11).

There was a significant overall effect of drug on total calls made ($F_{1,14} = 4.928$, $p = 0.045$). Further analysis revealed that inactivation of the rdACC caused a significant reduction in calls ($F_{1,8} = 6.74$, $p = 0.032$), whereas inactivation of the cdACC had no effect ($F_{1,4} < 1$).No significant effects of drug were seen on any of the other measures.

3.4 Discussion

The findings from this study have two major implications for our understanding and study of the dACC. First, specifically with respect to the marmoset, they provide insight into functional heterogeneity within this region that has not been identified by cytoarchitectonics. Second, they provide empirical support for the hypothesis that there is a functional dissociation between rostral and caudal regions of dACC, with the two regions having opposing effects on the regulation of anxiety. Inactivation of the rdACC induced an anxiolytic effect in response to an unfamiliar human intruder, as shown by the reduction in the EFA anxiety score and on the specific measures of average height and total calls. In contrast, inactivation of the cdACC produced an anxiogenic response, with a marked increase in the EFA anxiety score and a reduction on the specific measure of proportion of TSAF.

Detailed post-mortem analysis of cannulae placements, involving an integrated assessment of numerous anatomical landmarks and accounting for surgical revisions, revealed vast variation in the anatomy of the frontal region of the brain including the anterior cingulate region. A novel method of determining subregional boundaries within the dACC was developed based on relative distance from the LS and IC- (Figure 3.6). This revealed four topographically distinct subregions within the ACC (pgACC, rdACC, mdACC and cdACC). Subsequent surgeries have been modified allowing for greater precision in targeting dACC subregions in the marmoset in future studies.

Using these regional boundaries, the effect of temporary local inactivation of subregions of the dACC in response to uncertain threat, an unfamiliar human intruder, was assessed. A variety of behavioural measures were recorded and thus an EFA was used to identify the underlying relationship between these measured variables. One factor was extracted, and the pattern in which the measured variables clustered on this factor suggested that this represented the subject's anxiety response towards the human intruder. For example the distance measures of proportion of time spent at front and back loaded strongly on to the factor, and it has previously been demonstrated that anxiolytics affect the distance a marmoset maintains from a novel human intruder (Carey et al., 1992b). In addition tse-egg calls, which also loaded onto the factor, have been associated with vigilance behaviour (Bezerra and Souto, 2008).

Thus, based on the EFA score, inactivation of the cdACC produced an anxiogenic response to the human intruder, providing causal evidence for involvement of this area in anxiety regulation. Assessment of individual measures revealed a significant reduction in TSAF which is reflected in the EFA score. This is consistent with previous work carried out in

macaques, reporting reduced metabolic activity of the cdACC associated with impaired regulation of behavioural responses in situations of increased uncertainty (Kalin et al., 2005). In contrast, inactivation of the rdACC caused an anxiolytic response to the human intruder, as revealed by a reduction in average height which was reflected by a reduced EFA score and reductions in total calls made. Upward flight has previously been reported as a defensive response, particularly to terrestrial predators (Lipp, 1978; Searcy and Caine, 2003). Although, a reduction in total calls could reflect behavioural inhibition in a high anxious situation, given that it occurs alongside reduced defensive behaviour (height reduction), here it appears to reflect reduced anxiety. This result is consistent with functional imaging studies in humans which show increased activity of the rdACC in anxiety provoked by a partially reinforced aversive conditioned stimuli (Büchel et al., 1998). Furthermore, it supports the suggestion that the rdACC is specifically involved in conscious threat appraisal and catastrophising (Kalisch and Gerlicher, 2014), though this cannot directly be assessed in marmosets. It is interesting to note that although inactivation of the cdACC and rdACC had opposing effects on anxiety (anxiogenic and anxiolytic respectively) these effects were largely driven by different measures, TSAF and average height respectively. This suggests that these regions might regulate different aspects of the behavioural response to threat involving different defensive strategies. It might be that height reflects more of a typical “flight” response, whilst the TSAF involves more of a social element due to interaction with the human intruder.

Although the mdACC and pgACC were not key regions of interest, the effects of inactivation of these regions were also assessed. Interestingly, although inactivation of the mdACC had no overall effect on anxiety, assessment of inactivation of this region in individual subjects revealed that rather than no effect, most subjects showed either a clear anxiogenic response or a clear anxiolytic response. However, when looking at their site placements within the mdACC there was no clear anterior-posterior divide between anxiety responses. This suggests that rather than being a distinct functional region from the more anterior rdACC and the more posterior cdACC, the mdACC is a transition zone between these two regions, whose boundary presents a significant individual variation. Inactivation of the pgACC also had no overall effect on anxiety, however the sample size of this group was small and looking at the individual subjects 2 of the 3 showed large anxiogenic responses on the EFA score. Notably this is an opposing effect to that observed in the adjacent rdACC. Although this effect needs to be determined with a larger sample, it would be consistent with a structural association in marmosets between reduced pgACC volume and high trait anxiety (Mikheenko et al., 2015)

and observations of reduced volume and activity of this region in patients with anxiety disorders (Asami et al., 2008; Blair et al., 2012; Radua et al., 2010).

This study provides clear evidence for a functional dissociation between the rdACC and cdACC in marmoset, and in addition suggests that the pgACC may be a further functional division of the ACC. These subregions appear remarkably similar in terms of location relative to the genu of the corpus callosum, to dACC subregions proposed in humans based largely on cytological differences, the pgACC, aMCC and pMCC (Vogt et al., 2003). The pgACC is differentiated from the MCC on the basis of differences in neurofilament protein expression, whilst the aMCC and pMCC are differentiated by differences in neuronal density in layer V (Vogt et al., 2003). Correlative functional imaging studies support these divisions in human and similar divisions have also been proposed in macaques (Vogt et al., 2005). However, as of yet no such cytological differences have been reported in the anterior-posterior axis of marmoset dACC (area 24). Thus, detailed anatomical studies may reveal structural characteristics to support the functional dissociation in marmoset dACC subregions presented here. The work carried out in Chapter 7 begins to address this.

In summary, the findings of the present study demonstrate for the first time that topographically distinct subregions of the dACC are causally involved in the regulation of anxiety and further have opposing effects, with the rdACC promoting anxiogenic responses and the cdACC promoting anxiolytic responses. This provides causal evidence in support of previously reported findings from correlational studies in macaques and humans and have implications for translational research on the function of the dACC in anxiety regulation.

4 | THE ROLE OF THE dACC IN THE REGULATION OF BASELINE CARDIOVASCULAR ACTIVITY

4.1 Introduction

Since the 1960s, particularly in the case of cardiovascular activity, it has been recognised that autonomic activity is relevant to behaviour as well as metabolism (Obrist et al., 1970). The French physiologist, Claude Bernard, proposed that "when the heart is affected it reacts on the brain; and the state of the brain again reacts through the pneumo-gastric (vagus) nerve on the heart; so that under any excitement there will be much mutual action and reaction between these"(Darwin, 1965). This idea of a bidirectional interaction between the brain and the heart has greatly influenced current models of emotion regulation (Critchley, 2005; Thayer and Lane, 2000, 2009). Specifically, it has been proposed that higher cortical structures regulate autonomic activity, through bidirectional connections with autonomic nuclei, to meet affective as well as cognitive and motor challenges underlying adaptive goal-directed behaviour (Critchley, 2005; Thayer and Lane, 2000). The dACC has been identified as a key node in this network, particularly in mediating changes in sympathetic arousal (Critchley, 2005) and this may be critical to its wider involvement in emotion regulation.

4.1.1 The autonomic nervous system and emotion regulation

Claude Bernard is also credited with discovering the sympathetic regulation of blood pressure through his observations of vessel dilation upon transection of the spinal nerves in rabbits. This early experiment led to further characterisation of autonomic nervous system (ANS) function. The ANS consists of two anatomically and functionally distinct branches, which act together, often antagonistically, to maintain homeostasis by influencing activity of the heart and other effector tissues. The sympathetic branch is dominant during "fight or flight" situations in which it mobilises the body via adrenaline and noradrenaline neurotransmission,

preparing it for action. Conversely the parasympathetic branch is dominant during rest, in which it regulates basic bodily functions largely through cholinergic neurotransmission. However, both branches are tonically active, allowing for a balance of activity between them, and thus efferent tissue function to be precisely regulated (Uijtdehaage and Thayer, 2000). In turn, the ANS is primarily regulated by autonomic reflexes, which relay sensory information about bodily state to autonomic control centres in the brainstem and forebrain, including the hypothalamus, medulla, and pons, which have major outputs in the ANS. This system largely acts under reflex control, involuntarily and outside of consciousness.

The physiological response to threat, the fight-or-flight response, was first described by Walter Cannon (Cannon, 1915). It involves a general discharge of the sympathetic nervous system which has rapid and widespread physiological effects including increased heart rate (HR) and blood pressure (BP), increased blood flow to skeletal muscles, pupil dilation, slowed digestion and bladder relaxation (Everly and Lating, 2013). This stress response is pertinent to the study of the regulation of fear and anxiety and supports the notion that physiological arousal is a core feature of emotion (Critchley et al., 2013). Accordingly, physiological arousal, and sympathetic activity in particular, are important indices of emotion.

The discipline of psychophysiology is specifically concerned with the relationship between psychological processes and physiological responses. This is examined through simultaneous measurement of autonomic activity during tasks involving cognition or emotion. Various autonomic measurements can be taken, and these reflect different levels of sympathetic and parasympathetic control.

Electrodermal activity (EDA), also referred to as the skin conductance response (SCR) or galvanic skin response (GSR), measures the electrical conductance between two points on the surface of the skin. This is affected by moisture and therefore is a marker of sweat gland permeability, which is under the control of the sympathetic nervous system. Thus, EDA is often used in humans to measure sympathetic output as a marker of an emotional response. For example, it is commonly used as the conditioned response in fear conditioning studies (Milad et al., 2005, 2007b, 2007b).

HR is determined by the sinoatrial (SA) node of the heart. At rest this is under significant vagal tone (parasympathetic system) (Uijtdehaage and Thayer, 2000) which acts to reduce HR below the intrinsic rate of the SA node. An increase of HR above the intrinsic rate of SA node thus requires both withdrawal of vagal tone and increased sympathetic activity. Thus, HR reflects the balance of activity between the two branches of the ANS.

Blood pressure is determined by cardiac output and vascular resistance. Smooth muscle tone and therefore vascular resistance is under sympathetic control, however cardiac output is influenced by both autonomic branches (Guyenet, 2006). Short-term changes in blood pressure are minimised by the baroreceptor reflex, which acts to maintain blood pressure around a set range, mediated by both branches of the ANS. It is tonically active at normal blood pressure and is thus sensitive to both increased and decreased blood pressure. Increased sympathetic activity causes increased blood pressure through increased HR and heart contractility and vascular resistance causing greater baroceptor reflex activity, whilst parasympathetic activity causes reduced blood pressure through reduction of HR, causing reduced baroceptor activity. However, evidence suggests that during stress, the operating point of baroreceptor reflex shifts towards higher arterial pressure (Crestani, 2016), and thus blood pressure and HR can simultaneously be elevated during stress. Systolic blood pressure (sBP) refers to the pressure in the arteries following contraction (systole) when it is maximal, while diastolic blood pressure (dBP) is the arterial pressure between heart beats (diastole), when it is at its lowest. Mean arterial pressure (MAP) can be calculated from these measurements and reflects the average pressure during one cardiac cycle.

The autonomic measures discussed so far provide indices of autonomic arousal and have been used to characterise responses to fear and anxiety in humans, mostly using paradigms involving threatening stimuli and anticipation respectively (Kreibig, 2010). These share similar responses of increased HR, increased sBP and increased EDA, reflecting sympathetic activation and parasympathetic inhibition.

Heart rate variability (HRV), the beat-to-beat variation in heart rate, rather than reflecting autonomic arousal per se, measures the ability to flexibly transition between high (sympathetic driven) and low (parasympathetic driven) arousal states (Appelhans and Luecken, 2006), a key determinant of emotion regulation (Gross, 1998). Higher levels of resting HRV, reflect autonomic flexibility, and are reportedly associated with context-appropriate emotional responses. However, low HRV has emerged as an indicator of morbidity in disorders of negative emotion (Thayer et al., 2010, 2012), including depression (Kemp et al., 2012) and anxiety (Chalmers et al., 2014) which could explain the association between these disorders and cardiovascular disease (Gorman and Sloan, 2000; Khawaja et al., 2009). This autonomic imbalance is thought to arise from sympathetic hyperactivity and parasympathetic hypoactivity.

Different measures of HRV are thought to reflect these different aspects of ANS activity. Time domain measures involve simple calculations of the time interval between normal beats,

the inter-beat interval (IBI) or NN-interval. From this the root mean square of successive interval differences (RMSSD) is commonly derived and this provides an estimate of high-frequency variations in heart rate. Frequency domain analyses involve transformation of NN interval data from the time domain to the frequency domain using Fast Fourier Transform. This consistently reveals high frequency (HF: 0.15–0.40 Hz) and low frequency (LF: 0.04–0.15 Hz) components. HF is thought to be largely mediated by the parasympathetic nervous system and includes respiratory sinus arrhythmia (RSA), the natural occurrence of increased HR during inhalation and decreased HR during exhalation. The low frequency component (LF) is thought to be mediated by both sympathetic and parasympathetic branches of the ANS (Tarvainen et al., 2014; Thayer et al., 2010). Finally, nonlinear methods can be used to derive indices of cardiac vagal function and cardiac sympathetic function (Toichi et al., 1997).

4.1.2 The dACC and autonomic regulation

Early electrical stimulation and lesion experiments first revealed an association between the dACC and autonomic activity. Bilateral stimulation of sites along the ACC gyrus, including the pgACC, rdACC and mdACC, in psychotic patients (prior to further surgical procedures) caused "an autonomic effect of some sort" in 12 patients such as an increase in sBP and dBP occurring in 8 patients and a decrease in HR occurring in 7 but an increase in HR in 3 (Pool and Ransohoff, 1949). The variability of effects reported could have arisen from differences in stimulation parameters or from functional differences, with the authors suggesting that more caudal regions were involved in respiratory effects and more rostral regions in cardiovascular effects. Electrical stimulation of a similar region in other species are more consistent, eliciting reductions in heart rate and small reductions in BP in primates (Kaada, 1951), cats (Löfving, 1961) and rabbits (Buchanan and Powell, 1982). In the latter study, this effect was revealed to occur specifically at rdACC and mdACC stimulation sites but not cdACC.

EDA in humans has been associated more broadly with the dACC, with reduced SCRs found in patients with lesions (vascular or surgical resection) in the anterior cingulate gyrus (Tranel and Damasio, 1994) and direct electrical stimulation (Mangina and Beuzeron-Mangina, 1996), shown to elicit SCRs (largely ipsilaterally). These studies included the entire dACC region. More recently, electrical stimulation in humans prior to anterior cingulotomy or subcaudate tractotomy surgery has demonstrated a voltage response relationship between stimulation specifically targeting the mid-caudal dACC and EDA (i.e. higher voltage (1-3V)

stimulation, great EDA response) which was not observed when stimulating the subcaudate (Gentil et al., 2009).

Taken together, these studies broadly implicate a large area including the dACC in autonomic regulation, and suggest the rdACC and mdACC are specifically involved in regulation of HR and BP. However, it is important to note that electrical stimulation and the lesions mentioned can affect fibres of passage (axons coursing through the region on their way elsewhere) as well as the focal region and that this may contribute to the observed effects. Anatomical tracing studies in macaques do however show connectivity between the (entire) dACC, and autonomic regions such as the dorsal hypothalamus (Öngür et al., 1998) and the lateral periaqueductal gray (PAG) (An et al., 1998) supporting a role for the dACC in autonomic regulation.

4.1.3 The dACC and adaptive autonomic control

More recently, functional imaging studies in humans have enabled researchers to build on the anatomical and electrical stimulation studies in experimental animals. Based largely on results from these imaging studies it has been proposed that rather than simple control of autonomic activity, the dACC, and a network of regions termed the "central autonomic network", integrates autonomic activity with adaptive behaviour, making appropriate adjustments to support the metabolic demands on cognitive, emotional and motor challenges (Benarroch, 1993; Critchley, 2011, 2005; Thayer and Lane, 2000).

A number of imaging studies support this (Figure 4.1). In one of the earliest, Critchley and colleagues measured resting cerebral blood flow (rCBF) using PET, during cognitive (mental arithmetic) and physical (handgrip) tasks (Critchley et al., 2000). Activity of a large right dACC region, including areas 32 and 24, was found to covary with mean arterial blood pressure (MAP) (Figure 4.1A). Furthermore, during effortful versions of the tasks, increases in MAP and HR were associated with significant increases in activity in the mid to caudal dACC compared to the control effortless tasks.

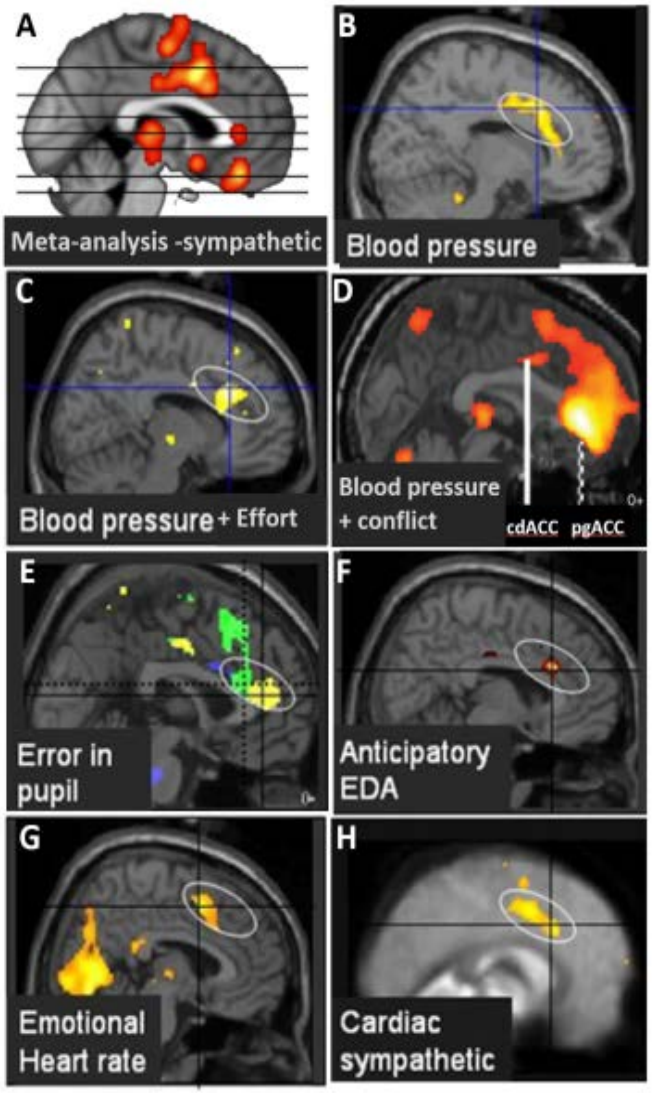

Figure 4.1 Functional neuroimaging studies show activity of the dACC across different tasks and different autonomic measures. Figure adapted from Critchley et al. 2005. A. Meta-analysis of neuroimaging studies measuring autonomic activity shows MCC and dACC activity is associated with sympathetic arousal (Beissner et al. 2013). B. Activity of the right dACC covaried with MAP (Critchley et al., 2000). C. Increased rCBF in the right dACC (caudal) during the effortful vs effortless tasks (Critchley et al., 2000). D.BOLD activity of a more caudal dACC region correlated with MAP during cognitive conflict (Gianaros et al., 2005). E. Activity of adjacent regions of the dACC increased in response to autonomic arousal alone (yellow) and to autonomic arousal and error (green) measured by pupillometry (Critchley et al. 2005a). F. Activity of the m/rdACC covaried with anticipatory EDA during uncertainty in a decision-making task and EDA (Critchley et al., 2001). G. Activity of a dorsal cdACC correlated with heart rate acceleration induced by emotional face stimuli (Critchley et al., 2005). H. A dorsal dACC region was also associated specifically with the low frequency component of HRV (Critchley et al., 2003)

Fewer studies have assessed the role of dACC in integrating emotion and autonomic arousal. likely due to the previous view of the dACC as the cognitive division of the ACC (Bush et al., 2000). However, activity of a more dorsal part of mid to caudal dACC predicts HR increases during presentation of emotional stimuli (faces of different categories) (Figure 4.1G) (Critchley et al., 2005a), and following an emotional stressor (participants told to mentally prepare a speech while being scanned, in preparation for a presentation after scan completion) (Wager et al., 2009).

There is much heterogeneity across studies in the location of the dACC ROIs showing activity. This is likely due to the variety of different tasks and autonomic arousal measures used but could possibly also reflect functional divisions. Addressing this issue, a recent meta-analysis, which included all studies that measured an autonomic activity metric in conjunction with neuroimaging, found activity in a dACC region, including mdACC and cdACC, that was specific to sympathetic over parasympathetic activity (Figure 4.1A)(Beissner et al., 2013) with this region consistently showing activity across cognitive, motor and affective tasks.

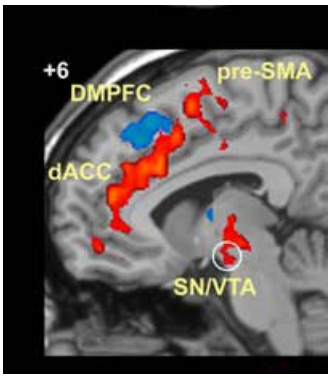

Figure 4.2 The dACC as a node in the "salience network"(shown in red) (Seeley et al. 2007).

An alternate but complementary account of dACC function, posits that it is part of a functionally connected network of regions, “the salience network” involved specifically in detecting behaviourally relevant events (Seeley et al., 2007). The dACC and the anterior insular are key nodes in the salience network (Figure 4.2), which is distinct from an “executive control network”. The latter includes the dorsolateral PFC and dorsomedial PFC as key nodes and is proposed to act on identified salience during tasks. This relates to autonomic regulation in that the salience network is proposed to detect the salience of interoceptive, homeostatically relevant stimuli and send a control signal to other regions to regulate arousal (Menon and Uddin, 2010), thus providing a means by which autonomic arousal is integrated with behavioural control.

To summarise, electrical stimulation and lesion studies implicate the dACC in autonomic arousal. Functional imaging studies support this role, and further specify a role for the dACC in the integration of sympathetic arousal with discrete subregions potentially responsible for integrating different cognitive and emotional behaviours with different aspects of autonomic arousal. However, to determine specific involvement of the dACC in autonomic arousal requires “task-free” conditions whilst in these neuroimaging studies it is difficult to disentangle autonomic arousal from task-related behavioural activity and from salience. Furthermore, they do not address the issue of causality.

Previous work in the Roberts laboratory has shown that temporary inactivation of area 32 (pgACC) increased MAP and inactivation of area 25 (sgACC) decreased HR and MAP and increased HRV (Wallis et al., 2017). However, the role of different subregions of the dACC in regulating cardiovascular activity in a task-free emotionally "neutral" condition has not been assessed. Following temporary pharmacological inactivation of the rdACC, mdACC or cdACC, subjects were placed in a behavioural testing apparatus to which they had been habituated. Blood pressure was measured online, and a range of cardiovascular measures were derived from this.

4.2 Methods

4.2.1 Subjects

A total of nine marmosets took part in this study (Table 2.1). All received dACC cannulation surgery targeting two sites and telemetry implantation surgery. One subject (Banshee) displayed inherent cardiac dysrhythmia and thus was not included in the HRV analysis as this would invalidate meaningful measurements but was included in assessments of other indices of cardiovascular function.

4.2.2 Behavioural testing

Once recovered from surgery, animals were habituated to the test apparatus (2.3). Habituation was defined as the point at which HR and blood pressure stopped declining and reached a relatively stable plateau alongside a reduction in a range of behaviours indicative of anxiety including vigilant posture, locomotion, and alarm calls (phee).

Following habituation, subjects continued to receive daily test sessions, in which they were placed in the test apparatus for 20 minutes, with the house light on (identical to habituation sessions). On manipulation days, an intracerebral infusion of saline (vehicle) or muscimol/baclofen, to transiently inhibit neuronal activity, was administered via implanted cannulae to the rdACC, mdACC or cdACC (2.5). Blood pressure was recorded via the implanted telemetric probe and transmitted to its receiver in the test box (2.6)

4.2.3 Data analysis

Systolic and diastolic blood pressure events were extracted from the blood pressure trace as local maxima or minima respectively. Inter-beat intervals (IBIs) were measured as the time interval between successive systolic blood pressure events and HR was derived from this (HR = IBI/60) . Data were processed to remove outliers (values outside the pressure range 20-200mmHg, and the IBI range of 0.1-0.4). Data from the first minute of each session were excluded as the offset period and the following 15 minutes were sampled (i.e. 60-960s) for calculation of average blood pressure and HR. The IBI data were imported into Kubios HRV version 2.2 (Tarvainen et al., 2014), and detrended using the smoothness priors method (lambda =500) (Tarvainen et al., 2002). The RMSSD, the square root of the mean squared standard deviation of the time difference between successive IBIs (a time-domain measure of HRV) was calculated and Poincaré (Lorenz) plots (a scatter plot of each IBI interval against the next one) were generated. The standard deviation of the points on the Poincaré plots,

perpendicular to the line of identity (SD1), and the standard deviation of the points along the line of identity (SD2) were used to calculate the Cardiac Vagal Index (CVI) and the Cardiac Sympathetic Index (CSI) (Toichi et al., 1997).

4.3 Results

4.3.1 Histological assessment of cannulae placements

Histological assessment of cannula placements was carried out as described in Chapter 3. Including predicted placements, a total of seven subjects had cannulae targeting rdACC, five targeting mdACC and four targeting cdACC (Table 4.1). Two subjects (Banshee and Trixie) are still alive and thus their cannulae placements remain to be verified post-mortem. As only two subjects (Wall-e and Yeti) had cannulae placements in the pgACC, data from this site is not included. However, data collected from the other cannulated site in these two animals is included (rdACC and mdACC respectively).

Table 4.1 Cannulation site placements for each subject included in the baseline cardiovascular activity study with totals per region and including predicted placements shown in italics/brackets.

SUBJECTS	Cannulation sites			
	pgACC	rdACC	mdACC	cdACC
Jalapeno		✓	✓	
Toba		✓	✓	
Garbanzos			✓	✓
Snowball		✓	✓	
Azuki		✓		✓
Wall-e	✓	✓		
Yeti	✓		✓	
Banshee		*(✓)*		*(✓)*
Trixie		*(✓)*		*(✓)*
TOTAL	2	7	5	4

4.3.2 Cardiovascular measurements reduced across habituation

Subjects took an average of 11.3 sessions (min = 7, max = 17, SD = 3.2) to habituate to the test apparatus and procedures before commencing infusions. A repeated measures one-way ANOVA revealed a significant reduction of HR ($F_{1,9}$ = 29.79, p = 0.0002) across habituation sessions. Tukey's multiple comparisons test showed a significant difference of session 1 vs n-1 (p = 0.0021) and session 1 vs n (p = 0.0009) but the difference between n-1 and n was not significant (p > 0.05) (Figure 4.3A).

Similarly, for MAP, a repeated measures one-way ANOVA also revealed a significant reduction ($F_{1,9} = 22.8$, $p = 0.0010$) across habituation sessions (n-1 = penultimate session, n = last session). Tukey's multiple comparisons test showed a significant difference of session 1 vs n-1 ($p = 0.0092$) and session 1 vs n ($p = 0.0008$) but the difference between n-1 and n was not significant ($p > 0.05$) (Figure 4.3B).

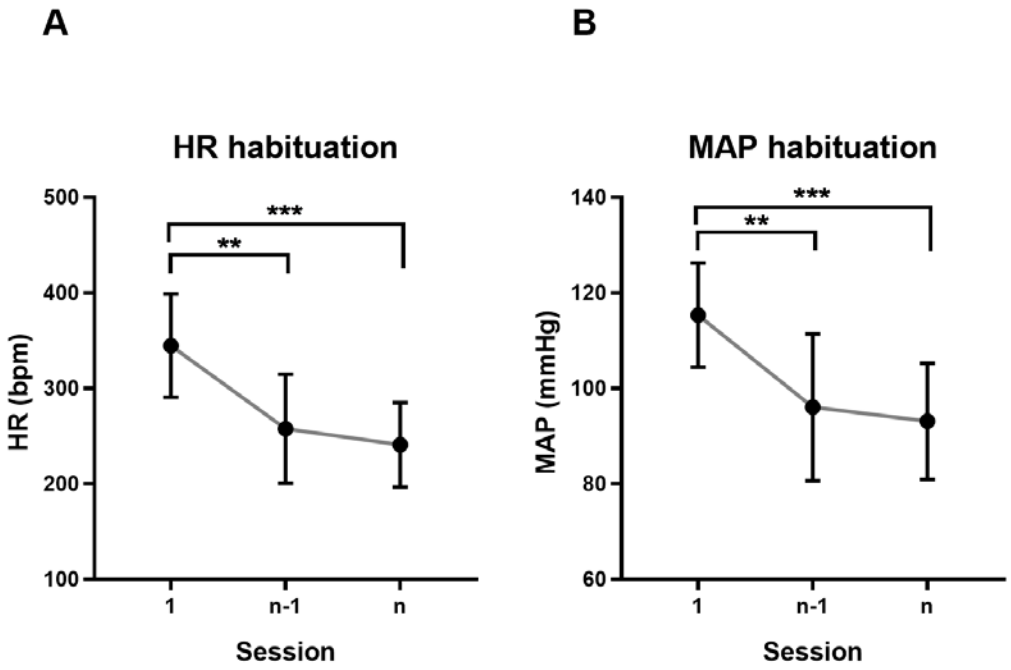

*Figure 4.3 A. Mean heart rate (HR) and B. mean arterial pressure (MAP) during habituation. A 15min sample was taken from the first, penultimate (n-1), and last (n) session of habituation. Error bars show ±SD. ** p<0.01 , **p<0.001 (Tukey's multiple comparisons test).*

4.3.3 Inactivation of rdACC, mdACC or cdACC had no effect on basic cardiovascular measures

Mixed model ANOVAs were performed to analyse the effect of inactivation on HR and mean arterial pressure. Fixed effect factors included: region (rdACC, mdACC or cdACC) and treatment (saline or mb), with subject as a random effect factor. There were no significant main effects of drug or region nor an interaction of drug by region on HR or MAP (Figure 4.4).

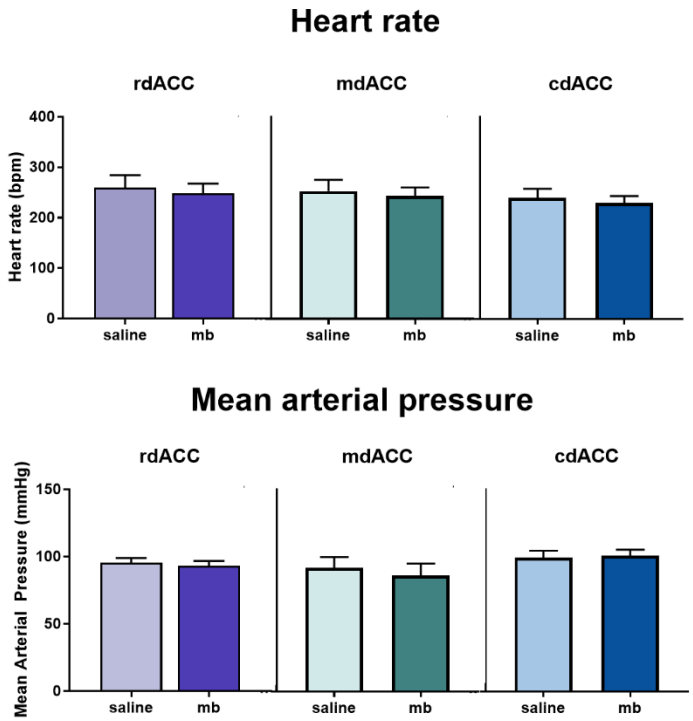

Figure 4.4 Effect of infusion of saline or mb in the rdACC, mdACC and cdACC on heart rate and mean arterial blood pressure. Bars show mean+SEM.

4.3.4 Inactivation of rdACC, mdACC or cdACC had no effect on HRV measures

Similar mixed model ANOVAs were performed to analyse the effect of inactivation on measures of heart rate variability (RMSSD, CVI and CSI) (Figure 4.5). There were no significant main effects of drug or region nor an interaction of drug by region on any measure.

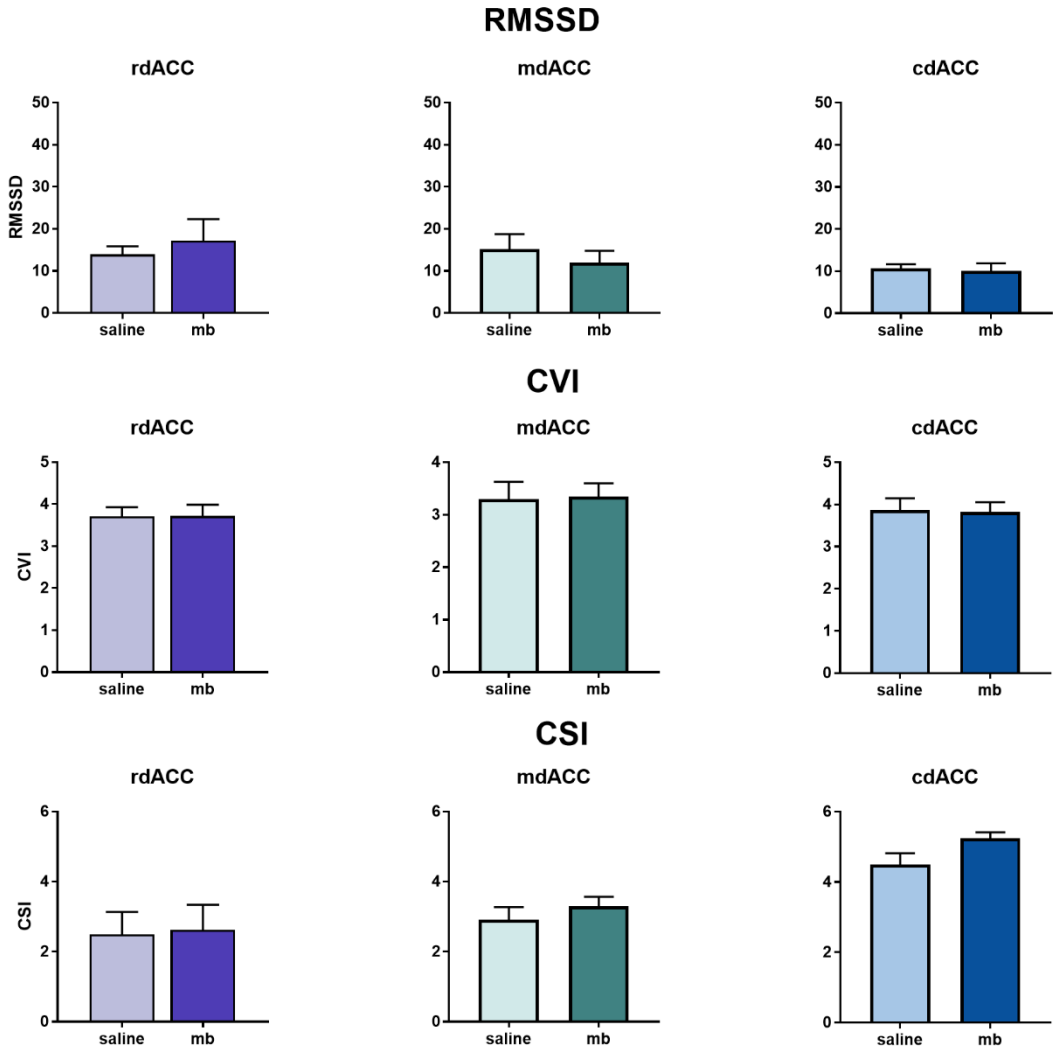

Figure 4.5 Effect of infusion of saline or mb in the rdACC, mdACC and cdACC on measures of HRV. Root mean sum of squares of IBI interval (RMSSD), cardiac vagal index (CVI), cardiac sympathetic index (CSI). Bars show mean+SEM.

4.4 Discussion

In this study the effects of pharmacological inactivation of the rdACC, mdACC, and cdACC were assessed in a task-free emotionally neutral condition. The results indicate that there were no significant effects of inactivation of these subregions on basic measures of cardiovascular autonomic activity (HR and MAP), nor on HRV measures (RMSSD, CVI, CSI).

This is the first study to assess the causal role of the dACC in autonomic arousal, in a relatively neutral context. Although, subjects were separated from their partners and taken away from their homecage environment, they had been well habituated to this procedure and to the test environment such that its novelty and arousal-inducing properties were minimised as can be seen in Figure 4.3. The lack of effect of dACC regional inactivation on the measured indices of cardiovascular activity in task-free conditions is consistent with the hypothesis that the dACC integrates autonomic regulation with volitional behaviour (Critchley et al., 2005a). Since in task-free conditions there is little observable volitional behaviour and an absence of salient stimuli, the dACC would not be expected to regulate autonomic activity. Of course, it remains to be determined whether these same manipulations do regulate autonomic activity in an emotional context.

Furthermore, whilst electrical stimulation studies do suggest that increased activity of the dACC can result in increased sympathetic activity as measured by HR responses and EDA (Gentil et al., 2009; Pool and Ransohoff, 1949) the lack of an effect of inactivation of the dACC in an emotionally neutral condition confirms that the dACC does not exert a tonic influence on the cardiovascular system. However, although activation of the dACC was not assessed in the present study, selective activation in future work, that does not alter activity in passing fibres, is required to establish whether the dACC does have a causal role in sympathetic upregulation.

5 |THE ROLE OF THE DACC IN THE REGULATION OF CONDITIONED FEAR

5.1 Introduction

Learning about direct threats and responding to them appropriately is essential for survival and is thus strongly conserved through evolution, suggesting that the neural circuitry of fear regulation is also conserved (LeDoux, 2012). Pavlovian fear conditioning has been used extensively to model acquisition, expression, and extinction of fear responses, in animal and human research, allowing for cross-species comparison of function (Milad and Quirk, 2012)(1.2.4.4.1). Dysregulation of fear is thought to contribute to certain anxiety disorders, namely PTSD and specific phobias, and extinction learning provides the basis for exposure therapy used as treatment. Studies of fear-associated learning in rodents (mostly rats) have given us tremendous insights into the neural circuits underlying regulation of fear. However, caution is required when translating findings from rodents to non-human primates and humans due to major differences in brain structure and organisation, particularly of the cerebral cortex (1.1.1.4). Of relevance to this thesis, the proposed anatomical homologies of the ACC appear inconsistent with functional findings (Myers-Schulz and Koenigs, 2011).

Classical rodent fear conditioning paradigms use an auditory tone as the CS, which is paired with foot shock. A freezing response (CR; conditioned response) is acquired to the CS and the duration of this taken as the behavioural expression of fear. A wealth of data using this paradigm has implicated two distinct regions of the ACC in fear regulation, and indicate that these have opposing functional roles (Sotres-Bayon and Quirk, 2010). The prelimbic cortex (PL) is involved in the expression of conditioned fear; as demonstrated by microstimulation (Vidal-Gonzalez et al., 2006), and transient pharmacological inactivation (Corcoran and Quirk, 2007; Laurent and Westbrook, 2009; Sierra-Mercado et al., 2011). In addition, electrical recordings of single neurons in the PL found sustained increases in firing rate in response to conditioned tones, which correlated with expression of fear (Burgos-Robles et al.,

2009). Conversely, the infralimbic cortex (IL) is required for extinction recall, and again this has been shown using various experimental techniques; lesion (Quirk et al., 2000), stimulation (Milad and Quirk, 2002; Milad et al., 2004) and transient pharmacological inactivation (Laurent and Westbrook, 2009; Sierra-Mercado et al., 2011). It is thought that the opposing roles of the IL and PL are mediated by projections to different targets in the amygdala (Sotres-Bayon and Quirk, 2010), a key site of plasticity for fear learning (LeDoux, 2000).

To enable translation of these findings from rodents to humans, researchers developed similar fear conditioning paradigms for use during human neuroimaging. These often include another cue (CS-) that is not linked to the US but a neutral outcome instead, to allow for measurement of differential responses between CS+ and CS-. The skin conductance response (SCR) is often used to measure conditioning and increases in this response reflect the conditioned response (CR). Although there is much variation in paradigm design, which could account for some of the discrepancy in findings (Sehlmeyer et al., 2009), the dACC, vmPFC and amygdala have each been identified to have distinct roles in fear conditioning and extinction in humans (Milad and Quirk, 2012).

Phelps and colleagues carried out the earliest fear conditioning studies in humans, using fMRI with a partial extinction reinforcement, to slow down the rate of extinction learning to allow its detailed examination (Phelps et al., 2004). They showed that amygdala activity correlated with the CR during both acquisition and extinction (Phelps et al., 2004). In addition, the vmPFC showed increased activity during extinction recall and the magnitude of this correlated with extinction success the next day. These findings have been replicated and extended, revealing that activity in the vmPFC also decreases during acquisition (Linnman et al., 2012b; Milad et al., 2007b). Functional activity of different parts of the vmPFC have been shown to correlate with extinction recall (Graham and Milad, 2011a). However, human vmPFC encompasses a number of distinct cytoarchitectonic areas, including sgACC (BA25, subgenual BA24) and adjacent regions including areas 14 and ventral area 32. Similarly, neuroimaging studies have shown that functional activity of the aMCC, as well as cortical thickness, positively correlates with the expression of conditioned fear, during acquisition (Milad et al.,2007b) and resting aMCC metabolism predicts differential fear expression during extinction recall (Linnman et al., 2012b). Furthermore, fear extinction is impaired in anxiety disorders, and evidence from fear extinction studies in patients with PTSD indicate abnormalities in the activity of the dACC and vmPFC. Specifically, PTSD patients show

impaired extinction recall compared to controls, and this is associated with greater activity of the pgACC/rdACC and lesser activity of the vmPFC (Milad et al., 2009).

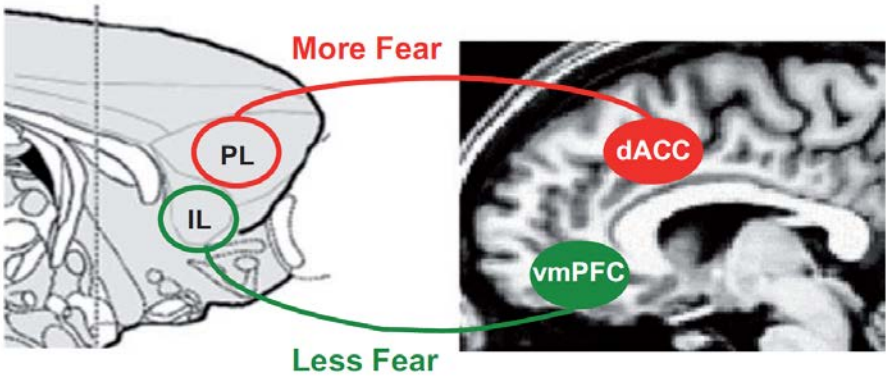

Figure 5.1 Proposed functional homologies with respect to fear between rodent (left) and human (right) mPFC. From (Milad and Quirk, 2012).

Thus, the dACC and vmPFC appear to have opposing roles in fear expression and extinction recall respectively in humans and have been likened, respectively, to the functional roles of the PL and IL in rodents (Figure 5.1) (Milad and Quirk, 2012). However, this apparent functional homology is discrepant with putative structural homology between the primate and rodent. Whereas the IL is a single cytoarchitectonically defined region of the rodent mPFC, as discussed, the vmPFC in humans is composed of a number of distinct cytoarchitectonic regions. On the basis of cytoarchitecture and connectivity the IL has been proposed homologous to primate area 25 (Heilbronner et al., 2016; Vogt and Paxinos, 2014), but area 25 is considerably more caudal than the vmPFC region generally implicated in extinction recall (Graham and Milad, 2011a).

Similarly, there is confusion with regards human homology to rodent PL. Whilst the PL and rdACC appear functionally homologous due to their apparently similar contribution to fear expression (Milad and Quirk, 2012), on the basis of cytoarchitecture and connectivity the PL is proposed homologous with primate area 32 (Heilbronner et al., 2016; Öngür et al., 2003; Passingham and Wise, 2012; Vogt and Paxinos, 2014), though its connectivity pattern also shows some similarity with pgACC. Moreover, the rodent AC shows greater structural homology with primate dACC than the PL does. However, in terms of function the rodent AC has been less studied in comparison to the PL in fear conditioning. In those few studies that have investigate rodent AC, Bissière and colleagues have studied the role of the ACd/Cg1, a subregion of the rodent AC which they show has excitatory projections to the BLA. Pharmacological inactivation of this region prior to acquisition of fear conditioning resulted in impaired acquisition and subsequent recall of fear (Bissière et al., 2008), whilst activation

facilitated it (measured by conditioned freezing response). There was no effect on fear expression when inactivation occurred prior to fear extinction, but it was enhanced following activation. Although the use of microstimulation to activate the ACd prior to acquisition found no effect on fear expression during acquisition, extinction or extinction recall (Vidal-Gonzalez et al., 2006) only the rostral portion of the ACd was targeted here. Thus, together these findings suggest that a subregion of the ACd/Cg1 is involved in the expression of fear and may also be involved in its acquisition. Hence, this region in rodent also shows functional similarity with the aMCC in humans with regards to fear expression during acquisition.

The difficulties in determining structural and functional homologies between rodent and human outlined here, highlight the need for similar fear conditioning studies in non-human primates. Recent work from the Roberts laboratory (Wallis et al., 2017), has revealed that inactivation of area 32 in marmoset enhanced expression of fear, while inactivation of 25 reduced it, opposite to what would be expected if these areas were homologous with the PL and IL respectively. In rhesus macaque, the dACC (a region spanning rdACC, mdACC and cdACC) has been implicated in fear (Klavir et al., 2012). Low-frequency stimulation (LFS) of the dACC, during extinction of conditioned fear had no effect on fear expression, however the following day, recall of fear memory was significantly reduced. This study implicates the dACC in the maintenance and expression of fear memory. It should be noted though that this effect differs from the observed effect of pharmacological inactivation of the PL during extinction which reduced fear expression but not fear recall (Sierra-Mercado et al., 2011). Such differences could be explained by the chosen method of inactivation - LFS has a minor and transient local effect with a long term accumulating effect on responsivity of the region in contrast to pharmacological inactivation (Klavir et al., 2012) or be due to differences in paradigm, as in the macaque study acquisition and extinction occurred within the same session.

Another important consideration when evaluating correlational findings from neuroimaging studies in humans is that activity of an area could reflect a number of different processes that are difficult to disentangle. In an attempt to isolate activity caused by fear appraisal vs fear expression a meta-analysis of fear conditioning studies including instructed fear studies, in which participants are consciously aware of CS-US contingencies and thus able to appraise fear, and classical Pavlovian fear studies in which participants learn task-associated CS-US contingencies was carried out (Mechias et al., 2010). This revealed that regardless of the paradigm type, the same mdACC region is consistently activated by conditioned fear stimuli (CS+). Thus, neither conscious appraisal nor fear expression exclusively explains activity in

this region during fear conditioning, rather its role is relevant to both. In contrast, another more rostral and dorsal region, the rostral dmPFC, was only activated during instructed fear, and was thus proposed to specifically mediate negative threat appraisal. Others have similarly proposed a role for the rdACC/dmPFC in negative appraisal processes (Kalisch and Gerlicher, 2014). For example, Kalisch and colleagues introduced high and low cognitive load during an instructed fear task and discovered that while both conditions elicited a similar conditioned response, during the low load condition, when cognitive resources enable greater conscious appraisal, activation of the rdACC was increased compared to the high load condition (Kalisch et al., 2006). These studies suggest that the rdACC may be more involved in conscious appraisal while the mdACC is more involved in fear expression.

To summarise, the dACC has been implicated in fear expression based on neuroimaging studies in humans, suggesting functional similarities between this region and the PL and ACd in rodents. However, the homologies between rodent and human areas involved in fear conditioning are difficult to determine with discrepancies apparent between structural and functional studies. Furthermore, it is suggested that different areas within the dACC may have different functional roles in fear conditioning. Thus, in this study we sought to determine the specific roles of subregions of the dACC by transiently inactivating these regions prior to the extinction of conditioned fear. To facilitate translation of results, a fear conditioning paradigm used in rodent studies (Sierra-Mercado et al., 2011) was adapted for use in marmosets (Wallis et al., 2017).

5.2 Methods

5.2.1 Subjects

A total of eight subjects took part in this study. All subjects had previously taken part in the experiments described in Chapters 2 and 4 (Table 2.1) (with the exception of Watercress who did not carry out the baseline study Chapter 4) and thus had prior telemetry implants, dACC cannulae and were habituated to the test apparatus.

5.2.2 Conditioned fear extinction paradigm

This paradigm consisted of 5 sessions, run over 5 consecutive days (Figure 5.2C). In the first two sessions, subjects were habituated to the context and the unconditioned stimulus (US^-). This involved 12 presentations with a variable intertrial interval (vITI) of 110-130s of a sliding black door opening for 5s to reveal an empty chamber behind.

In the 3rd session (acquisition), the conditioned stimulus (CS), an auditory sound (25s, 70db) was introduced. The first five CS presentations were paired with the US-. This was followed by 7 pairings of the CS with the US^+. The US^+ co-terminated with the last 5s of CS and involved the sliding black door opening for 5s to reveal a rubber snake in the chamber behind. CSs were presented with a vITI of 110-130s. In the 4th session (extinction), 20 CS-US^- pairings were presented with a vITI of 60-80s to promote extinction of conditioned fear. Infusion of saline or mb were carried out prior to the 4th session in order to assess the effect of inactivation on conditioned fear regulation and extinction. In the 5th and final session (extinction recall), 15 CS-US^- pairings were presented with a vITI of 60-80s to test for recall of fear extinction.

Blocks of 5 sessions were repeated 4 times within subject in order to carry out the 4 conditions (2 sites x 2 infusions), with a minimum of a week gap in between each. To minimise fear generalisation across blocks, patterned wall panels were used in the apparatus to change the context, and different sounds were used as the CS^+ so that each block would represented a new round of fear conditioning (Figure 5.2B). Wall panels and CS sounds were counterbalanced across conditions. Blocks were carried out in pairs such that block 1-2 and block 3-4 involved infusions in the same area, with area counterbalanced across subjects. Block 1 and block 3 were saline infusions. Watercress failed to show acquisition of conditioned fear on block 3 and 4 and thus this data is excluded.

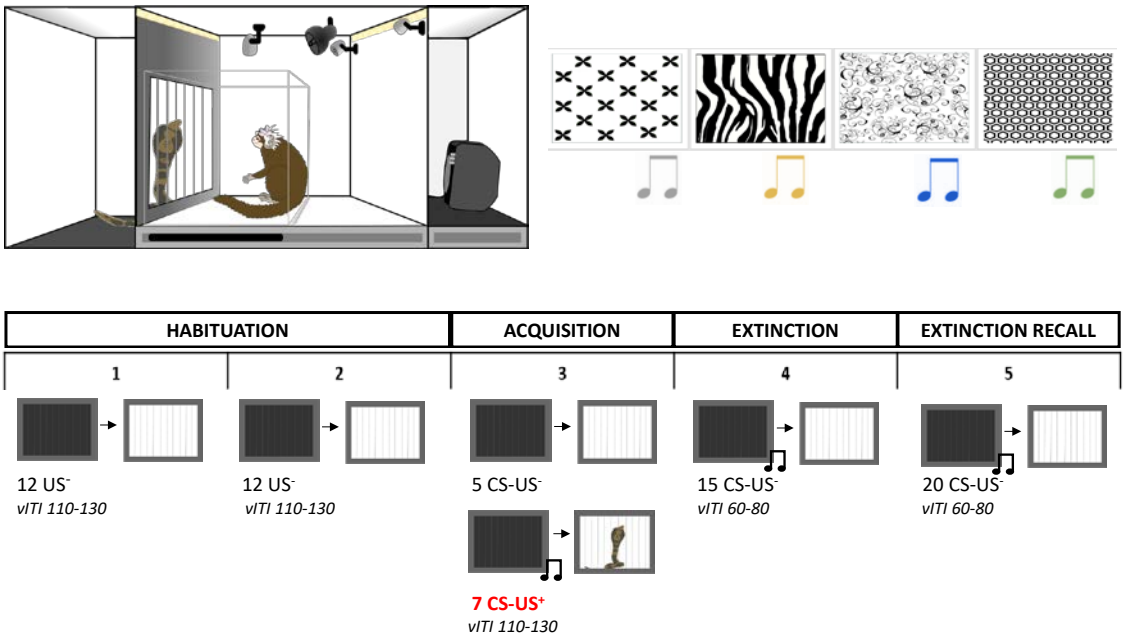

Figure 5.2 Fear conditioning paradigm. ***A*** *Diagram of marmoset in apparatus during US+ in which the black sliding door is open to reveal the rubber snake.* ***B*** *Different context wall panels (crosses, zebra, swirly, hexagon) and auditory cues (dreamharp, phone, bell, fishtank) were counterbalanced across blocks.* ***C*** *Fear extinction paradigm showing series of sessions in one block detailing the task parameters. CS = 25s, 70db auditory cue; US⁻=black door opening to empty chamber; US⁺=black door opening to rubber snake.*

5.2.3 Data analysis

5.2.3.1 Mean arterial pressure (MAP)

Telemetric data were collected and processed as described previously (2.6). The mean arterial pressure (MAP) was calculated from the systolic (sBP) and diastolic (dBP) blood pressure (MAP = 2/3 DBP + 1/3 sBP). The mean MAP during the 20s CS period and prior 20s BL period was calculated. In addition, a CS-specific MAP response was calculated for acquisition by subtracting the mean MAP during the BL from the CS.

5.2.3.2 Vigilant behaviours (VB)

All sessions were video recorded, and behaviour was scored offline. There was individual variation in the behaviours shown during the acquisition, and these varied according to the perceived threat. Thus, each animal's behaviour was assessed to identify any vigilant behaviours displayed by that animal. The identified behaviour was then scored for each 20s CS period.

Behaviours scored included:

Vigilant scanning (duration): attentive scanning of the surroundings accompanied by a tense body posture (Agustín-Pavón et al., 2012; Mikheenko et al., 2010).

Head jerks (count): rapid jerky movements of the head.

Stillness (duration): animal is still, apart from very slow subtle movements. Only occurs after presentation of the first US^{+}.

5.2.4 Data processing

For analysis of MAP and VB, trials were averaged in pairs (CS pairs) (Sierra-Mercado et al., 2011; Wallis et al., 2017). However, during the acquisition session, CS1 was excluded due to its novelty (novel CS presented), and CS2-5 were averaged as these represent baseline CS responding prior to formation of CS-US^{+} (pre-US^{+}). CS6 was also excluded as slight disruption was caused prior to this due to positioning of the snake in the chamber.

For analysis of fear extinction and extinction recall, % fear recall was calculated as follows: the MAP/VB value for each CS pair was divided by the MAP/VB value for the last CS pair of acquisition (Acq3) and converted to a percentage of conditioned responding.

5.3 Results

5.3.1 Histological assessment of cannulae placement

Histological assessment of cannula placements was carried out as described in Chapter 3. Including predicted placements, a total of six subjects had cannulae targeting rdACC, five targeting mdACC and five targeting the cdACC (Table 5.1). Two subjects (Banshee and Trixie) are still alive and thus their cannulae placements remain to be verified post-mortem.

Table 5.1 Cannulation site placements for each subject included in the conditioned fear extinction study with totals per region. Predicted placements shown in italics/brackets.

SUBJECTS	Cannulation sites		
	rdACC	mdACC	cdACC
Jalapeno	✓	✓	
Toba	✓	✓	
Garbanzos		✓	✓
Watercress		✓	✓
Snowball	✓	✓	
Azuki	✓		✓
Banshee	*(✓)*		*(✓)*
Trixie	*(✓)*		*(✓)*
TOTAL	**6**	**5**	**5**

5.3.2 Acquisition of conditioned fear as measured by MAP

All brain manipulations took place on extinction sessions so for each block the acquisition session took place before any manipulations took place. An overall mixed model ANOVA was performed on acquisition data from all four blocks for each subject (random factor) to analyse the effect of CS pair (fixed factor) on the MAP response during the CS period. This revealed a significant effect of CS pair on the MAP response indicating successful acquisition of conditioned fear ($F_{3,109}$= 146.91, p <0.001) (Figure 5.3). This was significant in each individual block (in all cases smallest p value (block 4): $F_{3,18}$ = 7.61, p <0.01). However, the MAP response was not CS-specific as there was also a significant effect of CS pair on the baseline MAP response ($F_{3,109}$ = 146.62, p <0.001) but no significant effect of CS pair on the CS-specific MAP response ($F_{3,109}$ <1), indicating conditioning to the context.

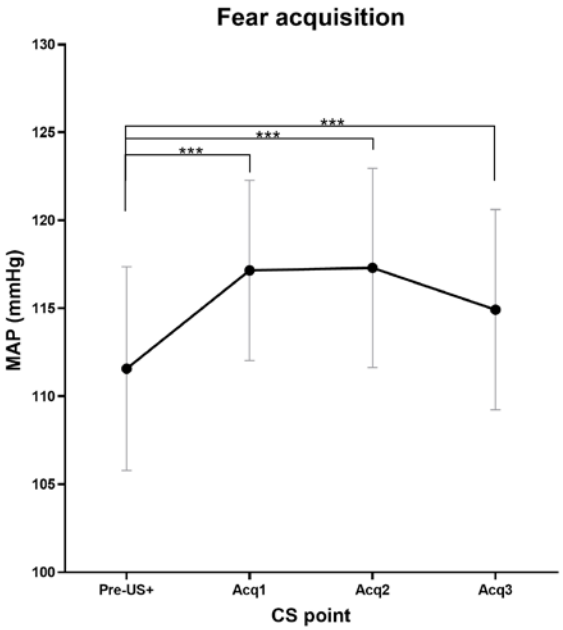

*Figure 5.3 Mean MAP during each CS pair across acquisition including all subjects (n=8) and all blocks (n=4). There was a significant effect of CS pair, and post-hoc multiple comparisons (Holm-Bonferroni correction) revealed significant differences between each acquisition point compared to the pre-US^{+} point (Pre- US^{+} vs Acq1 p p<0.001,***; Pre- US^{+} vs Acq2 p<0.001,***; pre- US^{+} vs Acq3 p<0.001,***). Symbols show mean ±SEM.*

Acquisition of fear diminished slightly across repeated blocks of conditioning indicating a degree of habituation to the paradigm (Figure 5.4). There was a trend effect of block on MAP response during the acquisition sessions (block: $F_{3,109}$ =2.18, p = 0.095). This was not significant between block pairs, (block 1 vs block 2: $F_{1,55}$ <1, block 3 vs block 4: $F_{1,48}$ <1), in which saline and drug treatments were directly compared.

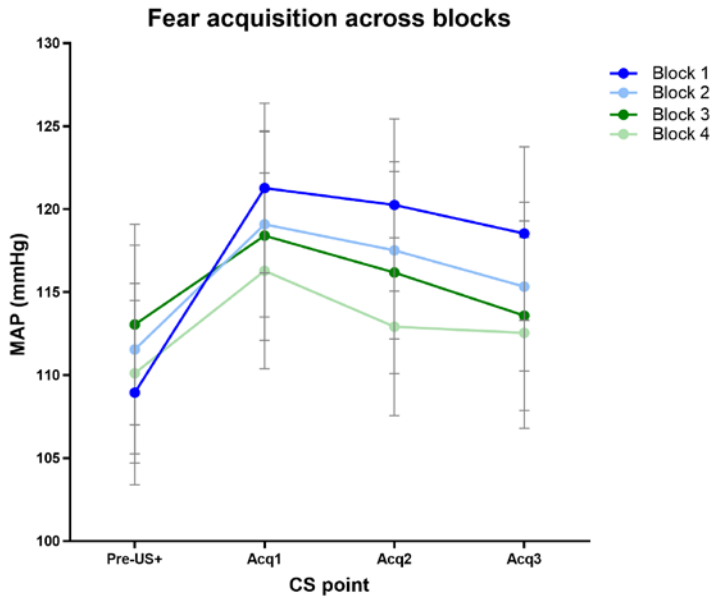

Figure 5.4 Mean MAP during each CS point across acquisition for each conditioning block.(Block 1 and 2, n=8; block 3 and 4 n=7). There was a trend effect of block on MAP response during acquisition sessions (block: $F_{3,109}$ = 2.18, p = 0.095). Symbols show mean ±SEM

Vigilant behaviour was also scored over acquisition. This has previously been observed in marmosets to develop during conditioning to a CS associated with an aversive loud noise (Mikheenko et al., 2010). However, while this behaviour was seen during extinction and extinction recall in the present paradigm, it was not very robust during acquisition when the US^+ was a rubber snake. Instead, there was large inter individual variability in the type of behaviours shown by each animal with some displaying increased vigilant behaviours across acquisition, others becoming 'still' following presentations of the US^+ ,and others becoming still in early acquisition but recovering vigilant behaviour by late acquisition (Table 5.2). This individual variation is likely due to differences in trait anxiety between animals and in state anxiety across acquisition blocks. This variation meant that it was not meaningful to group animals behavioural data during the acquisition session.

Table 5.2 Vigilant behaviour scores for all acquisition blocks for each subject.

Subject	CS point	Vigilant Behaviour across acquisition blocks				
		Block 1	Block 2	Block 3	Block 4	Average
Azuki	Pre-US+	3.71	3.48	3.69	2.62	**3.38**
	Acq1	5.00	3.33	2.71	2.77	**3.45**
	Acq2	3.73	3.55	2.70	3.31	**3.32**
	Acq3	5.03	2.99	3.13	2.39	**3.38**
Banshee	Pre-US+	2.83	2.09	1.90	1.57	**2.10**
	Acq1	1.54	2.15	3.21	5.14	**3.01**
	Acq2	1.29	4.34	4.89	3.23	**3.44**
	Acq3	3.56	1.97	5.14	3.65	**3.58**
Garbanzos	Pre-US+	2.49	0.58	2.26	0.21	**1.39**
	Acq1	2.95	1.01	5.29	0.82	**2.52**
	Acq2	2.59	2.90	3.37	1.57	**2.61**
	Acq3	2.32	1.66	4.21	1.81	**2.50**
Jalapeno	Pre-US+	1.62	2.32	1.70	1.21	**1.71**
	Acq1	2.28	3.00	2.11	2.52	**2.48**
	Acq2	1.31	1.06	3.79	1.79	**1.99**
	Acq3	2.19	1.72	3.67	2.66	**2.56**
Snowball	Pre-US+	2.50	5.22	2.65	3.78	**3.54**
	Acq1	3.04	5.03	2.69	6.47	**4.31**
	Acq2	1.80	7.75	4.13	3.09	**4.19**
	Acq3	6.36	4.28	2.17	4.24	**4.26**
Toba	Pre-US+	2.48	3.83	3.55	3.51	**3.34**
	Acq1	1.00	3.87	4.63	4.21	**3.43**
	Acq2	3.87	6.82	3.15	2.16	**4.00**
	Acq3	4.38	5.85	3.22	3.34	**4.19**
Trixie	Pre-US+	3.13	1.84	1.81	0.41	**1.79**
	Acq1	1.03	3.62	1.54	0.70	**1.72**
	Acq2	0.00	2.65	2.35	0.80	**1.45**
	Acq3	0.00	3.74	2.71	0.73	**1.79**
Watercress	Pre-US+	3.15	2.76			**2.96**
	Acq1	1.69	4.14			**2.92**
	Acq2	4.32	7.27			**5.79**
	Acq3	5.04	11.37			**8.20**

5.3.3 Extinction of conditioned fear in the first half of the extinction session

The data from all subjects during saline control infusions were analysed to assess if extinction occurred. There was a significant effect of CS pair on MAP %fear recall on control sessions ($F_{9,133}$ = 5.22, p <0.001). However, analysis of each half of extinction separately, revealed extinction occurred during the first half of the session only (ext half-1 CS pair: $F_{4,63}$ = 45.025, p <0.01; ext half-2 CS pair: $F_{4,63}$ <1). In contrast to the variable behavioral response observed during the CS period in acquisition, all animals at the beginning of the extinction session showed marked vigilant behaviour during the CS period in control sessions. This then declined across extinction and ANOVA revealed a main effect of CS pair ($F_{9,133}$ = 25.154, p<0.001). Again, this was only apparent in the first half of extinction and not the second (ext half-1 CS pair: $F_{4,63}$ = 15.95, p<0.001; ext half-2 CS pair: $F_{4,63}$ = 1.09, p = 0.37).

5.3.4 rdACC inactivation significantly reduced expression of fear during extinction

Saline (control) or muscimol/baclofen (to inactivate) were infused into either the rdACC, mdACC or cdACC prior to the fear extinction session (session 4) to investigate the roles of these regions in the expression and extinction of conditioned fear. An overall mixed model ANOVA was performed on MAP %fear recall with region, drug and CS pair as fixed factors and subject as a random factor. This revealed a significant main effect of drug ($F_{1,232}$ = 7.80, p<0.01, region ($F_{2,237}$ = 8.45, p<0.001) and a significant region by drug interaction on MAP % fear recall ($F_{2,232}$ = 5.03, p <0.01) which was independent of CS pair (region x drug x CS pair $F_{18,232}$ <1). However, analysis of the first and second half of extinction showed that this region by drug interaction was only significant during the first half of extinction (ext half-1 region x drug: $F_{2,113}$ = 6.32, p = 0.012; ext half-2 region x drug $F_{2,113}$ =1.06, p = 0.35). Thus, only the first half of extinction was analysed for each region.

Inactivation of the rdACC had a significant effect on MAP %fear recall ($F_{1,45}$ = 23.90, p < 0.001), however this occurred independently of CS pair (drug x CS pair: $F_{4,45}$=1.11, p = 0.36) indicating a general reduction in the expression of the fear response rather than a speeding up of the rate of extinction (Figure 5.5A). Neither inactivation of the mdACC nor cdACC had any effect on MAP % fear recall (mdACC drug: $F_{1,36}$ <1; cdACC drug: $F_{1,27}$ = 2.345, p = 0.137) (Figure 5.5A).

Analysis of VB revealed a significant main effect of drug ($F_{1,233}$ = 7.80, p<0.001, region ($F_{2,238}$ = 8.45, p<0.001) and a significant region by drug interaction ($F_{2,232}$ = 5.03, p<0.01) which was independent of CS pair (region x drug x CS pair $F_{18,233}$ =1.13, p=0.32). Again,

analysis of the first and second half of extinction showed that this region by drug interaction was only significant during the first half of extinction (ext half-1 region x drug: $F_{2,113} = 5.20$, $p<0.01$; ext half-2 region x drug $F_{2,112} <1$). Thus, only the first half of extinction was analysed for each region. This revealed a significant reduction in VB following inactivation of both the rdACC and mdACC with mb (rdACC: $F_{1,45} = 49.68$, $p<0.001$, mdACC: $F_{1,36} = 10.39$, $p<0.01$) but not the cdACC ($F_{1,27} =3.84$, $p=0.06$) (Figure 5.5B).

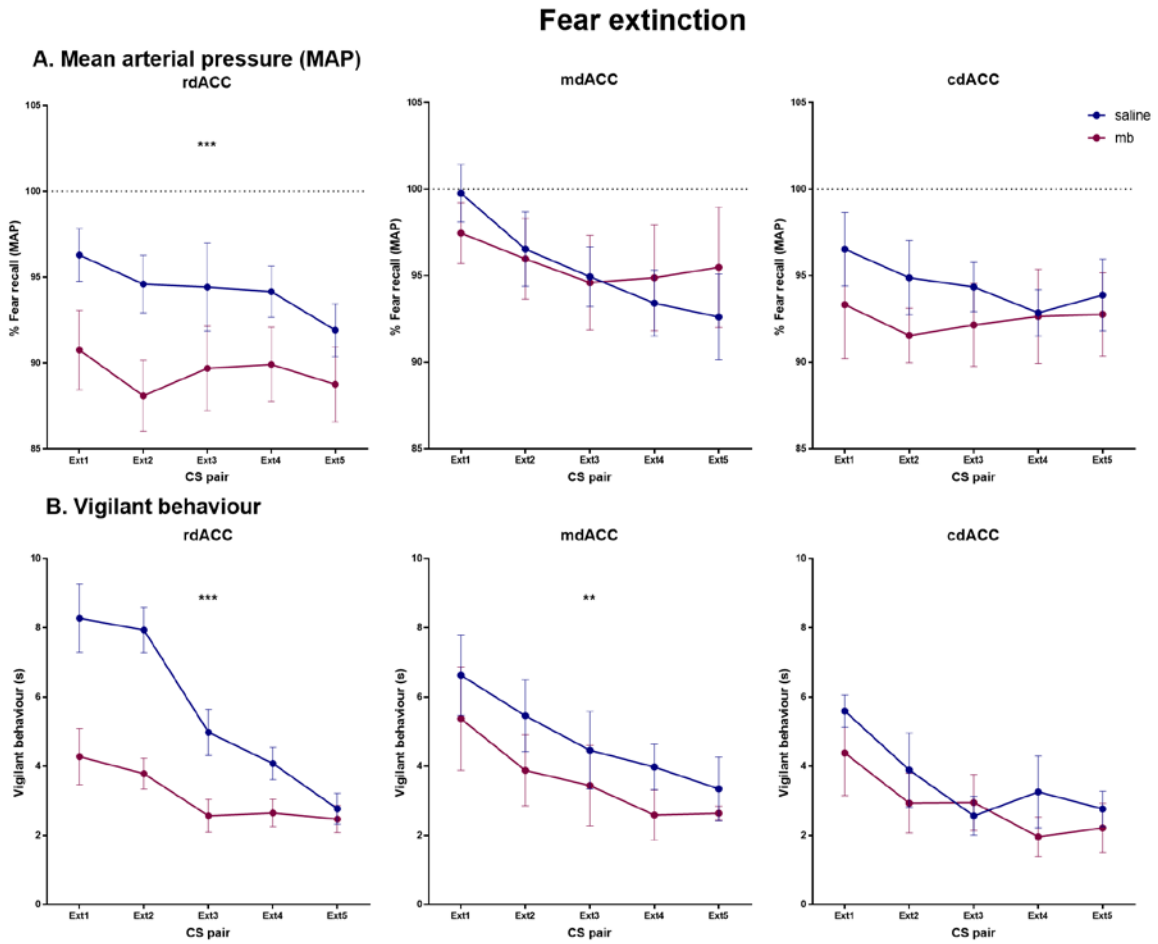

*Figure 5.5 Effect of infusion of saline or mb in dACC subregions on (A) % fear recall (MAP) and (B) vigilant behaviour during the first half of extinction. Inactivation of the rdACC significantly reduced %fear recall ($F_{1,45} = 23.90$, $p<0.001$***) but no significant effects were observed following inactivation of the mdACC or cdACC. Inactivation of the rdACC and mdACC but not cdACC significantly reduced vigilant behaviour (rdACC: $F_{1,45} = 49.68$, ***$p<0.001$, mdACC: $F_{1,36} = 10.39$, **$p<0.01$).Symbols show mean ±SEM.*

5.3.5 The dACC does not contribute to extinction recall

An overall mixed model ANOVA was performed on MAP % fear recall with region, drug and CS pair as fixed factors and subject as a random factor. There were no significant drug x region interactions on MAP % fear recall ($F_{2,155}$ <1) nor VB ($F_{2,155}$ <1) (Figure 5.6).

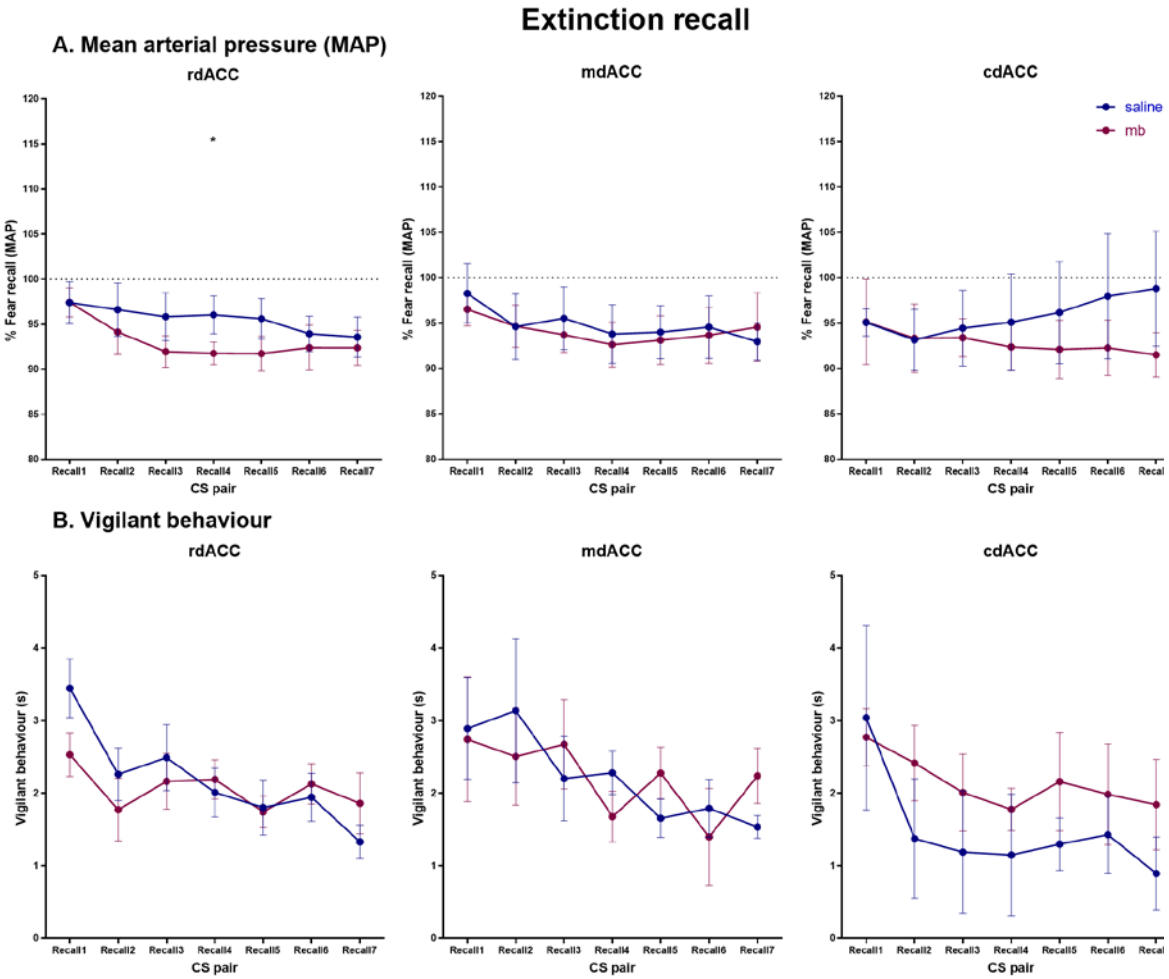

*Figure 5.6 Effect of infusion of saline or mb in dACC subregions on (A) % fear recall (MAP) and (B) vigilant behaviour during the extinction recall session. Inactivation of the rdACC significantly reduced %fear recall ($F_{1,65}$ =5.83, *p<0.05) but no significant effects were observed following inactivation of the mdACC or cdACC. There were no significant effects of drug on vigilant behaviour in any dACC subregion. Symbols show mean ±SEM.*

5.4 Discussion

The major finding of this study is that inactivation of the rdACC prior to fear extinction inhibits fear recall during the fear extinction session but had no subsequent effect on extinction recall. This effect was specific to the rdACC as inactivation of the mdACC and cdACC had no effect on fear recall nor extinction recall.

The paradigm used in this study was adapted from simple fear conditioning paradigms typically used in rodents (Sierra-Mercado et al., 2011; Wallis et al., 2017) to facilitate comparison of results. Instead of a foot-shock, commonly used as the US^+ in rodents, a rubber snake was used. Snakes are a predator of marmosets and are thus an evolutionarily conserved fearful stimulus in primates (Öhman and Mineka, 2001), and rubber snakes have previously been shown to provoke fear responses in captive marmosets (Barros and Tomaz, 2002; Shiba, 2013). Furthermore, the dACC has been implicated in pain (1.3.3) and thus use of a non-painful stimulus as the US^+ removes this potential confound. A potential flaw of the paradigm was the presentation of to-be-conditioned stimuli, CS-US^-pairing, prior to CS-US+ pairing. This was done to habituate the subject to the novel tone, but had the potential to cause latent inhibition, the reduction in fear conditioning caused by pre-exposure to the CS (Lubow, 1973). Despite some latent inhibition likely occurring, subjects were still able to acquire significant conditioned fear during the acquisition session (Figure 5.3).

It is important to note, that in the present study although CSs were presented, there was no CS-specific conditioning. Rather the conditioned MAP response likely reflected broader conditioning to the context. This could be due to the relatively short ITIs employed between successive trials during acquisition as it has been demonstrated that short ITIs promote associative conditioning with local contextual cues, diminishing CS-specific conditioning (Barnet et al., 1995). The majority of fear conditioning studies in experimental animals, do not report CS-specific conditioning (correcting for baseline levels of CR) and instead report absolute CS conditioning as done here (Burgos-Robles et al., 2009; Klavir et al., 2012; Sierra-Mercado et al., 2011; Vidal-Gonzalez et al., 2006). Although contextual conditioning occurred, this did not affect the repeated-measures design used in this study to allow within-subject comparison of fear regulation. The use of different patterned panels in the test chamber to vary the context between blocks (Figure 5.2) appears to have prevented any reduction or enhancement in fear acquisition across blocks despite being carried out in the same test apparatus.

The present result of blunted fear expression following pharmacological inactivation of the rdACC, but no effect on extinction memory, matches Sierra-Mercado and colleagues' finding following pharmacological inactivation of the PL prior to fear extinction (Sierra-Mercado et al., 2011). The paradigms used are comparable, and both likely reflect an effect on context conditioned fear. Inactivation of the PL has been reported to impair expression of both separately conditioned CS and contextual conditioned fear (Corcoran and Quirk, 2007). However, studies in which the competition between discrete cues and contextual cues was manipulated found that lesion of the PL only impaired fear expression when the competition between discrete and contextual cues was high (Sharpe and Killcross, 2015), suggesting the role of the PL in fear expression may be to modulate attention towards cues to direct fear responses appropriately. Whether this is also reflects the role of the rdACC in fear expression needs to be determined empirically with paradigms that distinguish between CS and contextual conditioning.

The ACd/Cg1 and the PL in rodents have been suggested homologous with the dACC (area 24), and area 32 respectively, although this remains contentious. (Heilbronner et al., 2016). There were no effects of mdACC and cdACC inactivation on fear expression in the present study but there was in the rdACC. Inactivation of the ACd/Cg1 found no effect on fear expression (Bissière et al., 2008), whilst various studies of the PL indicate its involvement in fear expression. Taken together, it would appear that the PL rather than the ACd is more similar in terms of function to the marmoset rdACC and the ACd may be more similar to the mdACC or cdACC. Although the PL is often proposed to be homologous with area 32 based on structural characteristics, this is contentious. Furthermore, recent work investigating the role of area 32 in marmoset found that inactivation had the opposite effect to that of PL, enhancing rather than reducing fear expression (Wallis et al., 2017).

Although the studies mentioned in rodents measured freezing as the conditioned fear response (CR), whilst the present study found a role for the rdACC in the MAP CR but not on vigilant behaviour, these findings are still comparable. MAP was a more reliable measure of fear conditioning, and showed a consistent pattern across subjects (Figure 5.3) and the pattern of MAP across acquisition, conditioning and extinction recall is very similar to that shown in rodent studies which use freezing as the CR. In addition, it is important to note that similar pharmacological inactivation of the rdACC during an emotionally neutral condition (Chapter 4) had no effect on MAP response, demonstrating that the present result is proposes a role of the rdACC on MAP that is specific to an aversive context.

The functional role of the rdACC in fear expression is also in agreement with neuroimaging studies in humans that correlate activity of the aMCC with fear expression (Linnman et al., 2012b; Milad et al., 2007a). It appears somewhat in conflict with findings in macaque in which inactivation of the dACC (largely rdACC but included anterior aspects of the cdACC) similarly reduced fear expression, but this occurred the following day during the recall session (Klavir et al., 2012). However, this is likely due to experimental differences. The latter study used LFS rather than pharmacological inactivation. The local effect of LFS is considered brief and minor but it can cause long lasting changes in synaptic plasticity, which may explain why expression of fear was affected the following day rather than the day of stimulation. Furthermore, they employed an immediate extinction paradigm (extinction occurs in the same session as acquisition) as opposed to delayed extinction (extinction occurs in a temporally distinct session from acquisition, usually the following day), which are likely to involve different neurobiological mechanisms (Myers and Davis, 2006). Thus, both the present result in marmosets and the previous result in macaque indicate involvement of the rdACC in fear expression.

The lack of effects of cdACC and mdACC inactivation suggest that these areas are functionally distinct from the rdACC with respect to fear conditioning. Neuroimaging studies in humans largely report involvement of the rdACC and larger regions incorporating rdACC and mdACC in fear expression (Mechias et al., 2010; Milad et al., 2007a). However, enhanced activity of the pMCC as well as exaggerated functional activity of this region, have been identified as risk factors for PTSD development (Shin et al., 2009, 2011). This suggests that overactivity of the cdACC might enhance expression of fear, but this remains to be determined experimentally.

In summary, the results of the present study indicate that the rdACC has a specific role in the expression of conditioned fear, a function that is comparable to that of the PL in rodents and that of the aMCC in humans. Given that exaggerated fear expression is often apparent in anxiety disorders, this finding has implications for the clinical treatment of these disorders.

6 | THE ROLE OF THE dACC IN APPROACH AND AVOIDANCE DECISION-MAKING

6.1 Introduction

When decision-making is optimal, actions are selected that maximise rewards and minimise punishments. To achieve this, organisms must flexibly modify behaviour in response to outcomes – a process driven by reinforcement learning. This involves appraisal of the available options, including assignment of values based on predicted costs and rewards, selection of the option with the highest predicted value, and finally an evaluation of the outcomes and updating of values. In patients suffering from disorders of negative emotion including anxiety and depression (see Introduction) decision-making is impaired. Although dominant models of dACC function highlight its role in reinforcement-guided action selection (Kennerley et al., 2006; Rushworth et al., 2004), the parallel role of the dACC in emotion regulation is rarely considered. Thus, an understanding of the joint contributions of the dACC to decision-making and emotion could give insights into the neurobiology underlying these disorders.

Often decisions need to be made that involve both rewards and costs, resulting in conflicting motivational drives of approach and avoidance. Excessive avoidance behaviour is characteristic of anxiety disorders (American Psychiatric Association, 2013) and this is likely driven by two main information processing biases: an attentional bias towards threat-related stimuli and an increased negative interpretation of ambiguous stimuli (Bar-Haim et al., 2007; Bishop et al., 2004; Dickson and MacLeod, 2004). These biases may influence decision-making during approach-avoidance conflict by altering the appraisal of options, inflating estimated costs of potential negative outcomes and thus leading to greater avoidance (Grupe and Nitschke, 2013; Paulus and Yu, 2012). However, avoidance alone is not diagnostic of anxiety; crucially, it is problematic when it becomes maladaptive such as when an active decision is made to forgo potential rewards to avoid potential negative outcomes (Aupperle

and Paulus, 2010). To assess this experimentally, tasks are required that involve approach-avoidance conflict, where the same action could result in either punishment or reward.

Few studies have specifically looked at the role of the dACC in approach-avoidance conflict. However, decision-making accounts of the dACC emphasize its role in reinforcement learning. Activity of the rdACC is reported to reflect interaction between both expected rewards and effort costs in a task involving effortful actions to gain reward (Croxson et al., 2009). Furthermore, in non-human primates, ablative lesions of the sulcus of the dACC impaired integration of rewards and cost history in a foraging task (Kennerley et al., 2006). In addition, the role of the dACC in conflict, conceptualised as situations that require cognitive control and subsequent adjustments in behaviour has been well-studied (Botvinick et al., 2001, 2004). This largely involves paradigms that create response conflict (when a choice between two competing incompatible responses must occur), and it has been suggested that conflict itself can act as an aversive signal in the dACC that drives avoidance learning away from further conflict (Botvinick, 2007). However, although effort and conflict are considered aversive, they are not threatening.

A broad area including the dACC and adjacent regions have been implicated in mediating a threat-related bias that sustains anxiety (Vytal et al., 2014). Thus, the dACC appears to be a common neural substrate for threat bias and conflict, both of which are relevant to approach-avoidance decision making. Aupperle and colleagues have specifically used an approach-avoidance conflict paradigm, and shown that in healthy participants, in comparison to decisions to simply approach reward (points) or avoid punishment (negative affective stimuli), decisions in which reward and punishment were both present, thus involving approach-avoidance conflict, greater activation of the rACC occurred. The opposite pattern was shown for the cdACC, which showed more activity during approach or avoid decisions than when approach-avoidance conflict occurred (Aupperle et al., 2015). This indicates that potential functional differences in the processing of threats in a decision-making context across the dACC.

Direct manipulations targeting the dACC in approach-avoidance conflict have not been carried out to my knowledge. However, microstimulation of a subzone in the adjacent pgACC in macaques (including rostral area 24 and dorsal area 32) in an approach-avoidance task increased avoidance decisions, and this effect was blocked by anxiolytic treatment (Amemori and Graybiel, 2012). Although the site of stimulation was more rostral than the dACC, the pgACC projects strongly to the dACC (Baleydier and Mauguiere, 1980) and thus the

observed effect could depend on downstream effects in the latter. However, this needs to be determined experimentally.

Decision-making impairments are also apparent in depression but differ to those in anxiety. Rather than being elicited by approach-avoidance conflict, impairments in depression are related more specifically to reward processing (Paulus and Yu, 2012). Broadly speaking, depressed patients are less sensitive to rewards, which is thought to underlie the core diagnostic symptom of anhedonia, the inability to feel pleasure (Eshel and Roiser, 2010; Pizzagalli et al., 2008). Clinically, reduced sensitivity to rewards is conceptualised as anhedonia – an inability to feel pleasure. More recently, there has been growing appreciation that anhedonia is not a unitary symptom and instead consists of distinct components: impaired reward anticipation (anticipatory anhedonia); impaired motivation to obtain rewards (motivational anhedonia); and impaired hedonic responses to reward (consummatory anhedonia) (Der-Avakian and Markou, 2012; Treadway and Zald, 2011). The combined effects of these impairments in reward processing result in 'decisional anhedonia: patients are impaired in decision making processes requiring a balance between the benefit of reward and the cost of effort. Behaviourally, this results in reduced approach responses to rewards (Treadway and Zald, 2011).

The dACC has been implicated in both reward-based decision-making and specific elements of anhedonia (Kennerley et al., 2006; Lally et al., 2014, 2015). Specifically, greater activity is observed in the rdACC (as measured by EEG current density) in response to reward feedback in participants that learnt to bias responding towards a more strongly reinforced “rich” reward stimulus compared to those that did not learn (Santesso et al., 2008). Previous work has shown that a response bias to the rich stimulus indicates reward sensitivity, and that impaired learning of this bias predicted anhedonia (Pizzagalli et al., 2005). Furthermore, activity of the rdACC has been implicated in mediating the anti-anhedonic effects of ketamine in depressed individuals (Lally et al., 2014, 2015). Thus, the rdACC appears to be a key region for reinforcement-guided reward learning and reduced activity in this region may contribute to anhedonia.

To summarise, various regions of the dACC have been implicated in a threat-related attentional bias thought to contribute to avoidance in anxiety, and in reward-based decision-making that is impaired in depressed patients with anhedonia. However, the causal role of the dACC in approach-avoidance decisions and reward sensitivity has not yet been determined. Further it is unclear whether specific regions of the dACC differentially contribute to these functions. Thus, the aim of this study was to assess the role of different dACC subregions to

changes in decision-making behaviour elicited by punishments and by rewards. This was investigated using an instrumental variable interval (VI) decision-making task that has previously been used in marmosets in the Roberts laboratory (Clarke et al., 2015). In this task a “reward + punishment” probe, was used to create an approach-avoidance conflict and thus assess threat sensitivity and avoidance behaviour, and a “rich reward” probe was used to assess reward sensitivity and approach behaviour. Subjects were well trained on this task and displayed stable performance over a long period of time. This meant that multiple manipulations could be carried out within subject without risk of affecting future performance. Therefore, the effects of both inactivation and activation of subregions of the dACC were assessed in different probe versions of the task.

6.2 Methods

6.2.1 Subjects

A total of eight marmosets took part in this study(Table 2.1). None had any prior experience of the testing apparatus.

6.2.2 Touchscreen Apparatus

This task was carried out in the same apparatus as the experiments in Chapters 4 and 5 (Figure 2.2). However, in this task, a licker was positioned centrally behind the cage bars and a touch-sensitive computer monitor or "touchscreen" (Campden Instruments, Loughborough, UK) was positioned in the chamber behind (Figure 6.1A).

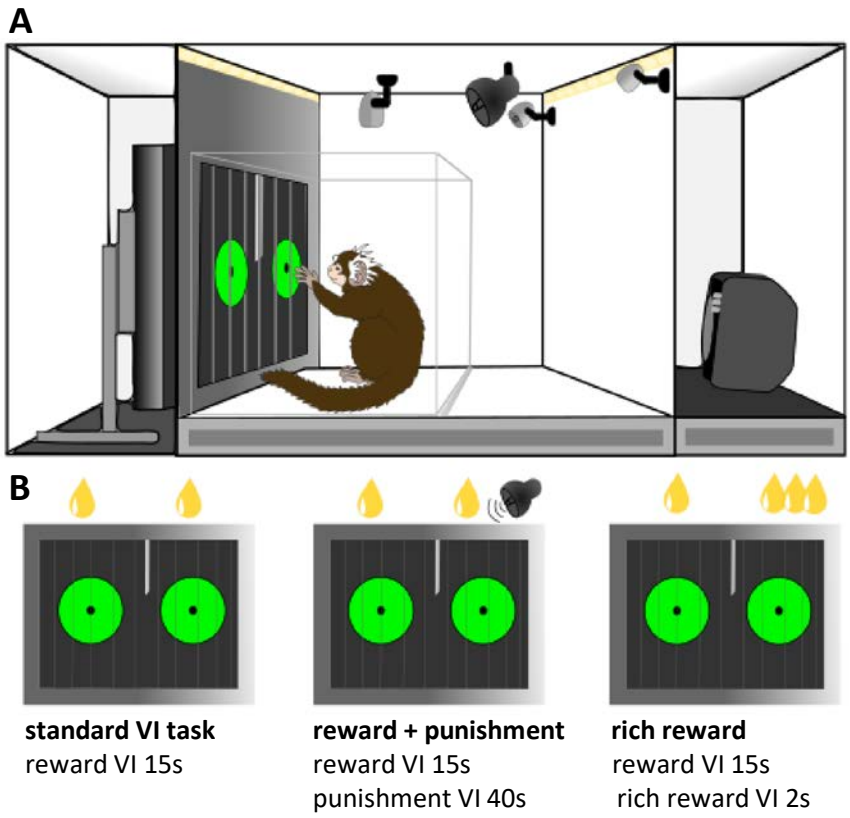

Figure 6.1 Variable interval (VI) decision-making task. ***A.*** *Diagram of a subject performing the VI decision-making task in the test apparatus.* ***B.*** *Description of the mean VI for each of the 3 different versions of the task. Milkshake droplet indicates reward, siren (loud noise) indicates punishment.*

6.2.3 Variable interval decision making task

6.2.3.1 Pretraining procedures

Subjects were first familiarised with banana milkshake reward (Nesquik, York, UK) by delivering this through a syringe in the homecage. They were then habituated to the

touchscreen apparatus and given milkshake from the syringe while in the test chamber. Next, milkshake was delivered freely though the licker in the apparatus. When at least 10 licks were made within a 12 min session, an 8s fixed time schedule of reward with 8s ITI was introduced with an auditory cue (recording of birdsong) signalling reward delivery. Subsequently, this auditory cue was always played during reward delivery and thus acted as a secondary reinforcer for reward. Next, subjects were trained to touch stimuli on the touchscreen to gain reward (8s milkshake delivery, 1s ITI). First, a green bar was presented across the width of the screen, followed by a smaller green square in the centre of the screen. Subjects were moved on to the next stage when they were reliably making at least 20 responses in a 12-minute session. In the final pretraining stages, the green square was randomly presented either to the left or the right of the licker, the reward length was gradually reduced from 8s to 5s and the ITI gradually increased from 1s to 3s.

6.2.3.2 Standard VI task

After pre-training, subjects learned to touch two identical stimuli (green circles, diameter = 6cm) presented simultaneously on the left and right of the licker (Figure 6.1A). Reward was made available to each stimulus on independent VI schedules with a mean of 15s (range from 5s to 25s in increments of 5s). If a response was rewarded, milkshake was freely available for 5s (~0.2ml) and the rewarded stimulus remained on screen for this duration. If a response was unrewarded, the stimuli disappeared and immediately reappeared, signalling the start of the next trial. Following training on the standard VI task, subjects responded fairly equally to both stimuli, however many showed a slight response bias indicating an innate preference for one stimulus location (left or right) over the other, likely due to their handedness.

6.2.3.3 Avoidance VI task (reward + punishment probe)

In reward + punishment probe sessions, the VI schedules for reward remained as in the standard VI task. However, in addition, an aversive noise (118-120 dB, 0.3-0.7s duration siren) was also presented on a VI schedule with a mean of 40s (range from 20s to 60s in 5s intervals) to the stimulus on one side only (Figure 6.1B). In training, this aversive noise was initially presented at 90dB (0.3-0.7s duration siren) and slowly incremented up to 118-120 dB over a number of sessions. The punishment was associated with the stimulus on the subject's preferred side, based on the subject's trend in response bias over a number of sessions. This ensured that any avoidance bias from the punished side would be against the direction of the subject's side preference.

6.2.3.4 Approach VI task (rich reward probe)

In rich reward probe sessions, the VI schedule for reward remained as in the standard VI task but on one side only. On the other side, the VI schedule for reward was changed to a mean of 2s (range of 0s to 4s in 2s interval) (Figure 6.1B) This meant reward availability was increased to one stimulus but not the other. The VI 2s reward schedule was linked to the stimulus on the subjects' non-preferred side, as judged by the subjects' trend in response bias over a number of sessions, to ensure that any approach bias would be opposite to the direction of the subjects' previous side preference.

6.2.4 Experimental Manipulations

When subjects were well trained well trained on the standard VI task, they underwent dACC cannulation surgery (2.4.4.2). After recovery and re-training on the task, data collection could begin. Subjects were infused with either muscimol/baclofen (mb) to inhibit activity, CGP/LY to enhance activity, or saline vehicle as a control (2.5) bilaterally into one of the cannulated brain regions prior to behavioural testing. They were given a 12-minute test session on one of the three task versions described above; the standard VI task, a "reward + punishment" probe session, or a "rich reward" probe session (Figure 6.1B). Reward + punishment and rich reward probe sessions were carried out infrequently (no more than once a week); subjects were otherwise trained daily on the standard VI task. As the rich reward probe was observed to affect the subjects' innate response bias, separate control infusions were carried out for comparison with each drug manipulation. Not all subjects received the full complement of drug infusions for all the task versions. Table 6.2 shows the drug and task manipulations carried out in each subregion for which there were sufficient data for subsequent statistical analyses. These are described in the results section.

6.2.5 Data analysis

A response bias measure was calculated for each test session (Box 6-1, 1-3). For the standard VI task this was calculated as a ratio of the number of responses made to the non-preferred stimulus/side over the number of responses made to the preferred stimulus/side. If responding were equal this would give a response bias of 1, however on average across subjects this was 0.84 (SD 0.12) indicating that subjects had a slight innate response bias. The response bias for the reward + punishment and rich reward probe sessions were calculated in the same way as for the standard VI task. As punishment was linked to the subjects preferred stimulus, an

increase in response bias indicated a bias away from punishment. Similarly, as rich reward was usually linked to the subjects non-preferred stimulus, an increase in response bias indicated a bias towards reward. Response bias values for day 1 (D1; day of infusion) and day 2 (D2; day after infusion) were normalised to day 0 (D0; day before infusion) (Box 6-1, 4,5), to account for inter-individual differences in innate response bias that could obscure drug-induced changes in task performance. Thus, a normalised response bias above 0 indicated either a punishment bias or a reward bias depending on the task version.

1. **standard VI task:**

   $$\text{response bias} = \frac{\text{total responses to non-preferred stimulus}}{\text{total responses to preferred stimulus}}$$

2. **reward + punishment probe:**

   $$\text{response bias (punishment bias)} = \frac{\text{total responses to non-preferred (non-punished) stimulus}}{\text{total responses to preferred (punished) stimulus}}$$

3. **rich reward probe:**

   $$\text{response bias (reward bias)} = \frac{\text{total responses to non-preferred (rich reward) stimulus}}{\text{total responses to preferred (normal reward) stimulus}}$$

4. **normalised response bias (D1):**

   $$\text{normalised response bias} = \text{D1 response bias} - \text{D0 response bias}$$

5. **normalised response bias (D2):**

   $$\text{normalised response bias} = \text{D2 response bias} - \text{D0 response bias}$$

Box 6-1Equations used to calculate response bias in the different task versions and normalisation of response bias.

6.3 Results

6.3.1 Histological assessment of cannulae placements

Histological assessment of cannula placements was carried out as described in Chapter 3. Of these, including predicted placements, a total of five subjects had cannulae targeting rdACC, four targeting mdACC and five targeting cdACC (Table 6.1). Two subjects (Jumbee and Buttercup) are still alive and thus their cannulae placements remain to be verified post-mortem. As only one subjects (Jumbee) had a cannulae placements in the pgACC, data from this site is not included. In addition, one subject had a cannulae placement more posteriorly in the PCC, and data from site is also excluded. However, data collected from the other cannulated site in these two animals is included (rdACC and mdACC respectively).

Table 6.1 Cannulation site placements for each subject included in the decision-making study with totals per region. Predicted placements shown in brackets.

SUBJECTS	Cannulation sites				
	pgACC	rdACC	mdACC	cdACC	PCC
Privet		✓		✓	
Ptolemy			✓	✓	
Golem		✓		✓	
Lilin			✓		✓
Twinkle			✓	✓	
Cucumber		✓		✓	
Jumbee	(✓)	(✓)			
Buttercup		(✓)	(✓)		
TOTAL	1	5	4	5	1

Table 6.2 Drug and task manipulations carried out in each subregion

VI task version:	Standard		Reward + punishment		Rich reward	
Manipulation:	mb	CGP/LY	mb	CGP/LY	mb	CGP/LY
Site						
rdACC	✓	✓	✓		✓	✓
mdACC			✓			
cdACC	✓	✓	✓		✓	✓

6.3.2 The rich reward probe significantly increased D1 response bias

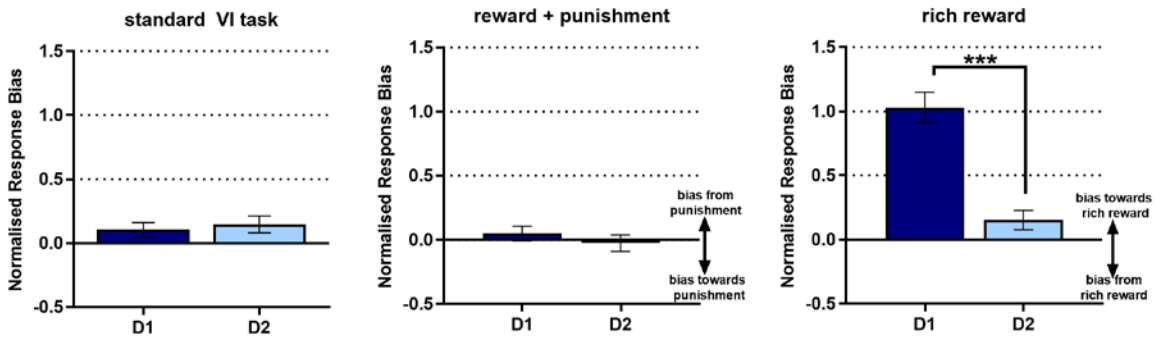

*Figure 6.2 Normalised response bias to the standard VI task, reward+ punishment probe and rich reward probe following control infusions . There was a significant effect of task on normalised response bias on D1 ($F_{2,67}$ = 33.808, p<0.001***) and a significant effect of day on normalised response bias during the rich reward probe session ($F_{1,69}$ = 25.683, p <0.001***).Bars show mean ±SEM.*

An overall mixed model ANOVA was performed on normalised response bias with task version (standard VI task, reward + punishment probe, rich reward probe) and day (D1, D2) as fixed factors and subject as a random factor. For this analysis, only data from control saline infusions (across all regions) was used. Significant effects of task version ($F_{2,67}$ = 33.808, p <0.001), day ($F_{1,69}$ = 25.683, p <0.001), and a task version by day interaction ($F_{2,66}$ = 22.249, p <0.001) were apparent. Separate analysis revealed a significant effect of task version on D1 response bias ($F_{2,36}$ = 46.096, p <0.001), due to the increased D1 response bias observed during the rich reward probe session, but not on D2 response bias ($F_{2,30}$ = 2.322, p = 0.115, ns). There was also a significant effect of day on response bias during the rich reward probe ($F_{1,15}$ = 73.64, p <0.001) (Figure 6.2).

6.3.3 Inactivation or activation of dACC subregions had no effect on response bias in the standard VI task

An overall mixed model ANOVA was run with fixed factors of region (rdACC and cdACC), drug (saline, mb, CGP/LY) and day (D1 or D2) and subject as a random factor to assess the effect of inactivation and activation on response bias on the standard VI task. No significant drug by region interactions were observed (drug x region: $F_{2,34}$ <1, drug x region x day: $F_{2,32}$ <1) (Figure 6.3).

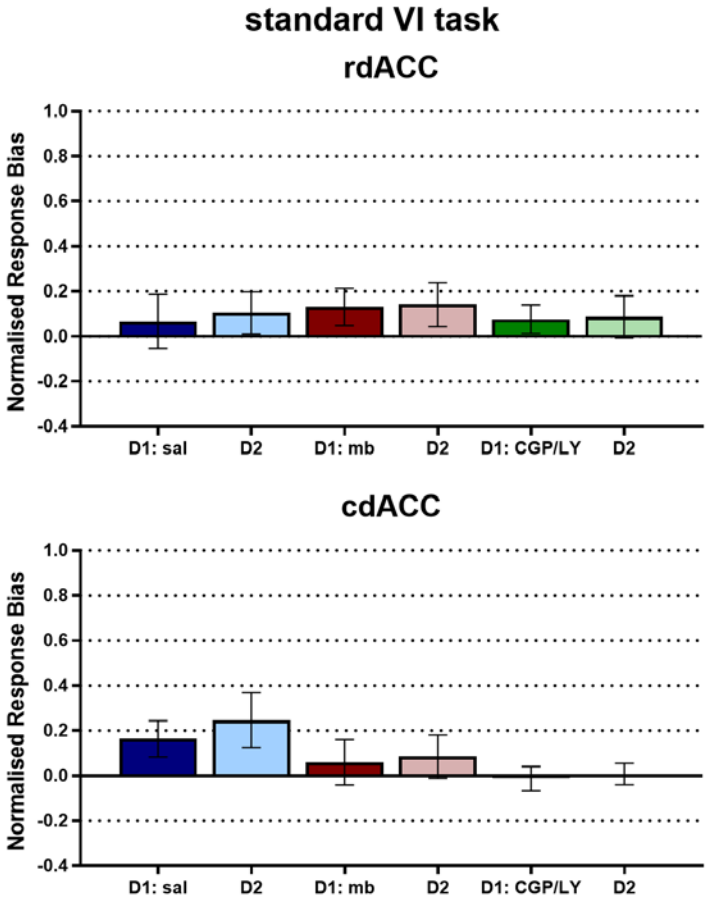

Figure 6.3 Effect of inactivation (mb) and activation(CGP/LY) of dACC subregions on normalised response bias in the standard VI task. No significant effects were observed. Bars show mean ±SEM. Darker bars indicate the day of infusion, with paler bars indicating the following day.

6.3.4 Inactivation of dACC subregions had no effect on the response bias in the reward + punishment probe

An overall mixed model ANOVA was run with fixed factors of region (rdACC, mdACC and cdACC), drug (saline or mb), and day (D1 or D2), and subject as a random factor to assess the effect of activation on response (punishment) bias on the reward + punishment probe (Figure 6.4). No significant drug by region interactions were observed (drug x region: $F_{2,34}$ =1.72, p = 0.192, drug x region x day: $F_{2,34}$ <1), nor were any significant effects observed following separate analyses run on each subregion (rdACC and cdACC).Thus, inactivation of dACC subregions had no effect on response bias on the reward + punishment probe

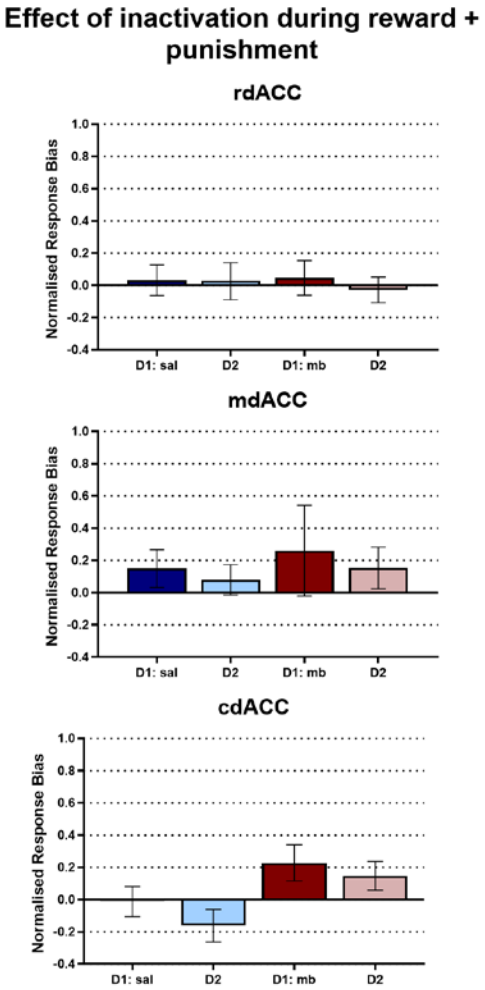

Figure 6.4 Effect of inactivation (mb) of dACC subregions on normalised response bias in the reward + punishment probe . No significant effects were observed. Bars show mean ±SEM. Darker bars indicate the day of infusion, with paler bars indicating the following day.

6.3.5 Activation of the cdACC blunted the D1 response bias in the rich reward probe

An overall mixed model ANOVA was run with fixed factors of region (rdACC and cdACC), drug (saline or mb), and day (D1 or D2), and subject as a random factor to assess the effect of

inactivation on response (reward) bias on the rich reward probe. A significant effect of day was apparent ($F_{1,23} = 26.1$, $p < 0.001$), reflecting the effect of this task version on response bias, but no significant drug by region interactions (drug x region: $F_{1,23} < 1$, drug x region x day $F_{1,23} < 1$). Separate mixed model ANOVAs were run on the rdACC, and cdACC with drug (saline, mb) and day (1 or 2) as fixed factors and subject as a random factor to assess the effects of inactivation if each region on response bias on the rich reward probe. There were significant effects of day in all regions but no significant effect of drug or a drug by day interaction (Figure 6.5)

An overall mixed model ANOVA was run with fixed factors of region (rdACC and cdACC). drug (saline or CGP/LY) and day (D1 or D2) and subject as a random factor to assess the effect of activation on response (reward) bias on the rich reward probe. A significant effect of day was apparent ($F_{1,20} = 25.66$, $p < 0.001$) reflecting the effect of this task version on response bias, but no significant effect of drug or a drug by day interaction. Separate mixed model ANOVAs were run on rdACC and cdACC with drug (saline, CGP/LY) and day (1 or 2) as fixed factors and subject as a random factor to assess the effects of activation on response (reward) bias on the rich reward probe. There were significant effects of day in both regions. In addition, although there were no significant effects of drug or a drug by day interaction in the rdACC, there was a significant effect of drug and drug by day interaction in the cdACC (cdACC drug: $F_{1,11} = 8.503$, $p = 0.0139$; cdACC drug x day: $F_{1,11} = 5.729$, $p = 0.035$ (Figure 6.5). This was only apparent on D1 (day of infusion and not the following day (D1 drug: $F_{1,3} = 10.424$, $p = 0.0482$, D2 drug: $F_{1,3} = 0.127$, $p = 0.745$).

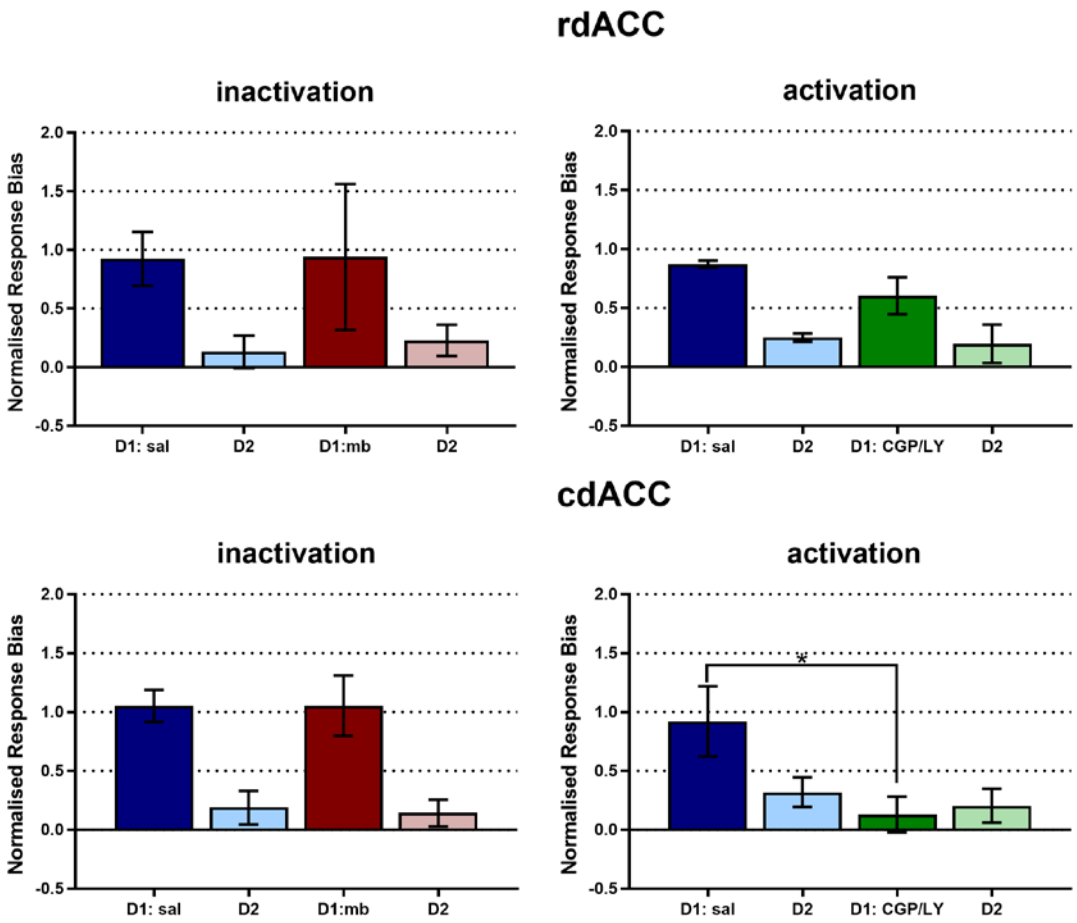

Figure 6.5Effect of inactivation and activation of the rdACC and cdACC on normalised response bias in the rich reward probe. There was no significant drug by region interaction, In the rdACC there were no significant effects of inactivation or activation, however there was a significant response bias on the day of infusion (D1). There was no significant effect of inactivation of cdACC, however activation significantly reduced the normalised response bias on D1. Bars show mean ±SEM.

6.4 Discussion

The major finding of this study is that enhanced activation of the cdACC abolishes a response bias towards reward. In contrast, activation of the rdACC had no effect on response bias towards reward, and neither inactivation of the rdACC or cdACC affected response bias away from punishment or towards reward.

Presentation of an asymmetric reinforcer ratio between two correct responses has previously been shown to produce a response bias– a preference to identify the stimulus paired with more frequent reward in healthy humans. However, subjects with higher depressive symptoms (sub-clinical) failed to acquire this response bias, and this predicted greater anhedonic symptoms one month later (Pizzagalli et al., 2005). Similarly, in the present study presentation of two identical stimuli with different VI schedules of reward such that response to one stimulus resulted in more frequent reward delivery (rich reward probe), elicited a response bias towards the rewarded stimulus in marmosets (Figure 6.2). This approach bias remained intact following inactivation of the cdACC, it was abolished following activation of the cdACC by infusion of CGP/LY (Figure 6.5).

It is difficult to deduce the physiological function of the cdACC based on impaired function following pharmacological activation. However, as inactivation had no effect on response bias to a rich reward, this suggests the cdACC is not causally involved in the learning of a response bias. This indicates that overactivity of the cdACC affects expression of this reward bias. A reduced sensitivity to reward is thought to underlie anhedonia, a core symptom of depression (Eshel and Roiser, 2010; Pizzagalli et al., 2008). Although, there are limited functional imaging studies implicating abnormalities in cdACC function in anhedonic symptomatology, clinical assessment of anhedonia typically involves self-report of consummatory pleasure rather than decisional aspects of anhedonia. In assessing only one element of anhedonia, studies of the neural correlates of anhedonia may be failing to identify brain regions (such as cdACC) involved in distinct components of the symptom. Overactivity of the cdACC may induce an anhedonia-like phenotype specifically in the decision-making domain. This may be caused by reduced hedonic capacity (Pizzagalli et al., 2008) or impaired integration of reinforcement history which is posited as a key function of the ACC (Rushworth et al., 2007).

Functional neuroimaging in humans has shown reduced activity of the caudate in response to reward, and reduced volume of this region correlates with anhedonic symptoms in unmedicated subjects with depression (Pizzagalli et al., 2009). Furthermore unmedicated

depressed patients show reduced functional connectivity between the caudate and cdACC in response to rewards, that normalises following antidepressant treatment (Admon et al., 2015). This suggests that abnormal functional connectivity between the cdACC and caudate may be responsible for reduced reward sensitivity in depression. Whether the reduced reward responsivity observed following cdACC activation in the present study is mediated by the caudate, remains to be determined.

Activity of the rdACC has been implicated in mediating the anti-anhedonic response of ketamine in the treatment of depression (Lally et al., 2014, 2015). One interpretation of this is that reduced rdACC activity is important in clinical anhedonia. However, no impairment was observed, following rdACC inactivation on the response bias to the rich reward probe (Figure 6.5), indicating that the rdACC is not causally involved in this. This suggests that the rdACC abnormalities observed in depression could reflect impairments in consummatory aspects of anhedonia rather than decisional. In addition, the present lack of effect of inactivation or activation of the rdACC in expression of a response bias, conflicts with a study carried out in healthy subjects in which activity of the rdACC in response to reward feedback is correlated with learning of a response bias using a decision-making task (Santesso et al., 2008). The findings of no effect of inactivation or of activation of the rdACC on the response bias to the rich reward probe conflict with this as they indicate that the rdACC is not causally involved in the learning of a response bias to reward. However, the latter finding was observed in the region of the rdACC directly above the corpus callosum, whilst the region targeted in marmosets was more dorsal, lying in area 24b and 24c.

In the reward + punishment probe sessions, a punishment VI schedule was superimposed on the normal VI reward schedule on one side only. This was used to create approach-avoidance decisional conflict and thus assess the extent to which subjects were willing to experience punishment in order to gain reward. A response bias away from the reward + punishment stimulus would hence indicate avoidance behaviour, and this has shown to be excessive in anxiety disorders. However, following control infusions, there was no change in response bias, as has previously been reported (Clarke et al., 2015), indicating that subjects were willing to experience occasional punishment in pursuit of reward. According to a model of cognitive mechanisms underlying threat processing (Bar-Haim et al., 2007), this suggests that the punishment, (118-122 dB, 0.3-0.7s duration siren on a VI 40s) is evaluated as a low threat, and processed such that current goals are pursued and “minor negative stimuli” are ignored. Excessive avoidance in anxiety disorders is proposed to result from evaluation of low threats as highly threatening, resulting in interruption of current goals and orienting to threat.

However, inactivation of rdACC or cdACC did not modify response bias indicating that normal activity of the dACC is not required to inhibit a threat-related bias. Furthermore, a neuroimaging study in humans indicates that depending on the intensity of a threat, activity of different subregions of the dACC is differentially recruited, with the cdACC associated with strong threat in particular (Straube et al., 2009). Thus, the lack of effect of inactivation of the cdACC in response to a weak threat, observed in the present study, is consistent with previous findings. Human functional imaging data, instead suggests that overactivity of the dACC is involved in a threat-related attentional bias during anxiety (Vytal et al., 2014), rather than underactivity. However, whether increased activity of the dACC causes the threat-related bias remains to be determined.

A potential limitation of this study was the use of CGP/LY to pharmacologically activate the target regions. CGP/LY has been shown to act by increasing presynaptic glutamate release (Marrocco et al., 2012). Glutamate can induce neuroplastic changes that can result in long-lasting changes in the function of a region. However, there was no evidence for a lasting alteration in response bias specifically following CGP/LY infusions indicating this did not occur. Indeed, response bias the following day was not significantly different to that following the control infusion, nor was the response bias to reward significantly diminished in the following rich reward probe session (data not shown).

Although the present study has assessed the role of the dACC in decisional aspects of reward processing, the dACC, and as discussed (Santesso et al., 2008) particularly the rdACC subregion may also contribute motivational and consummatory aspects of reward processing Future work should assess this causally in a task in which these distinct components can be assessed.

In summary, the results of the present study indicate that overactivity specifically of the cdACC plays an important role in mediating decisional anhedonia-like reductions in reward responsivity. This specific dACC subregion has not been well-studied in relation to anhedonia, and thus this finding has implications for understanding decision-making impairments in depression.

7 | A NEUROANATOMICAL STUDY OF THE dACC

7.1 Introduction

The brain consists of a network of interconnected neurons. To communicate information and thus influence function, these neurons must have structural, as well as chemical, connections between them. Knowledge of the anatomical connectivity of a region can therefore support functional findings. Accordingly, knowledge of the anatomical connectivity of the dACC might support functional differences between subregions.

Typically, anatomical tracing studies involve direct infusion of tracers into the region of interest, followed by post-mortem analysis of tracer labelling. This utilises the molecular machinery of neurons, which, like other cells, are continuously transporting macromolecules across the cell membrane. Macromolecules can be taken up from the extracellular space by the axon and transported towards the cell body (retrograde transport). Conversely, they can be taken up from the cell body and dendrites and transported along the axon to the periphery (anterograde transport). A variety of neuroanatomical tracers have been developed, and these can broadly be categorised as anterograde, retrograde, or trans-synaptic (transport occurs across synapses). Tracers differ in their mechanisms of uptake and transport, characteristics of cell labelling, and the methods used for their visualisation (Lanciego and Wouterlood, 2011). Biotinylated dextran amine (BDA) is one the most widely used anterograde tracers due to characteristics such as its robust homogeneous labelling of the neuronal cytoplasm along the entire trajectories of fibres.

The dACC has been identified as a key node for the integration of cognition and emotion; a suggestion supported by its anatomical connectivity with both higher cortical regions in the prefrontal cortex, and with limbic regions such as the amygdala (Bush et al., 2000; Ghashghaei and Barbas, 2002; Pessoa, 2008; Stevens et al., 2011). However, the invasive nature of tracing techniques, means that much of our knowledge of cingulate connectivity in humans has been deduced from studies in experimental animals, mainly macaques. More recently, the non-invasive MRI-based connectivity mapping technique, diffusion tensor imaging (DTI), has been used to specifically characterise white matter tracts in humans (Mori

and Zhang, 2006). In addition, resting-state functional connectivity, can be used to examine correlations in neural activity (fMRI) between brain regions at rest (Roy et al., 2009). Although this is reported to reflect structural connectivity, it can occur in its absence (Greicius et al., 2009). Thus, tract-tracing experiments are still considered the gold standard method for identifying structural connectivity in the brain.

Early tracing studies assessing the structural connectivity of the cingulate cortex involved infusions of both anterograde and retrograde tracers into large portions of the cingulate cortex in macaque. In addition, anterograde tracers were infused into subcortical structures to assess cingulate terminations (Baleydier and Mauguiere, 1980; Vogt and Pandya, 1987; Vogt et al., 1979). Clear differences in the connectivity with cortical regions, thalamic nuclei and other subcortical regions were found between the ACC and more posterior PCC. For example, the ACC primarily receives projections from the midline and intralaminar nuclei of the thalamus whilst the anterior and dorsolateral nuclei project to the PCC (Vogt et al., 1979). Thus, the connectivity findings supported cytoarchitectural and functional findings, distinguishing between the ACC and PCC. Furthermore, connectivity differences were found between the pgACC and dACC, with projections from the amygdala (lateral and basal accessory nuclei) to the cingulate cortex restricted to the former, and projections from the inferior parietal cortex occurring to the dACC, and continuing more posteriorly (Vogt and Pandya, 1987). Although at that time there was no evidence for cytoarchitectural differences along the rostrocaudal axis of area 24, an affective/cognitive functional distinction between pgACC and dACC had been suggested (Devinsky et al., 1995). More recently, cytoarchitectural differences between the pgACC and dACC have been shown in human and macaque, adding to connectivity and functional differences supporting the existence of the MCC as a distinct region from the ACC (Vogt, 2016; Vogt et al., 2005). In addition, cytoarchitectural differences have been described differentiating the pMCC from the aMCC (areas 24 and b). In humans, the pMCC contains more neurofilament protein (NFP)-expressing neurons than the aMCC in layer III and layer Va (Vogt et al., 2003). Although to my knowledge these cytoarchitectural differences have not specifically been assessed in marmosets, visual inspection of the marmoset atlas does suggest differences between the extreme rostral and caudal regions of dACC in terms of SMI 32 staining against NFP (Paxinos et al., 2011).

Thus, anatomical connectivity can provide a basis for parcellation, supporting differences in cytoarchitecture and function. In addition, it can provide important insights into function, particularly in cases where the function of afferent and efferent regions are well understood.

7.1.1 A review of the structural connectivity of the dACC

Tracing studies targeting the dACC, as well as studies in which tracers are infused in other regions which might be connected with the dACC, have been instrumental in identifying the major connections of the dACC with other brain structures. These connections are summarised below with a particular focus on regions involved in emotion (Figure 7.1).

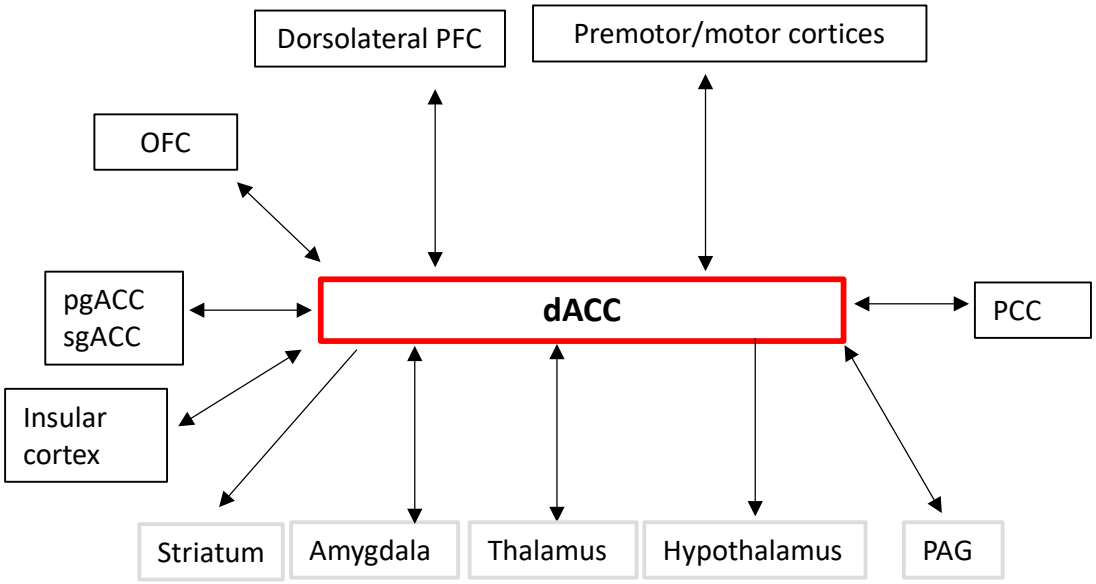

Figure 7.1 Summary of the major inputs and outputs of the dACC. Subcortical areas are shown in grey boxes and cortical areas in black boxes. Bidirectional arrows indication both anterograde and retrograde connections with the dACC whilst unidirectional arrows indicate anterograde projections from the dACC.

Cortex

In addition to the dACC, other cingulate regions, such as the pgACC (area 32) and sgACC (area 25), and cortical regions such as the dlPFC, mPFC and OFC have been implicated in the cognitive control of emotion (Ochsner et al., 2012).

Retrograde tracing of a large portion of ACC encompassing the mdACC and rdACC and extending beyond the genu revealed cortical input from the dlPFC, the lateral orbitofrontal cortex (OFC), the insular cortex and the caudal parahippocampal gyrus (TF and TH), as well as extensive input from adjacent ACC and PCC (Baleydier and Mauguiere, 1980; Vogt and Pandya, 1987; Vogt et al., 1979). Cortical connectivity was found to be ipsilateral, except at the injection site, where labelling of the contralateral dACC was apparent (Baleydier and Mauguiere, 1980). Analysis of connectivity of a more restricted region, area 24a and b of the mid-anterior dACC, confirmed reciprocal connectivity of many of the above regions, as well as strong reciprocal connectivity with the premotor cortex, and weak connectivity with the motor cortex (Arikuni et al., 1994). However, infusion of retrograde tracer into the OFC

revealed that while projections from area 24 were extensive, they were largely restricted to area 24c, particularly in more posterior dACC (Cavada et al., 2000).

Amygdala

The amygdala is a large structure located in the medial temporal lobes. This region has been intensely studied in relation to emotion since it was first discovered that lesions in macaques abolished fear (Weiskrantz, 1956). In both primates and rodents, the amygdala is composed of a number of nuclei; the basal nuclei (basolateral and basomedial), the lateral nucleus (LA), the central nucleus (CeA) with intercalated cell masses (ITC) positioned in between these. These nuclei have been distinguished functionally, in relation to fear processing in rodents (Killcross et al., 1997; LeDoux, 2003; Maren and Quirk, 2004), and on the basis of differences in anatomy, and connectivity patterns (John et al., 2013; Sah et al., 2003). Thus, the LA is considered the major input zone, receiving sensory signals from cortical and thalamic structures, while the CeA is considered the major output zone. The basal nuclei and ITC carry out intermediate processing. Of particular interest, rodent and human imaging studies have highlighted the role of medial prefrontal regions in the control of the amygdala during fear regulation (Milad and Quirk, 2012)

The dACC has strong bidirectional connectivity with the basal amygdala (Amaral and Price, 1984; Baleydier and Mauguiere, 1980; Ghashghaei et al., 2007). An extensive study of cortical connectivity with the basal nuclei of the amygdala using tracers in macaques, revealed that the density of connections with area 24 was one of the strongest amongst the prefrontal regions (Ghashghaei et al., 2007). Output to the basal amygdala from area 24 were greater than input received from it. Furthermore, analysis of the laminar pattern of input and output connections to the basal amygdala resembled reciprocal corticocortical feedforward and feedback projections i.e. output from layer 3 positively correlated with input to superficial layers 1-3. This suggests that a feedback loop exists between the dACC and basal amygdala. Interestingly, the density of projections differed along the rostrocaudal axis –a region within the cdACC projected heavily to the amygdala and had much lighter reciprocal projections, while a more rostral part of the dACC projected moderately to the amygdala but received heavy reciprocal projections. Also in the temporal lobe, the entorhinal cortex and perirhinal cortex have been shown to be reciprocally connected with the rdACC (Arikuni et al., 1994; Carmichael and Price, 1995).

Thalamus

The thalamus is a large structure located in the hindbrain, which is densely connected with the prefrontal cortex and other brain structures (Barbas et al., 1991; Darian-Smith et al., 1990). Based on this connectivity, it is reported to have a key function in relaying sensory and subcortical information to the cerebral cortex, as well as within the cortex via cortico-thalamo-cortical projections (Guillery and Sherman, 2002). The thalamus is composed of multiple cytoarchitectonically distinct nuclei, each with differing patterns of anatomical connectivity. Indeed, thalamocortical connectivity has been used as a means to parcellate the frontal cortex (Rose and Woolsey, 1948).

Infusion of retrograde tracer into the rdACC in macaques resulted in labelling of the mediodorsal nucleus and the anteromedial nucleus (AM), a cluster in the dorsolateral region of the ventral anterior nucleus (VA) as well as some of the intralaminar nuclei (Baleydier and Mauguiere, 1980). Anterograde tracers also showed projections from the rdACC to these thalamic nuclei.

Autonomic regions (hypothalamus and PAG)

Emotional arousal involves physiological responses such as changes in heart rate and a galvanic skin response, and therefore involves activation of autonomic centres in the brain. The hypothalamus has been proposed to act as a key relay in a pathway by which the prefrontal cortex can rapidly influence emotional expression activity in low-level spinal and brainstem autonomic structures (Barbas et al., 2003). In comparison to other medial frontal regions (area 25 and area 32), projections from area 24 to the hypothalamus are less dense (Öngür et al., 1998). However, following BDA infusion into rdACC (area 24b) in macaques, most hypothalamic regions were labelled, with densest labelling found in the dorsal hypothalamus.

The periaqueductal gray (PAG) is a midbrain structure surrounding the aqueduct, that has also been implicated in autonomic regulation, as well as defensive behaviours(Satpute et al., 2013). The PAG is organised in distinct longitudinal columns which differ in connectivity and function (Bandler and Shipley, 1994; Keay and Bandler, 2001). The lateral PAG reportedly mediates active coping strategies (“fight or flight”), while the ventrolateral PAG mediates passive coping strategies, and the dorsolateral PAG in particular, is associated with mediating fear learning (Kincheski et al., 2012). Anterograde tracers infused into in rostral 24b in macaque labelled the lateral and ventrolateral PAG, with some sparser labelling in the dorsomedial and dorsolateral PAG (An et al., 1998). Retrograde tracing of the dorsolateral

PAG revealed cell bodies across the extent of the dACC (area 24b), which were most dense in the rdACC. A similar labelling pattern was found following retrograde tracing of the lateral and ventrolateral PAG, although these resulted in cell bodies in both 24b and 24c (An et al., 1998).

Striatum

The striatum is divided into the dorsal striatum which consists of the caudate and putamen, separated by the internal capsule in primates, and the ventral striatum which largely consists of the nucleus accumbens. Although there is no distinct boundary, these regions are associated with different functions; the dorsal striatum with cognition and sensorimotor function, and the ventral striatum with more emotion-relevant functions such as motivation and reward (Haber, 2016).

The striatum was reported as a main projection zone of the cingulate gyrus following anterograde tracer injection in the rdACC (Baleydier and Mauguiere, 1980). Dense labelling was found in the dorsal caudate and dorsal putamen, both ipsilaterally and contralaterally, though the latter was weaker, and the nucleus accumbens. Cingulo-striatal projections have been characterised in more detail by injection of retrograde tracers into different regions of the striatum (Kunishio and Haber, 1994). This revealed that the ventromedial striatum primarily receives input from the anterior area 24a and b (rdACC), while the central and ventrolateral striatum receives input across area 24a and b. In contrast, the majority of input to the dorsal striatum arose from sulcal regions, namely area 24c extending posteriorly into area 23c. Recently, Heilbronner and colleagues analysed the network homologies between rodent and non-human primate based on connectivity with the striatum (Heilbronner et al., 2016). They also found differential striatal projections across area 24 in primates, with the rdACC projecting strongly to the dorsal and ventral striatum and weaker cdACC projections to the dorsal striatum.

In summary, the dACC has connections with multiple brain regions implicated in emotional processing and other diverse functions. However, connectivity with various regions appears to differ along the rostro-caudal axis of the dACC, indicating the potential existence of functional divisions. This pattern of differential connectivity has been gleaned through synthesis of a variety of tracing studies, largely in macaques, often involving either very large infusion sites, very restricted infusion sites or focussed primarily on efferent regions. However, a specific assessment of global differences in connectivity across the dACC has not yet been carried out.

Differences in function, primarily between the rdACC and cdACC in the marmoset have been demonstrated throughout this thesis. However, differences in cytoarchitecture have not yet been clearly identified within the rostro-caudal axis to distinguish between these areas. Although the forebrain connectivity of the marmoset has begun to be established (Roberts et al., 2007), the pattern of cingulate connectivity is largely unknown. In the experiments in this chapter, I perform a preliminary inspection of NFP cytoarchitecture in the rdACC and cdACC in marmoset, followed by a detailed comparison of the ipsilateral anterograde projections of these subregions of the dACC, with a view to uncover differential structural connectivity that might support observed differences in function.

7.2 Methods

7.2.1 Subjects

A total of four marmosets were used in the experiments described in this chapter (Table 7.1). Of these, three (Watercress and Snowball) had previously taken part in the HIT, baseline, and fear extinction studies, and had received a telemetry implant, and dACC cannulation surgery.

*Table 7.1 Subjects included in the tracing study with tracer infusion sites. Subjects with * received infusions through implanted cannulae.*

SUBJECTS	Infusion sites		
	rdACC	mdACC	cdACC
Lemongrass	BDA		
Nemesis		BDA	
Watercress*			BDA
Snowball*		BDA	
Total	1	2	1

7.2.2 Tracer infusions

Biotinylated dextran amine (BDA-10000, D1956; Molecular Probes, Cambridge Bioscience, Cambridgeshire, UK) was used as an anterograde tracer. This was made up as a 5% w/w solution in 0.01M phosphate buffer, (pH7.4) then aliquoted, and stored at -20°C until ready for use.

High molecular weight BDA has been recommended over low molecular weight BDA for its preferential anterograde labelling (Reiner et al., 2000). Although some retrograde labelling of cell bodies did occur, as has been recently characterised (Zhang et al., 2017), in this study only anterogradely-labelled axon terminals were analysed. These were differentiated from fibres of passage by the appearance of bead-like structures along the axon suggestive of synaptic terminals, and the absence of cut ends (Figure 7.2).

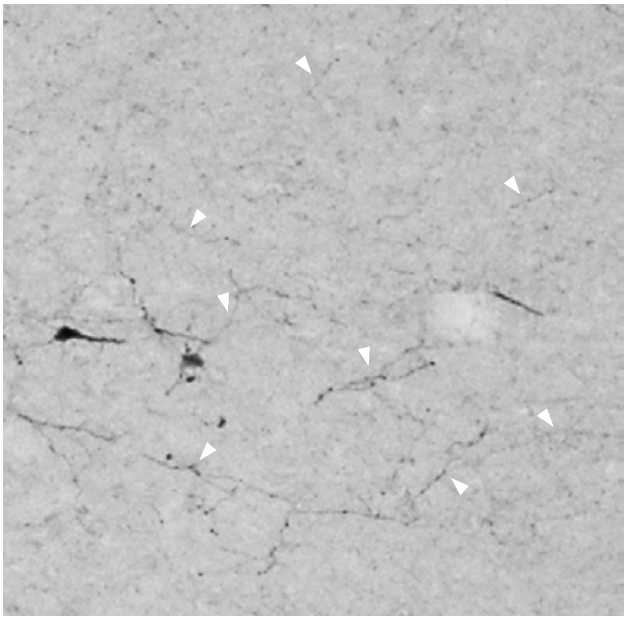

Figure 7.2 Example of anterograde labelling of axons by BDA. White arrowheads indicate prominent axon fibres.

In subjects with pre-existing cannulae implants targeting the dACC (Table 7.1), 0.2 µl of BDA was infused unilaterally at a rate of 0.1 µl per min via the indwelling cannulae as previously described (2.5.2), followed by a period of 25 minutes during which injectors were left in place to allow for diffusion.

7.2.3 Tracing surgery

Two further subjects (Lemongrass and Nemesis) had not previously undergone any surgical manipulations, and thus BDA was infused stereotaxically in a dedicated surgery. Surgical coordinates and tracer volumes are given in (Table 7.2).

Table 7.2 Infusion coordinates for subjects that received stereotaxic tracer infusions.

Subject	Tracer	Volume (µl)	AP (mm)	LM (mm)	DV (mm)
Lemongrass	BDA	0.2	13.5	-1.0	3.3
		0.1	13.0	-1.0	3.3
Nemesis	BDA	0.2	11.0	-1.0	-4.0

Following standard pre-surgical procedures, anaesthesia induction, and stereotaxic surgical procedures (2.4.4), a craniotomy was made at the depth-adjusted target coordinates, and the dura was pierced with a needle. A bevelled 31 gage injector (Plastics One, Roanake, VA, USA) was attached to a gas-tight 10µl Hamilton syringe using PTFE tubing (inner diameter 0.3mm; VWR International Ltd, UK) and solva tubing (inner diameter 0.38mm; Pulse Instrumentation, Wisconsin, USA), and secured onto the stereotaxic arm. The tubing and syringe were filled with saline (sodium chloride 0.9% w/v; Hameln Pharmaceuticals Ltd., Gloucester, UK), and an air bubble, then BDA were loaded by drawing back the syringe plunger. The Hamilton syringe was placed in a microinfusion pump set to 0.495mm diameter, and a rate of 0.1ul per min. The injector was slowly lowered to the target site +0.1mm further ventral, and then brought back up to the target DV coordinate (to promote uniform liquid flow). The air bubble was marked on the tubing, and the microinfusion pump was started. The pump was stopped at the appropriate time according to the desired infusion volume, and the air bubble was inspected to verify the infusion had worked. The injector was left in situ for 25 min to allow for diffusion. Finally, the injector was slowly removed from the brain. The skin at the incision was sewn back together using single sutures (3.0 Vicryl, polygactin 910, re-absorbable, Ethicon, Puerto Rico, USA). Standard procedures for post-surgical care were carried out (2.4.5)

7.2.4 Histological procedures

Subjects were put down a minimum of 10 days after infusion to allow for the tracer to spread. Each brain was dissected, post-fixed, and cryoprotected as described in section 2.4.5. A brain was then frozen on a sledge microtome, and coronal sections were cut at 40µm. These were placed in well plates containing 0.01M PBS 0.01% azide, and arranged in series, with 200µm between each. Two series were processed, one for Nissl visualisation using cresyl violet staining as previously described (2.8), and a second to visualise BDA staining.

3,3'-diaminobenzidine (DAB) immunohistochemistry was performed to visualise neuronal labelling of BDA. Free-floating sections were washed in 0.05M Tris-NaCl with 0.5% Triton X-100 (all washes 3 x 10mins). Sections were then incubated for 2hrs in room temperature in ready-to-use Avidin-biotin complex-horseradish peroxidase reagent (ABC-HRP; Vectorstain elite, Vector Laboratories, Peterborough, UK) to enable binding of BDA. Next, sections were incubated in ImmPACT DAB (Vector Laboratories), during which DAB was oxidised to form an insoluble brown reaction product. A pilot section was stained first, with the incubation length determined empirically (20-150s) to check for adequate staining. Sections were

mounted on gelatine-coated slides and left to dry overnight at room temperature. Finally, sections were dehydrated, and the slides coverslipped with DPX mountant.

7.2.5 Data analysis

7.2.5.1 Image acquisition

Sections were visualised and imaged under bright-field using a stereomicroscope (M205 FA; Leica, Wetzlar, Germany). Low magnification images were taken of every section in the series, and high magnification images were taken of regions of interest. Images were subsequently cropped and adjusted for tone, brightness, and contrast, and arranged in Microsoft PowerPoint.

7.2.5.2 Analysis of NFP cytoarchitecture

Coronal sections of the marmoset forebrain that had previously been stained against NFP using SMI32 (unpublished data, Roberts lab), were inspected to assess differences in cytoarchitecture between the rdACC and cdACC.

7.2.5.3 Analysis of anterograde terminal labelling

For the purpose of this chapter, the primary comparison was made between ipsilateral terminal labelling following rdACC infusion vs cdACC infusion. However, data from subjects that received mdACC infusions was also assessed where there were differences in rdACC and cdACC labelling, to assess whether these were graded or more abrupt.

DAB-stained sections were visually scanned under high magnification, and compared with corresponding cresyl-stained sections to facilitate identification of labelled structures and Brodmann areas alongside careful consultation of a marmoset atlas (Paxinos et al., 2011). Thus, the nomenclature used here matches that used in the atlas. Labelling in each region of interest was scored according to density of labelling using the following scale:

- = no labelling

(+) = very weak positive labelling

+ = weak positive labelling

++ = positive labelling

+++ = moderate positive labelling

++++ = strong positive labelling

+++++ = very strong positive labelling

7.3 Results

7.3.1 NFP chemoarchitecture

SMI32 labelling of the rdACC reveals sparse expression of NFP restricted to layer V of area 24b and 24c, and few labelled neurons in layer III of area 24c only (Figure 7.3A,B,C). In the cdACC, extensive labelling is found throughout area 24 (A-D), though expression is greatest in 24b, with cell bodies in layers III and V (Figure 7.3D,E,F).

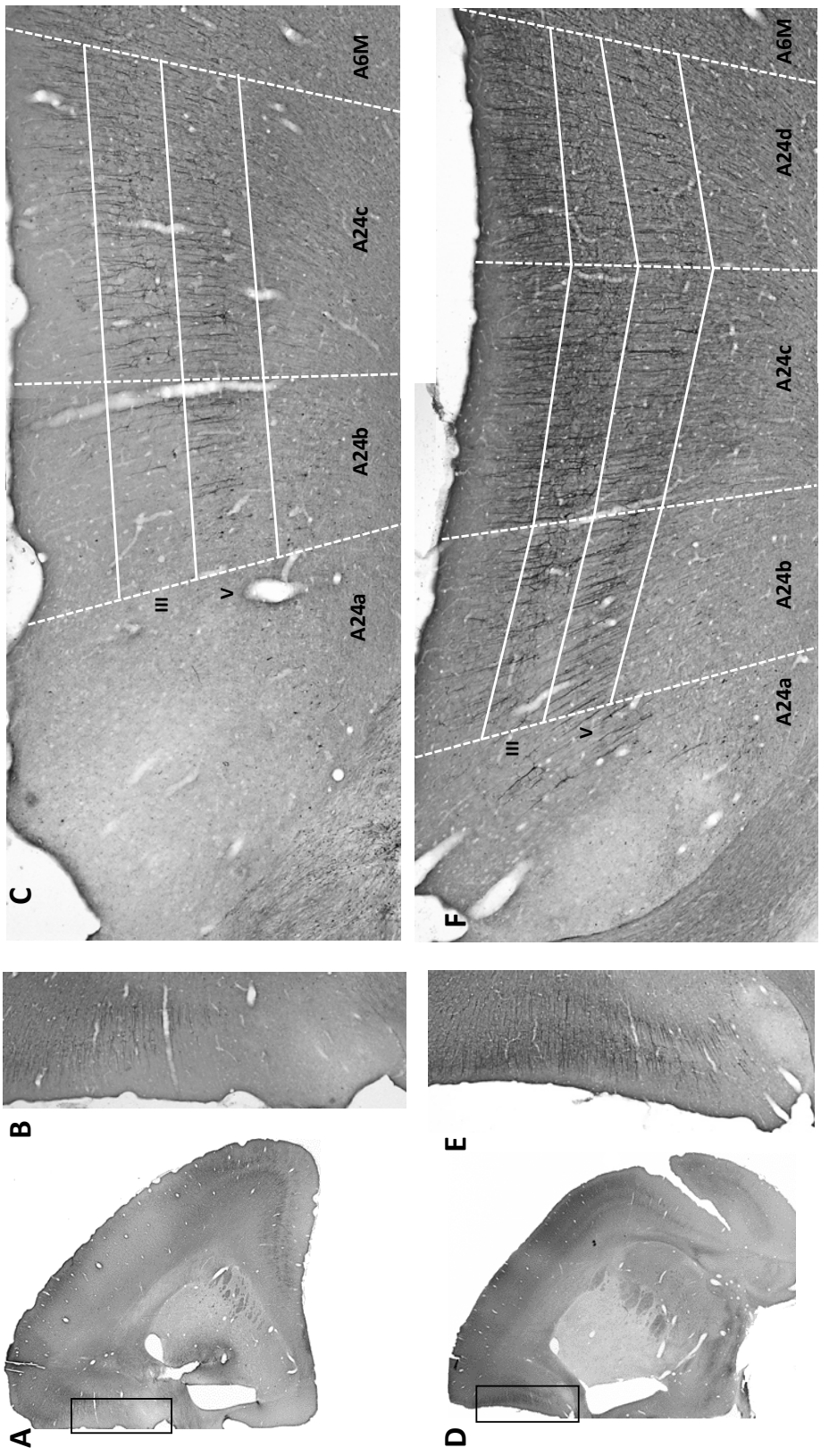

Figure 7.3 SMI32 labelling of NFP in the rdACC (A,B,C) and cdACC (D,E,F). Black boxes indicate the regions shown in the high-power photomicrographs. C and F show rotated view of the regions of interest with cytoarchitectonic areas labelled and bounded according to the marmoset atlas (Paxinos et al. 2011) and cortical layers labelled. NFP expression is denser in the cdACC compared to the rdACC, and occurs in layers III and V.

7.3.2 Infusion sites

The location of infusion sites relative to anatomical landmarks was calculated as described in Chapter 3 (Figure 7.4), also taking into account the tracer spread by visual inspection of adjacent sections. For infusions performed stereotaxically, stained sections were visually inspected to determine both the infusion site and spread. Infusions were largely restricted to area 24b and 24c of the dACC (Figure 7.5) .

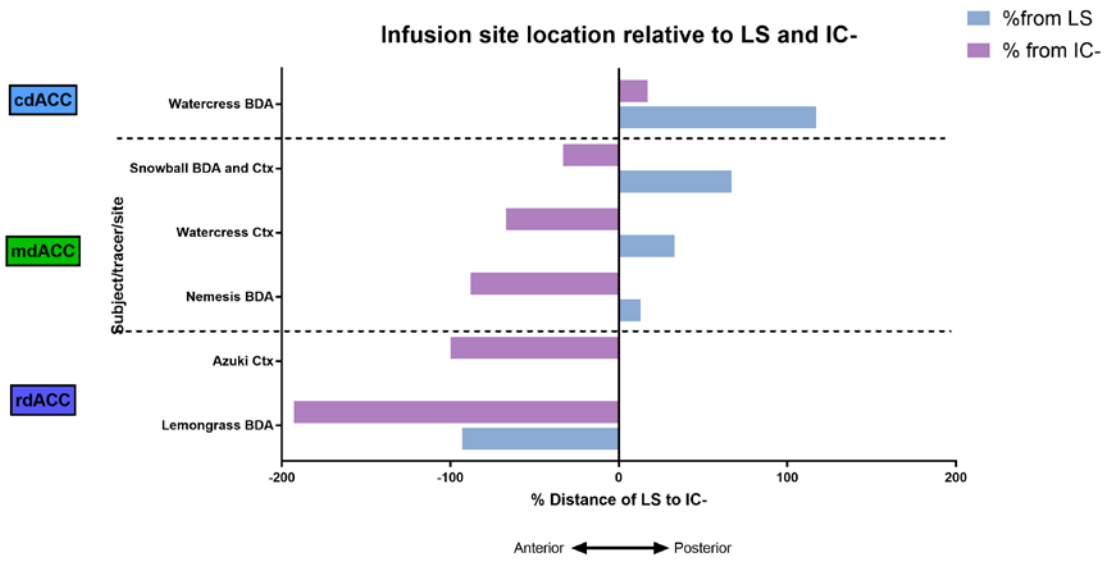

Figure 7.4 Location of tracer infusion sites. Bars plot the distance of each tracer infusion site from the lateral septum (LS) and the disappearance of the islands of Calleja standardised to the entire LS to IC-.

7.3.3 Overview of BDA anterograde terminal labelling

As can be seen in Table 7.3 and summarised in Figure 7.6, differences in anterograde projections from the rdACC and cdACC were apparent in a number of areas. Some regions (e.g. lateral PAG) were only labelled by the rdACC infusion and not the cdACC infusion. In other regions, (e.g. proisocortical motor area) there were differences in the density of projections from the rdACC compared to the cdACC. Finally, some regions (e.g. area 9) did not differ in relative labelling from infusions along the rostro-caudal axis of the dACC. The pattern of labelling following infusion in the mdACC showed greater similarity to the rdACC terminal labelling in some regions (e.g. dorsal striatum), but greater similarity to the cdACC terminal labelling in other regions (e.g. PAG). Only the parafasicular nucleus of the thalamus received projections from the mdACC, that were absent following rdACC and cdACC infusions.

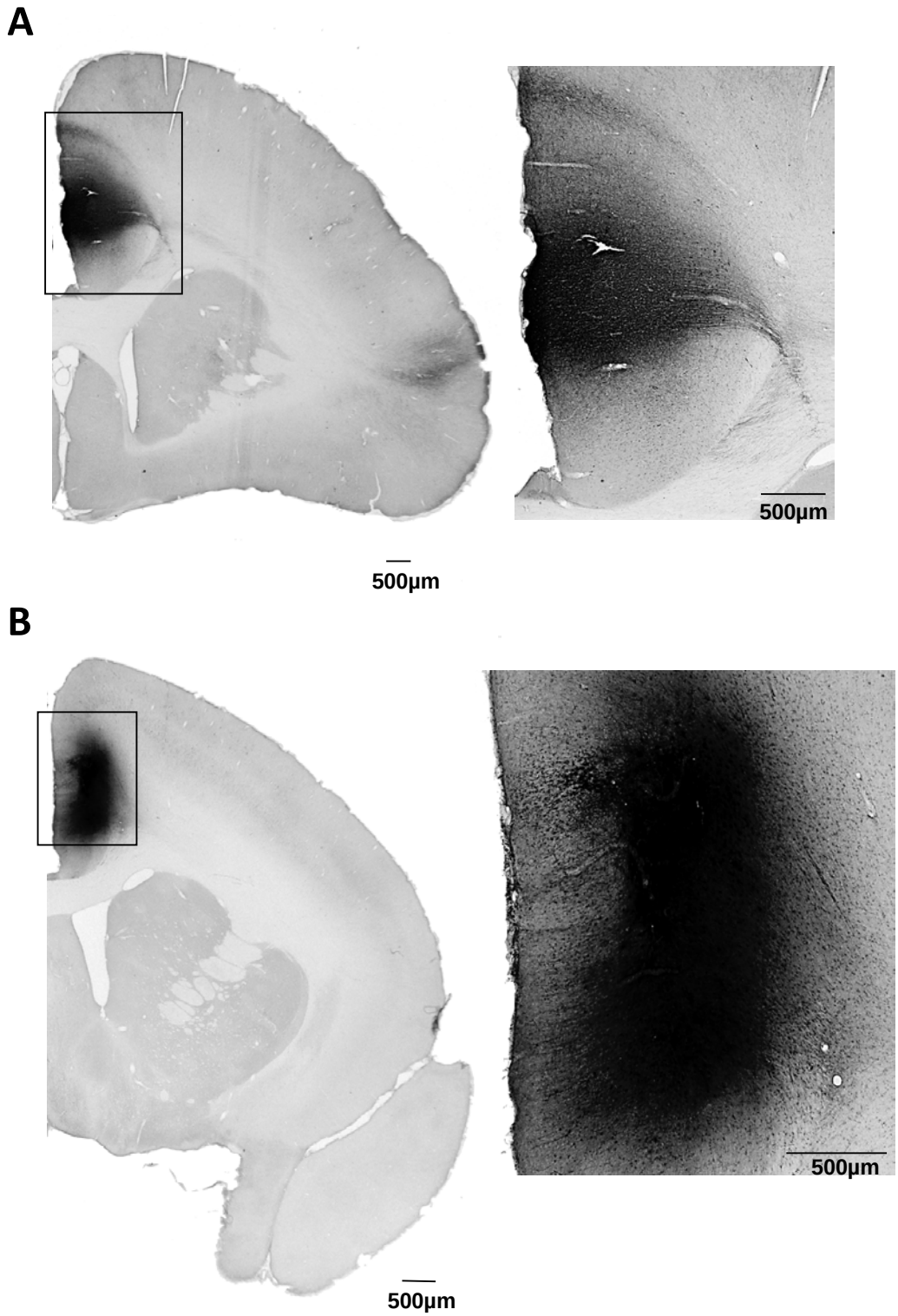

Figure 7.5 Low-power Brightfield photographs showing BDA infusion sites in the dACC. A. infusion in the right rdACC (Lemongrass) B. infusion in the right cdACC (Watercress). Black boxes indicate the regions shown in the high-power photomicrographs.

Table 7.3Comparison of BDA labelling in regions of interest following infusion into either the rdACC, mdACC or cdACC. See methods for key. Areas in which differences in BDA-labelling in rdACC vs cdACC are highlighted. Table continues on the next page.

Area	Infusion site		
	rdACC	mdACC	cdACC
Area 10	+	+	++
Area 9	+	+	+
Area 46	+	++	++
Area 8a	+	++	+++
Area 8b	++	++	++
Area 6M	+++	++++	++
Area 6D	++	+++	++
Area 11	++	++	+
Area 13	+	++	++++
Area 14	-	-	-
Area 24 - rostral	+++++	+++	++
Area 24 - mid	+++	+++++	+++
Area 24 - caudal	++	++++	+++
Area 25	-	-	-
Area 32	+	+	+
Area 47/12	**(+)**	+	++
Proisocortical Motor	++	++	+
Temporal area 3	+	-	-
Granular	++	+++	+
Dysgranular	+++	+	-
Agranular	++	**(+)**	-
Endopiriform cortex	+	-	-
Entorhinal	-	-	-
Perirhinal (A35)	-	-	-

Area	Infusion site		
	rdACC	mdACC	cdACC
Caudate (anterior)	++	+	+
Caudate (mid)	++	++	+
Caudate (posterior)	+	(+)	+
Putamen (anterior)	++	+	+
Putamen (mid)	+++	+++	+
Putamen (posterior)	+	+	+
Claustrum	(+)	++	+
Nucleus accumbens core	-	-	-
Nucleus accumbens shell	-	-	-
Bed nucleus of the stria terminalis	+	-	-
Thalamus:			
Anterodorsal (AD)	-	-	-
Anteromedial (AM)	-	+	+
Anteroventral (AV)	-	+	-
Ventral anterior lateral (VAL)	++	+++	++
Ventral anterior medial (VAM)	+	+	+
Paraventricular (PVA)	-	-	-
Interanteromedial (IAM)	+	+	-
Central medial (CM)	++	++	-
Reuniens	++	+	+
Retrouniens	+	-	-
Medial dorsal (medial)	++	++	-
Medial dorsal (central)	+++	+++	+
Medial dorsal (lateral)	+	+	+
Parafasicular (PaF)	-	++	-
Reticular nucleus	++	+	+
Hypothalamus:			
Anterior	-	-	-
Lateral	+	+	-
Posterior	+	+	-
Hippocampus	-	-	-
Amygdala:			
Basolateral	(+)	-	-
Basomedial	-	-	-
Lateral	-	-	-
Central nucleus	(+)	-	-
Extended	-	-	-
Periaqueductal gray:			
Dorsal medial	-	-	-
Dorsal lateral	-	-	-
Lateral	++	-	-
Ventrolateral	++	-	-
Ventromedial	-	-	-

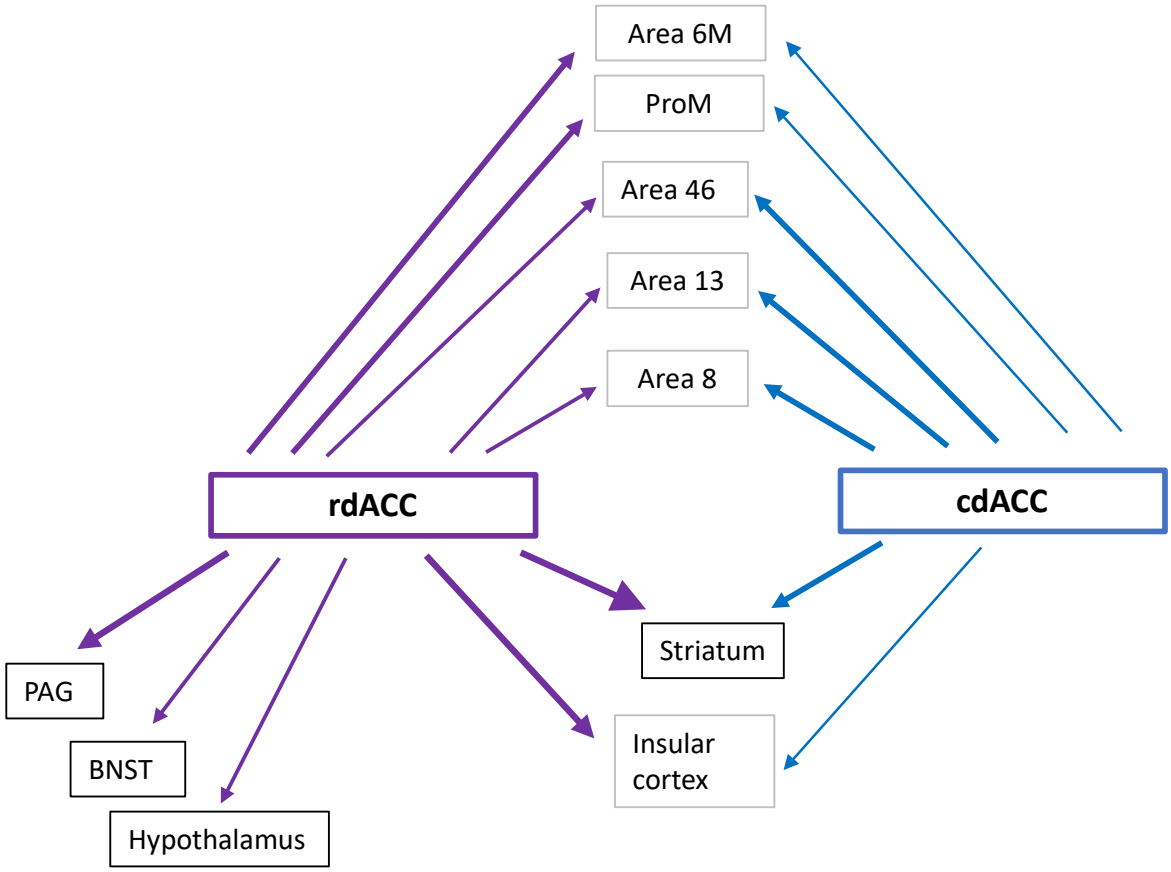

Figure 7.6 Schematic summary of differences in anterograde labelling following BDA infusions into the rdACC and cdACC. Thickness of arrows reflects relative density of labelling. Grey boxes show cortical regions.

7.3.4 Intra-cingulate labelling

There was strong intra-cingulate labelling following infusions in to both the rdACC and cdACC. However, the extent of cingulate labelling from the rdACC infusion site (Figure 7.7) was more anterior, spreading to the pgACC, than from the cdACC infusion site, which labelled more posterior cingulate areas (Figure 7.8). Labelling of the mdACC was similar following infusions from either the rdACC or cdACC. In addition, though not the focus of this analysis, it is noteworthy that the rdACC infusion labelled the contralateral hemisphere to a greater degree than the cdACC infusion. Weak labelling of area 32 was observed from both infusion sites, however neither labelled area 25 (sgACC).

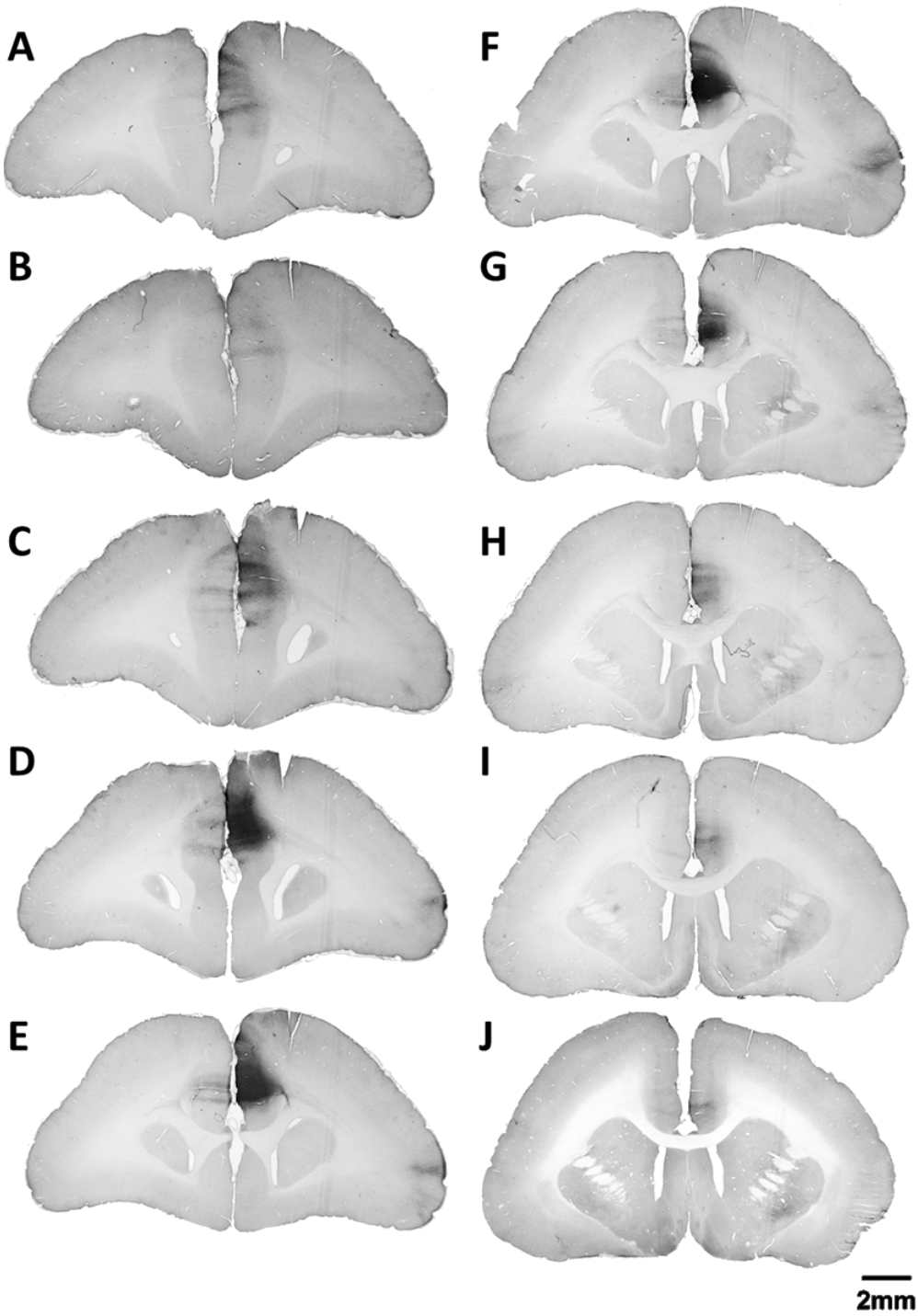

Figure 7.7 BDA labelling of the cingulate cortex following in the right rostral dACC (Lemongrass). Sections are 400µm apart.

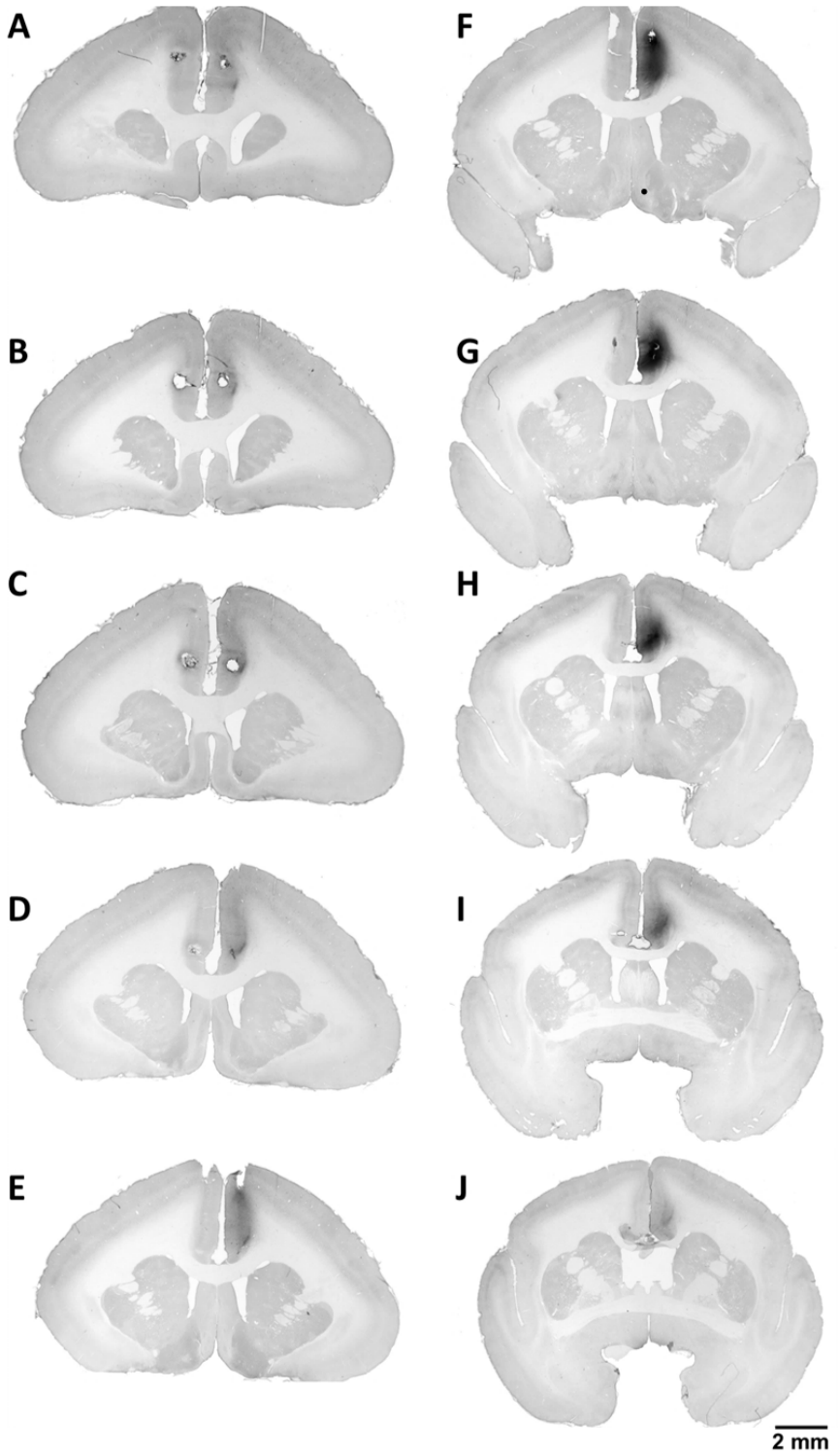

Figure 7.8 BDA-labelling of the cingulate cortex following infusion in the right caudal dACC (Watercress). Sections are 400µm apart. Note some damage was caused by the rdACC cannula implants as can be seen in A-G.

7.3.5 Cortical labelling

Following infusion in the rdACC, only a small cluster of fibres were observed on the dorsal edge of area 46 (dlPFC) (Figure 7.9A). However, more widespread labelling was observed across area 46 following cdACC infusion (Figure 7.9B). Both area 8a, and area 13 (orbitofrontal cortex; OFC) were labelled sparsely following infusion into rdACC, but more strongly following infusion into cdACC (Figure 7.10). Medial area 6 (supplementary motor cortex) and the proisocortical motor cortex were however labelled more strongly following rdACC infusion (Figure 7.11A).

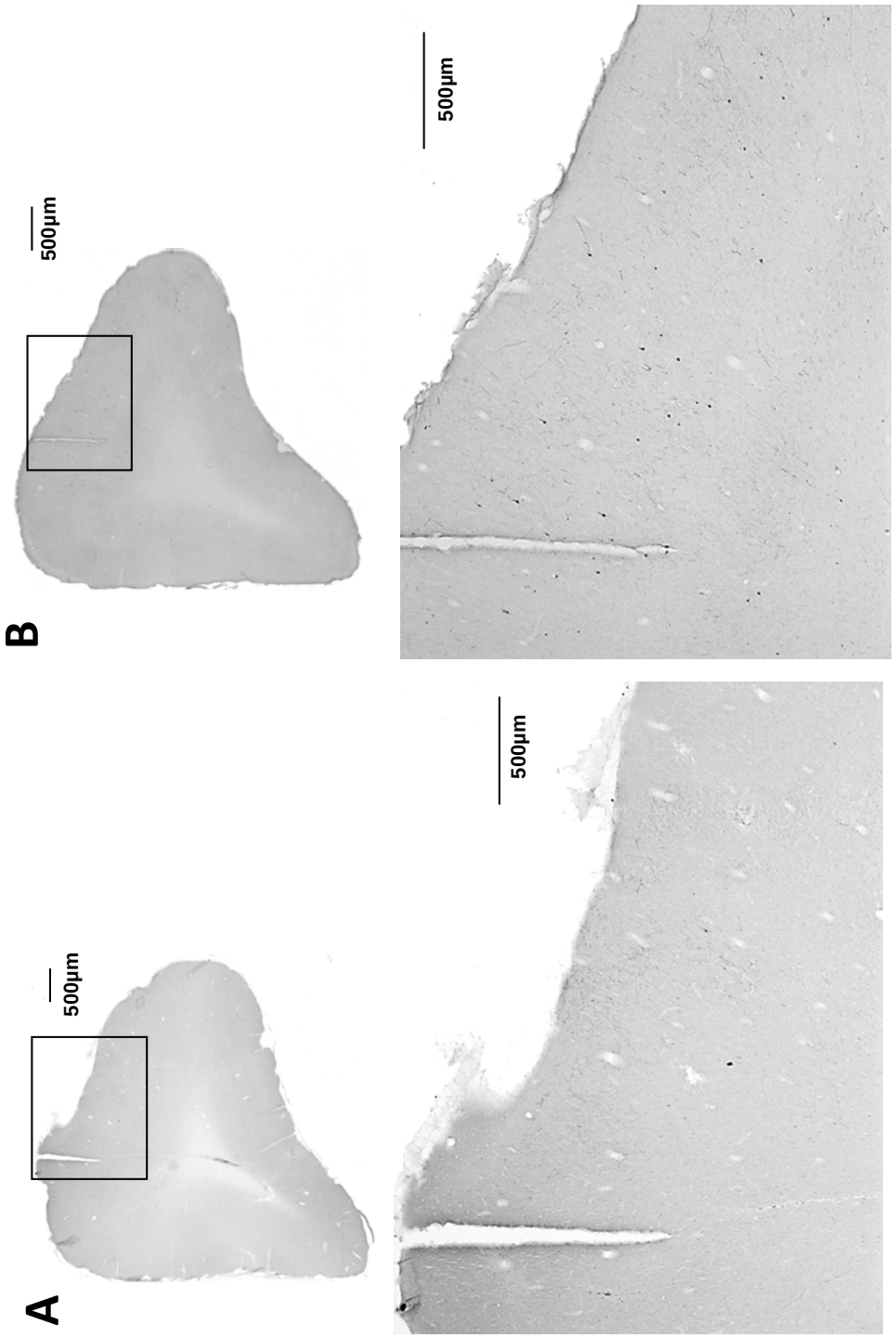

Figure 7.9 BDA-labelling of area 46 following injections in rdACC (A) and cdACC (B). Black boxes indicate the regions shown in the high-power photomicrographs. A small cluster was observed following rdACC infusion but more widespread labelling following cdACC infusion.

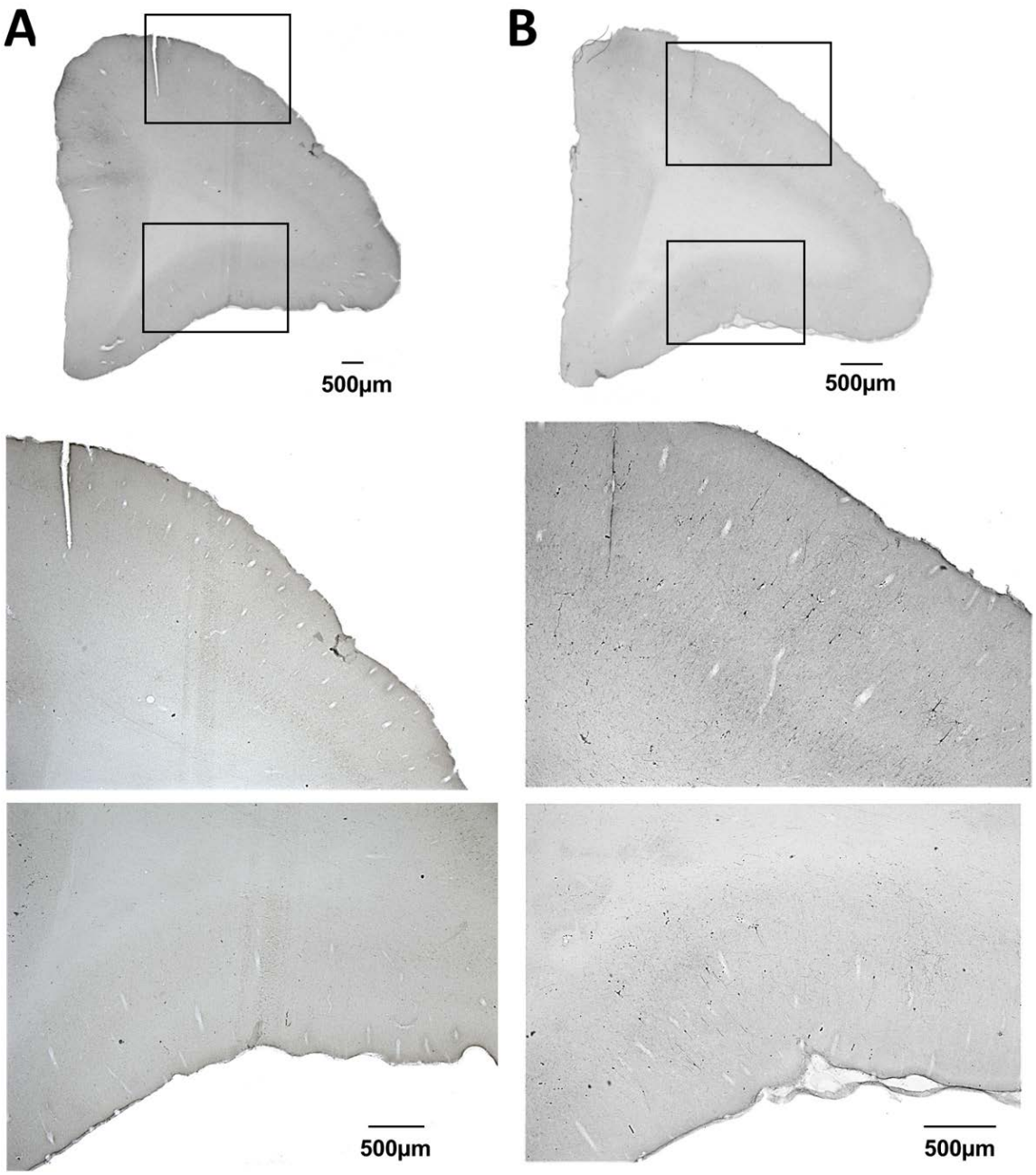

Figure 7.10 BDA-labelling of area 8a (top) and area 13 (bottom) following infusions in rdACC (A) and cdACC (B). Black boxes indicate the regions shown in the high-power photomicrographs. Minimal labelling of these areas was observed following rdACC infusion, but more was observed following cdACC infusion.

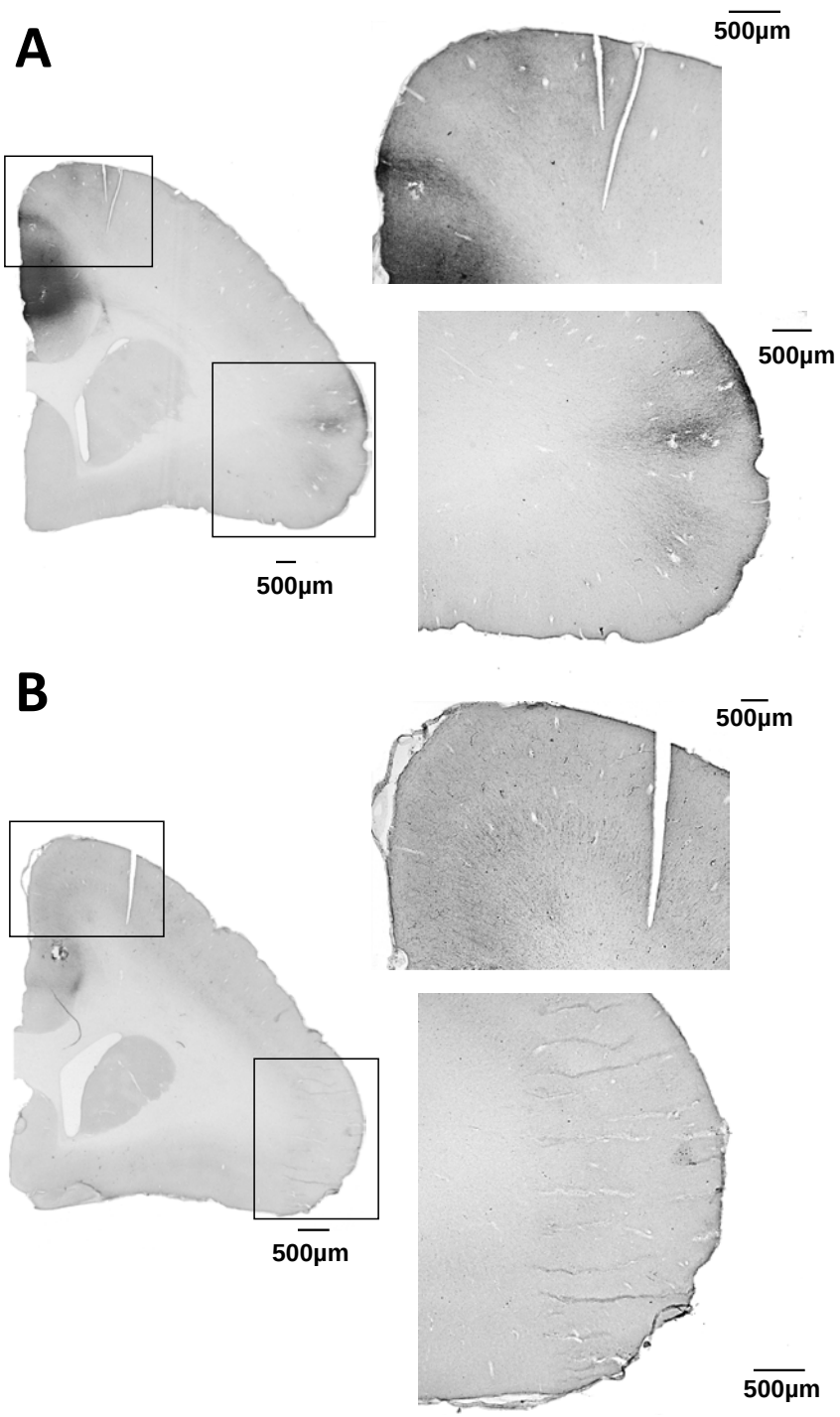

Figure 7.11 BDA-labelling of medial area 6 (top) and proisocortical motor cortex (ProM) (bottom) following infusions in rdACC (A) and cdACC (B). Black boxes indicate the regions shown in the high-power photomicrographs. Labelling of the ProM was stronger following the rdACC infusion, with minimal fibres observed following the cdACC infusion. Similarly labelling of medial area 6 was stronger following the rdACC infusion with a cluster of fibres observable, whereas fibres were much sparser following cdACC infusion.

7.3.6 Subcortical labelling

Dense clusters of fibres were observed in the ventromedial caudate and putamen following rdACC infusion (Figure 7.12A) with sparser labelling primarily in more dorsolateral aspects of the caudate and putamen were observed following cdACC infusion ((Figure 7.12B). Labelling of the bed nucleus of the stria terminalis (BNST) was weak following rdACC infusion and no fibres were observed following cdACC infusion (Figure 7.13). Minimal labelling restricted to only the granular insular cortex was found following cdACC infusion (Figure 7.14B). Labelling of the insular cortex was much stronger following rdACC infusion with (Figure 7.14B) dense clusters of fibres observed in the agranular and dysgranular regions. In addition, a dense column of fibres was observed in the claustrum. Labelling of both the PAG (Figure 7.15) and the hypothalamus (Figure 7.16) were observed following rdACC infusion but not cdACC infusion. Labelling was observed primarily in the lateral and ventrolateral regions of the PAG and in the lateral hypothalamus.

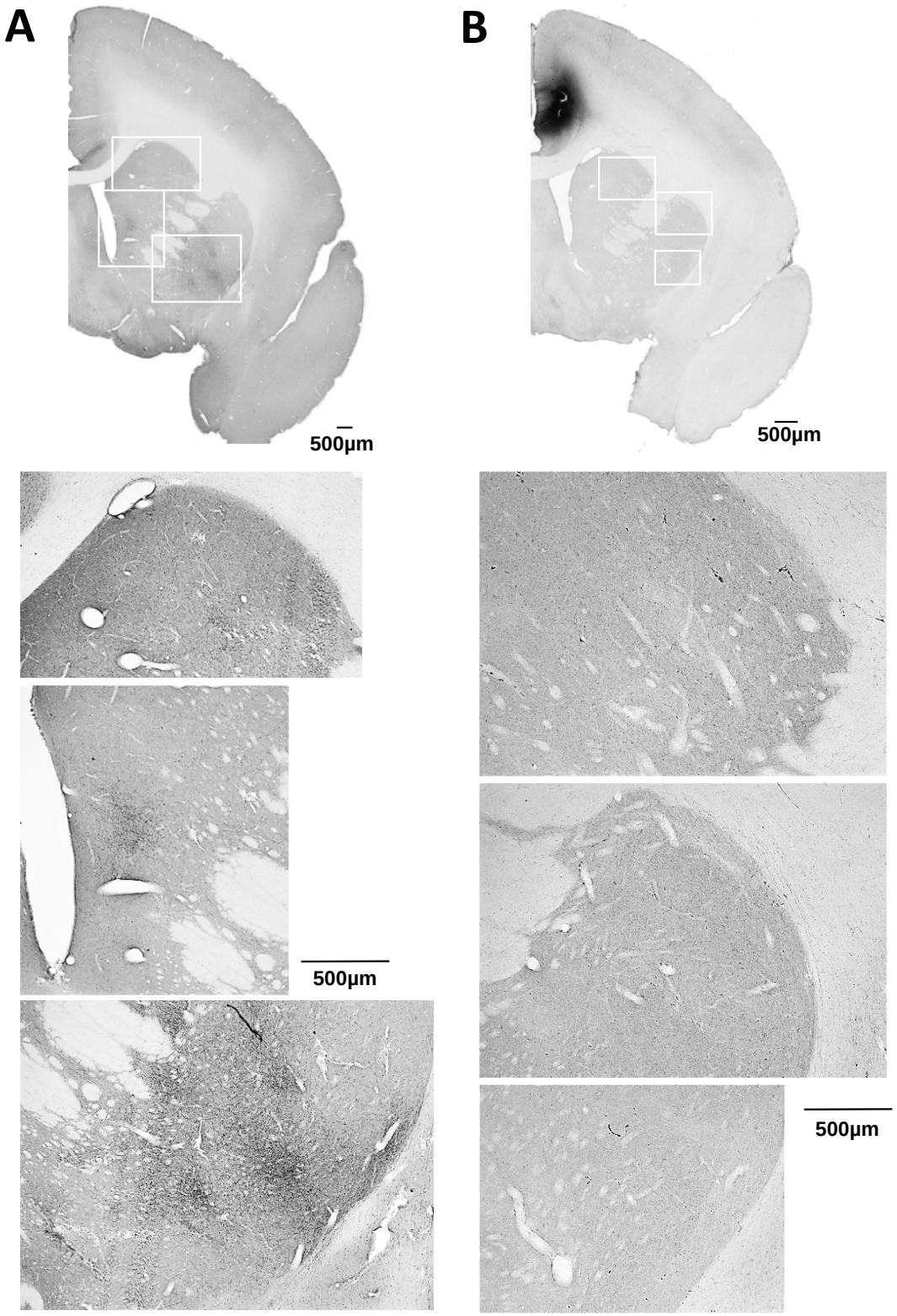

Figure 7.12 BDA- labelling of the striatum following infusions in rdACC (A) and cdACC (B). White boxes indicate the regions shown in the high-power photomicrographs. Dense clusters of fibres were observed in the ventromedial caudate and putamen following rdACC infusion. Sparser labelling primarily in more lateral aspects of the caudate and putamen were observed following cdACC infusion.

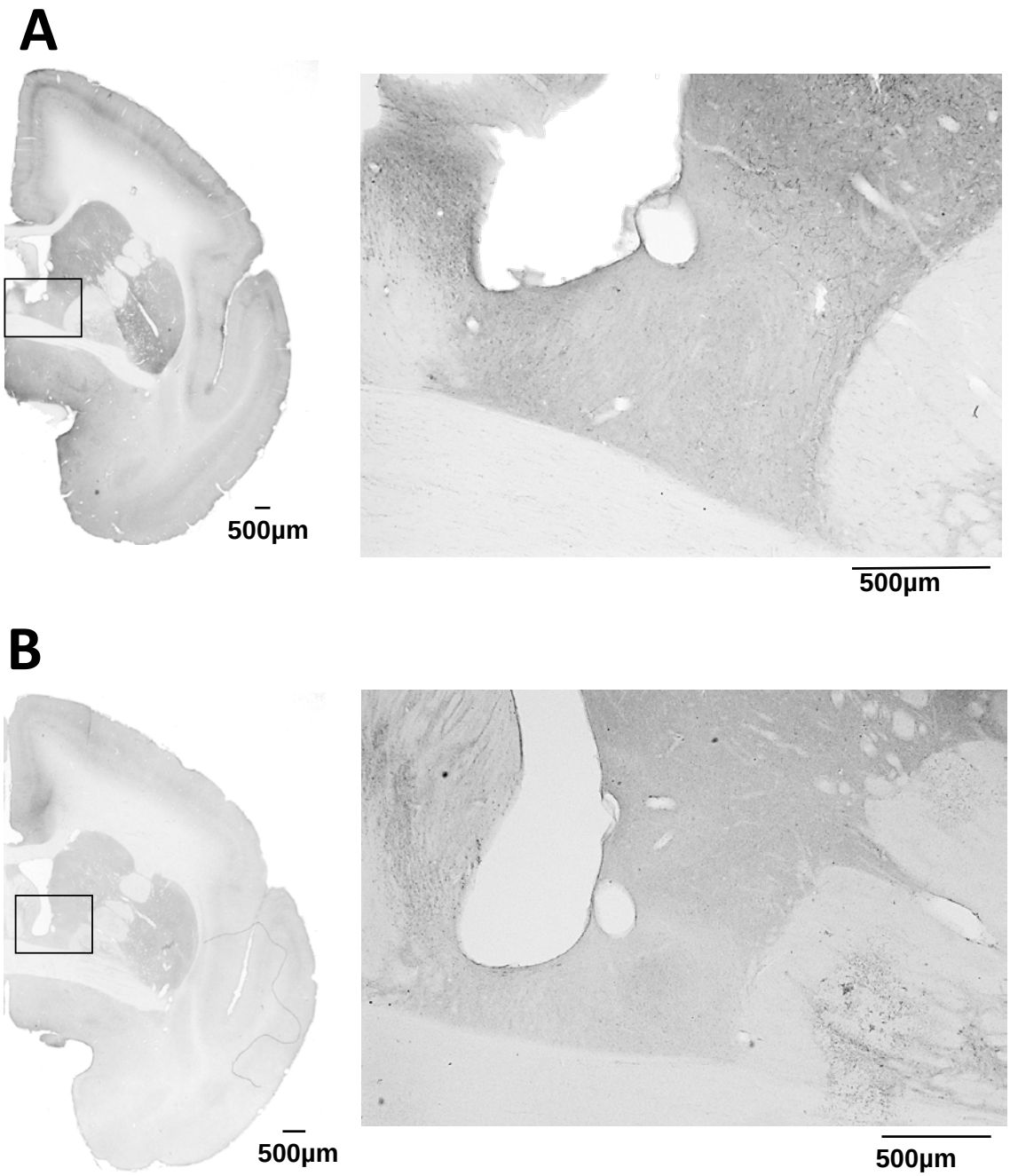

Figure 7.13 BDA-labelling of the bed nucleus of the stria terminalis (BNST) following infusions in rdACC (A) and cdACC (B). White boxes indicate the regions shown in the high-power photomicrographs. Weak labelling was observed only following rdACC infusion.

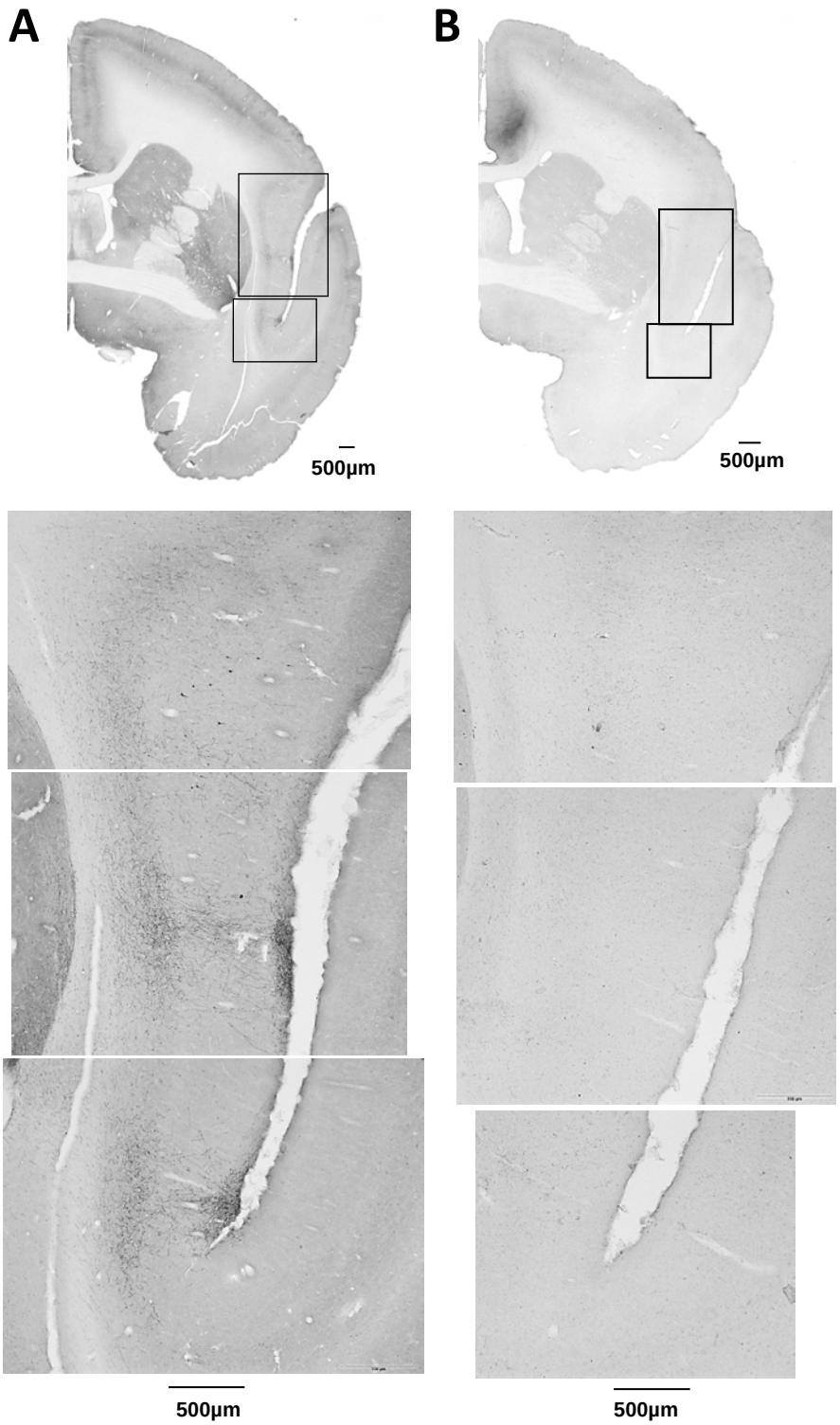

Figure 7.14 BDA-labelling of the claustrum and insular cortex following infusions in rdACC (A) and cdACC (B). White boxes indicate the regions shown in the high-power photomicrographs. A column of fibres was observed along the claustrum following rdACC infusion. Clusters of fibres were labelled in the agranular and dysgranular insular cortex with more diffuse labelling in the granular insular cortex. Only weak labelling was observed in the granular insular cortex following cdACC infusion.

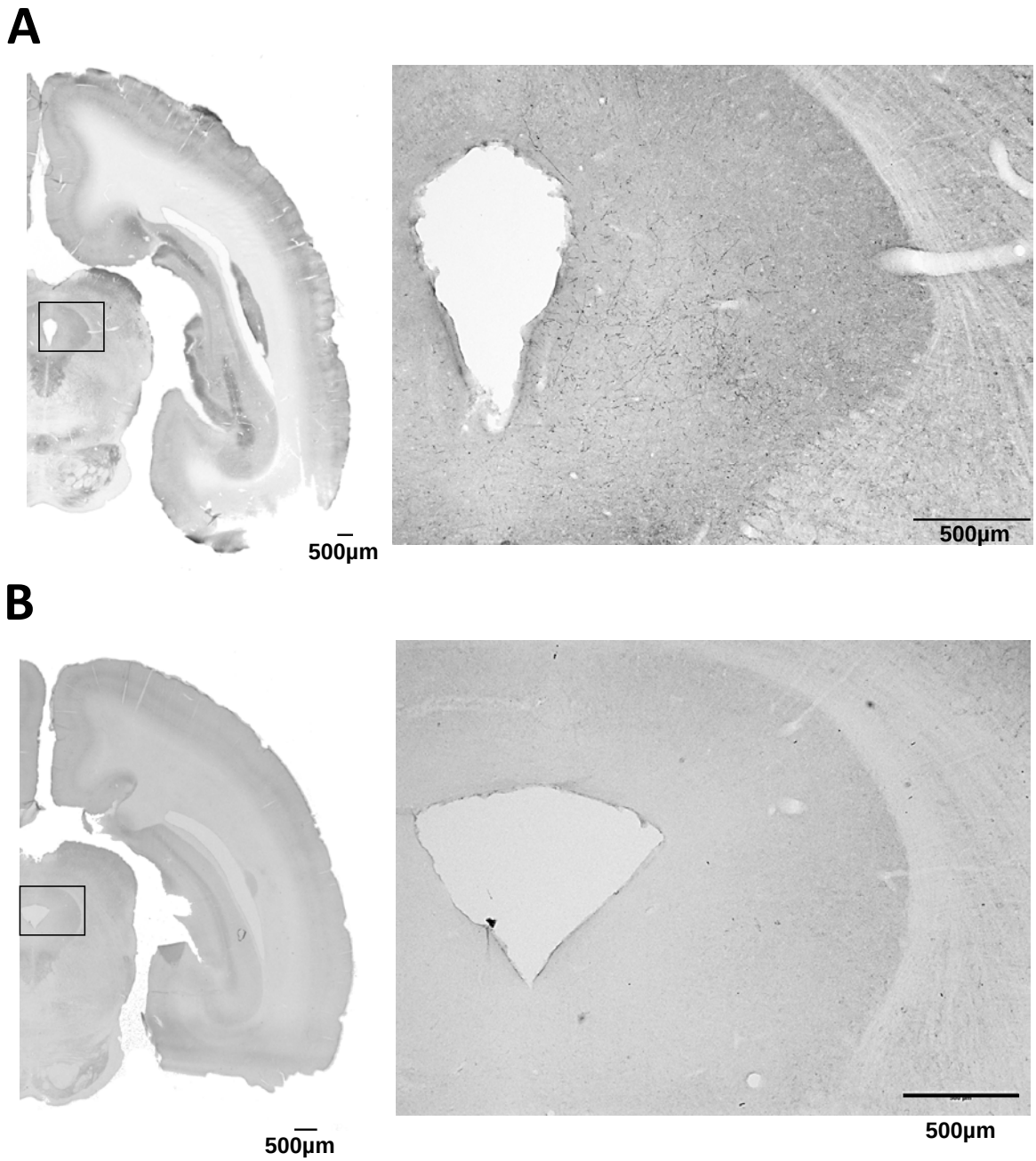

Figure 7.15 BDA-labelling of the periaqueductal gray following infusions in rdACC (A) and cdACC (B). White boxes indicate the regions shown in the high-power photomicrographs. Labelled terminals were observed in the lateral and ventrolateral PAG following rdACC infusion. No labelling was observed in the PAG following cdACC infusion.

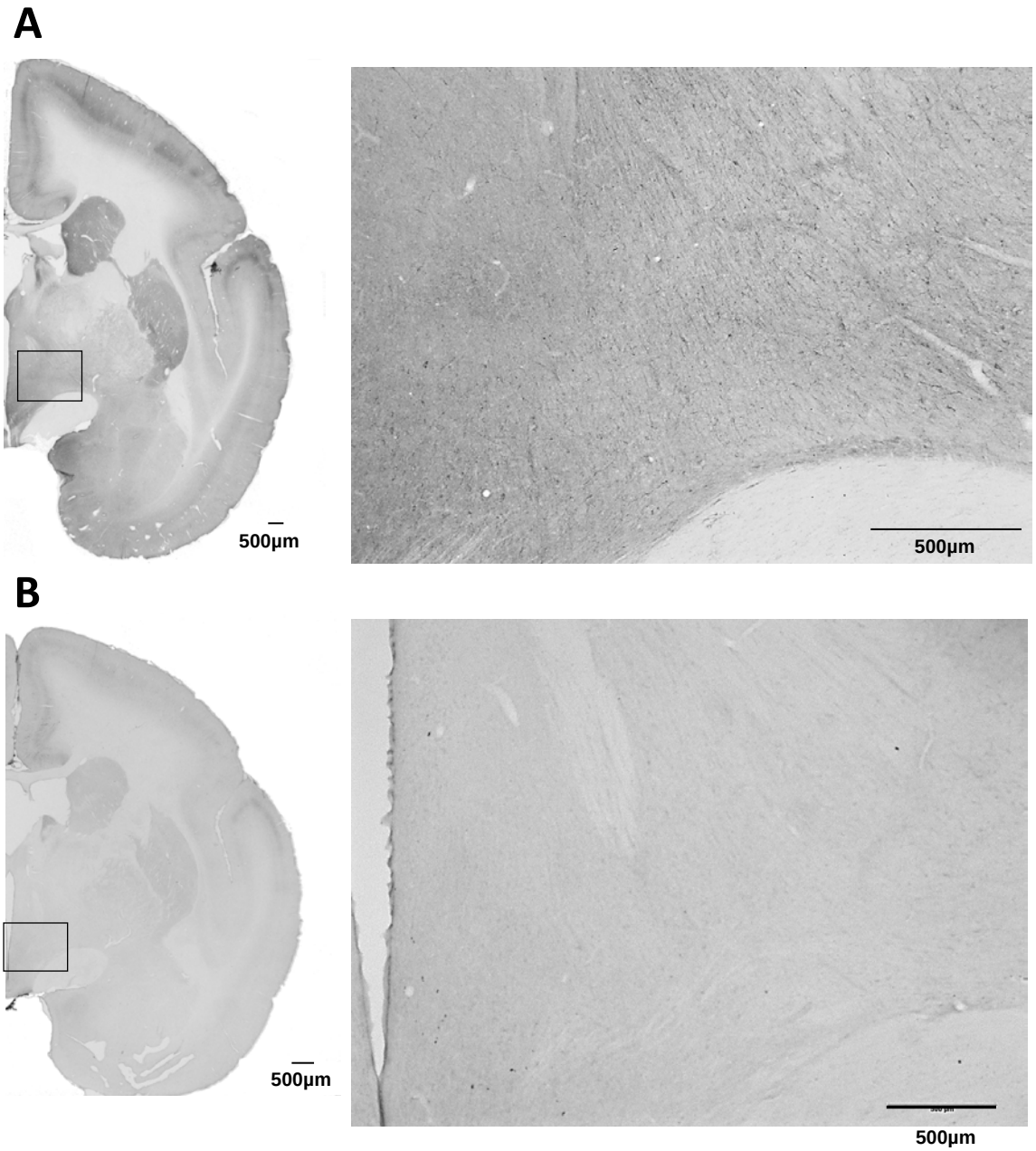

Figure 7.16 BDA-labelling of the hypothalamus following infusions in rdACC (A) and cdACC (B). White boxes indicate the regions shown in the high-power photomicrographs. Labelled terminals were observed in the lateral posterior hypothalamus following rdACC infusion. No labelling was observed in the hypothalamus following cdACC infusion.

7.4 Discussion

In this study, first a comparison of NFP expression in the rdACC vs cdACC was made, which indicated chemoarchitectural differences between these regions. Second, a comparison of the anterograde ipsilateral projections of the rdACC vs cdACC was made, revealing large differences in the efferent targets of these regions. Together these findings support the existence of a functional dissociation between the rdACC and cdACC in the marmoset. In addition, terminal labelling from the mdACC region, supports the hypothesis that this region may be a transitional border region between the more anatomically distinct rdACC and cdACC.

The differences in NFP expression between the rdACC and cdACC reported here, are remarkably similar to those reported in humans between the aMCC and pMCC (Vogt et al., 2003). That is, greater NFP-expressing neurons in layers III and V of the cdACC/pMCC compared to the rdACC/aMCC. This is significant as it provides evidence for a chemoarchitectonic distinction within a region presently described as cytoarchitecturally homogeneous along the rostro-caudal axis (area 24) (Burman and Rosa, 2009; Paxinos et al., 2011). Furthermore, it suggests that the rdACC and cdACC in marmoset are homologous to the aMCC and pMCC in human.

BDA was infused into the rdACC and cdACC, with the infusions largely targeting areas 24b and 24c, as identified by dense labelling at the infusion sites (Figure 7.5). The pattern of terminal labelling following infusions into these subregions of the dACC was assessed and found to differ significantly between the rdACC and cdACC. Previous chapters in this thesis have identified key differences in the function of the rdACC and cdACC in the processing of negative emotion, suggesting a functional dissociation between these subregions of the dACC. Differences in structure can support differences in function and give an insight into their cause as if one region has anterograde/output projections to another it has the potential to influence its activity and function. Thus, the results of this study provide anatomical evidence to support functional differences in the dACC.

It is first important to note that there was dense interconnectivity between the rdACC and cdACC, suggesting each subregion can exert a strong influence on the function of the other. Beyond the cingulate cortex, in general, projections from the rdACC were more widespread and denser than projections from the cdACC, particularly in subcortical areas and the insular cortex. However, the cdACC did label certain anterior regions in the frontal cortex more strongly than the rdACC.

The rdACC was found to project to a number of subcortical regions (PAG, LH and BNST) that did not receive projections from the cdACC. In agreement with tracing studies in macaque, the rdACC projected to the lateral and ventrolateral PAG (An et al., 1998). The PAG has been implicated in defensive behaviours (Bandler and Shipley, 1994; Keay and Bandler, 2001), and recently human functional neuroimaging has associated activity of the ventrolateral PAG with fear (Satpute et al., 2013). In addition weak projections of the lateral hypothalamus and the BNST were observed from the rdACC but not cdACC, both of which are strongly implicated in the expression of fear and anxiety responses (Avery et al., 2016; Barbas et al., 2003; Walker et al., 2003). These regions have all been implicated in the autonomic regulation of emotion (Crestani et al., 2013; Critchley et al., 2013), and thus support the finding in Chapter 5 in which inactivation of the rdACC, but not cdACC, blunted autonomic expression of fear.

The rdACC had stronger projections to the insular cortex than that of the cdACC. This is noteworthy as the dACC and insular cortex are proposed to form a functional network involved in salience detection in humans (Seeley et al., 2007). This proposal is based on functional connectivity analyses, that show correlated activity between these regions during the processing of behaviourally salient stimuli. The functional ROI encompasses the entire dACC from the pgACC posteriorly but ends at the level of the cdACC. Thus, the structural connectivity finding here appears to match the functional connectivity finding in humans.

In contrast, projections to area 13 (anterior OFC) were denser from cdACC than from rdACC. This finding is in agreement with retrograde tracing studies in the OFC of macaque showing stronger labelling of cdACC compared to rdACC (Cavada et al., 2000). Previous work in the Roberts laboratory has shown that excitotoxic lesions of the anterior OFC causes increased anxiety in response to a novel human intruder (Agustín-Pavón et al., 2012), similar to the result presented in Chapter 3 following inactivation of the cdACC. Although this needs to be examined empirically, this raises the possibility that this anxiogenic effect may be caused by a functional interaction between the cdACC and anterior OFC. Area 46, which is an important component of dlPFC, was another region in which BDA labelling from the cdACC infusion was denser than from rdACC infusion. The dlPFC has been implicated in cognitive control (Duncan and Owen, 2000), and functional connectivity with the dACC is thought to be important in the adaptive regulation of emotion, and proposed to be aberrant in depression (Pizzagalli, 2011).

Both the rdACC and cdACC projected to the striatum. However, projections were denser from the rdACC than cdACC and the pattern of labelling differed, with the former primarily

labelling dorsomedial striatum and the latter labelling the dorsolateral striatum. This pattern of striatal connectivity has previously been described in macaques (Heilbronner et al., 2016). These regions of the striatum have different proposed roles – the dorsolateral striatum in habitual and the dorsomedial striatum involved in goal-directed decision-making (Ostlund et al., 2009; Yin et al., 2004).

It was surprising that no anterograde projections from the dACC were observed in the amygdala. Tracing studies in macaques have shown dense anterograde projections from the dACC to amygdala (Ghashghaei et al., 2007). However, these appear to occur at relatively localised "hotspots" and thus the lack of positive labelling in the present study is thus likely due to the BDA infusions not including these key regions within the dACC that densely project to the amygdala. Supporting this suggestion, previous data (unpublished, Roberts lab) involving infusion of anterograde and retrograde tracers into the marmoset basolateral amygdala revealed labelling of the rdACC that was restricted to area 24a, directly above the corpus callosum, whereas the present BDA infusions largely targeted area 24b and c.

In addition, there were no anterograde projections from the dACC to area 25, the sgACC. This was also surprising given that the aMCC and sgACC are thought to form a functional network that is dysregulated in depression but resolves following antidepressant treatment (Mayberg et al., 1999, 2005). However, area 25 is observed to project to the dACC (unpublished data, Roberts lab), and these projections may be more important in this network (Riva-Posse et al., 2014).

It was suggested in Chapter 3 that the mdACC may be a transitional border zone between the more anterior rdACC and the more posterior cdACC, rather than a distinct functional area, as inactivation of this region produced an effect similar to inactivation of the rdACC in some subjects (anxiolytic effects), and an effect similar to inactivation of the cdACC in others. This suggestion is supported by the pattern of terminal labelling following BDA infusion in the mdACC, which showed greater similarity to rdACC terminal labelling in some regions (e.g. dorsal striatum), but greater similarity to the cdACC terminal labelling in other regions (e.g. PAG). The only region in which terminal labelling uniquely differentiated the mdACC from both the rdACC and cdACC was in the parafasicular nucleus of the thalamus, a region that is suggested to be involved in pain processing (Vogt et al., 2008).

One potential flaw of this study was the use of subjects with implanted cannulae, through which they had received prior infusions. The posterior dACC cannulae was implanted vertically and thus causes relatively localised and minimal damage at the infusion site and

directly above it. However, the anterior cannulae was inserted at an angle and thus caused wider damage to the peripheral cortex. However as can be seen from Figure 7.5, damage was relatively restricted. Prior infusions in the area did not appear to affect uptake of BDA, which showed widespread labelling at the infusion site and beyond. In addition, the data from the two surgically naïve subjects that then received stereotaxic infusions of BDA corroborated the data found from the subjects that received infusions through cannulae, indicating that the latter method did not significantly affect labelling.

To summarise, this study has shown cytoarchitectural differences between the rdACC and cdACC, similar to those between the aMCC and pMCC in human, and furthermore has uncovered significant differences in the anatomical projections from these subregions in key areas implicated in emotion. These include the dlPFC, the striatum and the PAG. Although discussion of the potential functional implications of differences in monosynaptic projections between the rdACC and cdACC remain speculative, previous work in this thesis has provided evidence for differences in function between these subregions. The results of this study hence provide anatomical evidence in support of a functional dissociation between the rdACC and cdACC.

8 | GENERAL DISCUSSION

Since the integral positioning of the cingulate cortex in Papez's circuit for the control of emotional expression, followed by the use of anterior cingulotomy for the treatment of disorders involving negative affect, alongside the wealth of neuroimaging studies investigating this region in recent decades, the dACC has consistently been implicated in negative emotion. The former studies are based on gross, non-specific damage to this region, and the latter are correlative, and so the precise contribution of the dACC to the regulation of emotion remains unclear and poorly specified.

Human neuroimaging studies provide correlational evidence for functional heterogeneity within the dACC with regards to its involvement in negative emotion and related disorders. Although this suggests that there might be functional differences within the dACC that contribute to different aspects of negative emotion, this possibility has not been investigated causally.

The work in this thesis has addressed the causal contributions of the dACC to the regulation of negative emotion in the common marmoset, taking into account potential anatomical and functional heterogeneity within its rostral (rdACC) and caudal (cdACC) extents. In this chapter the results from this thesis will be summarised and then synthesised in relation to the existing literature. The broader implications of this work and future directions will then be discussed.

8.1 Summary of results

Uncertainty is a core driver of anxiety and an excessive response to uncertain threats is often observed in anxiety disorders (Bishop, 2007; Grupe and Nitschke, 2013). In Chapter 3, the contributions of the dACC to the regulation of anxiety in response to an uncertain threat (in the form of an unfamiliar human intruder) were evaluated, taking into account a possible dissociation between its rostral and caudal aspects. In order to resolve the issues arising from the considerable individual variation in the location and extent of the dorsal cingulate cortex in marmosets and the lack of a clear rostral-caudal division documented in the marmoset atlas, novel methods were developed to determine subregional boundaries within the dACC. This allowed us to effectively target them with stereotaxic surgery, which has important implications for future studies of this brain region in the marmoset.

The major findings in this chapter were that the inactivation of the rdACC and cdACC had opposing effects on the anxiety response observed in response to an uncertain threat. In particular, the former was shown to promote an anxiolytic response and the latter an anxiogenic one. Furthermore, inactivation of the mdACC, located in between the rdACC and cdACC, resulted in mixed anxiolytic and anxiogenic effects which differed by subject, suggesting it might be a transitional region located at this functional border. These findings provide the first causal evidence supporting a functional distinction between the rdACC and cdACC in the regulation of anxiety.

Physiological arousal is a core feature of emotion and this is often reflected in changes in cardiovascular activity. Thus regions involved in autonomic regulation are often also involved in emotion (Critchley et al., 2005b). In Chapter 4, the effects of inactivating the rdACC, mdACC and cdACC on a number of measures of cardiovascular activity were assessed in a task-free emotionally neutral condition. None of these dACC subregions had an effect on baseline cardiovascular measures, including HR, MAP, and a number of measures of HRV. These findings suggest the dACC does not have a causal role in regulating cardiovascular activity under neutral/baseline conditions.

Building on the results from Chapter 4, the experiments in Chapter 5 assessed the effect of inactivation of the rdACC, mdACC and cdACC on measures of cardiovascular activity in the context of negative emotion. This specifically involved Pavlovian fear conditioning, a much used model for anxiety disorders (Milad and Quirk, 2012). Inactivation of the rdACC blunted the expression of fear using the cardiovascular measure of MAP as the conditioned response.

There was no effect on extinction recall when subjects were tested the next day without any drug manipulation. This extends the findings of Chapter 3, suggesting the rdACC has a broad role in the expression of negative emotion, contributing to both anxiety and fear. Furthermore, it shows that in contrast to an emotionally neutral context, in a negative emotional context the rdACC contributes to the regulation of cardiovascular activity. Inactivation of the mdACC or cdACC had no effects on fear expression or fear recall. This also causally supports the functional dissociation between the rdACC and cdACC.

Decision-making is often impaired in disorders of negative emotion (Paulus and Yu, 2012) and thus, in Chapter 6 the contributions of the rdACC and cdACC to decision-making were assessed in a reward based decision-making task. A 'rich reward' probe session was given to assess the ability of animals to modify their response selection based on the relative value of reward cues. Although inactivation of both the rdACC and cdACC had no effect on the generation of a response bias to a more richly rewarded stimulus, activation of the cdACC but not rdACC blunted this reward bias.

Finally, in Chapter 7, an anatomical analysis of the anterograde (output) connections of the rdACC, mdACC and cdACC was carried out with a particular focus on characterising differential connectivity of these regions, following infusions of BDA. Widespread differences were observed in the projections of the rdACC and cdACC, which were particularly notable in subcortical structures involved in autonomic regulation (hypothalamus and PAG). These areas received projections from the rdACC but not cdACC. In addition, chemoarchitectural evidence for a distinction between the rdACC and cdACC was made based on differences in the expression of NFP, similar to those described in the aMCC/pMCC in humans. Thus, the findings of this chapter add anatomical evidence in support of a functional dissociation between the rdACC and cdACC.

8.2 Synthesis of results

8.2.1 The rdACC is causally involved in the expression of anxiety

Inactivation of the rdACC reduced both anxious behaviour (Chapter 3) and autonomic correlates of fear expression (Chapter 5). On the contrary, inactivation of the rdACC had no effect on the control of baseline autonomic activity (Chapter 4) or on rewarded approach decision-making (Chapter 6).

Uncertain threats are ambiguous (Bishop, 2007; Grupe and Nitschke, 2013) whilst expression of conditioned fear reflects the response to a learned threat(Maren, 2001). Although fear and anxiety differ, anxiety disorders are characterised by excessive fear, so both of these paradigms are relevant to anxiety (1.2.4.4). Thus, taken together these findings causally implicate the rdACC in the broader expression of anxiety and the regulation of negative emotional responses to anxiogenic stimuli. In addition, they support the suggestion that the aMCC integrates autonomic regulation with volitional behaviour (Critchley et al., 2005a).

Consistent with its functional role in negative emotion regulation, anterograde tracing studies (Chapter 7) revealed output projections to the hypothalamus, the PAG, which has been linked to active and passive emotional coping (Keay and Bandler, 2001), and the BNST, which has been identified as important for mediating long-lasting threat related responses (Walker et al., 2003) and anxiety in humans (Avery et al., 2016). Given the implication of these regions in the autonomic regulation of emotion (Crestani et al., 2013; Critchley et al., 2013), they support a role for the rdACC, but not cdACC, in blunting the autonomic expression of fear.

These findings add causal support to the wealth of correlative fear-related neuroimaging studies in which activity predominantly occurs in the aMCC (1.2.4.5) (Etkin et al., 2011; Mechias et al., 2010; Milad et al., 2007a; Vogt et al., 2003). Furthermore, they suggest that excessive anxiety could result from overactivity of the aMCC. Anterior cingulotomy, in which the aMCC is ablated, has been reported effective in reducing symptoms of anxiety disorders (Ballantine et al., 1987; Meyer et al., 1973). The present findings add further support to this idea, indicating that normalising activity in the aMCC might be an effective strategy for treating anxiety.

8.2.2 The cdACC is causally involved in regulating anxiety related to uncertain threats

Inactivation of the cdACC increased expression of anxiety, specifically in the context of an uncertain threat (Chapter 3), indicating a causal role for the cdACC in the regulation of

anxiety. However, it had no effect on the control of baseline autonomic activity (Chapter 4) nor the autonomic expression of conditioned fear (Chapter 5). These findings appear somewhat conflicting, given that anxiety is often characterised by excessive fear, but this may reflect a specific role of the cdACC in regulating anxiety related to uncertain threats.

At the beginning of the extinction session prior to which this manipulation was carried out, subjects had learned that the cue and context were aversive and thus they are associated with a certain threat. However, as the extinction session progresses, uncertainty increases as the new learning occurs now associating the cue and context with the US^- which is thought to inhibit the original fear response (Mauk and Ohyama, 2004), and as this strengthens, certainty increases again. This suggests that the lack of effect of cdACC inactivation, which might be expected to increase fear expression, could be due to the cdACC having a specific role in uncertain threats that is not captured by this extinction paradigm. A fear extinction paradigm involving partial extinction reinforcement in which uncertainty is increased, would provide further insights into this potential function.

Other task differences may also provide insights into the function of the cdACC. The HI test is carried out in the homecage, a familiar environment to the experimental marmosets, in which a range of coping behaviours can be carried out to mitigate the effects of anxiety. However, the fear extinction paradigm is carried out in more of a confined context, and an autonomic rather than behavioural measure is used as the primary measure of fear expression. Thus, the cdACC may specifically be involved in mediating behavioural coping strategies when presented with an anxiety-provoking stimulus. This might be considered more of a habitual trait-like response (Schwabe and Wolf, 2011), a suggestion that is supported by the finding in Chapter 7 of projections from the cdACC to the dorsolateral striatum, a region typically involved in habitual behaviours.

In addition, in Chapter 6, inactivation of the cdACC had no effect on approach behaviour to a richly rewarded stimulus, yet activation of the cdACC blunted this. This indicates that whilst the cdACC has no physiological role in the response bias to reward in this particular task, abnormal overactivity of this region in a decision-making context, which could occur in disorders of negative emotion, impairs this function. However, to my knowledge, the function of the cdACC has not specifically been assessed in humans in relation to decisional anhedonia, thus the present finding suggests this warrants investigation.

A blunted reward bias could reflect reduced hedonic capacity or deficits in goal-directed behaviour. This latter suggestion is again supported by the finding in Chapter 7 of projections

from the cdACC to the dorsolateral striatum, which indicate that increased activity of the cdACC activity might increase habitual behaviour through interaction with the dorsolateral striatum.

These findings are relevant to our understanding of anxiety disorders. The pMCC appears to be consistently hyperactive across different emotional paradigms in PTSD (Hayes et al., 2012). Similarly, recent work has shown a specific involvement of the MCC during threat processing in GAD, compared to SAD or PD (Buff et al., 2016). Activation of this region in response to threatening stimuli, was greater than for healthy controls, and further functional connectivity specifically between the pMCC and amygdala was greater. Taken with the present finding of a causal role of the cdACC in regulating responses to uncertain threats, this suggests that hyperactivity of this region might cause an impairment in threat processing such that ambiguous threats are overestimated, leading to hypervigilance. Hyperactivity of the cdACC in combat veterans with PTSD and their co-twins compared to non-PTSD veterans and their twins, during a cognitive task involving conflict has also been reported (Shin et al., 2011), suggesting that overactivity of the pMCC is a familial risk factor for the development of PTSD following trauma. This suggests that the cdACC may have a more general role in the processing of conflict, which can be driven by threat uncertainty or uncertainty in the cognitive domain. In addition, goal-directed behaviour is also impaired in PTSD and GAD, consistent with the present finding of impaired goal-directed behaviour following overactivation of the cdACC.

8.2.4 The rdACC and cdACC are functionally dissociable

The results presented throughout this thesis provide causal evidence for a functional dissociation between the rdACC and cdACC, as well as anatomical evidence supporting this claim.

In Chapter 3, inactivation of the rdACC reduced anxiety in response to an uncertain threat whereas inactivation of cdACC increased it, thus these subregions had opposing roles in the expression and regulation of anxiety. Inactivation of the rdACC blunted conditioned fear expression, consistent for a role in the expression of negative emotion, whereas inactivation of cdACC had no effect on fear expression (Chapter 5). Finally, activation of rdACC had no effect on the response bias to a richly rewarded stimulus whereas activation of the cdACC blunted this response bias (Chapter 6).

Chapter 7 revealed differences in chemoarchitecture and anterograde projections between the rdACC and cdACC providing anatomical support for differences in function. The rdACC

projects to the PAG, LH and BNST, key regions involved in autonomic regulation (Crestani et al., 2013; Critchley et al., 2013), whereas the cdACC does not. The density of projections from the rdACC to the dlPFC and OFC, regions implicated in executive functions are weaker than from the cdACC. Furthermore the pattern of striatal connectivity differed, with the rdACC projecting to the dorsomedial striatum, a region implicated in goal-directed behaviour, and the cdACC projecting to the dorsolateral striatum, a region implicated in habitual behaviour (Schwabe and Wolf, 2011).

Furthermore, the current evidence suggests that rather than a graded functional distinction between the rdACC and cdACC, there is a binary change in function as one progresses from the rdACC to the cdACC. This border between the dACC subregions could not easily be defined spatially, likely due to difference between individual subjects. Thus, the placement of the mdACC varied across this border. The key evidence for this is listed below:

- Inactivation of the mdACC resulted in both anxiolytic (similar to rdACC) and anxiogenic (similar to cdACC) effects in different animals (Chapter 3)
- The anterograde projections from the mdACC to cortical and subcortical regions across the brain were not obviously distinct to those from the rdACC or cdACC. In some instances, they were more similar to the rdACC and in others they were more similar to the cdACC.

The cannulae targets for the rdACC and cdACC were relatively restricted, but the presence of the mdACC site provides insights into where a functional boundary might lie, which is suggested to be somewhere in this mdACC region (Figure 8.1B).

In Chapter 3, preliminary work assessing the role of the pgACC in anxiety was also carried out, and although this constitutes preliminary evidence, it suggested that the pgACC is also functionally distinct from the rdACC, as inactivation of this subregion tended to cause an anxiogenic rather than anxiolytic effect.

8.2.4.1 Relation to Vogt's neurobiological model of the cingulate cortex

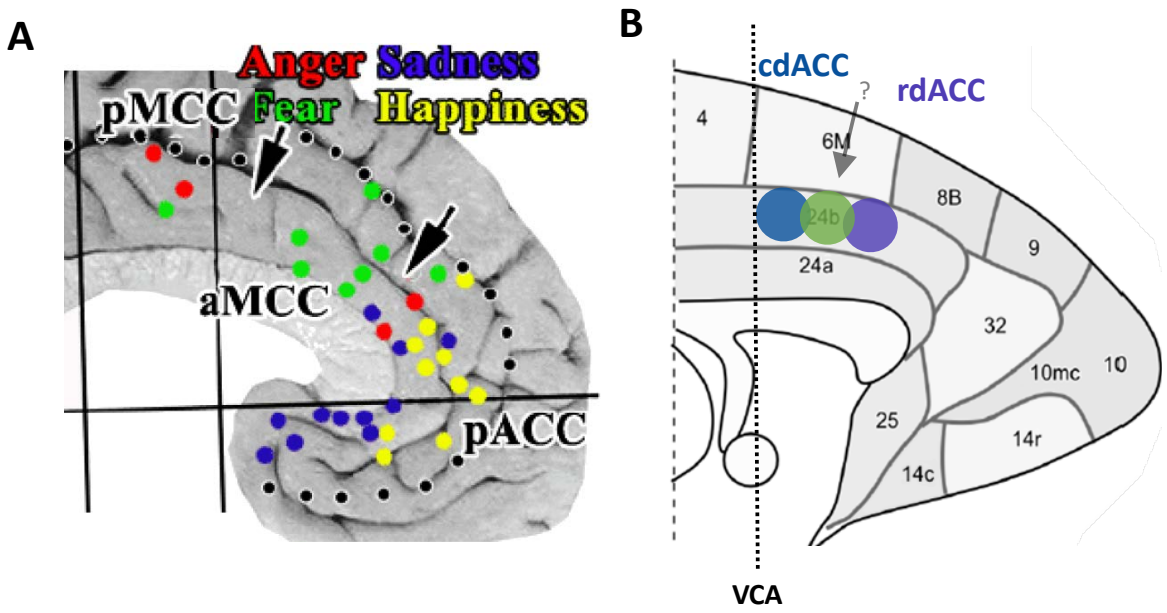

Figure 8.1 Distinction between the aMCC/pMCC in humans compared to rdACC/cdACC in marmoset. Peak voxels from emotion-generating tasks plotted onto cingulate subregions (figure from Vogt et al. 2003). B. The rdACC, mdACC(green) and cdACC cannulae placements in the present study. The grey arrow indicates the potential functional boundary between these regions.

An anterior and posterior division of the MCC, a region similar to the dACC in terms of its spatial location but qualitatively distinct from the ACC, has been proposed in both humans and macaques. This division is largely based on architectural evidence, though there has also been some functional support (Figure 8.1A).

In humans, layer Va of the pMCC (areas 24a and 24b) is thicker, includes a greater density of neurons, and more NFP-expressing neurons than the aMCC. In addition the pMCC contains NFP-expressing neurons in deep layer III, which are barely detectable in the aMCC (Vogt et al., 2003). Differences in receptor architecture between the aMCC and pMCC, such as reduced GABAb binding density in the aMCC versus pMCC have also been described (Palomero-Gallagher et al., 2008, 2009). Furthermore, analysis of neuroimaging studies during emotion-generating tasks revealed relatively greater fear-related activity in the aMCC compared to the pMCC (Figure 8.1a) (Vogt et al., 2003). In macaques, the aMCC and pMCC have also been identified, and these can be differentiated by the presence of more dense parvalbumin-expressing neurons in layer Va of the aMCC compared to the pMCC (Vogt et al., 2005).

Although the work in this thesis does not address whether the dACC in marmoset is qualitatively distinct from the ACC in terms of cytoarchitecture and chemoarchitecture, and thus homology with the MCC in other species cannot be directly inferred, the functional

dissociation between the rdACC and cdACC, differences in connectivity, and differences in chemoarchitecture, align well with the aMCC/pMCC distinction as can be seen in Figure 8.1C. The chemoarchitectural evidence presented in Chapter 7 particularly strengthens this claim as the differences in NFP expression between the rdACC and cdACC in layers III and V are remarkably similar to those reported in humans between the aMCC and pMCC (Vogt et al., 2003). Furthermore, the causal role of the rdACC in fear expression identified here is consistent with the involvement of the aMCC in fear expression (Milad et al., 2007a; Vogt et al., 2003). Similarly, the cdACC in marmosets, which is not involved in fear expression, appears to spatially map on to the anterior portion of the pMCC, which also has little fear related activity. Thus, the rdACC and cdACC in the marmoset may be considered functionally homologous to the aMCC and pMCC, respectively in humans. However, future studies should include a detailed architectural analysis of the ACC in marmosets, including assessment of cytoarchitecture, chemoarchitecture and receptor architecture to further corroborate this with structural evidence.

8.3 Implications for the study of the dACC

8.3.1 The dACC should not be considered functional homogeneous

The findings of this thesis provide the first causal evidence for a functional dissociation between the rdACC and cdACC in the regulation of negative emotion. Although the dACC was once considered a single entity, the work carried out in this thesis in addition to other supporting evidence discussed, means that this position is no longer tenable.

Throughout this thesis, I have borne in mind a potential functional dissociation between the aMCC and pMCC when discussing regional activations in functional imaging studies and thus attempted to describe these accordingly. However, to do so precisely requires co-registration of regional boundaries to standard co-ordinates, as described by Vogt and colleagues (Vogt et al., 2003). The dACC has largely been considered as a single functional entity in the neuroimaging literature, with only spatial designations usually given. The present work strengthens the call to re-interpret the vast array of functional imaging studies involving the dACC in negative emotion and beyond, in light of this heterogeneity. This would bring us closer to understanding the functional organisation of the dACC and further break down the complexity of this region.

However, negative emotion is just one of several functions that have been attributed to the dACC, including cognitive control, action selection and pain (1.3). Future studies should causally assess whether or not these subregions differentially contribute to other specific functions of the dACC, which may be related to its role in negative emotion.

8.3.2 The rdACC and cdACC are part of a network of regions involved in negative emotion

In the present work it was revealed that the rdACC and cdACC project to many of the regions that are implicated in negative emotion and other findings (unpublished data, Roberts lab) indicate it also receives projections from them. Whilst the work in this thesis has investigated the distinct functional contributions of the rdACC and cdACC to negative emotion, as highlighted, these are just two regions in a network of likely interacting regions implicated in this function. This network includes other regions of the ACC, namely the pgACC and sgACC, as well as additional structures such as the amygdala, dlPFC and striatum.

Particularly pertinent in furthering our understanding of depression, are the interactions between the aMCC and area 25, which are thought to form a functional network that is

dysregulated in depression but resolves following antidepressant treatment (Kozel et al., 2011; Mayberg et al., 1999, 2005). Furthermore, it has been suggested that the DBS antidepressant response is mediated by white matter tracts between these regions (Riva-Posse et al., 2014). The receptor architecture of area 25 shows great similarity with the aMCC suggesting common circuit organisation (Palomero-Gallagher et al., 2009).

The amygdala is also strongly implicated in the expression of negative emotion and receives projections from multiple prefrontal and cingulate regions, including from the dACC (Ghashghaei and Barbas, 2002; Ghashghaei et al., 2007). This suggests that these regions might converge on the amygdala to regulate negative emotion (Delgado et al., 2008; Ochsner and Gross, 2005; Ochsner et al., 2004). Furthermore specific abnormalities in cingulate-amygdala interactions have been described in disordered negative emotion (Pezawas et al., 2005; Robinson et al., 2013).

8.4 Implications for future translational studies investigating the role of the dACC in disorders of negative emotion

Translational studies in experimental animals are essential to further our understanding of the dACC as these allow for causal manipulations that cannot be carried out in humans. The findings of this thesis are pertinent to the understanding of the role of the dACC in disorders of negative emotion such as anxiety and depression. Anxiety disorders are characterised by excessive fear responses to uncertain threats and the results of this thesis, suggest the rdACC is involved in the expression of these responses whilst the cdACC is involved in regulating these responses. However further work is needed to more precisely characterise these functions of the rdACC and cdACC.

8.4.1 The common marmoset as a model for the study of ACC function

The experiments conducted in this thesis were carried out using the common marmoset (*Callithrix jacchus*). Similar to other non-human primates, marmosets have a well-developed frontal lobe, which resembles the human frontal lobe in terms of structural and functional organisation (Burman and Rosa, 2009). However, the precise structural and functional parcellation of the dACC and adjacent regions is an issue that is yet to be resolved. The present work shows that pharmacological manipulations in the common marmoset can shed light on the functional complexity of the dACC and I propose that this is the ideal species with which to carry out further studies towards this aim as this will further our understanding of the functions supported by this region in humans.

This thesis primarily focused on the function of the dACC in marmoset during the regulation and expression of negative emotion. However, in Chapter 3, surgical modifications and post-mortem analyses are described, detailing methods used to specifically target the cdACC, rdACC and another subregion the pgACC, in which only preliminary functional studies were carried out. Although studies have already begun to assess the role of the pgACC in negative emotion in the common marmoset, these have targeted a distinct cytoarchitectonic area, area 32 (Wallis et al., 2017). Given that evidence in humans and macaques suggests that the pgACC (area 24) is also functionally distinct from the aMCC and pMCC, this warrants further investigation.

As shown in Chapter 7, both the rdACC and cdACC project to many regions that are also implicated in negative emotion. Ultimately, these regions are likely to work together concertedly, to regulate negative emotion, and. Thus, an understanding of how these regions interact, involving an analysis of their bidirectional anatomical connectivity and causal

investigation into their functional interactions is needed to give further insights into disorders of negative emotion.

Previous work in the Roberts laboratory has assessed the roles of area 25 and area 32 in the regulation of negative emotion in some of the same tasks used in the present work (Wallis et al., 2017). This has revealed that inactivation of area 25 enhanced conditioned fear extinction, whilst inactivation of area 32 impaired it, whilst having no effect on actual fear expression. In contrast, inactivation of rdACC in the present study had no effect on extinction per se but blunted fear expression. This highlights the distinct effects these different regions of ACC have on the regulation of fear. In addition, the vlPFC and OFC have also been implicated in the regulation of negative emotion, with lesions of both these regions resulting in heightened anxiety in the HI task (Agustín-Pavón et al., 2012), similarly to the present effect observed following cdACC inactivation. However the vlPFC and OFC have been reported to have different effects on an avoidance bias in the VI reward + punishment probe (Clarke et al., 2015). Thus, a number of prefrontal and cingulate regions besides the dACC have been causally implicated in the regulation of negative emotion. The work carried out in Chapter 7 has shown that the dACC projects and/or receives projections from (data not shown) all of these regions. This highlights the importance of a neural circuit-based approach when assessing the function of the dACC in negative emotion regulation.

A novel technique that can be used to study the function of neuronal circuits involving the dACC in marmosets is Designer Receptors Exclusively Activated by Designer Drugs (DREADDs) (El-Shamayleh et al., 2016; Roth, 2016; Watakabe et al., 2016). DREADDs are engineered receptors that are no longer activated by their endogenous ligand but are instead activated by an otherwise inert ligand. An anterograde virus containing an inverted floxed sequence for a DREADD can be infused stereotaxically into the dACC, in a similar manner to infusions of tracers, whilst another retrograde virus encoding cre-recombinase can be infused into an efferent target region e.g. OFC. Thus the DREADD will only express in neurons projecting from the dACC to the target region allowing for specific transient manipulation of this circuitry (Boender et al., 2014). By utilising this approach, it is possible to dissect out how these distinct prefrontal and ACC regions interact in the control of emotion.

In addition, various other tasks have been developed in the Roberts lab, which assess precise functions relevant to negative emotion and cognition (Oikonomidis et al., 2017). Of particular relevance for furthering our understanding of the role of the cdACC in regulating anxiety related to uncertain threats is the discriminative fear conditioning paradigm which can be used to assess anxiety responses to an ambiguous stimulus (Mikheenko et al., 2010; Shiba et al.,

2014). In addition, the discriminative appetitive conditioning paradigm can be used to parse the consummatory and anticipatory aspects of reward. Given that in the present work no impairments were found in decisional aspects of anhedonia following activation of the rdACC, yet overactivity of the aMCC has been associated with an anti-anhedonic effect in depressed individuals (Lally et al., 2015), investigation of the function of the aMCC in this task could be particularly insightful.

Another line of research in which the marmoset is particularly useful is the study of social behaviour. Similar to humans but different from some other non-human primates such as macaques, marmosets live in a cooperative breeding system, which is thought important for social cognition (Burkart et al., 2009). Study of the social behaviours of marmosets following an encounter with other unfamiliar marmosets has revealed a significant association between serotonin transporter binding in the pgACC in those showing trait social anxiety (Yokoyama and Onoe, 2015; Yokoyama et al., 2012). Experiments to assess whether the pgACC is causal to social anxiety is an important next step, alongside determining its modulation by serotonin, a target for many anti-depressant and anti-anxiety pharmaceuticals.

Cognitive control is another function in which the dACC is implicated (Ullsperger et al., 2014) and it has been suggested that the dACC is a key node in the brain for the integration of cognition and emotion, which may be particularly relevant for neuropsychiatric disorders (Ray and Zald, 2012; Stevens et al., 2011). Although, in humans there is a wealth of evidence implicating the dACC in cognitive conflict, studies in non-human primates have only recently identified conflict-related activity in the dACC using single-unit recordings (Amemori and Graybiel, 2012; Ebitz and Platt, 2015; Shenhav and Botvinick, 2015). Thus, further work causally assessing this function of the dACC is required.

8.4.2 Implications for the study of the dACC in rat

Rats have been used extensively to model neuropsychiatric disorders, and have undoubtedly provided key insights into the neurobiology underlying these (Fernando and Robbins, 2011; Milad and Quirk, 2012; Nestler and Hyman, 2010). However, the difficulty in determining homologies between frontal regions of the brain in rats with those in non-human primates and human, hampers the translation of findings (1.1.1.4).

This homology is particularly contentious with regards to the dACC. On the basis of function in fear expression, the PL has been proposed homologous with the aMCC (Graham and Milad, 2011b; Milad et al., 2007a). However on the basis of anatomical projections to the thalamus it is considered by some more similar to the dlPFC (Vertes, 2002), and on the basis

of cytoarchitecture (Carmichael and Price, 1994; Vogt et al., 2005) and projections to the striatum it is considered more similar to area 32 (Heilbronner and Haber, 2014). Similarly the AC in rodents has also been proposed to be homologous to the dACC, on the basis of cytoarchitecture (Carmichael and Price, 1994; Vogt et al., 2005) and some similarity in striatal projections (Heilbronner et al., 2016).

It could be that these different regions in rat (PL and AC) show greater similarity to different respective subregions of the dACC in primate. In Chapter 5, a fear conditioning paradigm similar to that used in rats was used to assess the roles of subregions of the dACC in fear expression. Inactivation of the rdACC had a similar effect to previous work inactivating the PL in rats, indicating a degree of functional homology (Graham and Milad, 2011b; Sierra-Mercado et al., 2011). However, this finding needs to be considered with caution, as a similar behavioural output could be driven by different underlying mechanisms. Although more work should be done to characterise the homology between rodent and primate frontal regions, recent work has suggested their functions may have diverged too much to be meaningfully comparable in functional studies of behaviour (Wallis et al., 2017).

8.5 Conclusion

The major aim of this thesis was to investigate and causally assess whether a functional dissociation between the rdACC and cdACC in the regulation and expression of negative emotion existed. The experiments performed as part of this thesis have confirmed that the rdACC and cdACC have distinct contributions to the expression and regulation of negative emotion. This has widespread implications for our understanding of anxiety disorders and depression, in which negative emotion regulation, expression and modulation are impaired, as well as implications for our understanding of the structural and functional organisation of the dACC.

REFERENCES

Admon, R., Nickerson, L.D., Dillon, D.G., Holmes, A.J., Bogdan, R., Kumar, P., Dougherty, D.D., Iosifescu, D.V., Mischoulon, D., Fava, M., et al. (2015). Dissociable cortico-striatal connectivity abnormalities in major depression in response to monetary gains and penalties. Psychol. Med. *45*, 121–131.

Agustín-Pavón, C., Parkinson, J., Man, M.-S., and Roberts, A.C. (2011). Contribution of the amygdala, but not orbitofrontal or medial prefrontal cortices, to the expression of flavour preferences in marmoset monkeys. Eur. J. Neurosci. *34*, 1006–1017.

Agustín-Pavón, C., Braesicke, K., Shiba, Y., Santangelo, A.M., Mikheenko, Y., Cockroft, G., Asma, F., Clarke, H., Man, M.-S., and Roberts, A.C. (2012). Lesions of ventrolateral prefrontal or anterior orbitofrontal cortex in primates heighten negative emotion. Biol. Psychiatry *72*, 266–272.

Allen, T.A., Narayanan, N.S., Kholodar-Smith, D.B., Zhao, Y., Laubach, M., and Brown, T.H. (2008). Imaging the spread of reversible brain inactivations using fluorescent muscimol. J. Neurosci. Methods *171*, 30–38.

Amaral, D.G., and Price, J.L. (1984). Amygdalo-cortical projections in the monkey (Macaca fascicularis). J. Comp. Neurol. *230*, 465–496.

Amemori, K., and Graybiel, A.M. (2012). Localized microstimulation of primate pregenual cingulate cortex induces negative decision-making. Nat. Neurosci. *15*, 776–785.

American Psychiatric Association (2013). Diagnostic and statistical manual of mental disorders (DSM-5®) (American Psychiatric Pub).

An, X., Bandler, R., Öngür, D., and Price, J.L. (1998). Prefrontal cortical projections to longitudinal columns in the midbrain periaqueductal gray in macaque monkeys. J. Comp. Neurol. *401*, 455–479.

Andrews, G., Issakidis, C., Sanderson, K., Corry, J., and Lapsley, H. (2004). Utilising survey data to inform public policy: comparison of the cost-effectiveness of treatment of ten mental disorders. Br. J. Psychiatry *184*, 526–533.

Appelhans, B.M., and Luecken, L.J. (2006). Heart rate variability as an index of regulated emotional responding. Rev. Gen. Psychol. *10*, 229.

Arikuni, T., Sako, H., and Murata, A. (1994). Ipsilateral connections of the anterior cingulate cortex with the frontal and medial temporal cortices in the macaque monkey. Neurosci. Res. *21*, 19–39.

Asami, T., Hayano, F., Nakamura, M., Yamasue, H., Uehara, K., Otsuka, T., Roppongi, T., Nihashi, N., Inoue, T., and Hirayasu, Y. (2008). Anterior cingulate cortex volume reduction in patients with panic disorder. Psychiatry Clin. Neurosci. *62*, 322–330.

Ash, H., Smith, T.E., Knight, S., and Buchanan-Smith, H.M. (2018). Measuring physiological stress in the common marmoset (Callithrix jacchus): Validation of a salivary cortisol collection and assay technique. Physiol. Behav. *185*, 14–22.

Aupperle, R.L., and Paulus, M.P. (2010). Neural systems underlying approach and avoidance in anxiety disorders. Dialogues Clin. Neurosci. *12*, 517.

Aupperle, R.L., Melrose, A.J., Francisco, A., Paulus, M.P., and Stein, M.B. (2015). Neural substrates of approach-avoidance conflict decision-making. Hum. Brain Mapp. *36*, 449–462.

Avery, S.N., Clauss, J.A., and Blackford, J.U. (2016). The human BNST: functional role in anxiety and addiction. Neuropsychopharmacology *41*, 126.

Baleydier, C., and Mauguiere, F. (1980). The duality of the cingulate gyrus in monkey. Neuroanatomical study and functional hypothesis. Brain J. Neurol. *103*, 525–554.

Ballantine, H.T., Bouckoms, A.J., Thomas, E.K., and Giriunas, I.E. (1987). Treatment of psychiatric illness by stereotactic cingulotomy. Biol. Psychiatry *22*, 807–819.

Bandelow, B., Sher, L., Bunevicius, R., Hollander, E., Kasper, S., Zohar, J., Möller, H.-J., Care, W.T.F. on M.D. in P., WFSBP Task Force on Anxiety Disorders, O.C.D., and PTSD (2012). Guidelines for the pharmacological treatment of anxiety disorders, obsessive–compulsive disorder and posttraumatic stress disorder in primary care. Int. J. Psychiatry Clin. Pract. *16*, 77–84.

Bandler, R., and Shipley, M.T. (1994). Columnar organization in the midbrain periaqueductal gray: modules for emotional expression? Trends Neurosci. *17*, 379–389.

Barahal, H.S. (1958). 1,000 prefrontal lobotomies—A five-to-10-year follow-up study. Psychiatr. Q. *32*, 653–678.

Barbas, H., Henion, T.H.H., and Dermon, C.R. (1991). Diverse thalamic projections to the prefrontal cortex in the rhesus monkey. J. Comp. Neurol. *313*, 65–94.

Barbas, H., Saha, S., Rempel-Clower, N., and Ghashghaei, T. (2003). Serial pathways from primate prefrontal cortex to autonomic areas may influence emotional expression. BMC Neurosci. *4*, 1–12.

Bard, P. (1934). On emotional expression after decortication with some remarks on certain theoretical views: Part I. Psychol. Rev. *41*, 309.

Bar-Haim, Y., Lamy, D., Pergamin, L., Bakermans-Kranenburg, M.J., and Van Ijzendoorn, M.H. (2007). Threat-related attentional bias in anxious and nonanxious individuals: a meta-analytic study. (American Psychological Association).

Barnet, R.C., Grahame, N.J., and Miller, R.R. (1995). Trial spacing effects in Pavlovian conditioning: A role for local context. Anim. Learn. Behav. *23*, 340–348.

Barros, M., and Tomaz, C. (2002). Non-human primate models for investigating fear and anxiety. Neurosci. Biobehav. Rev. *26*, 187–201.

Baxter, A.J., Vos, T., Scott, K.M., Ferrari, A.J., and Whiteford, H.A. (2014). The global burden of anxiety disorders in 2010. Psychol. Med. *44*, 2363–2374.

Beissner, F., Meissner, K., Bär, K.-J., and Napadow, V. (2013). The Autonomic Brain: An Activation Likelihood Estimation Meta-Analysis for Central Processing of Autonomic Function. J. Neurosci. *33*, 10503–10511.

Benarroch, E.E. (1993). The Central Autonomic Network: Functional Organization, Dysfunction, and Perspective. Mayo Clin. Proc. *68*, 988–1001.

Bezerra, B.M., and Souto, A. (2008). Structure and usage of the vocal repertoire of Callithrix jacchus. Int. J. Primatol. *29*, 671–701.

Bishop, S.J. (2007). Neurocognitive mechanisms of anxiety: an integrative account. Trends Cogn. Sci. *11*, 307–316.

Bishop, S., Duncan, J., Brett, M., and Lawrence, A.D. (2004). Prefrontal cortical function and anxiety: controlling attention to threat-related stimuli. Nat. Neurosci. *7*, 184–188.

Bissiere, S., McAllister, K.H., Olpe, H.-R., and Cryan, J.F. (2006). The rostral anterior cingulate cortex modulates depression but not anxiety-related behaviour in the rat. Behav. Brain Res. *175*, 195–199.

Bissière, S., Plachta, N., Hoyer, D., McAllister, K.H., Olpe, H.-R., Grace, A.A., and Cryan, J.F. (2008). The Rostral Anterior Cingulate Cortex Modulates the Efficiency of Amygdala-Dependent Fear Learning. Biol. Psychiatry *63*, 821–831.

Blair, K.S., Geraci, M., Smith, B.W., Hollon, N., DeVido, J., Otero, M., Blair, J.R., and Pine, D.S. (2012). Reduced Dorsal Anterior Cingulate Cortical Activity During Emotional Regulation and Top-Down Attentional Control in Generalized Social Phobia, Generalized Anxiety Disorder, and Comorbid Generalized Social Phobia/Generalized Anxiety Disorder. Biol. Psychiatry *72*, 476–482.

Boccard, S.G.J., Fitzgerald, J.J., Pereira, E.A.C., Moir, L., Van Hartevelt, T.J., Kringelbach, M.L., Green, A.L., and Aziz, T.Z. (2014). Targeting the Affective Component of Chronic Pain: A Case Series of Deep Brain Stimulation of the Anterior Cingulate Cortex. Neurosurgery *74*, 628–637.

Boender, A.J., de Jong, J.W., Boekhoudt, L., Luijendijk, M.C.M., van der Plasse, G., and Adan, R.A.H. (2014). Combined Use of the Canine Adenovirus-2 and DREADD-Technology to Activate Specific Neural Pathways In Vivo. PLoS ONE *9*, e95392.

Boldrini, M., Hen, R., Underwood, M.D., Rosoklija, G.B., Dwork, A.J., Mann, J.J., and Arango, V. (2012). Hippocampal Angiogenesis and Progenitor Cell Proliferation Are Increased with Antidepressant Use in Major Depression. Biol. Psychiatry *72*, 562–571.

Botvinick, M.M. (2007). Conflict monitoring and decision making: reconciling two perspectives on anterior cingulate function. Cogn. Affect. Behav. Neurosci. *7*, 356–366.

Botvinick, M.M., Braver, T.S., Barch, D.M., Carter, C.S., and Cohen, J.D. (2001). Conflict monitoring and cognitive control. Psychol. Rev. *108*, 624.

Botvinick, M.M., Cohen, J.D., and Carter, C.S. (2004). Conflict monitoring and anterior cingulate cortex: an update. Trends Cogn. Sci. *8*, 539–546.

Bouton, M.E., and Moody, E.W. (2004). Memory processes in classical conditioning. Neurosci. Biobehav. Rev. *28*, 663–674.

Brett, M., Johnsrude, I.S., and Owen, A.M. (2002). The problem of functional localization in the human brain. Nat. Rev. Neurosci. *3*, nrn756.

Brodmann, K. (1909). Vergleichende Lokalisationslehre der Groshirnrinde (Barth).

Brown, M.H., and Lighthill, J.A. (1968). Selective anterior cingulotomy: a psychosurgical evaluation. J. Neurosurg. *29*, 513–519.

Buchanan, S.L., and Powell, D.A. (1982). Cingulate cortex: Its role in Pavlovian conditioning. J. Comp. Physiol. Psychol. *96*, 755.

Büchel, C., Morris, J., Dolan, R.J., and Friston, K.J. (1998). Brain Systems Mediating Aversive Conditioning: an Event-Related fMRI Study. Neuron *20*, 947–957.

Buff, C., Brinkmann, L., Neumeister, P., Feldker, K., Heitmann, C., Gathmann, B., Andor, T., and Straube, T. (2016). Specifically altered brain responses to threat in generalized anxiety disorder relative to social anxiety disorder and panic disorder. NeuroImage Clin. *12*, 698–706.

Burcusa, S.L., and Iacono, W.G. (2007). Risk for Recurrence in Depression. Clin. Psychol. Rev. *27*, 959–985.

Burgos-Robles, A., Vidal-Gonzalez, I., and Quirk, G.J. (2009). Sustained Conditioned Responses in Prelimbic Prefrontal Neurons Are Correlated with Fear Expression and Extinction Failure. J. Neurosci. *29*, 8474–8482.

Burkart, J.M., Hrdy, S.B., and Van Schaik, C.P. (2009). Cooperative breeding and human cognitive evolution. Evol. Anthropol. Issues News Rev. *18*, 175–186.

Burman, K.J., and Rosa, M.G.P. (2009). Architectural subdivisions of medial and orbital frontal cortices in the marmoset monkey (Callithrix jacchus). J. Comp. Neurol. *514*, 11–29.

Bush, G., Luu, P., and Posner, M.I. (2000). Cognitive and emotional influences in anterior cingulate cortex. Trends Cogn. Sci. *4*, 215–222.

Bush, G., Vogt, B.A., Holmes, J., Dale, A.M., Greve, D., Jenike, M.A., and Rosen, B.R. (2002). Dorsal anterior cingulate cortex: a role in reward-based decision making. Proc. Natl. Acad. Sci. *99*, 523–528.

Caetano, S.C., Kaur, S., Brambilla, P., Nicoletti, M., Hatch, J.P., Sassi, R.B., Mallinger, A.G., Keshavan, M.S., Kupfer, D.J., Frank, E., et al. (2006). Smaller cingulate volumes in unipolar depressed patients. Biol. Psychiatry *59*, 702–706.

Cagni, P., Gonçalves, I., Ziller, F., Emile, N., and Barros, M. (2009). Humans and natural predators induce different fear/anxiety reactions and response pattern to diazepam in marmoset monkeys. Pharmacol. Biochem. Behav. *93*, 134–140.

Cannon, W.B. (1915). Bodily changes in pain, hunger, fear and rage: An account of recent researches into the function of emotional excitement. (New York, NY, US: D Appleton & Company).

Cannon, W.B. (1927). The James-Lange theory of emotions: A critical examination and an alternative theory. Am. J. Psychol. *39*, 106–124.

Carey, G.J., Costall, B., Domeney, A.M., Jones, D.N.C., and Naylor, R.J. (1992a). Behavioural effects of anxiogenic agents in the common marmoset. Pharmacol. Biochem. Behav. *42*, 143–153.

Carey, G.J., Costall, B., Domeney, A.M., Jones, D.N.C., and Naylor, R.J. (1992b). Behavioural effects of anxiogenic agents in the common marmoset. Pharmacol. Biochem. Behav. *42*, 143–153.

Carmichael, S.T., and Price, J.L. (1994). Architectonic subdivision of the orbital and medial prefrontal cortex in the macaque monkey. J. Comp. Neurol. *346*, 366–402.

Carmichael, S.T., and Price, J.L. (1995). Limbic connections of the orbital and medial prefrontal cortex in macaque monkeys. J. Comp. Neurol. *363*, 615–641.

Carter, C.S., Braver, T.S., Barch, D.M., Botvinick, M.M., Noll, D., and Cohen, J.D. (1998). Anterior cingulate cortex, error detection, and the online monitoring of performance. Science *280*, 747–749.

Caspi, A., Sugden, K., Moffitt, T.E., Taylor, A., Craig, I.W., Harrington, H., McClay, J., Mill, J., Martin, J., and Braithwaite, A. (2003). Influence of life stress on depression: moderation by a polymorphism in the 5-HTT gene. Sci. Signal. *301*, 386.

Cavada, C., Compañy, T., Tejedor, J., Cruz-Rizzolo, R.J., and Reinoso-Suárez, F. (2000). The Anatomical Connections of the Macaque Monkey Orbitofrontal Cortex. A Review. Cereb. Cortex *10*, 220–242.

Chalmers, J.A., Quintana, D.S., Abbott, M.J.-A., and Kemp, A.H. (2014). Anxiety Disorders are Associated with Reduced Heart Rate Variability: A Meta-Analysis. Front. Psychiatry *5*.

Chen, C.-H., Ridler, K., Suckling, J., Williams, S., Fu, C.H.Y., Merlo-Pich, E., and Bullmore, E. (2007). Brain Imaging Correlates of Depressive Symptom Severity and Predictors of Symptom Improvement After Antidepressant Treatment. Biol. Psychiatry *62*, 407–414.

Cisler, J.M., and Koster, E.H. (2010). Mechanisms of attentional biases towards threat in anxiety disorders: An integrative review. Clin. Psychol. Rev. *30*, 203–216.

Clarke, H.F., Horst, N.K., and Roberts, A.C. (2015). Regional inactivations of primate ventral prefrontal cortex reveal two distinct mechanisms underlying negative bias in decision making. Proc. Natl. Acad. Sci. *112*, 4176–4181.

Cole, M.W., Yeung, N., Freiwald, W.A., and Botvinick, M. (2009). Cingulate cortex: diverging data from humans and monkeys. Trends Neurosci. *32*, 566–574.

Coleman, K., and Pierre, P.J. (2014). Assessing Anxiety in Nonhuman Primates. ILAR J. *55*, 333–346.

Corcoran, K.A., and Quirk, G.J. (2007). Activity in prelimbic cortex is necessary for the expression of learned, but not innate, fears. J. Neurosci. *27*, 840–844.

Costall, B., Domeney, A.M., Gerrard, P.A., Kelly, M.E., and Naylor, R.J. (1988). Zacopride: anxiolytic profile in rodent and primate models of anxiety. J. Pharm. Pharmacol. *40*, 302–305.

Costall, B., Domeney, A.M., Farre, A.J., Kelly, M.E., Martinez, L., and Naylor, R.J. (1992). Profile of action of a novel 5-hydroxytryptamine1A receptor ligand E-4424 to inhibit aversive behavior in the mouse, rat and marmoset. J. Pharmacol. Exp. Ther. *262*, 90–98.

Cotter D, Mackay D, Landau S, Kerwin R, and Everall I (2001). REduced glial cell density and neuronal size in the anterior cingulate cortex in major depressive disorder. Arch. Gen. Psychiatry *58*, 545–553.

Craig, A.D. (2009). How do you feel—now? the anterior insula and human awareness.

Crestani, C.C. (2016). Emotional Stress and Cardiovascular Complications in Animal Models: A Review of the Influence of Stress Type. Front. Physiol. *7*.

Crestani, C.C., Alves, F.H., Gomes, F.V., Resstel, L., Correa, F., and Herman, J.P. (2013). Mechanisms in the bed nucleus of the stria terminalis involved in control of autonomic and neuroendocrine functions: a review. Curr. Neuropharmacol. *11*, 141–159.

Critchley, H. (2011). Dissecting axes of autonomic control in humans: Insights from neuroimaging. Auton. Neurosci. *161*, 34–42.

Critchley, H.D. (2005). Neural mechanisms of autonomic, affective, and cognitive integration. J. Comp. Neurol. *493*, 154–166.

Critchley, H., Eccles, J., and Garfinkel, S. (2013). Interaction between cognition, emotion, and the autonomic nervous system.

Critchley, H.D., Corfield, D.R., Chandler, M.P., Mathias, C.J., and Dolan, R.J. (2000). Cerebral correlates of autonomic cardiovascular arousal: a functional neuroimaging investigation in humans. J. Physiol. *523*, 259–270.

Critchley, H.D., Mathias, C.J., Josephs, O., O'Doherty, J., Zanini, S., Dewar, B.-K., Cipolotti, L., Shallice, T., and Dolan, R.J. (2003). Human cingulate cortex and autonomic control: converging neuroimaging and clinical evidence. Brain *126*, 2139–2152.

Critchley, H.D., Rotshtein, P., Nagai, Y., O'Doherty, J., Mathias, C.J., and Dolan, R.J. (2005a). Activity in the human brain predicting differential heart rate responses to emotional facial expressions. NeuroImage *24*, 751–762.

Critchley, H.D., Tang, J., Glaser, D., Butterworth, B., and Dolan, R.J. (2005b). Anterior cingulate activity during error and autonomic response. NeuroImage *27*, 885–895.

Croxson, P.L., Walton, M.E., O'Reilly, J.X., Behrens, T.E.J., and Rushworth, M.F.S. (2009). Effort-Based Cost–Benefit Valuation and the Human Brain. J. Neurosci. *29*, 4531–4541.

Culverhouse, R.C., Saccone, N.L., Horton, A.C., Ma, Y., Anstey, K.J., Banaschewski, T., Burmeister, M., Cohen-Woods, S., Etain, B., Fisher, H.L., et al. (2018). Collaborative meta-analysis finds no evidence of a strong interaction between stress and 5-HTTLPR genotype contributing to the development of depression. Mol. Psychiatry *23*, 133–142.

Damasio, A., and Carvalho, G.B. (2013). The nature of feelings: evolutionary and neurobiological origins. Nat. Rev. Neurosci. *14*, 143–152.

Darian-Smith, C., Darian-Smith, I., and Cheema, S.S. (1990). Thalamic projections to sensorimotor cortex in the macaque monkey: Use of multiple retrograde fluorescent tracers. J. Comp. Neurol. *299*, 17–46.

Darwin, C. (1965). The expression of the emotions in man and animals (University of Chicago press).

Davidson, R.J., Irwin, W., Anderle, M.J., and Kalin, N.H. (2003). The neural substrates of affective processing in depressed patients treated with venlafaxine. Am. J. Psychiatry.

Dehaene, S., Posner, M.I., and Tucker, D.M. (1994). Localization of a neural system for error detection and compensation. Psychol. Sci. *5*, 303–305.

Delgado, M.R., Nearing, K.I., LeDoux, J.E., and Phelps, E.A. (2008). Neural circuitry underlying the regulation of conditioned fear and its relation to extinction. Neuron *59*, 829–838.

Der-Avakian, A., and Markou, A. (2012). The neurobiology of anhedonia and other reward-related deficits. Trends Neurosci. *35*, 68–77.

Devinsky, O., Morrell, M.J., and Vogt, B.A. (1995). Contributions of anterior cingulate cortex to behaviour. Brain *118*, 279–306.

Dickson, J.M., and MacLeod, A.K. (2004). Approach and avoidance goals and plans: Their relationship to anxiety and depression. Cogn. Ther. Res. *28*, 415–432.

Disner, S.G., Beevers, C.G., Haigh, E.A.P., and Beck, A.T. (2011). Neural mechanisms of the cognitive model of depression. Nat. Rev. Neurosci. *12*, 467–477.

Drevets, W.C., Price, J.L., Simpson, J.R., Todd, R.D., Reich, T., Vannier, M., and Raichle, M.E. (1997). Subgenual prefrontal cortex abnormalities in mood disorders.

Dum, R.P., and Strick, P.L. (1993). Cingulate Motor Areas. In Neurobiology of Cingulate Cortex and Limbic Thalamus, (Birkhäuser, Boston, MA), pp. 415–441.

Duncan, J., and Owen, A.M. (2000). Common regions of the human frontal lobe recruited by diverse cognitive demands. Trends Neurosci. *23*, 475–483.

Ebitz, R.B., and Platt, M.L. (2015). Neuronal Activity in Primate Dorsal Anterior Cingulate Cortex Signals Task Conflict and Predicts Adjustments in Pupil-Linked Arousal. Neuron *85*, 628–640.

Eddy, M.C., Todd, T.P., Bouton, M.E., and Green, J.T. (2016). Medial prefrontal cortex involvement in the expression of extinction and ABA renewal of instrumental behavior for a food reinforcer. Neurobiol. Learn. Mem. *128*, 33–39.

Eisenberger, N.I. (2012). The pain of social disconnection: examining the shared neural underpinnings of physical and social pain. Nat. Rev. Neurosci. *13*, 421–434.

Eisenberger, N.I., and Lieberman, M.D. (2004). Why rejection hurts: a common neural alarm system for physical and social pain. Trends Cogn. Sci. *8*, 294–300.

Eisenberger, N.I., Lieberman, M.D., and Williams, K.D. (2003). Does rejection hurt? An fMRI study of social exclusion. Science *302*, 290–292.

Ekman, P. (2016). What Scientists Who Study Emotion Agree About. Perspect. Psychol. Sci. *11*, 31–34.

Ekman, P., Sorenson, E.R., and Friesen, W.V. (1969). Pan-cultural elements in facial displays of emotion. Science *164*, 86–88.

Ekman, P., Levenson, R.W., and Friesen, W.V. (1983). Autonomic nervous system activity distinguishes among emotions. Science *221*, 1208–1210.

Elliott, R., Sahakian, B.J., McKay, A.P., Herrod, J.J., Robbins, T.W., and Paykel, E.S. (1996). Neuropsychological impairments in unipolar depression: the influence of perceived failure on subsequent performance. Psychol. Med. *26*, 975–989.

El-Shamayleh, Y., Ni, A.M., and Horwitz, G.D. (2016). Strategies for targeting primate neural circuits with viral vectors. J. Neurophysiol. *116*, 122–134.

Eshel, N., and Roiser, J.P. (2010). Reward and punishment processing in depression. Biol. Psychiatry *68*, 118–124.

Etkin, A., and Wager, T. (2007). Functional neuroimaging of anxiety: a meta-analysis of emotional processing in PTSD, social anxiety disorder, and specific phobia. Am. J. Psychiatry *164*, 1476–1488.

Etkin, A., Egner, T., and Kalisch, R. (2011). Emotional processing in anterior cingulate and medial prefrontal cortex. Trends Cogn. Sci. *15*, 85–93.

Everly, G.S., and Lating, J.M. (2013). The Anatomy and Physiology of the Human Stress Response. In A Clinical Guide to the Treatment of the Human Stress Response, (Springer, New York, NY), pp. 17–51.

Fernando, A.B.P., and Robbins, T.W. (2011). Animal models of neuropsychiatric disorders. Annu. Rev. Clin. Psychol. *7*, 39–61.

Field, A. (2013). Discovering statistics using IBM SPSS statistics (Sage).

Foltz, E.L., and White Jr, L.E. (1962). Pain “relief” by frontal cingulumotomy. J. Neurosurg. *19*, 89–100.

Fulton, J.F., and Jacobsen, C.F. (1935). The functions of the frontal lobes: A comparative study in monkeys, chimpanzees and man. Adv Mod Biol Mosc. *4*, 113–125.

Galatzer-Levy, I.R., and Bryant, R.A. (2013). 636,120 Ways to Have Posttraumatic Stress Disorder. Perspect. Psychol. Sci. *8*, 651–662.

Gehring, W.J., Goss, B., Coles, M.G., Meyer, D.E., and Donchin, E. (1993). A neural system for error detection and compensation. Psychol. Sci. *4*, 385–390.

Gentil, A.F., Eskandar, E.N., Marci, C.D., Evans, K.C., and Dougherty, D.D. (2009). Physiological responses to brain stimulation during limbic surgery: further evidence of anterior cingulate modulation of autonomic arousal. Biol. Psychiatry *66*, 695–701.

Ghashghaei, H.T., and Barbas, H. (2002). Pathways for emotion: interactions of prefrontal and anterior temporal pathways in the amygdala of the rhesus monkey. Neuroscience *115*, 1261–1279.

Ghashghaei, H.T., Hilgetag, C.C., and Barbas, H. (2007). Sequence of information processing for emotions based on the anatomic dialogue between prefrontal cortex and amygdala. NeuroImage *34*, 905–923.

Gilmer, W.S., and McKinney, W.T. (2003). Early experience and depressive disorders: human and non-human primate studies. J. Affect. Disord. *75*, 97–113.

Gorman, J.M. (1996). Comorbid depression and anxiety spectrum disorders. Depress. Anxiety *4*, 160–168.

Gorman, J.M., and Sloan, R.P. (2000). Heart rate variability in depressive and anxiety disorders. Am. Heart J. *140*, 77–83.

Gotlib, I.H., and Joormann, J. (2010). Cognition and Depression: Current Status and Future Directions. Annu. Rev. Clin. Psychol. *6*, 285–312.

Graham, B.M., and Milad, M.R. (2011a). The Study of Fear Extinction: Implications for Anxiety Disorders. Am. J. Psychiatry *168*, 1255–1265.

Graham, B.M., and Milad, M.R. (2011b). Translational Research in the Neuroscience of Fear Extinction: Implications for Anxiety Disorders. Am. J. Psychiatry *168*, 1255–1265.

Greicius, M.D., Supekar, K., Menon, V., and Dougherty, R.F. (2009). Resting-state functional connectivity reflects structural connectivity in the default mode network. Cereb. Cortex *19*, 72–78.

Griebel, G., and Holmes, A. (2013). 50 years of hurdles and hope in anxiolytic drug discovery. Nat. Rev. Drug Discov. *12*, 667–687.

Gross, J.J. (1998). The emerging field of emotion regulation: an integrative review. Rev. Gen. Psychol. *2*, 271.

Gross, C.T., and Canteras, N.S. (2012). The many paths to fear. Nat. Rev. Neurosci. *13*, 651–658.

Gross, J.J., and Jazaieri, H. (2014). Emotion, emotion regulation, and psychopathology: An affective science perspective. Clin. Psychol. Sci. *2*, 387–401.

Grupe, D.W., and Nitschke, J.B. (2013). Uncertainty and anticipation in anxiety: an integrated neurobiological and psychological perspective. Nat. Rev. Neurosci. *14*, 488–501.

Guillery, R.W., and Sherman, S.M. (2002). Thalamic Relay Functions and Their Role in Corticocortical Communication: Generalizations from the Visual System. Neuron *33*, 163–175.

Guyenet, P.G. (2006). The sympathetic control of blood pressure. Nat. Rev. Neurosci. *7*, 335–346.

Haber, S.N. (2016). Corticostriatal circuitry. Dialogues Clin. Neurosci. *18*, 7–21.

Haber, S.N., and Knutson, B. (2010). The Reward Circuit: Linking Primate Anatomy and Human Imaging. Neuropsychopharmacology *35*, 4–26.

Haller, J., Aliczki, M., and Pelczer, K.G. (2013). Classical and novel approaches to the preclinical testing of anxiolytics: a critical evaluation. Neurosci. Biobehav. Rev. *37*, 2318–2330.

Hamilton, J.P., Etkin, A., Furman, D.J., Lemus, M.G., Johnson, R.F., and Gotlib, I.H. (2012). Functional neuroimaging of major depressive disorder: a meta-analysis and new integration of baseline activation and neural response data. Am. J. Psychiatry *169*, 693–703.

Hariri, A.R., Mattay, V.S., Tessitore, A., Kolachana, B., Fera, F., Goldman, D., Egan, M.F., and Weinberger, D.R. (2002). Serotonin transporter genetic variation and the response of the human amygdala. Science *297*, 400–403.

Hariri, A.R., Drabant, E.M., Munoz, K.E., Kolachana, B.S., Mattay, V.S., Egan, M.F., and Weinberger, D.R. (2005). A susceptibility gene for affective disorders and the response of the human amygdala. Arch. Gen. Psychiatry *62*, 146–152.

Harmer, C.J., Goodwin, G.M., and Cowen, P.J. (2009). Why do antidepressants take so long to work? A cognitive neuropsychological model of antidepressant drug action. Br. J. Psychiatry *195*, 102–108.

Hawton, K., Casañas i Comabella, C., Haw, C., and Saunders, K. (2013). Risk factors for suicide in individuals with depression: A systematic review. J. Affect. Disord. *147*, 17–28.

Hayden, B.Y., Heilbronner, S.R., Pearson, J.M., and Platt, M.L. (2011). Surprise signals in anterior cingulate cortex: neuronal encoding of unsigned reward prediction errors driving adjustment in behavior. J. Neurosci. *31*, 4178–4187.

Hayes, J.P., Hayes, S.M., and Mikedis, A.M. (2012). Quantitative meta-analysis of neural activity in posttraumatic stress disorder. Biol. Mood Anxiety Disord. *2*, 1.

Heilbronner, S.R., and Haber, S.N. (2014). Frontal Cortical and Subcortical Projections Provide a Basis for Segmenting the Cingulum Bundle: Implications for Neuroimaging and Psychiatric Disorders. J. Neurosci. *34*, 10041–10054.

Heilbronner, S.R., Rodriguez-Romaguera, J., Quirk, G.J., Groenewegen, H.J., and Haber, S.N. (2016). Circuit-Based Corticostriatal Homologies Between Rat and Primate. Biol. Psychiatry *80*, 509–521.

Hofmann, S.G. (2008). Cognitive processes during fear acquisition and extinction in animals and humans. Clin. Psychol. Rev. *28*, 199–210.

Hutcheson, G.D., and Sofroniou, N. (1999). The multivariate social scientist: Introductory statistics using generalized linear models (Sage).

Insel, T., Cuthbert, B., Garvey, M., Heinssen, R., Pine, D.S., Quinn, K., Sanislow, C., and Wang, P. (2010). Research Domain Criteria (RDoC): Toward a New Classification Framework for Research on Mental Disorders. Am. J. Psychiatry *167*, 748–751.

Jacobs, B.L., van Praag, H., and Gage, F.H. (2000). Adult brain neurogenesis and psychiatry: a novel theory of depression. Mol. Psychiatry *5*, 262–269.

Jinks, A.L., and McGregor, I.S. (1997). Modulation of anxiety-related behaviours following lesions of the prelimbic or infralimbic cortex in the rat. Brain Res. *772*, 181–190.

John, Y.J., Bullock, D., Zikopoulos, B., and Barbas, H. (2013). Anatomy and computational modeling of networks underlying cognitive-emotional interaction. Front. Hum. Neurosci. *7*.

Kaada, B.R. (1951). Somato-motor, autonomic and electrocorticographic responses to electrical stimulation of rhinencephalic and other structures in primates, cat, and dog; a study of responses from the limbic, subcallosal, orbito-insular, piriform and temporal cortex, hippocampus-fornix and amygdala. Acta Physiol. Scand. Suppl. *24*, 1.

Kalin, N.H. (2004). Studying non-human primates: a gateway to understanding anxiety disorders. Psychopharmacol. Bull. *38*, 8–13.

Kalin, N.H., and Shelton, S.E. (1989). Defensive behaviors in infant rhesus monkeys: environmental cues and neurochemical regulation. Science *243*, 1718–1722.

Kalin, N.H., Shelton, S.E., and Turner, J.G. (1992). Effects of \s s-carboline on fear-related behavioral and neurohormonal responses in infant rhesus monkeys. Biol. Psychiatry *31*, 1008–1019.

Kalin, N.H., Shelton, S.E., Davidson, R.J., and Kelley, A.E. (2001). The Primate Amygdala Mediates Acute Fear But Not the Behavioral and Physiological Components of Anxious Temperament. J. Neurosci. *21*, 2067–2074.

Kalin, N.H., Shelton, S.E., Fox, A.S., Oakes, T.R., and Davidson, R.J. (2005). Brain Regions Associated with the Expression and Contextual Regulation of Anxiety in Primates. Biol. Psychiatry *58*, 796–804.

Kalisch, R., and Gerlicher, A.M.V. (2014). Making a mountain out of a molehill: On the role of the rostral dorsal anterior cingulate and dorsomedial prefrontal cortex in conscious threat appraisal, catastrophizing, and worrying. Neurosci. Biobehav. Rev. *42*, 1–8.

Kalisch, R., Wiech, K., Critchley, H.D., and Dolan, R.J. (2006). Levels of appraisal: a medial prefrontal role in high-level appraisal of emotional material. Neuroimage *30*, 1458–1466.

Kassam, K.S., Markey, A.R., Cherkassky, V.L., Loewenstein, G., and Just, M.A. (2013). Identifying emotions on the basis of neural activation. PloS One *8*, e66032.

Keay, K.A., and Bandler, R. (2001). Parallel circuits mediating distinct emotional coping reactions to different types of stress. Neurosci. Biobehav. Rev. *25*, 669–678.

Kemp, A.H., Quintana, D.S., Felmingham, K.L., Matthews, S., and Jelinek, H.F. (2012). Depression, Comorbid Anxiety Disorders, and Heart Rate Variability in Physically Healthy, Unmedicated Patients: Implications for Cardiovascular Risk. PLOS ONE *7*, e30777.

Kendler, K.S., Karkowski, L.M., and Prescott, C.A. (1999). Causal Relationship Between Stressful Life Events and the Onset of Major Depression. Am. J. Psychiatry *156*, 837–841.

Kennerley, S.W., and Walton, M.E. (2011). Decision Making and Reward in Frontal Cortex. Behav. Neurosci. *125*, 297–317.

Kennerley, S.W., Walton, M.E., Behrens, T.E., Buckley, M.J., and Rushworth, M.F. (2006). Optimal decision making and the anterior cingulate cortex. Nat. Neurosci. *9*, 940–947.

Kessler, R.C., Berglund, P., Demler, O., Jin, R., Merikangas, K.R., and Walters, E.E. (2005a). Lifetime prevalence and age-of-onset distributions of DSM-IV disorders in the National Comorbidity Survey Replication. Arch. Gen. Psychiatry *62*, 593–602.

Kessler, R.C., Chiu, W.T., Demler, O., and Walters, E.E. (2005b). Prevalence, severity, and comorbidity of 12-month DSM-IV disorders in the National Comorbidity Survey Replication. Arch. Gen. Psychiatry *62*, 617–627.

Kessler, R.C., Aguilar-Gaxiola, S., Alonso, J., Chatterji, S., Lee, S., Ormel, J., Ustün, T.B., and Wang, P.S. (2009). The global burden of mental disorders: an update from the WHO World Mental Health (WMH) surveys. Epidemiol. Psichiatr. Soc. *18*, 23–33.

Khawaja, I.S., Westermeyer, J.J., Gajwani, P., and Feinstein, R.E. (2009). Depression and Coronary Artery Disease. Psychiatry Edgmont *6*, 38–51.

Killcross, S., Robbins, T.W., and Everitt, B.J. (1997). Different types of fear-conditioned behaviour mediated by separate nuclei within amygdala. Nature *388*, 377.

Kincheski, G.C., Mota-Ortiz, S.R., Pavesi, E., Canteras, N.S., and Carobrez, A.P. (2012). The Dorsolateral Periaqueductal Gray and Its Role in Mediating Fear Learning to Life Threatening Events. PLOS ONE *7*, e50361.

Klavir, O., Genud-Gabai, R., and Paz, R. (2012). Low-Frequency Stimulation Depresses the Primate Anterior-Cingulate-Cortex and Prevents Spontaneous Recovery of Aversive Memories. J. Neurosci. *32*, 8589–8597.

Kolling, N., Wittmann, M.K., Behrens, T.E.J., Boorman, E.D., Mars, R.B., and Rushworth, M.F.S. (2016). Value, search, persistence and model updating in anterior cingulate cortex. Nat. Neurosci. *19*, 1280–1285.

Koolschijn, P., van Haren, N.E., Lensvelt-Mulders, G.J., Pol, H., Hilleke, E., and Kahn, R.S. (2009). Brain volume abnormalities in major depressive disorder: A meta-analysis of magnetic resonance imaging studies. Hum. Brain Mapp. *30*, 3719–3735.

Kötter, R., and Meyer, N. (1992). The limbic system: a review of its empirical foundation. Behav. Brain Res. *52*, 105–127.

Kozel, F.A., Rao, U., Lu, H., Nakonezny, P.A., Grannemann, B., McGregor, T., Croarkin, P.E., Mapes, K.S., Tamminga, C.A., and Trivedi, M.H. (2011). Functional Connectivity of Brain Structures Correlates with Treatment Outcome in Major Depressive Disorder. Front. Psychiatry *2*.

Kreibig, S.D. (2010). Autonomic nervous system activity in emotion: A review. Biol. Psychol. *84*, 394–421.

Krettek, J.E., and Price, J.L. (1977). The cortical projections of the mediodorsal nucleus and adjacent thalamic nuclei in the rat. J. Comp. Neurol. *171*, 157–191.

Kunishio, K., and Haber, S.N. (1994). Primate cingulostriatal projection: Limbic striatal versus sensorimotor striatal input. J. Comp. Neurol. *350*, 337–356.

Lally, N., Nugent, A.C., Luckenbaugh, D.A., Ameli, R., Roiser, J.P., and Zarate, C.A. (2014). Anti-anhedonic effect of ketamine and its neural correlates in treatment-resistant bipolar depression. Transl. Psychiatry *4*, e469.

Lally, N., Nugent, A.C., Luckenbaugh, D.A., Niciu, M.J., Roiser, J.P., and Zarate, C.A. (2015). Neural correlates of change in major depressive disorder anhedonia following open-label ketamine. J. Psychopharmacol. (Oxf.) 0269881114568041.

Lanciego, J.L., and Wouterlood, F.G. (2011). A half century of experimental neuroanatomical tracing. J. Chem. Neuroanat. *42*, 157–183.

Lanza, M., Fassio, A., Gemignani, A., Bonanno, G., and Raiteri, M. (1993). CGP 52432: a novel potent and selective GABAB autoreceptor antagonist in rat cerebral cortex. Eur. J. Pharmacol. *237*, 191–195.

Laurent, V., and Westbrook, R.F. (2009). Inactivation of the infralimbic but not the prelimbic cortex impairs consolidation and retrieval of fear extinction. Learn. Mem. *16*, 520–529.

LeDoux, J. (2003). The emotional brain, fear, and the amygdala. Cell. Mol. Neurobiol. *23*, 727–738.

LeDoux, J.E. (2000). Emotion circuits in the brain. Annu. Rev. Neurosci. *23*, 155–184.

LeDoux, J.E. (2012). Evolution of human emotion. Prog. Brain Res. *195*, 431–442.

LeDoux, J.E., and Brown, R. (2017). A higher-order theory of emotional consciousness. Proc. Natl. Acad. Sci. *114*, E2016–E2025.

LeDoux, J.E., and Pine, D.S. (2016). Using Neuroscience to Help Understand Fear and Anxiety: A Two-System Framework. Am. J. Psychiatry *173*, 1083–1093.

Li, M., Metzger, C.D., Li, W., Safron, A., van Tol, M.-J., Lord, A., Krause, A.L., Borchardt, V., Dou, W., Genz, A., et al. (2014). Dissociation of glutamate and cortical thickness is restricted to regions subserving trait but not state markers in major depressive disorder. J. Affect. Disord. *169*, 91–100.

Lieberman, M.D., and Eisenberger, N.I. (2015). The dorsal anterior cingulate cortex is selective for pain: Results from large-scale reverse inference. Proc. Natl. Acad. Sci. 201515083.

Lindquist, K.A., Wager, T.D., Kober, H., Bliss-Moreau, E., and Barrett, L.F. (2012). The brain basis of emotion: A meta-analytic review. Behav. Brain Sci. *35*, 121–143.

Linnman, C., Zeidan, M.A., Furtak, S.C., Pitman, R.K., Quirk, G.J., and Milad, M.R. (2012b). Resting amygdala and medial prefrontal metabolism predicts functional activation of the fear extinction circuit. Am. J. Psychiatry *169*, 415–423.

Linnman, C., Zeidan, M.A., Pitman, R.K., and Milad, M.R. (2012a). Resting cerebral metabolism correlates with skin conductance and functional brain activation during fear conditioning. Biol. Psychol. *89*, 450–459.

Lipp, H.P. (1978). Aggression and flight behaviour of the marmoset monkey Callithrix jacchus: an ethogram for brain stimulation studies. Brain. Behav. Evol. *15*, 241–259.

Lissek, S., Powers, A.S., McClure, E.B., Phelps, E.A., Woldehawariat, G., Grillon, C., and Pine, D.S. (2005). Classical fear conditioning in the anxiety disorders: a meta-analysis. Behav. Res. Ther. *43*, 1391–1424.

Lissek, S., Kaczkurkin, A.N., Rabin, S., Geraci, M., Pine, D.S., and Grillon, C. (2014). Generalized Anxiety Disorder is Associated with Overgeneralization of Classically Conditioned-Fear. Biol. Psychiatry *75*, 909–915.

Löfving, B. (1961). Cardiovascular adjustments induced from the rostral cingulate gyrus: with special reference to sympatho-inhibitory mechanisms (Acta physiologica Scandinavica).

Lubow, R.E. (1973). Latent inhibition. Psychol. Bull. *79*, 398.

Luppino, G., Matelli, M., Camarda, R.M., Gallese, V., and Rizzolatti, G. (1991). Multiple representations of body movements in mesial area 6 and the adjacent cingulate cortex: an intracortical microstimulation study in the macaque monkey. J. Comp. Neurol. *311*, 463–482.

Machado, C.J., and Bachevalier, J. (2008). Behavioral and hormonal reactivity to threat: Effects of selective amygdala, hippocampal or orbital frontal lesions in monkeys. Psychoneuroendocrinology *33*, 926–941.

MacLean, P.D. (1990). The triune brain in evolution: Role in paleocerebral functions (Springer Science & Business Media).

Maier, S., Szalkowski, A., Kamphausen, S., Perlov, E., Feige, B., Blechert, J., Philipsen, A., van Elst, L.T., Kalisch, R., and Tüscher, O. (2012). Clarifying the role of the rostral dmPFC/dACC in fear/anxiety: learning, appraisal or expression? PloS One *7*, e50120.

Malberg, J.E., Eisch, A.J., Nestler, E.J., and Duman, R.S. (2000). Chronic antidepressant treatment increases neurogenesis in adult rat hippocampus. J. Neurosci. *20*, 9104–9110.

Mangina, C.A., and Beuzeron-Mangina, J.H. (1996). Direct electrical stimulation of specific human brain structures and bilateral electrodermal activity. Int. J. Psychophysiol. *22*, 1–8.

Maren, S. (2001). Neurobiology of Pavlovian fear conditioning. Annu. Rev. Neurosci. *24*, 897–931.

Maren, S., and Quirk, G.J. (2004). Neuronal signalling of fear memory. Nat. Rev. Neurosci. *5*, 844–852.

Marrocco, J., Mairesse, J., Ngomba, R.T., Silletti, V., Van Camp, G., Bouwalerh, H., Summa, M., Pittaluga, A., Nicoletti, F., Maccari, S., et al. (2012). Anxiety-Like Behavior of Prenatally Stressed Rats Is Associated with a Selective Reduction of Glutamate Release in the Ventral Hippocampus. J. Neurosci. *32*, 17143–17154.

Mathews, A., and MacLeod, C. (2002). Induced processing biases have causal effects on anxiety. Cogn. Emot. *16*, 331–354.

Mauk, M.D., and Ohyama, T. (2004). Extinction as New Learning Versus Unlearning: Considerations from a Computer Simulation of the Cerebellum. Learn. Mem. *11*, 566–571.

Mayberg, H.S. (1997). Limbic-cortical dysregulation: a proposed model of depression. J. Neuropsychiatry Clin. Neurosci.

Mayberg, H.S., Brannan, S.K., Mahurin, R.K., Jerabek, P.A., Brickman, J.S., Tekell, J.L., Silva, J.A., McGinnis, S., Glass, T.G., Martin, C.C., et al. (1997). Cingulate function in depression: a potential predictor of treatment response. Neuroreport *8*, 1057–1061.

Mayberg, H.S., Liotti, M., Brannan, S.K., McGinnis, S., Mahurin, R.K., Jerabek, P.A., Silva, J.A., Tekell, J.L., Martin, C.C., Lancaster, J.L., et al. (1999). Reciprocal Limbic-Cortical Function and Negative Mood: Converging PET Findings in Depression and Normal Sadness. Am. J. Psychiatry *156*, 675–682.

Mayberg, H.S., Brannan, S.K., Tekell, J.L., Silva, J.A., Mahurin, R.K., McGinnis, S., and Jerabek, P.A. (2000). Regional metabolic effects of fluoxetine in major depression: serial changes and relationship to clinical response. Biol. Psychiatry *48*, 830–843.

Mayberg, H.S., Lozano, A.M., Voon, V., McNeely, H.E., Seminowicz, D., Hamani, C., Schwalb, J.M., and Kennedy, S.H. (2005). Deep brain stimulation for treatment-resistant depression. Neuron *45*, 651–660.

Mechias, M.-L., Etkin, A., and Kalisch, R. (2010). A meta-analysis of instructed fear studies: implications for conscious appraisal of threat. Neuroimage *49*, 1760–1768.

Menon, V., and Uddin, L.Q. (2010). Saliency, switching, attention and control: a network model of insula function. Brain Struct. Funct. *214*, 655–667.

Meyer, G., McElhaney, M., Martin, W., and McGraw, C.P. (1973). Stereotactic cingulotomy with results of acute stimulation and serial psychological testing. Surg. Approaches Psychiatry 39–58.

Michael, T., Blechert, J., Vriends, N., Margraf, J., and Wilhelm, F.H. (2007). Fear conditioning in panic disorder: Enhanced resistance to extinction. J. Abnorm. Psychol. *116*, 612.

Mikheenko, Y., Man, M.-S., Braesicke, K., Johns, M.E., Hill, G., Agustín-Pavón, C., and Roberts, A.C. (2010). Autonomic, behavioral, and neural analyses of mild conditioned negative affect in marmosets. Behav. Neurosci. *124*, 192–203.

Mikheenko, Y., Shiba, Y., Sawiak, S., Braesicke, K., Cockcroft, G., Clarke, H., and Roberts, A.C. (2015). Serotonergic, Brain Volume and Attentional Correlates of Trait Anxiety in Primates. Neuropsychopharmacology *40*, 1395–1404.

Milad, M.R., and Quirk, G.J. (2002). Neurons in medial prefrontal cortex signal memory for fear extinction. Nature *420*, 70–74.

Milad, M.R., and Quirk, G.J. (2012). Fear Extinction as a Model for Translational Neuroscience: Ten Years of Progress. Annu. Rev. Psychol. *63*, 129–151.

Milad, M.R., Vidal-Gonzalez, I., and Quirk, G.J. (2004). Electrical stimulation of medial prefrontal cortex reduces conditioned fear in a temporally specific manner. Behav. Neurosci. *118*, 389.

Milad, M.R., Quinn, B.T., Pitman, R.K., Orr, S.P., Fischl, B., and Rauch, S.L. (2005). Thickness of ventromedial prefrontal cortex in humans is correlated with extinction memory. Proc. Natl. Acad. Sci. U. S. A. *102*, 10706–10711.

Milad, M.R., Quirk, G.J., Pitman, R.K., Orr, S.P., Fischl, B., and Rauch, S.L. (2007a). A Role for the Human Dorsal Anterior Cingulate Cortex in Fear Expression. Biol. Psychiatry *62*, 1191–1194.

Milad, M.R., Wright, C.I., Orr, S.P., Pitman, R.K., Quirk, G.J., and Rauch, S.L. (2007b). Recall of fear extinction in humans activates the ventromedial prefrontal cortex and hippocampus in concert. Biol. Psychiatry *62*, 446–454.

Milad, M.R., Orr, S.P., Lasko, N.B., Chang, Y., Rauch, S.L., and Pitman, R.K. (2008). Presence and acquired origin of reduced recall for fear extinction in PTSD: results of a twin study. J. Psychiatr. Res. *42*, 515–520.

Milad, M.R., Pitman, R.K., Ellis, C.B., Gold, A.L., Shin, L.M., Lasko, N.B., Zeidan, M.A., Handwerger, K., Orr, S.P., and Rauch, S.L. (2009). Neurobiological Basis of Failure to Recall Extinction Memory in Posttraumatic Stress Disorder. Biol. Psychiatry *66*, 1075–1082.

Miller, C.T., Freiwald, W.A., Leopold, D.A., Mitchell, J.F., Silva, A.C., and Wang, X. (2016). Marmosets: A Neuroscientific Model of Human Social Behavior. Neuron *90*, 219–233.

Mitchell, J.F., and Leopold, D.A. (2015). The marmoset monkey as a model for visual neuroscience. Neurosci. Res. *93*, 20–46.

Mogg, K., and Bradley, B.P. (2005). Attentional bias in generalized anxiety disorder versus depressive disorder. Cogn. Ther. Res. *29*, 29–45.

Mohanty, A., Engels, A.S., Herrington, J.D., Heller, W., Ringo Ho, M.-H., Banich, M.T., Webb, A.G., Warren, S.L., and Miller, G.A. (2007). Differential engagement of anterior cingulate cortex subdivisions for cognitive and emotional function. Psychophysiology *44*, 343–351.

Moniz, E. (1937). Prefrontal leucotomy in the treatment of mental disorders. Am. J. Psychiatry *93*, 1379–1385.

Mori, S., and Zhang, J. (2006). Principles of Diffusion Tensor Imaging and Its Applications to Basic Neuroscience Research. Neuron *51*, 527–539.

Mullins, N., and Lewis, C.M. (2017). Genetics of Depression: Progress at Last. Curr. Psychiatry Rep. *19*, 43.

Murphy, F.C., Michael, A., Robbins, T.W., and Sahakian, B.J. (2003). Neuropsychological impairment in patients with major depressive disorder: the effects of feedback on task performance. Psychol. Med. *33*, 455–467.

Myers, K.M., and Davis, M. (2006). Mechanisms of fear extinction. Mol. Psychiatry *12*, 120–150.

Myers-Schulz, B., and Koenigs, M. (2011). Functional anatomy of ventromedial prefrontal cortex: implications for mood and anxiety disorders. Mol. Psychiatry *17*, 132–141.

Nestler, E.J., and Hyman, S.E. (2010). Animal models of neuropsychiatric disorders. Nat. Neurosci. *13*, 1161–1169.

Nitschke, J.B., Sarinopoulos, I., Oathes, D.J., Johnstone, T., Whalen, P.J., Davidson, R.J., and Kalin, N.H. (2009). Anticipatory Activation in the Amygdala and Anterior Cingulate in Generalized Anxiety Disorder and Prediction of Treatment Response. Am. J. Psychiatry *166*, 302–310.

Norrholm, S.D., Jovanovic, T., Olin, I.W., Sands, L.A., Karapanou, I., Bradley, B., and Ressler, K.J. (2011). Fear Extinction in Traumatized Civilians with Posttraumatic Stress Disorder: Relation to Symptom Severity. Biol. Psychiatry *69*, 556–563.

Obrist, P.A., Webb, R.A., Sutterer, J.R., and Howard, J.L. (1970). The cardiac-somatic relationship: some reformulations. Psychophysiology *6*, 569–587.

Ochsner, K.N., and Gross, J.J. (2005). The cognitive control of emotion. Trends Cogn. Sci. *9*, 242–249.

Ochsner, K.N., Ray, R.D., Cooper, J.C., Robertson, E.R., Chopra, S., Gabrieli, J.D.E., and Gross, J.J. (2004). For better or for worse: neural systems supporting the cognitive down- and up-regulation of negative emotion. NeuroImage *23*, 483–499.

Ochsner, K.N., Silvers, J.A., and Buhle, J.T. (2012). Functional imaging studies of emotion regulation: a synthetic review and evolving model of the cognitive control of emotion. Ann. N. Y. Acad. Sci. *1251*.

Öhman, A. (2005). The role of the amygdala in human fear: automatic detection of threat. Psychoneuroendocrinology *30*, 953–958.

Öhman, A., and Mineka, S. (2001). Fears, phobias, and preparedness: toward an evolved module of fear and fear learning. Psychol. Rev. *108*, 483.

Oikonomidis, L., Santangelo, A.M., Shiba, Y., Clarke, F.H., Robbins, T.W., and Roberts, A.C. (2017). A dimensional approach to modeling symptoms of neuropsychiatric disorders in the marmoset monkey. Dev. Neurobiol. *77*, 328–353.

Öngür, D., and Price, J.L. (2000). The Organization of Networks within the Orbital and Medial Prefrontal Cortex of Rats, Monkeys and Humans. Cereb. Cortex *10*, 206–219.

Öngür, D., An, X., and Price, J. l. (1998). Prefrontal cortical projections to the hypothalamus in Macaque monkeys. J. Comp. Neurol. *401*, 480–505.

Öngür, D., Ferry, A.T., and Price, J.L. (2003). Architectonic subdivision of the human orbital and medial prefrontal cortex. J. Comp. Neurol. *460*, 425–449.

Orr, S.P., Metzger, L.J., Lasko, N.B., Macklin, M.L., Peri, T., and Pitman, R.K. (2000). De novo conditioning in trauma-exposed individuals with and without posttraumatic stress disorder. J. Abnorm. Psychol. *109*, 290.

Ostlund, S.B., Winterbauer, N.E., and Balleine, B.W. (2009). Evidence of action sequence chunking in goal-directed instrumental conditioning and its dependence on the dorsomedial prefrontal cortex. J. Neurosci. *29*, 8280–8287.

Otowa, T., Hek, K., Lee, M., Byrne, E.M., Mirza, S.S., Nivard, M.G., Bigdeli, T., Aggen, S.H., Adkins, D., Wolen, A., et al. (2016). Meta-analysis of genome-wide association studies of anxiety disorders. Mol. Psychiatry *21*, 1391.

Palomero-Gallagher, N., Mohlberg, H., Zilles, K., and Vogt, B.A. (2008). Cytology and Receptor Architecture of Human Anterior Cingulate Cortex. J. Comp. Neurol. *508*, 906–926.

Palomero-Gallagher, N., Vogt, B.A., Schleicher, A., Mayberg, H.S., and Zilles, K. (2009). Receptor architecture of human cingulate cortex: Evaluation of the four-region neurobiological model. Hum. Brain Mapp. *30*, 2336–2355.

Papez, J.W. (1937). A proposed mechanism of emotion. Arch. Neurol. Psychiatry *38*, 725–743.

Passingham, R.E., and Wise, S.P. (2012). The neurobiology of the prefrontal cortex: anatomy, evolution, and the origin of insight (Oxford University Press).

Paulus, M.P., and Yu, A.J. (2012). Emotion and decision-making: affect-driven belief systems in anxiety and depression. Trends Cogn. Sci. *16*, 476–483.

Paxinos, Watson, C., Petrides, M., Rosa, M., and Tokuno, H. (2011). The Marmoset Brain in Stereotaxic Coordinates (Academic Press).

Pessoa, L. (2008). On the relationship between emotion and cognition. Nat. Rev. Neurosci. *9*, 148.

Petrides, M., and Pandya, D.N. (1994). Comparative architectonic analysis of the human and the macaque frontal cortex. Handb. Neuropsychol. *9*, 17–58.

Petrides, M., and Pandya, D.N. (2002). Comparative cytoarchitectonic analysis of the human and the macaque ventrolateral prefrontal cortex and corticocortical connection patterns in the monkey. Eur. J. Neurosci. *16*, 291–310.

Petrides, M., Tomaiuolo, F., Yeterian, E.H., and Pandya, D.N. (2012). The prefrontal cortex: comparative architectonic organization in the human and the macaque monkey brains. Cortex *48*, 46–57.

Peyron, R., Laurent, B., and Garcia-Larrea, L. (2000). Functional imaging of brain responses to pain. A review and meta-analysis (2000). Neurophysiol. Clin. Neurophysiol. *30*, 263–288.

Pezawas, L., Meyer-Lindenberg, A., Drabant, E.M., Verchinski, B.A., Munoz, K.E., Kolachana, B.S., Egan, M.F., Mattay, V.S., Hariri, A.R., and Weinberger, D.R. (2005). 5-HTTLPR polymorphism impacts human cingulate-amygdala interactions: a genetic susceptibility mechanism for depression. Nat. Neurosci. *8*, 828–834.

Phelps, E.A., Delgado, M.R., Nearing, K.I., and LeDoux, J.E. (2004). Extinction learning in humans: role of the amygdala and vmPFC. Neuron *43*, 897–905.

Picard, N., and Strick, P.L. (1996). Motor areas of the medial wall: a review of their location and functional activation. Cereb. Cortex *6*, 342–353.

Picard, N., and Strick, P.L. (2001). Imaging the premotor areas. Curr. Opin. Neurobiol. *11*, 663–672.

Pitman, R.K., Rasmusson, A.M., Koenen, K.C., Shin, L.M., Orr, S.P., Gilbertson, M.W., Milad, M.R., and Liberzon, I. (2012). Biological studies of post-traumatic stress disorder. Nat. Rev. Neurosci. *13*, 769–787.

Pittenger, C., and Duman, R.S. (2008). Stress, Depression, and Neuroplasticity: A Convergence of Mechanisms. Neuropsychopharmacology *33*, 88–109.

Pizzagalli, D.A. (2011). Frontocingulate dysfunction in depression: toward biomarkers of treatment response. Neuropsychopharmacol. Off. Publ. Am. Coll. Neuropsychopharmacol. *36*, 183–206.

Pizzagalli, D., Pascual-Marqui, R.D., Nitschke, J.B., Oakes, T.R., Larson, C.L., Abercrombie, H.C., Schaefer, S.M., Koger, J.V., Benca, R.M., and Davidson, R.J. (2001). Anterior cingulate activity as a predictor of degree of treatment response in major depression: evidence from brain electrical tomography analysis. Am. J. Psychiatry *158*, 405–415.

Pizzagalli, D.A., Jahn, A.L., and O'Shea, J.P. (2005). Toward an objective characterization of an anhedonic phenotype: a signal-detection approach. Biol. Psychiatry *57*, 319–327.

Pizzagalli, D.A., Iosifescu, D., Hallett, L.A., Ratner, K.G., and Fava, M. (2008). Reduced Hedonic Capacity in Major Depressive Disorder: Evidence from a Probabilistic Reward Task. J. Psychiatr. Res. *43*, 76–87.

Pizzagalli, D.A., Holmes, A.J., Dillon, D.G., Goetz, E.L., Birk, J.L., Bogdan, R., Dougherty, D.D., Iosifescu, D.V., Rauch, S.L., and Fava, M. (2009). Reduced Caudate and Nucleus Accumbens Response to Rewards in Unmedicated Subjects with Major Depressive Disorder. Am. J. Psychiatry *166*, 702–710.

Pool, J.L., and Ransohoff, J. (1949). Autonomic effects on stimulating rostral portion of cingulate gyri in man. J. Neurophysiol. *12*, 385–392.

Posner, J., Russell, J.A., and Peterson, B.S. (2005). The circumplex model of affect: An integrative approach to affective neuroscience, cognitive development, and psychopathology. Dev. Psychopathol. *17*, 715–734.

Prins, N.W., Pohlmeyer, E., Debnath, S., Mylavarapu, R., Geng, S., Sanchez, J.C., Rothen, D., and Prasad, A. (2017). Common marmoset (Callithrix jacchus) as a primate model for behavioral neuroscience studies. J. Neurosci. Methods.

Quirk, G.J., Russo, G.K., Barron, J.L., and Lebron, K. (2000). The role of ventromedial prefrontal cortex in the recovery of extinguished fear. J. Neurosci. *20*, 6225–6231.

R Core Team (2017). R: A language and environment for statistical computing [Internet]. Vienna, Austria; 2014.

Radua, J., Heuvel, O.A. van den, Surguladze, S., and Mataix-Cols, D. (2010). Meta-analytical Comparison of Voxel-Based Morphometry Studies in Obsessive-Compulsive Disorder vs Other Anxiety Disorders. Arch. Gen. Psychiatry *67*, 701–711.

Raichle, M.E., MacLeod, A.M., Snyder, A.Z., Powers, W.J., Gusnard, D.A., and Shulman, G.L. (2001). A default mode of brain function. Proc. Natl. Acad. Sci. *98*, 676–682.

Rauch, S.L., Shin, L.M., and Phelps, E.A. (2006). Neurocircuitry models of posttraumatic stress disorder and extinction: human neuroimaging research—past, present, and future. Biol. Psychiatry *60*, 376–382.

Ray, R.D., and Zald, D.H. (2012). Anatomical insights into the interaction of emotion and cognition in the prefrontal cortex. Neurosci. Biobehav. Rev. *36*, 479–501.

Reif, A., Fritzen, S., Finger, M., Strobel, A., Lauer, M., Schmitt, A., and Lesch, K.P. (2006). Neural stem cell proliferation is decreased in schizophrenia, but not in depression. Mol. Psychiatry *11*, 514.

Reiner, A., Veenman, C.L., Medina, L., Jiao, Y., Del Mar, N., and Honig, M.G. (2000). Pathway tracing using biotinylated dextran amines. J. Neurosci. Methods *103*, 23–37.

Ressler, K.J., and Mayberg, H.S. (2007). Targeting abnormal neural circuits in mood and anxiety disorders: from the laboratory to the clinic. Nat. Neurosci. *10*, 1116–1124.

Ripke, S., Wray, N.R., Lewis, C.M., Hamilton, S.P., Weissman, M.M., Breen, G., Byrne, E.M., Blackwood, D.H., Boomsma, D.I., and Cichon, S. (2013). A mega-analysis of genome-wide association studies for major depressive disorder. Mol. Psychiatry *18*, 497.

Riva-Posse, P., Choi, K.S., Holtzheimer, P.E., McIntyre, C.C., Gross, R.E., Chaturvedi, A., Crowell, A.L., Garlow, S.J., Rajendra, J.K., and Mayberg, H.S. (2014). Defining critical white matter pathways mediating successful subcallosal cingulate deep brain stimulation for treatment-resistant depression. Biol. Psychiatry *76*, 963–969.

Roberts, A.C., Tomic, D.L., Parkinson, C.H., Roeling, T.A., Cutter, D.J., Robbins, T.W., and Everitt, B.J. (2007). Forebrain connectivity of the prefrontal cortex in the marmoset monkey (Callithrix jacchus): an anterograde and retrograde tract-tracing study. J. Comp. Neurol. *502*, 86–112.

Robinson, O.J., Charney, D.R., Overstreet, C., Vytal, K., and Grillon, C. (2012). The adaptive threat bias in anxiety: Amygdala–dorsomedial prefrontal cortex coupling and aversive amplification. NeuroImage *60*, 523–529.

Robinson, O.J., Overstreet, C., Allen, P.S., Letkiewicz, A., Vytal, K., Pine, D.S., and Grillon, C. (2013). The role of serotonin in the neurocircuitry of negative affective bias: Serotonergic modulation of the dorsal medial prefrontal-amygdala 'aversive amplification' circuit. NeuroImage *78*, 217–223.

Robinson, O.J., Krimsky, M., Lieberman, L., Allen, P., Vytal, K., and Grillon, C. (2014). The dorsal medial prefrontal (anterior cingulate) cortex–amygdala aversive amplification circuit in unmedicated generalised and social anxiety disorders: an observational study. Lancet Psychiatry *1*, 294–302.

Rolls, E.T. (2005). Emotion explained (Oxford University Press, USA).

Rose, J.E., and Woolsey, C.N. (1948). Structure and relations of limbic cortex and anterior thalamic nuclei in rabbit and cat. J. Comp. Neurol. *89*, 279–347.

Roth, B.L. (2016). DREADDs for Neuroscientists. Neuron *89*, 683–694.

Roy, A.K., Shehzad, Z., Margulies, D.S., Kelly, A.M., Uddin, L.Q., Gotimer, K., Biswal, B.B., Castellanos, F.X., and Milham, M.P. (2009). Functional connectivity of the human amygdala using resting state fMRI. Neuroimage *45*, 614–626.

Rudebeck, P.H., Putnam, P.T., Daniels, T.E., Yang, T., Mitz, A.R., Rhodes, S.E.V., and Murray, E.A. (2014). A role for primate subgenual cingulate cortex in sustaining autonomic arousal. Proc. Natl. Acad. Sci. *111*, 5391–5396.

Rush, A.J., Trivedi, M.H., Wisniewski, S.R., Nierenberg, A.A., Stewart, J.W., Warden, D., Niederehe, G., Thase, M.E., Lavori, P.W., Lebowitz, B.D., et al. (2006). Acute and longer-term outcomes in depressed outpatients requiring one or several treatment steps: a STAR* D report. Am. J. Psychiatry *163*, 1905–1917.

Rushworth, M.F., Kolling, N., Sallet, J., and Mars, R.B. (2012). Valuation and decision-making in frontal cortex: one or many serial or parallel systems? Curr. Opin. Neurobiol. *22*, 946–955.

Rushworth, M.F.S., Walton, M.E., Kennerley, S.W., and Bannerman, D.M. (2004). Action sets and decisions in the medial frontal cortex. Trends Cogn. Sci. *8*, 410–417.

Rushworth, M.F.S., Behrens, T.E.J., Rudebeck, P.H., and Walton, M.E. (2007). Contrasting roles for cingulate and orbitofrontal cortex in decisions and social behaviour. Trends Cogn. Sci. *11*, 168–176.

Sah, P., Faber, E.S.L., Lopez De Armentia, M., and Power, J. (2003). The Amygdaloid Complex: Anatomy and Physiology. Physiol. Rev. *83*, 803–834.

Santangelo, A.M., Ito, M., Shiba, Y., Clarke, H.F., Schut, E.H., Cockcroft, G., Ferguson-Smith, A.C., and Roberts, A.C. (2016). Novel Primate Model of Serotonin Transporter Genetic Polymorphisms Associated with Gene Expression, Anxiety and Sensitivity to Antidepressants. Neuropsychopharmacology.

Santesso, D.L., Dillon, D.G., Birk, J.L., Holmes, A.J., Goetz, E., Bogdan, R., and Pizzagalli, D.A. (2008). Individual Differences in Reinforcement Learning: Behavioral, Electrophysiological, and Neuroimaging Correlates. NeuroImage *42*, 807–816.

Satpute, A.B., Wager, T.D., Cohen-Adad, J., Bianciardi, M., Choi, J.-K., Buhle, J.T., Wald, L.L., and Barrett, L.F. (2013). Identification of discrete functional subregions of the human periaqueductal gray. Proc. Natl. Acad. Sci. *110*, 17101–17106.

Schmaal, L., Hibar, D.P., Sämann, P.G., Hall, G.B., Baune, B.T., Jahanshad, N., Cheung, J.W., van Erp, T.G.M., Bos, D., Ikram, M.A., et al. (2017). Cortical abnormalities in adults and adolescents with major depression based on brain scans from 20 cohorts worldwide in the ENIGMA Major Depressive Disorder Working Group. Mol. Psychiatry *22*, 900–909.

Schoepp, D.D., Jane, D.E., and Monn, J.A. (1999). Pharmacological agents acting at subtypes of metabotropic glutamate receptors. Neuropharmacology *38*, 1431–1476.

Schwabe, L., and Wolf, O.T. (2011). Stress-induced modulation of instrumental behavior: from goal-directed to habitual control of action. Behav. Brain Res. *219*, 321–328.

Seamans, J.K., Lapish, C.C., and Durstewitz, D. (2008). Comparing the prefrontal cortex of rats and primates: insights from electrophysiology. Neurotox. Res. *14*, 249–262.

Searcy, Y.M., and Caine, N.G. (2003). Hawk calls elicit alarm and defensive reactions in captive Geoffroy's marmosets (Callithrix geoffroyi). Folia Primatol. (Basel) *74*, 115–125.

Seeley, W.W., Menon, V., Schatzberg, A.F., Keller, J., Glover, G.H., Kenna, H., Reiss, A.L., and Greicius, M.D. (2007). Dissociable intrinsic connectivity networks for salience processing and executive control. J. Neurosci. *27*, 2349–2356.

Sehlmeyer, C., Schöning, S., Zwitserlood, P., Pfleiderer, B., Kircher, T., Arolt, V., and Konrad, C. (2009). Human fear conditioning and extinction in neuroimaging: a systematic review. PloS One *4*, e5865.

Shackman, A. (2015). The importance of respecting variation in cingulate anatomy: Comment on Lieberman & Eisenberger 2015 and Yarkoni.

Shackman, A.J., Salomons, T.V., Slagter, H.A., Fox, A.S., Winter, J.J., and Davidson, R.J. (2011). The Integration of Negative Affect, Pain, and Cognitive Control in the Cingulate Cortex. Nat. Rev. Neurosci. *12*, 154–167.

Shah, A.A., and Treit, D. (2003). Excitotoxic lesions of the medial prefrontal cortex attenuate fear responses in the elevated-plus maze, social interaction and shock probe burying tests. Brain Res. *969*, 183–194.

Shah, A.A., Sjovold, T., and Treit, D. (2004). Inactivation of the medial prefrontal cortex with the GABA A receptor agonist muscimol increases open-arm activity in the elevated plus-maze and attenuates shock-probe burying in rats. Brain Res. *1028*, 112–115.

Shapero, B.G., Black, S.K., Liu, R.T., Klugman, J., Bender, R.E., Abramson, L.Y., and Alloy, L.B. (2014). Stressful Life Events and Depression Symptoms: The Effect of Childhood Emotional Abuse on Stress Reactivity. J. Clin. Psychol. *70*, 209–223.

Sharpe, M.J., and Killcross, S. (2015). The prelimbic cortex directs attention toward predictive cues during fear learning. Learn. Mem. *22*, 289–293.

Shenhav, A., and Botvinick, M. (2015). Uncovering a Missing Link in Anterior Cingulate Research. Neuron *85*, 455–457.

Shenhav, A., Botvinick, M.M., and Cohen, J.D. (2013). The Expected Value of Control: An Integrative Theory of Anterior Cingulate Cortex Function. Neuron *79*, 217–240.

Shenhav, A., Cohen, J.D., and Botvinick, M.M. (2016). Dorsal anterior cingulate cortex and the value of control. Nat. Neurosci. *19*, 1286–1291.

Shiba, Y. (2013). Characterising trait anxiety in the common marmoset (Callithrix jacchus) : investigations into behavioural, psychophysiological and cognitive phenotypes. Ph.D. University of Cambridge.

Shiba, Y., Santangelo, A.M., Braesicke, K., Agustín-Pavón, C., Cockcroft, G., Haggard, M., and Roberts, A.C. (2014). Individual differences in behavioral and cardiovascular reactivity to emotive stimuli and their relationship to cognitive flexibility in a primate model of trait anxiety. Front. Behav. Neurosci. *8*, 137.

Shima, K., and Tanji, J. (1998). Role for cingulate motor area cells in voluntary movement selection based on reward. Science *282*, 1335–1338.

Shin, L.M., and Liberzon, I. (2010). The Neurocircuitry of Fear, Stress, and Anxiety Disorders. Neuropsychopharmacology *35*, 169–191.

Shin, L.M., Lasko, N.B., Macklin, M.L., Karpf, R.D., Milad, M.R., Orr, S.P., Goetz, J.M., Fischman, A.J., Rauch, S.L., and Pitman, R.K. (2009). Resting metabolic activity in the cingulate cortex and vulnerability to posttraumatic stress disorder. Arch. Gen. Psychiatry *66*, 1099–1107.

Shin, L.M., Bush, G., Milad, M.R., Lasko, N.B., Brohawn, K.H., Hughes, K.C., Macklin, M.L., Gold, A.L., Karpf, R.D., Orr, S.P., et al. (2011). Exaggerated Activation of Dorsal Anterior Cingulate Cortex During Cognitive Interference: A Monozygotic Twin Study of Posttraumatic Stress Disorder. Am. J. Psychiatry *168*, 979–985.

Sierra-Mercado, D., Padilla-Coreano, N., and Quirk, G.J. (2011). Dissociable roles of prelimbic and infralimbic cortices, ventral hippocampus, and basolateral amygdala in the expression and extinction of conditioned fear. Neuropsychopharmacology *36*, 529–538.

Smith, C.U.M.C. (2010). The triune brain in antiquity: Plato, Aristotle, Erasistratus. J. Hist. Neurosci. *19*, 1–14.

Smith, G.E. (1907). A new topographical survey of the human cerebral cortex, being an account of the distribution of the anatomically distinct cortical areas and their relationship to the cerebral sulci. J. Anat. Physiol. *41*, 237.

Sotres-Bayon, F., and Quirk, G.J. (2010). Prefrontal control of fear: more than just extinction. Curr. Opin. Neurobiol. *20*, 231–235.

Sridharan, D., Levitin, D.J., and Menon, V. (2008). A critical role for the right fronto-insular cortex in switching between central-executive and default-mode networks. Proc. Natl. Acad. Sci. *105*, 12569–12574.

Steele, J.D., Currie, J., Lawrie, S.M., and Reid, I. (2007). Prefrontal cortical functional abnormality in major depressive disorder: A stereotactic meta-analysis. J. Affect. Disord. *101*, 1–11.

Steele, J.D., Christmas, D., Eljamel, M.S., and Matthews, K. (2008). Anterior Cingulotomy for Major Depression: Clinical Outcome and Relationship to Lesion Characteristics. Biol. Psychiatry *63*, 670–677.

Stern, C.A.J., Do Monte, F.H.M., Gazarini, L., Carobrez, A.P., and Bertoglio, L.J. (2010). Activity in prelimbic cortex is required for adjusting the anxiety response level during the elevated plus-maze retest. Neuroscience *170*, 214–222.

Stevens, F.L., Hurley, R.A., and Taber, K.H. (2011). Anterior Cingulate Cortex: Unique Role in Cognition and Emotion. J. Neuropsychiatry Clin. Neurosci.

Stevenson, M.F., and Poole, T.B. (1976). An ethogram of the common marmoset (Calithrix jacchus jacchus): general behavioural repertoire. Anim. Behav. *24*, 428–451.

Straube, T., Schmidt, S., Weiss, T., Mentzel, H.-J., and Miltner, W.H.R. (2009). Dynamic activation of the anterior cingulate cortex during anticipatory anxiety. NeuroImage *44*, 975–981.

Sullivan, P.F., Neale, M.C., and Kendler, K.S. (2000). Genetic epidemiology of major depression: review and meta-analysis. Am. J. Psychiatry *157*, 1552–1562.

Suzuki, K., Nosyreva, E., Hunt, K.W., Kavalali, E.T., and Monteggia, L.M. (2017). Effects of a ketamine metabolite on synaptic NMDAR function. Nature *546*, E1–E3.

Sylvers, P., Lilienfeld, S.O., and LaPrairie, J.L. (2011). Differences between trait fear and trait anxiety: Implications for psychopathology. Clin. Psychol. Rev. *31*, 122–137.

Talairach, J., and Tournoux, P. (1988). Co-Planar Stereotaxic Atlas of the Human Brain: 3-D Proportional System: An Approach to Cerebral Imaging (Thieme).

Tarvainen, M.P., Ranta-Aho, P.O., Karjalainen, P.A., and others (2002). An advanced detrending method with application to HRV analysis. IEEE Trans. Biomed. Eng. *49*, 172–175.

Tarvainen, M.P., Niskanen, J.-P., Lipponen, J.A., Ranta-aho, P.O., and Karjalainen, P.A. (2014). Kubios HRV – Heart rate variability analysis software. Comput. Methods Programs Biomed. *113*, 210–220.

Thayer, J.F., and Lane, R.D. (2000). A model of neurovisceral integration in emotion regulation and dysregulation. J. Affect. Disord. *61*, 201–216.

Thayer, J.F., and Lane, R.D. (2009). Claude Bernard and the heart–brain connection: Further elaboration of a model of neurovisceral integration. Neurosci. Biobehav. Rev. *33*, 81–88.

Thayer, J.F., Yamamoto, S.S., and Brosschot, J.F. (2010). The relationship of autonomic imbalance, heart rate variability and cardiovascular disease risk factors. Int. J. Cardiol. *141*, 122–131.

Thayer, J.F., \AAhs, F., Fredrikson, M., Sollers III, J.J., and Wager, T.D. (2012). A meta-analysis of heart rate variability and neuroimaging studies: implications for heart rate variability as a marker of stress and health. Neurosci. Biobehav. Rev. *36*, 747–756.

Thompson, R.A. (1994). Emotion regulation: A theme in search of definition. Monogr. Soc. Res. Child Dev. *59*, 25–52.

Toichi, M., Sugiura, T., Murai, T., and Sengoku, a (1997). A new method of assessing cardiac autonomic function and its comparison with spectral analysis and coefficient of variation of R-R interval. J. Auton. Nerv. Syst. *62*, 79–84.

Tovote, P., Fadok, J.P., and Lüthi, A. (2015). Neuronal circuits for fear and anxiety. Nat. Rev. Neurosci. *16*, 317.

Tranel, D., and Damasio, H. (1994). Neuroanatomical correlates of electrodermal skin conductance responses. Psychophysiology *31*, 427–438.

Treadway, M.T., and Zald, D.H. (2011). Reconsidering anhedonia in depression: Lessons from translational neuroscience. Neurosci. Biobehav. Rev. *35*, 537–555.

Trivedi, M.H., Rush, A.J., Wisniewski, S.R., Nierenberg, A.A., Warden, D., Ritz, L., Norquist, G., Howland, R.H., Lebowitz, B., McGrath, P.J., et al. (2006). Evaluation of Outcomes With Citalopram for Depression Using Measurement-Based Care in STAR*D: Implications for Clinical Practice. Am. J. Psychiatry *163*, 28–40.

Uijtdehaage, S.H.J., and Thayer, J.F. (2000). Accentuated antagonism in the control of human heart rate. Clin. Auton. Res. *10*, 107–110.

Ullsperger, M., Danielmeier, C., and Jocham, G. (2014). Neurophysiology of Performance Monitoring and Adaptive Behavior. Physiol. Rev. *94*, 35–79.

Uylings, H., Groenewegen, H.J., and Kolb, B. (2003). Do rats have a prefrontal cortex? Behav. Brain Res. *146*, 3–17.

Vertes, R.P. (2002). Analysis of projections from the medial prefrontal cortex to the thalamus in the rat, with emphasis on nucleus reuniens. J. Comp. Neurol. *442*, 163–187.

Vidal-Gonzalez, I., Vidal-Gonzalez, B., Rauch, S.L., and Quirk, G.J. (2006). Microstimulation reveals opposing influences of prelimbic and infralimbic cortex on the expression of conditioned fear. Learn. Mem. *13*, 728–733.

Videbech, P., and Ravnkilde, B. (2004). Hippocampal Volume and Depression: A Meta-Analysis of MRI Studies. Am. J. Psychiatry *161*, 1957–1966.

Vogt (1987). Cingulate cortex of the rhesus monkey: I. Cytoarchitecture and thalamic afferents. J. Comp. Neurol.

Vogt, B. (2009). Cingulate Neurobiology and Disease (OUP Oxford).

Vogt, B.A. (2016). Midcingulate cortex: structure, connections, homologies, functions and diseases. J. Chem. Neuroanat. *74*, 28–46.

Vogt, B.A., and Pandya, D.N. (1987). Cingulate cortex of the rhesus monkey: II. Cortical afferents. J. Comp. Neurol. *262*, 271–289.

Vogt, B.A., and Paxinos, G. (2014). Cytoarchitecture of mouse and rat cingulate cortex with human homologies. Brain Struct. Funct. *219*, 185–192.

Vogt, B.A., and Peters, A. (1981). Form and distribution of neurons in rat cingulate cortex: Areas 32, 24, and 29. J. Comp. Neurol. *195*, 603–625.

Vogt, B.A., and Vogt, L. (2003). Cytology of human dorsal midcingulate and supplementary motor cortices. J. Chem. Neuroanat. *26*, 301–309.

Vogt, C., and Vogt, O. (1919). Allgemeine Ergebnisse unserer Hirnforschung.

Vogt, B., Rosene, D., and Pandya, D. (1979). Thalamic and cortical afferents differentiate anterior from posterior cingulate cortex in the monkey. Science *204*, 205–207.

Vogt, B.A., Berger, G.R., and Derbyshire, S.W. (2003). Structural and functional dichotomy of human midcingulate cortex. Eur. J. Neurosci. *18*, 3134–3144.

Vogt, B.A., Vogt, L., Farber, N.B., and Bush, G. (2005). Architecture and Neurocytology of Monkey Cingulate Gyrus. J. Comp. Neurol. *485*, 218–239.

Vogt, B.A., Hof, P.R., Friedman, D.P., Sikes, R.W., and Vogt, L.J. (2008). Norepinephrinergic afferents and cytology of the macaque monkey midline, mediodorsal, and intralaminar thalamic nuclei. Brain Struct. Funct. *212*, 465–479.

Vogt, B.A., Hof, P.R., Zilles, K., Vogt, L.J., Herold, C., and Palomero-Gallagher, N. (2013). Cingulate area 32 homologies in mouse, rat, macaque and human: Cytoarchitecture and receptor architecture. J. Comp. Neurol. *521*, 4189–4204.

Vytal, K.E., Overstreet, C., Charney, D.R., Robinson, O.J., and Grillon, C. (2014). Sustained anxiety increases amygdala–dorsomedial prefrontal coupling: a mechanism for maintaining an anxious state in healthy adults. J. Psychiatry Neurosci. JPN *39*, 130145.

Wager, T.D., van Ast, V.A., Hughes, B.L., Davidson, M.L., Lindquist, M.A., and Ochsner, K.N. (2009). Brain mediators of cardiovascular responses to social threat, Part II: Prefrontal-subcortical pathways and relationship with anxiety. NeuroImage *47*, 836–851.

Wager, T.D., Atlas, L.Y., Botvinick, M.M., Chang, L.J., Coghill, R.C., Davis, K.D., Iannetti, G.D., Poldrack, R.A., Shackman, A.J., and Yarkoni, T. (2016). Pain in the ACC? Proc. Natl. Acad. Sci. 201600282.

Wagner, G., Koch, K., Schachtzabel, C., Schultz, C.C., Sauer, H., and Schlösser, R.G. (2011). Structural brain alterations in patients with major depressive disorder and high risk for suicide: Evidence for a distinct neurobiological entity? NeuroImage *54*, 1607–1614.

Walker, A.E. (1940). A cytoarchitectural study of the prefrontal area of the macaque monkey. J. Comp. Neurol. *73*, 59–86.

Walker, D.L., Toufexis, D.J., and Davis, M. (2003). Role of the bed nucleus of the stria terminalis versus the amygdala in fear, stress, and anxiety. Eur. J. Pharmacol. *463*, 199–216.

Wallis, J.D. (2012). Cross-species studies of orbitofrontal cortex and value-based decision-making. Nat. Neurosci. *15*, 13–19.

Wallis, C.U., Cardinal, R.N., Alexander, L., Roberts, A.C., and Clarke, H.F. (2017). Opposing roles of primate areas 25 and 32 and their putative rodent homologs in the regulation of negative emotion. Proc. Natl. Acad. Sci. 201620115.

Watakabe, A., Sadakane, O., Hata, K., Ohtsuka, M., Takaji, M., and Yamamori, T. (2016). Application of viral vectors to the study of neural connectivities and neural circuits in the marmoset brain. Dev. Neurobiol.

Weiskrantz, L. (1956). Behavioral changes associated with ablation of the amygdaloid complex in monkeys. J. Comp. Physiol. Psychol. *49*, 381.

Wendy, J.S., Cosgrove, G.R., Ballantine Jr, H.T., Edwin, H.C., Scott, L.R., Andrew, N., and Bruce, H.P. (1996). Magnetic resonance image-guided stereotactic cingulotomy for intractable psychiatric disease. Neurosurgery *38*, 1071–1078.

Whiteford, H., Degenhardt, L., and Rehm, J. (2013). Global burden of disease attributable to mental and substance use disorders: findings from the Global Burden of Disease Study 2010. The Lancet.

Whitty, C.W.M., Duffield, J.E., Tow, P.M., and Cairns, H. (1952). Anterior cingulectomy in the treatment of mental disease. The Lancet *259*, 475–481.

WHO WHO | Depression and Other Common Mental Disorders.

Wilkinson, H.A., Davidson, K.M., and Davidson, R.I. (1999). Bilateral Anterior Cingulotomy for Chronic Noncancer Pain. Neurosurgery *45*, 1129–1136.

Williams, Z.M., Bush, G., Rauch, S.L., Cosgrove, G.R., and Eskandar, E.N. (2004). Human anterior cingulate neurons and the integration of monetary reward with motor responses. Nat. Neurosci. *7*, 1370.

Wong, M.-L., and Licinio, J. (2004). From monoamines to genomic targets: a paradigm shift for drug discovery in depression. Nat. Rev. Drug Discov. *3*, 136.

World Health Organization (2017). Depression and other common mental disorders: global health estimates.

Yarkoni, A.T. (2015). No, the dorsal anterior cingulate is not selective for pain: comment on Lieberman and Eisenberger (2015).

Yarkoni, T., Poldrack, R.A., Nichols, T.E., Van Essen, D.C., and Wager, T.D. (2011). Large-scale automated synthesis of human functional neuroimaging data. Nat. Methods *8*, 665–670.

Yin, H.H., Knowlton, B.J., and Balleine, B.W. (2004). Lesions of dorsolateral striatum preserve outcome expectancy but disrupt habit formation in instrumental learning. Eur. J. Neurosci. *19*, 181–189.

Yokoyama, C., and Onoe, H. (2015). Positron emission tomography imaging of the social brain of common marmosets. Neurosci. Res.

Yokoyama, C., Kawasaki, A., Hayashi, T., and Onoe, H. (2012). Linkage Between the Midline Cortical Serotonergic System and Social Behavior Traits: Positron Emission Tomography Studies of Common Marmosets. Cereb. Cortex bhs196.

Zanos, P., Moaddel, R., Morris, P.J., Georgiou, P., Fischell, J., Elmer, G.I., Alkondon, M., Yuan, P., Pribut, H.J., Singh, N.S., et al. (2017). Zanos et al. reply. Nature *546*, E4–E5.

Zanos P, Moaddel R, Morris Pj, Georgiou P, Fischell J, Elmer Gi, Alkondon M, Yuan P, Pribut Hj, Singh Ns, et al. (2016). NMDAR inhibition-independent antidepressant actions of ketamine metabolites., NMDAR inhibition-independent antidepressant actions of ketamine metabolites. Nat. Nat. *533*, *533*, 481, 481–486.

Zarate, C.A., Singh, J.B., Carlson, P.J., Brutsche, N.E., Ameli, R., Luckenbaugh, D.A., Charney, D.S., and Manji, H.K. (2006). A Randomized Trial of an N-methyl-D-aspartate Antagonist in Treatment-Resistant Major Depression. Arch. Gen. Psychiatry *63*, 856–864.

Zhang, W., Xu, D., Cui, J., Jing, X., Xu, N., Liu, J., and Bai, W. (2017). Anterograde and retrograde tracing with high molecular weight biotinylated dextran amine through thalamocortical and corticothalamic pathways. Microsc. Res. Tech. *80*, 260–266.

Zilles, K., and Amunts, K. (2010). Centenary of Brodmann's map — conception and fate. Nat. Rev. Neurosci. *11*, nrn2776.

Zoellner, L.A., Rothbaum, B.O., and Feeny, N.C. (2011). PTSD not an anxiety disorder? DSM committe proposal turns back the hands of time. Depress. Anxiety *28*, 853–856.